ASSOCIATION AND INTERACTIONS OF PULMONARY SURFACTANT LIPIDS AND PROTEINS IN MODEL MEMBRANES AT THE AIR - WATER INTERFACE.

Kaushik Nag

A thesis submitted in partial fulfilment of the requirements for the degree of Doctor of Philosophy.

Department of Biochemistry,

Memorial University of Newfoundland,

St. John's, Canada.

1996.

ABSTRACT

Pulmonary surfactant (PS) a lipid-protein complex secreted by type-II pneumocytes is responsible for alveolar stability and prevents lung collapse at low volumes. PS lines the air-alveolar fluid interface with a putative ultra-thin monomolecular film, which by reducing the surface tension of that interface counteracts the contractile forces of lung collapse at low volumes. Monomolecular films (monolayers) are appropriate models for studying biological membranes, in which the lipids and proteins are organized in bilayers, and for pulmonary surfactant films.

Interactions of the main phospholipid component of PS, dipalmitoylphosphatidylcholine (DPPC) were studied with the other component lipids and proteins of PS at the air-water interface in monolayers. Over the last decade, epifluorescence microscopy has become a novel and powerful tool to study the organization of molecules in films. Epifluorescence microscopy of films formed in a surface balance of DPPC in combination with unsaturated phosphatidylcholine (dioleyl-PC or DOPC); dipalmitoylphosphatidylglycerol (DPPG); cholesterol; and fluorescently labelled surfactant proteins SP-A, SP-B and SP-C were performed. Visual observation of such lipid-lipid and lipid-protein films using epifluorescence microscopy allowed for the semi-quantitative understanding of the surface chemistry, phase transition, association and interactions of such components of PS with each other, at the air-water interface.

The unsaturated phosphatidylcholine, DOPC, fluidized films of DPPC and were squeezed out of such films upon dynamic cycling (Chapter 3). Phosphatidylglycerol

(DPPG) condensed films of DPPC under the influence of calcium (Chapter 4). Cholesterol drastically altered the DPPC condensed phase structures and fluidized such films (Chapter 5). Hydrophobic surfactant protein - C (SP-C) perturbed the packing of DPPC and DPPC:DPPG films, occupied the fluid phase and was present in the films up to high packing states (Chapter 6). Films adsorbed from liposomes and solvent-spread ones of some PS components were found to display similar micro-architecture and phase properties in equivalent packing states, and SP-C enhanced the adsorption of DPPC vesicles (Chapter 7). Hydrophobic surfactant protein - B (SP-B) also perturbed the packing and associated with the fluid phase of DPPC, albeit differently than did SP-C (Chapter 8 and 9). Hydrophilic surfactant protein - A (SP-A) adsorbed to DPPC films, and was associated with the condensed-fluid phase boundaries of the lipid, and perturbed the packing of such films (Chapter 10). Porcine lipid surfactant extract (LSE) films showed fluid to condensed phase transition upon compression, and probably other complex transitions which was indicated by a decrease in the amount of condensed domains with increasing packing states (Chapter 11). The condensed phase of LSE films were increased under the influence of millimolar calcium dissolved in the subphase compared to the ones without the cation. Dissolved SP-A in the subphase, adsorbed on to solvent-spread LSE films and altered the distribution of condensed domains (Chapter 11). Some of the properties of LSE films (Chapter 11) were correlated to those exhibited by its component combinations in films (Chapters 3-10).

These studies, using a novel technique, elucidate some of the possible modes of association and interactions between the major pulmonary surfactant components at the

air-water interface. This study may also indicate feasible lipid-lipid and lipid-protein associations and micro-organisation in model of biological membranes.

ACKNOWLEDGEMENTS

I would like to express my gratitude to my supervisor Dr. Kevin M. W. Keough for his patience, understanding and supervision during the course of this work. I would also like to thank him especially for the critical and meticulous changes of my English writing style (from Bengali thinking process and writing in Benglish (Bengali + English = Benglish), for which he has shown exceptional patience.

I would like to thank my supervisory committee members Dr. Philip J. Davis (Biochemistry, MUN) for his periodical moral boosts during the course of this work and critical reading of this thesis, and Dr. Nathan H. Rich (Physics, MUN) for his support and help with instrumentation during the course of this work. I would also like to express my gratitude to the following for help, advice and discussions during the course of this work, Drs. Michael Morrow (Physics, MUN); David Pink (Physics, St.Francis Xavier University, Nova Scotia); Jesus Perez-Gil (University Complutens Madrid, Spain). A special acknowledgment goes to Dr. Sailen Mookerjea (Biochemistry, MUN) for his unending ethical support during the depression years, and for discussions ranging from world politics to cyberspace, as a distraction from the boredom of laboratory work.

I would also like to extend my gratitude to the numerous support staff who had helped me in various ways during the course of this research, especially Roy Ficken (Photography, Biology, MUN) and Donna Osborne (Secretary, VP Research, MUN) for deciphering complex hieroglyphics; Lynn Anne D. Worthman (Biochemistry, MUN); June Stewart (Biochemistry, MUN) for helping me with laboratory work. I would also

like to acknowledge the assistance provided by Lorne Taylor (Chemistry, University of Waterloo) and Ronald C. Beavis (Skirball Institute of Bimolecular Medicine, New York), in analysis of the surfactant proteins. Finally a special thanks goes to my girlfriend Doreen Broaders Miron, for typing parts of this thesis, and for moral support over the years.

A special acknowledgement also goes out to the funding agencies which have supported different aspects of this project, especially the School of Graduate Studies, MUN; Medical Research Council, Canada and NATO.

TABLE OF CONTENTS

LIST OF FIGURES

ABBREVIATIONS

Å	Angstrom unit (10^{-10} meter)
AFM	Atomic force microscopy
BAM	Brewster angle microscopy
Da	Dalton
DPPC	1,2-dipalmitoyl-*sn*-glycero-3-phosphocholine
DPPG	1,2-dipalmitoyl-*sn*-glycero-3-phospho-*rac*-glycerol
DMPC	1,2-dimyristoyl-*sn*-glycero-3-phosphocholine
DOPC	1,2-dioleyl-*sn*-glycero-3-phosphocholine
DSPC	1,2-distearoyl-*sn*-glycero-3-phosphocholine
ESR	electron spin resonance
ϕ	degree of crystallization
FTIR	Fourier transform infrared
γ	surface tension
^{2}H NMR	deuterium nuclear magnetic resonance
IRRAS	infrared reflectance attenuated spectroscopy
kDa	kilo Dalton
L_α	liquid crystalline
L_β	gel
LA	large aggregates
LB	Langmuir-Blodgett

LC	liquid condensed
LE	liquid expanded
LSE	lipid surfactant extract
μ	micro (10^{-6})
M	molar
mN/m	milliNewton per meter
nm	nanometre (10^{-9} meter)
MALDI	matrix assisted laser desorption/ionization
π	surface pressure
PS	pulmonary surfactant
SA	small aggregates
SAM	surface active material
SP-A	surfactant protein - A
SP-B	surfactant protein - B
SP-C	surfactant protein - C
Tc	gel to liquid crystalline phase transition temperature
TM	tubular myelin
TOF	time of flight

INTRODUCTION

"Surfactants allow us to protect a water surface and to generate beautiful soap bubbles, which delight our children."

Pierre-Gilles DeGennes,

Soft Matter (Nobel Lectures, 1992)

Pulmonary surfactant (PS), a frothy material found in the lungs of most air-breathing species, is responsible for alveolar stability. The material is secreted by type - II alveolar cells and is composed mainly of lipids and small amounts of proteins. The lung tissues, which have elastic recoil like stretched rubber, during low lung volume tend to collapse the alveoli due to contractile tissue forces. The lipid-protein complex of pulmonary surfactant lines the alveolar air-fluid interface with a thin film, and reduces the air-fluid interfacial tension counteracting the contractile forces of lung collapse. A number of disease conditions such as neonatal Respiratory Distress Syndrome (RDS) and Adult-RDS (ARDS) arise due to altered levels, composition, and *in vivo* inhibition of pulmonary surfactant. Some of these situations are treatable by instilling surfactant (natural and synthetic) or a combination of some of the pulmonary surfactants lipid-protein components into the diseased lung. The search for better and improved artificial surfactants for therapy has been the focus of intensive research efforts over the last few decades, although the surface activity, nature and composition of the PS films in the alveoli and the biophysical transformations that PS undergoes from its cellular secretory

stage to film formation are not yet completely clear. At present, despite some intense basic and clinical research efforts integrating the fields of biology, physical chemistry and physiology to study PS, functional comprehension at the molecular level of the complex in the air-alveolar fluid interface is limited. Nevertheless research in this area has indicated some important facts which have lead to improved clinical treatments of PS related disorders.

Pulmonary surfactant is rich in some unusual phospholipids such as dipalmitoylphosphatidylcholine (DPPC) and phosphatidylglycerol which are not found in any eukaryotic lipid-containing cellular organelles such as biological membranes. Pulmonary surfactant (PS) also contains significant amounts of unsaturated lipids and cholesterol which are normally found in most mammalian biological membranes. The proteins of PS although present in small amounts ($\sim$5-10 wt% of the lipids), play significant roles in its surface activity. The combination of lipid-protein complexes of PS allows for the material to be uniquely surface-active. *In vitro* the material can rapidly adsorb and spread at an air-water interface to form films, and these films upon compression can reduce the surface tension of the interface to near 0 mN/m, and such films quickly re-spread from highly compressed states. Some of these biophysical processes are currently not well understood. The purpose of this thesis is to examine the structures and surface properties of the pulmonary surfactant and its component films using a novel custom designed surface balance with microscopic attachments. This instrument not only allows one to measure surface activity of materials at an air-water interface but also microscopically observe the association and semi-quantitatively assay

the interactions of lipids and proteins in films. We have examined the surface properties, interactions and associations of the main lipid component of pulmonary surfactant, DPPC, in combination with other components such as unsaturated lipid, acidic lipid, cholesterol, surfactant proteins A, B and C, and extracts of porcine pulmonary surfactant. Because of the nature of the films and their constituents, these studies are not only relevant to PS but may also be considered as models for lipid-lipid and lipid-protein organizations in biological membranes. Also since monomolecular films are unusual structures in biological systems (only pulmonary surfactant and apolipoprotein particles have monolayers), these studies may indicate some general characteristics of lipid-protein associations in these structures, as well as in single leaflets (monolayers) of bilayer membranes.

The style and content of this thesis (except the first 2 chapters) is written in publication fromat, since most of the data presented has been previously published or in submission for publication. The content of the organization of the thesis is that the first two chapters are introduction to surfactant and biological membranes, and the rest description of data obtained on *in vitro* interactions of the various surfactant components in films.

Chapter 1.

PULMONARY SURFACTANT

1.1] Historical Development.

It was reported in 1671 by Frederic Marten, that "When the whales blow up the water, they fling out with it some fattish substance that floats upon the sea like sperm, and this fat the Mallemucks (bird) devour greedily" (cited from Goerke, 1974). This was probably the first detection of pulmonary surfactant in the giant mammal. Alexander Graham Bell in 1889, in trying to construct artificial ventilators for babies, stated that some babies die from inability to expand their lungs sufficiently when they take their first breath (citation from, Stern et al. 1970). As early as 1929, Von Neegard recognized that surface tension was presumably responsible for closure or lung recoil during breathing (Obladen, 1992). Later Macklin (1954) described the possibility of an alveolar mucoid like film on the pulmonary cell walls which were able to maintain a consistent favourable surface tension. Around the same period Pattle (1955) reported that the foamy substance of the lungs, originated from the alveolar cellular lining. John Clements, measured the surface activity of the foamy material at an air-water interface, and concluded that the material is highly surface active (Clements, 1956; 1957). Avery and Mead (1959), discovered that Respiratory Distress Syndrome (RDS), previously called the Hyaline Membrane Disease in human neonates, was caused by surfactant deficiency, leading to a spurt of clinical research in the area.

King and Clements extracted the surface active material from dog lungs and reported a method of its isolation in a relatively "pure" form (King and Clements, 1972a). They also studied its composition (King and Clements, 1972b) and physical

properties (King and Clements, 1972c). Schürch et al., (1976) first determined the surface tension of the lung air-alveolar fluid interface *in situ*, by a novel alveolar micro-puncture technique. This study indicated that at low lung volumes the interfacial surface tension was below 9 mN/m, and varied between below 9 to 20 mN/m during deflation to inflation of the lungs. They also measured the dynamic dependency of this surface tension on lung volumes, supporting the proposals made earlier, that surface activity of pulmonary surfactant allows for the surface tension of the air-alveolar fluid interface to be reduced (Schürch et al., 1976, 1978). Recently the fluid lining layer of the lungs has been shown to be continuous (Bastacky et al., 1995), and multilayers of lipidic film lining the air-alveolar fluid interface have been demonstrated (Schürch and Bachofen, 1995). Research in pulmonary surfactant over the last 60 years has lead to clinicians and surfactologists meeting in floating (surface active !) conferences on the rivers Danube and Rhine (Lachman, 1995). Some of the earlier historical developments of pulmonary surfactant research have been well documented and reviewed (Comroe, 1977; Goerke, 1974; Obladen, 1992; Smith, 1995).

1.2] Surface Tension in the Lungs.

The concept of how surfactant effects or changes surface tension of the lungs during the normal respiratory process, came from some seminal studies on measurement of lung volume and morphometry under different conditions of surface tension and pressures, created by filling the lungs with different fluids. Such studies showed that during lung deflation and inflation, the pressure - volume characteristics of the lungs

could be drastically altered and almost abolished once the lungs were washed with detergents (Clements, 1956; Mead et al., 1957). Later studies have shown, that by filling lungs with different fluids such as saline, hydrocarbons or fluorocarbons, the alveolar microstructure, lung area and morphometry can be altered, from those of air-filled lungs (Schürch and Bachofen, 1995; Wilson and Bachofen, 1982). Figure 1.1 shows the morphological structure of the lungs filled with saline (A), air (B) and air after the lungs have been washed with detergent (C), where in each case the lung volume was 70 % of the total lung capacity (TLC) (Wilson and Bachofen, 1982). The air-alveolar fluid interface had different interfacial or surface tension in contact with saline (A) than with air (B), since in the former case the air-alveolar fluid interface was abolished, and in the detergent washed lung filled with air (C) since the surface tension controlling lining (or surfactant) was removed by detergent washing. These studies indicate indirectly that the lung air-fluid interface has some material which controls the surface tension of that interface and thus alveolar morphometry, and any alteration of this surface tension (by using saline to abolish the air-alveolar fluid interface) or removal of this material (by detergent washing) leads to altered alveolar stability and structure, compared to normal air-filled lung. These and other studies have implied that the surface tension of the lung is a crucial factor in determining alveolar stability, morphometry and gas exchanges in normal air-breathing species (Bachofen et al., 1987; Schürch and Bachofen, 1995; Wilson and Bachofen, 1982). Studies have shown that the surface tension of the lungs *in vivo* can be measured by alveolar micropuncture and the values at low lung volume are very low ($\sim$ 1 mN/m) (Schürch et al., 1976). Recent studies indicate that

Figure 1.1 Internal morphology of lungs filled with saline (A), air (B) and air after detergent washing of the alveolus (C), fixed at 70 % of total lung capacity. Scale bar is 400 μm.

The surface tension in the lungs filled with air (A) was higher than the one with saline (B) since the saline abolished the interface between air and the alveolar fluid. In case of (C), the material (surfactant) which controls alveolar surface tension was removed by detergent washing, thereby altering the surface-tension from that of the air-filled lungs (A) with the material. The surface morphometry and total areas are also different in A, B and C indicating that alveolar ultra-structure and surface area depend on the surface tension of the air-alveolar fluid interface. The highly corrugated surface of the alveoli in (A) allows for larger area of gas exchange, in contrast to the smoother (smaller surface area) surfaces seen in (B). [From Wilson and Bachofen (1982), ©American Physiological Society; reprinted with the permission of the authors and publisher].

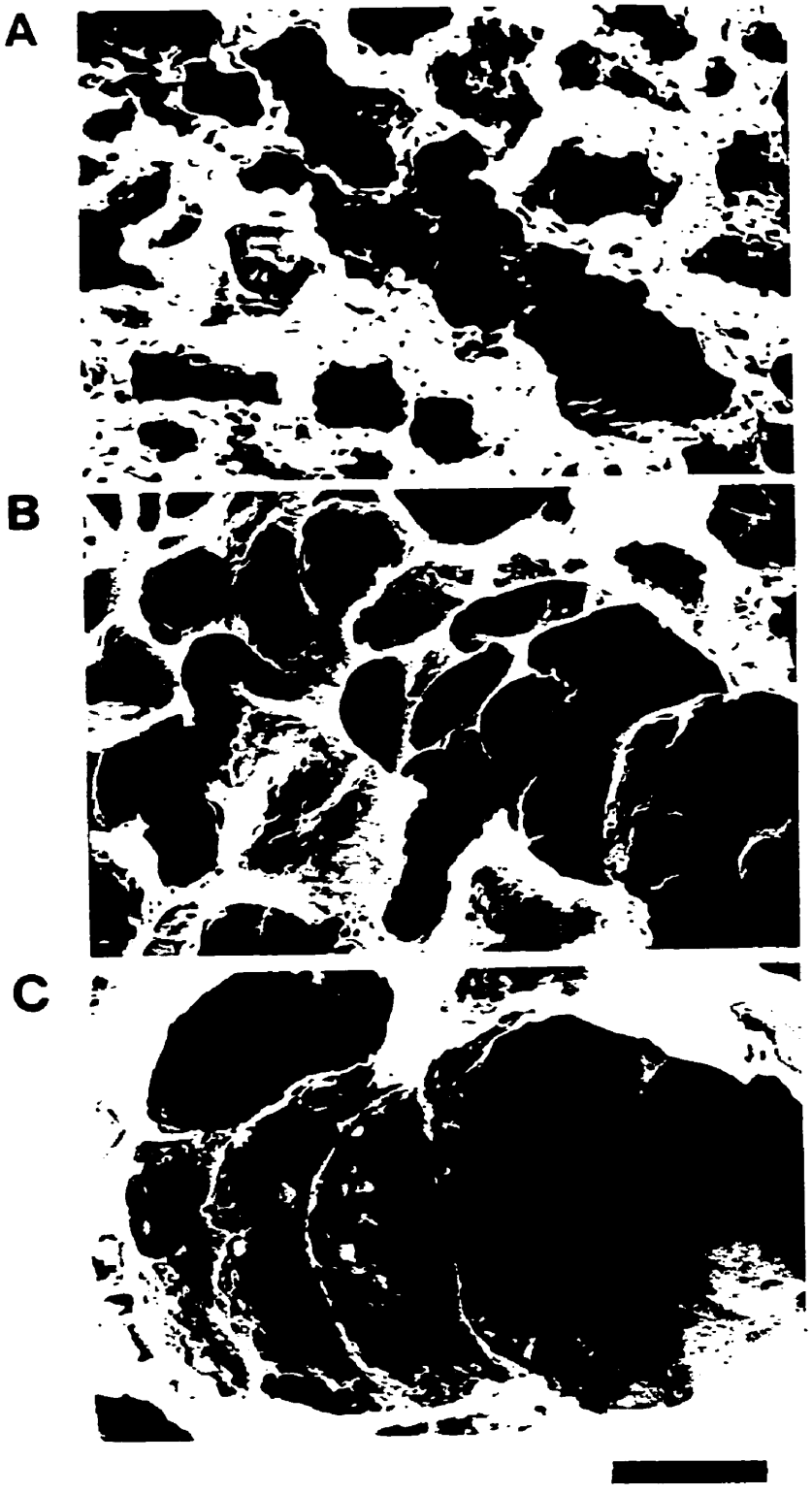

8a

for lungs deflated to functional residual capacity at (FRC - maximal deflational lung volume during normal breathing) at 37°C, the surface tension of the air-alveolar fluid interface is near 1 mN/m and the values are very stable, when the lungs are held at low volumes (Schürch and Bachofen, 1995). To achieve such low surface tension the lungs do not have to be deflated quasi-statically and a minimum deflational rate is not required to achieve low surface tension in the lungs (Schürch and Bachofen, 1995). This reduction of surface tension (γ) at low lung volumes counters various forces (such as contractile collapsing force of lung parenchyma or tissue surrounding the alveoli) trying to collapse the lung.

Clements proposed a model from several *in vitro* studies of pulmonary surfactant. His model suggests that pulmonary surfactant lines the air-alveolar fluid interface with a thin mono-molecular (monolayer) film. The lining film layer (Figure 1.2, bottom, 6) of pulmonary surfactant reduces the air-alveolar fluid interfacial tension possibly by the molecules forming a compact film or solid surface at low alveolar volumes. Träuble et al., (1974) suggested that the function of pulmonary surfactant other than reducing surface tension, is to induce critical spontaneous opening and closing of the alveoli. Others have suggested that the pulmonary surfactant can act as an anti-glue in some amphibian and non-mammalian species (Daniels et al., 1995). The concept that surface-tension in the lungs is near 0 mN/m has been challenged, since arguments that an interfacial layer of molecules (in a compact solid state) above the surface of the alveolar fluid may abolish that interface, and thereby create an interface between air-solid surface above the alveolar fluid has been put forward (Bangham, 1987). The term surface

Figure 1.2 Diagram of a terminal air-space or alveoli with the surfactant lining film (top) and the possible lipid layered structures (multi-, bi- or mono- layers) found during the formation of the film (bottom) [The top figure was reproduced from Hawgood and Clements, 1990, ©The Rockefeller University Press, NY with permission of the authors and publisher.]

The type-II cells are involved in synthesis and secretion of pulmonary surfactant (top). The material is packaged in multi-bilayer lamellar bodies (LB, 4). After secretion into the alveolar fluid, the lamellar bodies transform into peculiar tube-like structures called tubular myelin (TM, 5). Tubular myelin is presumed to be the precursor of the surface active film (6) at the air-alveolar fluid interface. Some other vesicular structures such as small and large bilayer aggregates (7) may also be found in association with pulmonary surfactant extracted from alveolar fluid, and upon dynamic cycling of pulmonary surfactant at an air-water interface *in vitro*.

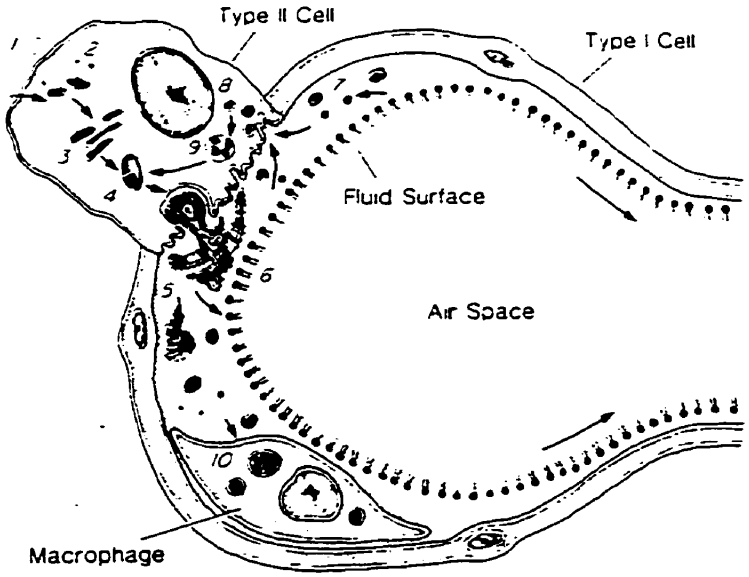
Type II Cell
Type I Cell
Fluid Surface
Air Space
Macrophage

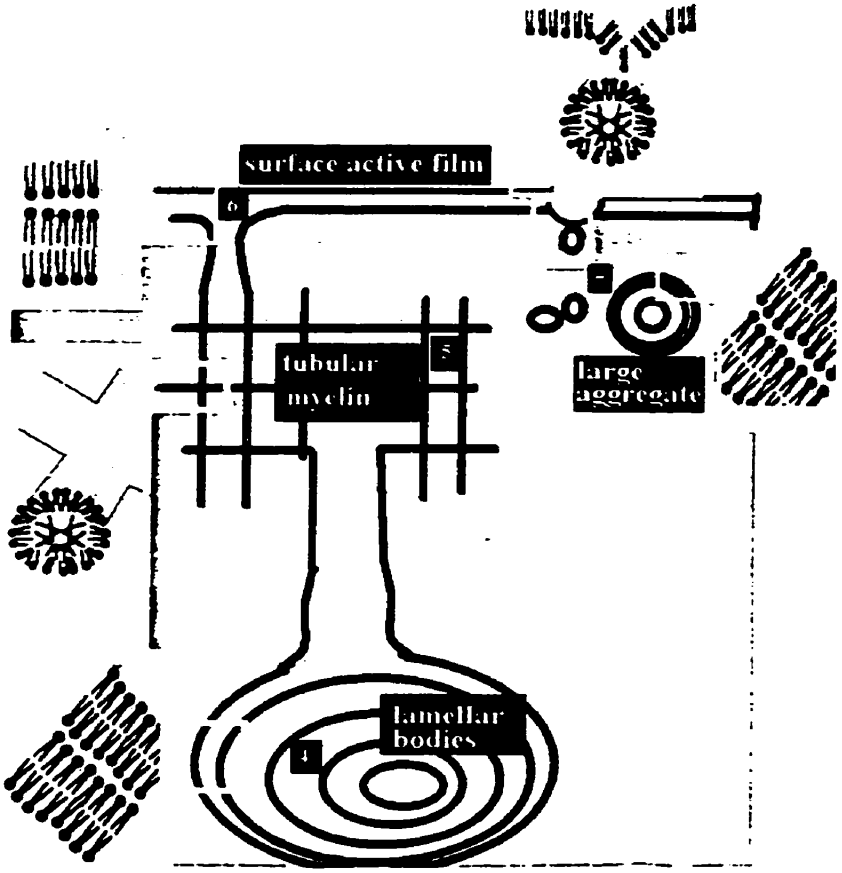
surface active film
tubular myelin
large aggregate
lamellar bodies

tension has been modified to surface pressure or π by surfactant researchers, or γ when discussing pulmonary surfactant films (Keough, 1992), although the term surface tension is frequently used by many (see Keough, 1992 for the arguments). Surface pressure (π) can be defined as the difference of surface tension (γ) of an interface with a film (γ_f) and without (γ_w) or $\pi = (\gamma_f - \gamma_w)$ [see chapter 2 for further discussion on surface pressure]. Also the Clements model describing the film lining the alveoli being open and exposed to air, or the two ends of the film ending at each alveoli (as shown in the Figure 1.2 A) has been debated, and suggestions have been made that the film may be closed or lines a spherical bubble in each alveolar unit (Scarpelli and Mautone, 1994).

1.3] Extracellular Transformations

Pulmonary surfactant is normally extracted from mammalian and other lungs by means of gently lavaging or washing out the lungs with a physiological saline. The extracted material is then centrifuged to separate surfactant from extracelluar debris and other materials associated with the lung fluid. Although the location of the synthesis and secretion of pulmonary surfactant has been well established to be the type - II pneumocyte (Figure 1.2 (A)), the lavaged material consists of various structures such as lamellar bodies, tubular myelin and vesicular aggregates, whose exact functions at the air-alveolar fluid interface are not completely clear. These structures are presumed to be pulmonary surfactant at the various levels of transformations in the alveoli to achieve surface active films at the air-alveolar fluid interface. Most of these "enigmatic", structural forms stain well with electron microscopic lipid stains, and are considered as

different forms or ranks of phospholipid molecules "arrayed shoulder to shoulder as in unit biological membranes" (Gross, 1995b). A general schematics of transformation of pulmonary surfactant from its secretory states, to its film formation, and then re-uptake at the air-alveolar fluid interface is shown in Figure 1.2 (bottom), and the direction of these processes shown by the arrows (top). The types of lipid layered structure, each of these forms are presumed to be in are shown in box of Figure 1.2 (bottom).

The extracelluar transformation (termed "metabolism") that these structures undergo has been proposed from localization of various surfactant lipids and proteins in the different lung cellular compartments and extracelluar regions. Lamellar bodies (LB), tubular myelin (TM) and some vesicular aggregates have been identified, with natural extracted pulmonary surfactant. Small and large aggregates (SA and LA) are mainly formed by *in vitro* compression-expansion cycling of pulmonary surfactant suspensions at an air-water interface, and are presumed to be structures formed during exchange of material between the interfacial films and the bulk phase. Typical electron micrographs of some of these structures, stained using electron-dense lipidic stains which identify individual unit bilayer membranes are shown in Figure 1.3 (Williams, 1992). The schematics of such transformations indicate that the main form secreted by type-II cells is lamellar bodies (LB). Lamellar bodies consist of multi-lamellated or concentric layered structures (Figure 1.3, A). The LB transforms at the air- alveolar interface into peculiar tube-like structures, called tubular myelin (TM, Figure 1.3 (B)). The TM is presumed to be the precursor of the surface active film which lines the alveoli (film discussed in next section). During dynamic cycling of the film at the air-alveolar fluid

Figure 1.3. Electron micrographs of lamellar bodies (A), tubular myelin (B), large aggregates (C) and small aggregates (D). Scale bar is 1 μm.

A) Lamellar bodies (LB) are multi-bilayer structures. Each of the single bilayers (dark lining) is arranged in concentric layers with probably a thin water layer between them. Some attached tubular myelin (TM) structures (square lattice, box) can also be seen in the top of the micrograph, and thus it is presumed that TM are formed by unfolding of the lamellas of LB.

B) Tubular myelin (TM) is formed by thin bilayer tubes (see Figure 1.2, B) crisscrossing each other in a square lattice. Each of the TM network is arranged on top of another, and can be seen by slight displacement of one network layer from the next in the micrograph. [Micrographs LB and TM were a generous gift from Dr. Mary C. Williams, of the Boston University School of Medicine].

C) Large aggregates (LA) and D) small aggregates (SA) are bilayer vesicular or liposomal structures. Small aggregates are formed (probably from LA) by dynamic cycling of pulmonary surfactant at an air-water interface *in vitro*. [The micrographs of LA and SA were reprinted from Veldhuizen et al., (1993), ©Biochemical Journal, Portland Press, UK, with kind permission of the authors and publisher]

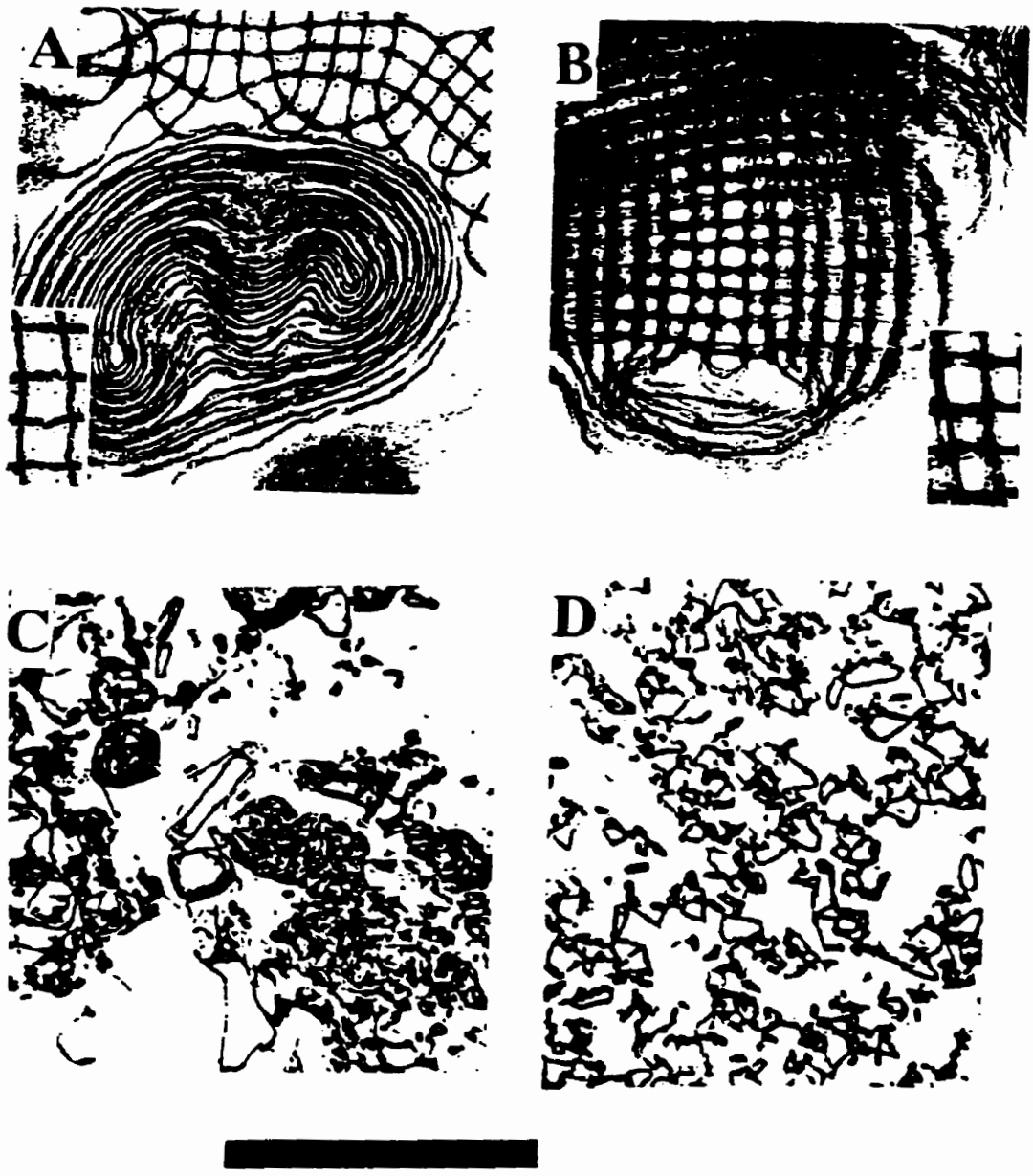
A
B
C
D

interface, or at an air-water interface *in vitro*, materials are probably squeezed out and adsorbed specifically into this film, to enrich the film with certain surfactant components. By dynamic cycling of pulmonary surfactant suspensions which contain mainly LB, TM and large aggregates (Figure 1.3, C) an increase in number of small aggregates (Figure 1.3,D) in the cycled suspensions can be observed (Gross, 1995a). It is presumed that such conversions are an indication of the material exchange between TM, film and bulk subphase (by squeeze out of materials from films), ultimately enriching the pulmonary surface active films with one component of PS over all the others (details of some of the process, discussed in the next section). The conversion of these various forms from LB to TM to film to LA/SA are dependent on particular components of the surfactant (not yet clearly identified), and the process is called "extracelluar metabolism of pulmonary surfactant" (Gross, 1995a). Recent studies although have indicated that the type and amounts of surfactant proteins present in some of these structural forms vary considerably.

Gross (1995a) has recently indicated that there may be an extracellular, yet unidentified, enzyme (they call serine protease) involved in conversion of these various structural forms (Gross and Schultz, 1992). These structures indicate that pulmonary surfactant seems to be an unusual biological material, which transforms "extracellularly" into multiple heterogenous and some atypical, structures (Gross and Naraine, 1989; Gross and Schultz, 1992). Most biological systems undergo transformations intra-cellularly and various metabolic biochemical pathways are involved. In the case of pulmonary surfactant, the extracellular material undergoes these transformations by

biophysical and biochemical mechanisms. Thus, comprehension of the processes involved in pulmonary surfactant transformations may be aided by biophysical studies of the material *in vitro* at an air-fluid interface by surface physico-chemical measurements. Although much is known about the biochemistry and intra-cellular metabolism of the pulmonary surfactant components, their main functional roles in "lining the alveoli with surface active films" are not yet fully clear. Also the composition and structure of the surfactant film in the alveoli is not yet known. The composition of the surface film *in situ* can also be understood from simple componential film studies *in vitro*. The main purpose of this thesis is to study surfactant *in vitro* at an air-water interface, using a recently developed biophysical technique of epifluorescence microscopy, which allows combining surface chemistry and micro-structural analysis of films surfactant and its component.

1.4] Nature of the Air-Alveolar Lining Film.

From the time of its discovery, until recently, the question which plagued PS researchers was, "Is there a thin film lining the air - alveolar fluid interface ?", since no direct demonstration of such a film could be made in the lungs. It was also not clear that the alveolar fluid lining the lung air-water interface is continuous or if the fluid exists in distinct pools at the corners of single alveoli. Early reports of the alveolar lining by traditional electron microscopy showed heterogenous "thin osmiophilic lining on a grey subphase" when aqueous glutaraldehyde fixation and osmium tetroxide (lipid-stain) staining of the alveoli were performed (Gil, 1985; Weibel and Gill, 1968). This

osmiophilic lining also had various phospholipid structures, broken bilayer vesicles and other lipidic or osmium staining structures floating on top of them (Gil, 1985). Attempts to isolate and stain pulmonary surfactant films *in situ*, were plagued by the fact that the alveolar-fluid lining the epithelial cells is extremely thin and possibly discontinuous, and if a film existed on such a fluid interface, it was too close to the epithelial cells to be discriminated from the normal bilayer membrane of epithelial cells by conventional electron microscopy. Schürch and Bachofen (1995) used a unique technique of perfusion of the lungs with fluid (edema) so that any interfacial layer existing between the lung epithelial cells and air would be lifted off the epithelial cellular lining by the extraneous fluids applied by perfusion. Using this technique they demonstrated the nature and structure of the pulmonary surfactant lining layer which is shown in Figure 1.4 (Schürch and Bachofen, 1995).

The layers (S) shown in Figure 1.4 (A) seemed on further examination (higher magnification, Figure 1.4, C) to be thicker than a single bilayer or a monolayer. They described the layer as "rather polymorphous or the lining layer covering the increased volume of the hypophase appeared to be made of amorphous materials, and at other sites, triple layers or even multilayers can be recognized " (Schürch and Bachofen, 1995). They explained the tri-layered structures as a monolayer on top of an underlying bilayer of lipids (see Figure 1.2, B), the bilayer probably acting as a pool or reservoir for the monolayer or film of surfactant. It is presumed that this bilayer pool replenishes the surface film of pulmonary surfactant with essential phospholipid components, which makes such films highly surface active. Also recently the question whether or not

Figure 1.4 Electron micrographs of the alveolar surfactant lining layer, and underlying alveolar cells and fluid are shown. The layers (S) were observed by lifting the material from the alveolar epithelial cells (Ef in A) towards the air by vascular perfusion of fluid (AH in B) in the alveolus. The lining layer was found to be thin and continuous, and had an average thickness of a trilayer (C), a monolayer on top of a bilayer. Scale bar is 1 μm. [From Schürch and Bachofen, 1995; reprinted with the permission of the author and publisher, ©Mercel Dekker Inc., NY]

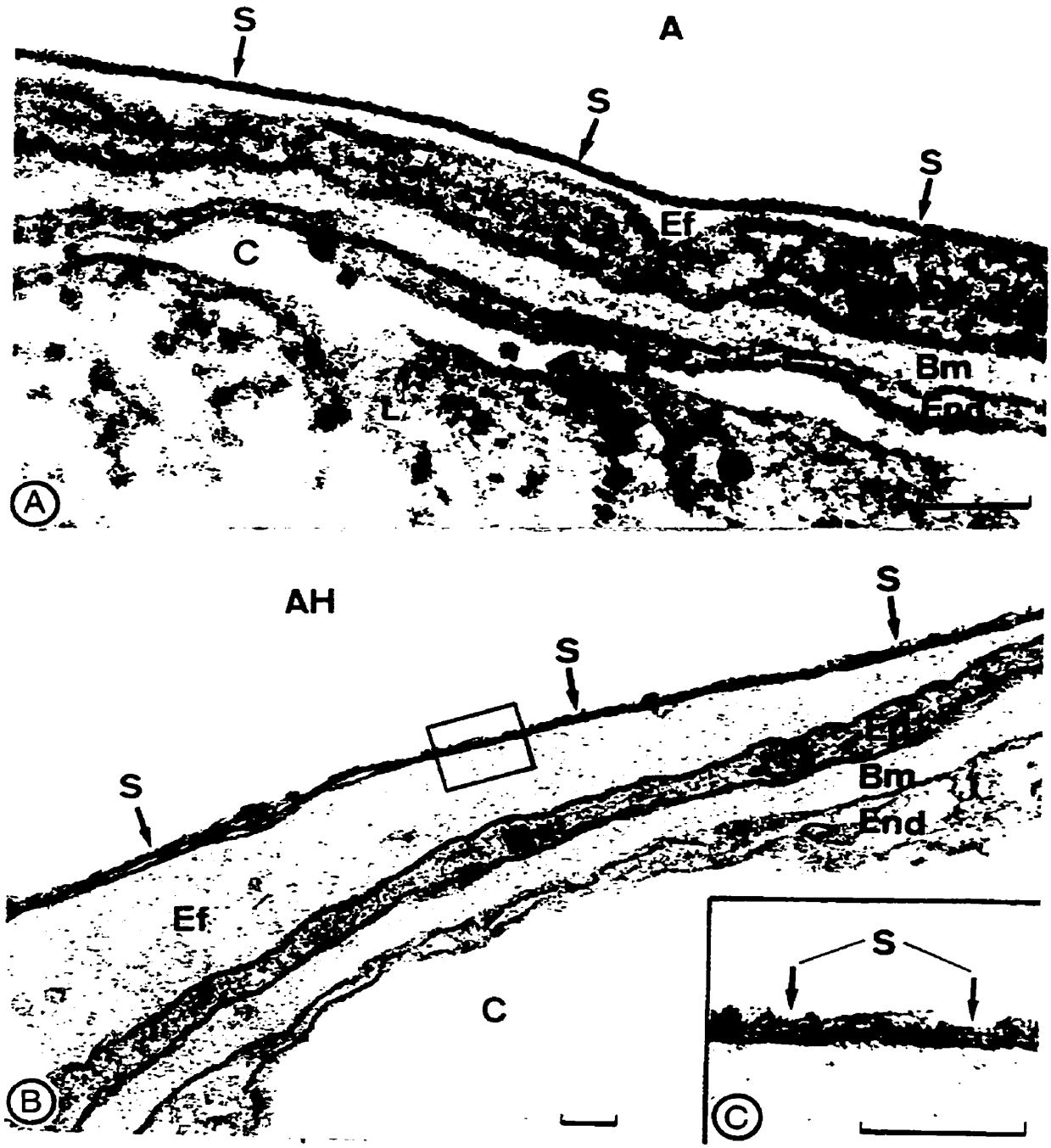
S
A
S
S
Ef
C
Bm
End
L
A
AH
S
S
S
Bm
End
Ef
C
B
S
C

normal alveoli are lined with a thin layer of alveolar fluid, on which such films or layers can form has been put to rest. Bastacky et al., (1995) using low temperature electron microscopy, (which preserves structures at liquid nitrogen temperature) demonstrated that the alveolar fluid layer appears continuous, submerging epithelial cells lining the alveoli. They determined that the thickness of the fluid layer was about 0.2 μm thick on average, and varied from a few nanometres to several micrometers from one alveolus to another (Bastacky et al., 1995).

Although the lining film of surfactant has been demonstrated, there are only few indications to date on the composition, nature and structure of the pulmonary surfactant film *in vivo*. It is also not clear whether the surface active film in the lungs contains all or some of the pulmonary surfactant components, or whether such components can be present in the surface film at low surface tension. We have examined the structure of such surfactant films (last chapter) and the association, interactions and presence of various components of pulmonary surfactant *in vitro* in films (Chapters 3-11).

1.5] Composition of Pulmonary Surfactant.

Pulmonary surfactant of various mammalian and vertebral species consists mainly of lipids and small amounts of protein. The lipid and protein composition of surfactant of humans is shown in table I (A). The lipids of most mammalian species consist of mainly phospholipid, such as phosphatidylcholine (PC), phosphatidylglycerol (PG), phosphatidylethanolamine (PE), phosphatidylserine and significant amounts of cholesterol among other neutral lipids (table 1, B). The proteins, although detected in pulmonary

surfactant two decades ago, have only recently been completely analyzed for their gene and structures, and have been termed as surfactant protein - A (SP-A), -B (SP-B), -C (SP-C) and -D (SP-D) in their chronological order of discovery (Possmayer, 1988). Although the surfactant associated proteins are only present in small amounts (5-10 weight % of surfactant lipids), they play important roles in assembly, secretion, transformation and surface activity of pulmonary surfactant, and some of the functional role these proteins play in the alveoli have recently begun to emerge.

Surfactant Lipids : In pulmonary surfactant of most species, about 75 % of the lipids are phospholipids, of which ~65% is phosphatidylcholine (Table 1., A) (Hawgood, 1991). The phosphatidylcholine (PC) species is about 45 % dipalmitoylated or has saturated 16 carbon palmitoyl chains in the sn-1 and sn-2 positions (16:0/16:0-PC) called dipalmitoylphosphatidylcholine or DPPC (Akino, 1992; Hawgood, 1991). Recently the amounts of DPPC in PS of calf has been re-estimated to be lower than the ones reported previously, that is DPPC constitutes about only 40 % of the total diacyl phosphatidylcholine species of surfactant, and therefor less than half of surfactant lipids (Kahn et al., 1995a; 1995b). The typical chain distribution of the other PC species in pulmonary surfactant is shown in table 1 (C) (Akino, 1992). Although DPPC is an unusual molecular species in most mammalian tissues, (since most tissue PC are 1-saturated, 2-unsaturated-PC, as in biological membranes), some DPPC is also present in small amounts in other tissues such as the brain. It is thus not specific for surfactant, as reported in some earlier publications, but its occurrence in such high amounts

TABLE 1.

(a) COMPOSITION.

*Composition of Pulmonary Surfactant	% by weight
LIPIDS	90-95
Phospholipid	75
Saturated phosphatidylcholine (DPPC)	45
Unsaturated phosphatidylcholine	20
Phosphatidylglycerol (PG)	8
Others (Phosphatidylethanolamine, phosphatidylinositol, phosphatidylserine)	5
Neutral lipids (Cholesterol, di-/tri-glycerides)	10
Other lipids (Fatty acids)	2
PROTEINS	5-10
Loosely associated (mainly serum)	2
Surfactant apoproteins (SP-A,SP-B,SP-C & SP-D)	5

* Modified from Hawgood, 1991

b) PHOSPHOLIPID COMPOSITION

# Species	% (by weight)
PC	82.3
PG	7.5
PE	6.1
PI	1.8
PS	0.1
Lyso-PC	0.3
Others	1.2

From, Akino (1992).

c) CHAIN DISTRIBUTION

# sn-1/sn-2	PC	PG
16:0/16:0	50.3	34.7
16:0/18:0	2.5	4.0
16:0/16:1	8.8	3.5
16:0/18:1	15.3	32.0
16:0/18:2	12.9	10.5

"ubiquitously" in surfactant is unique (Hawgood, 1991). Among other PC (table 1, C), monoenoic species such as palmitoyl-oleyl (16:0/18:1) and palmitoyl-pamitoleoyl (16:0/16:1), dienoic species like palmitoyl-linoleoyl (16:0/18:2), are also present in lung surfactant (Akino, 1992, Kahn et al., 1995b).

Phosphatidylglycerol (PG) is the major acidic lipid in the pulmonary surfactant of most adult mammalian species, but it is, however, absent in the PS of some animals such as Rhesus monkey. PG seems to be a specific constituent of pulmonary surfactant, especially in such high amounts, about 7 % by weight (table 1, B), as it is not found in any other mammalian tissue. This acidic phospholipid is only found in significant amounts in some bacterial membranes. The PG species in surfactant is present only in small amounts before birth as detected in the mothers amniotic fluid, and increases with the gestational age of fetus. Thus PG has become a clinical marker for analyzing fetal lung maturity and development, from analysis of amniotic fluid of surfactant phospholipids, since this fluid bathes the fetal lungs. Fetal pulmonary surfactant although low in PG, contains significant amounts of another acidic phospholipid, phosphatidylinositol (PI), which is almost completely replaced by PG after birth. With lung maturity after birth, PI levels in matured surfactant drops below 2 % (table 1, B) whereas PG increases to about 8-10 weight % in the surfactant phospholipid pool. Other phospholipids such as phosphadtidylserine and free fatty acids (palmitic acid) are also found in minor amounts in adult pulmonary surfactant. The PG species in the extracelluar components of pulmonary surfactant of adult rabbits contain mainly 16:0/16:0, followed by 16:0/18:1 and 16:1/18:2 species (Hayashi et al., 1990). Analysis

of human bronchio-alveolar lavage extracts indicated that PG consists of about 11.8 % of phospholipid by weight in normal individuals, whereas in patients with adult respiratory failure the level dropped to 0.3 % and in alveolar proteinosis to about 4 % (Hallman et al., 1982).

Cholesterol accounts for the largest amount of neutral lipids present in pulmonary surfactant (Yu et al., 1983). The amount of cholesterol expressed as percentage of total phospholipid varies among animal species, reaching as high as 30 % in Australian lung fish to as low as 7 % in humans (Daniels et al, 1995). The variation of some of the lipids in surfactant of various animals and their alteration in diseased conditions indicates that pulmonary surfactant lipid components have some definitive functional roles in normal lung functioning.

Other lipids such as phosphatidylethanolamine (PE), lyso-phosphatidylcholine (lyso-PC), tri- and di- acylglycerols are also found in pulmonary surfactant in minor amounts in various species, although their individual functional roles in surfactant are not well defined (Keough, 1992). Recently, pulmonary type-II cells responsible for secretion of all the surfactant components, were shown also to secrete vitamin-E (tocopherol) and some plamologens (ether-lipids) with the surfactant lipids, and these are regarded as constituents of pulmonary surfactant (Rüstow et al., 1993, 1994). The composition of pulmonary surfactant from different species and some of their roles in surfactant functions have been reviewed (Akino 1992; Daniels et al., 1995; Hawgood 1991). Discussion on the roles some of these lipids play in pulmonary surfactant are given in the chapters on unsaturated lipid (Chapter 3), phosphatidylglycerol (Chapter 4) and

cholesterol (Chapter 5).

Surfactant Proteins: Pulmonary surfactant contains small amounts of hydrophilic and hydrophobic proteins. Surfactant protein -A (SP-A) and -D (SP-D) are multimeric, glycoproteins, of monomer molecular weights around 30-45 kilo Dalton, and belong to the family of proteins which binds carbohydrates called collectins. Surfactant protein -B (SP-B) and -C (SP-C) are highly hydrophobic, smaller, 4-17 kDa proteins which can be extracted with organic solvents from lung lavage along with surfactant lipids. The tertiary structures and the relative sizes of SP-A, SP-B and SP-C are shown in Figure 1.5.

Native SP-A is a glycoprotein, found as an octadecamer (18 monomers) in surfactant (Figure 1.5, A), having an approximate molecular weight of 650 kDa. The protein has a long collagenous N-terminal region, a short neck, and a globular region (pink regions in Figure 1.5, A) containing some glycosylated residues near its C terminal. The protein binds lipids such as DPPC, calcium and carbohydrate. Some of these interactions allow for transformation of surfactant at the alveolar space to form surface active films. The protein has also been shown to have certain immune functions. Detailed structure-function relationship, sequence, synthesis and functional roles of SP-A in pulmonary surfactant are discussed in Chapter 10. Recently discovered SP-D is a glycoprotein, found in lung lavage, although its association with pulmonary surfactant lipids and its functional roles in surfactant is not clear.

Native SP-B is a hydrophobic 8.7 kDa (monomer), non glycosylated, disulphide

Figure 1.5 The secondary structures of surfactant proteins SP-A (A), SP-B (B) and SP-C (C) are shown. The relative size of each protein is shown in the left panel with the scale bar. [The Figure was a generous gift from Dr. J. Perez-Gil, University of Madrid, Spain].

The pink-red regions of SP-A (A) indicate the globular domains which are the glycosylated regions of the protein, and the inter-twined filamentous stretch is the collagenous domain.

The charged amphipathic helical regions in SP-B are shown by the positive charges (+++), and are presumed to give this hydrophobic protein slightly polar character compared to SP-C. The alpha helix of the SP-C is probably oriented with its axis parallel to the acyl chains in bilayer lipid membranes, and the 3 charged residues (+ signs) are thought to interact with polar solvents or lipid headgroups.

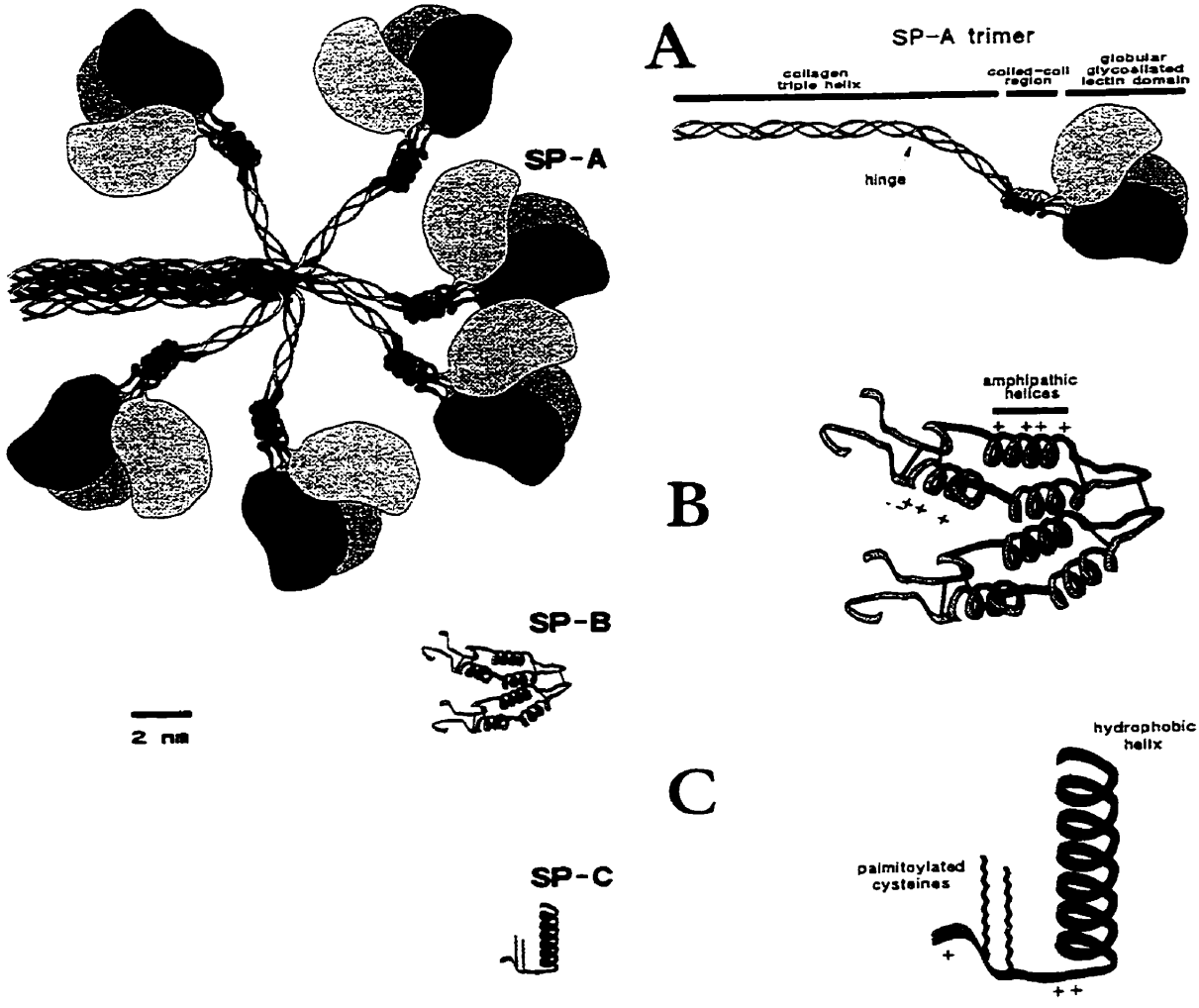
SP-A
SP-B
SP-C
2 nm
A
SP-A trimer
collagen triple helix
coiled-coil region
globular glycosilated lectin domain
hinge
B
amphipathic helices
C
hydrophobic helix
palmitoylated cysteines

linked dimer, having amphipathic helices distributed through out its sequence. The amphipathic helices are made of charged residues with an excess of positive charges (Figure 1.5 B, ++ signs) dispersed between the sequence of hydrophobic residues. Native SP-C is an acylated (dipalmitoylated), extremely hydrophobic, α-helical peptide of MW of 4.2 kDa, the acylation being at the cysteine residues near its N-terminal (Figure 1.5, C). The structure-function properties of SP-B and SP-C are discussed in details in chapter 6-9; although it should be mentioned here that the function of hydrophobic proteins is to enhance the surface activity of surfactant lipids.

The sequence describing some of the functional roles of the surfactant proteins, and the cellular compartments in the alveoli with which they are associated, are shown in Figure 1.6. The proteins are synthesized by the type-II pneumocytes, packaged with the lipids into lamellar bodies and secreted to the air-alveolar fluid interface. From *in vitro* experiments it can be demonstrated that SP-A and SP-B in combination with calcium ions transform bilayer lipids into tubular myelin (TM) (Williams, 1992), and TM is believed to form the surface active film by rapid adsorption of the surfactant lipids in combination with SP-C. SP-A also helps in the recycling of the materials from the surface film back into the type-II cells for reutilization and also in stimulating macrophages in the alveolar fluid to engulf viral and bacterial particles.

1.6] Fluidity and Dysfunctions.

DPPC is the only component of pulmonary surfactant, films of which at 37°C (body temperature of most mammalian species) can be packed or compressed to reduce

Figure 1.6 Schematics of synthesis, secretion and functional roles of pulmonary surfactant proteins, SP-A (A), SP-B (B) and SP-C (C). Abbreviations used are: LB-lamellar bodies; RER-rough endoplasmic reticulum; TM-tubular myelin; ERY-erythrocytes; AM-alveolar macrophage; MES-mesenchymal cells; Cap-capillary].

The type-II cells synthesize and secrete the proteins, which help in various transformations of pulmonary surfactant to ultimately achieve a surface active film lining the air-alveolar fluid interface. The + and - signs indicate whether each of the proteins are effective in performing certain processes *in vitro*, such as formation of tubular myelin (TM), macrophage stimulation to engulf viruses or bacteria. The arrows indicate pathways of secretion and recycling of the proteins associated with pulmonary surfactant lipidic structures. Note that none of the proteins are shown in association or interacting with the surface active film, since whether this occurs *in situ* is not clear to date. [From Van Golde et al., (1994) reprinted with the kind permission of the author and publisher, © American Physiological Society, MD]

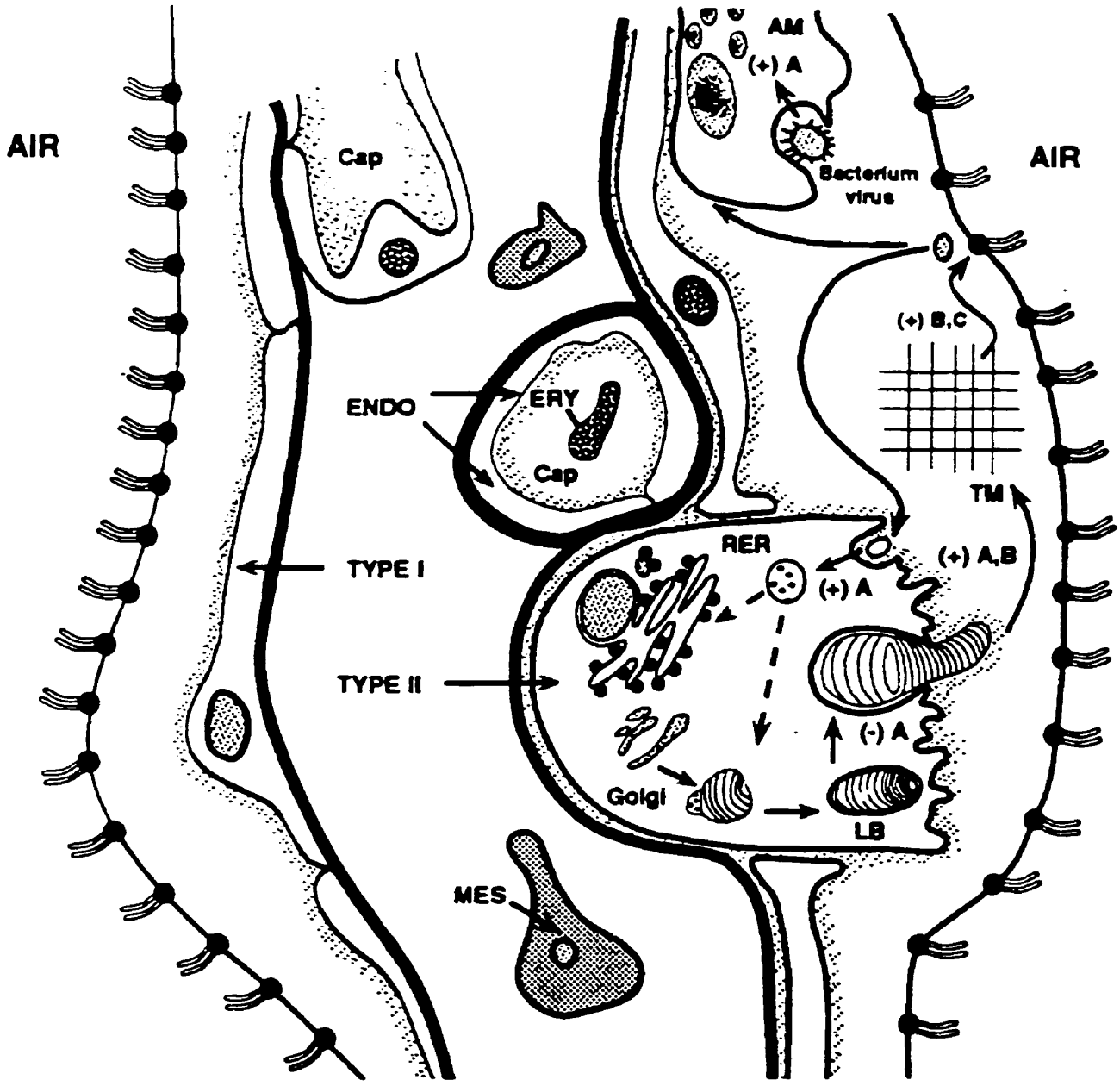
AIR
Cap
AM
(+) A
Bacterium virus
AIR
(+) B,C
ENDO
ERY
Cap
TM
RER
(+) A,B
TYPE I
(+) A
TYPE II
(-) A
Golgi
LB
MES

the surface tension of an air-water interface to near 0 mN/m. None of the other component lipids or proteins of surfactant in films can achieve such low surface tension. Films of these components readily collapse at lower surface pressures or higher surface tensions upon compression. It is presumed that, by a process of selective exclusion of other components such as unsaturated lipids or selective insertion of DPPC in to the alveolar surface films, or both, pulmonary surfactant films are enriched with DPPC or the lipid having rigid acyl chains. DPPC has poor adsorptivity and spreadability, properties which are detrimental to the surface activity of PS. Spreadability and adsorptivity of DPPC at an air-water interface are enhanced by addition of small amounts of other surfactant lipids or proteins. The unsaturated lipids, cholesterol, and the hydrophobic SP-B and SP-C can enhance the surface activity of DPPC, by enhancing the fluidizing of the phospholipid in bilayers. Thus it is presumed that there is a delicate balance between rigid and fluid lipids in pulmonary surfactant for optimal surface activity of the material.

Lau and Keough (1981) recognized that cold acclimatized turtles had higher unsaturated lipids in their PS than control animals kept at higher temperatures. Later Daniels et al., (1990) observed that the amount of surfactant cholesterol increased with decreasing body temperatures in lizards acclimatized to different temperatures. Also PS from lung fish and amphibians which maintain low body temperatures, have higher cholesterol to disaturated PC ratios (cholesterol being about 20-30 % of the lipids) compared to mammals and reptiles living at higher body temperatures (Daniels et al., 1995). From these studies there is some indication that PS composition in various

species is probably delicately controlled depending on the surrounding or environmental temperature of the species. Thus it was suggested, that PS control its rigid and fluid lipids, according to the thermal environment in which it is required to function (Daniels et al., 1995; Lau and Keough, 1981). By increasing cholesterol and fluid lipid content, animals living at low temperature would fluidize the rigid lipid to increase maximal absorption and spreadability whereas they also might require less DPPC for to reduce the surface tension of the air-alveolar fluid interface (Daniels et al., 1995; Lau and Keough, 1981). Animals living at higher temperature, would not require as much fluidizing lipids since the amounts present in PS makes it exist in an almost fluid state because the rigid chain phospholipid DPPC, is very close to its chain melting temperature (see chapter 3 for a discussion on rigid and fluid chains). This control of the composition of biological systems for optimal performance is termed "homioviscous adaptation", or adaptation of fluidity of membranes or other systems by producing or reducing one type of fluid or rigid molecules (Hadley, 1985).

Also the composition of PS and presumably its fluidity is altered in surfactant related diseases such as respiratory diseases syndrome (RDS), and adult respiratory distress syndrome (ARDS). The total saturated PC content of patients with idiopathic lung diseases, is about 80 % less than that in normal human lungs (Günther et al., 1995). Avery and Mead, (1959) detected that PS from lungs of neonates with RDS showed altered surface activity, and others have shown that the pulmonary surfactant of such patients had lower PG content compared to the ones from normal individuals (Hallman and Gluck, 1982). There are consistent reports in the literature from several groups

indicating that PS of neonates with RDS had higher unsaturated PC/saturated-PC (DPPC) ratios compared to normal neonatal PS (reviewed by Keough, 1985), although the exact roles of the lipids in such disorders are unclear. Pulmonary surfactant proteins also play an important role in normal PS, since targeted disruption of surfactant protein genes, can induce respiratory distress. The lipid and protein components of PS, and the amounts in which they are produced, may have some significant roles for optimal surface activity of the material at the air-alveolar fluid interface. Fluidity of the material seems to be an important criterion for PS function or dysfunction, and understanding the fluidity of the films of DPPC in combination with other PS components are one of the major focus of this thesis. Further discussion of the possible fluidizing roles of unsaturated lipids, cholesterol and the proteins play in PS are discussed in chapters 3-10, and that of porcine pulmonary surfactant extracts in chapter 11.

Chapter 2.

BIOLOGICAL MEMBRANE

2.1] The Bilayer Membrane

The story of the discovery that biological membranes are phospholipid bilayers dates back to the early part of this century, and is interesting in its connections to monolayer films (Cadenhead, 1985). As early as 1925, Gorter and Grendel, performed seminal experiments which led to our understanding of the biological membrane as being a lipid bilayer, or two monolayers with the molecules in the layers having their hydrophobic parts facing each other. These workers extracted lipids from red blood cells and studied these lipids by spreading the molecules in monomolecular films at a fixed area air-water interface (Gorter and Grendel, 1925). From measurement of the areas occupied by the lipid molecules, they computed the area of the erythrocyte as half of that of the closely packed lipid films, and indicated for the first time that the lipids were packed into two layers in the plasma membrane of the blood cells (Gorter and Grendal, 1925). Their calculations of the lipid bilayer areas were slightly flawed, since they could not take into account the presence of proteins in biological membrane. With the advent of electron microscopy, the models of the biomembrane were modified as a lipid bilayer containing proteins embedded in the lipid matrix, and the proteins could be observed as dotted, globular structures on the surface of one or the other monolayer or leaflet of the membranes. Spectroscopic studies of biomembranes showed that some of the proteins embedded in the interior of the bilayer were α-helical and non-polar (Leonard and Singer, 1966). From such accumulating evidence, Singer and Nicholson (1972) proposed the "fluid mosaic model" of the biological membrane. This model, suggests that biomembranes are dynamic structure where lipids and proteins diffuse

Figure 2.1 Shows the typical molecular arrangements in biological membranes based on the fluid mosaic model (A), the molecular structure of a phospholipid bilayer (B) and a molecule (C). [(A) was reprinted from Bretscher, (1985) with permission from the author and publisher ©Scientific American, NY]

The phospholipid molecules (C) in a bilayer (B) have the polar headgroups located in water and the hydrophobic chains facing each other. The bilayer membrane (B) not only consists of phospholipids, but other lipids such as cholesterol and glycolipids (A). The proteins are of different varieties, including the transmembrane α-helical, glycosylated, globular and peripheral proteins (A). [Note: similarities of some of the structures of membrane proteins with those found in pulmonary surfactant, such as the alpha-helix one with SP-C in figure 1.5]. Some of the proteins embedded in the interior of the bilayer matrix have α-helical trans-membrane segments of non-polar residues, with the polar residues located near or outside the bilayer. Most of the proteins and lipids shown can diffuse laterally in the plane of the bilayer, but cannot traverse from one monolayer to the other.

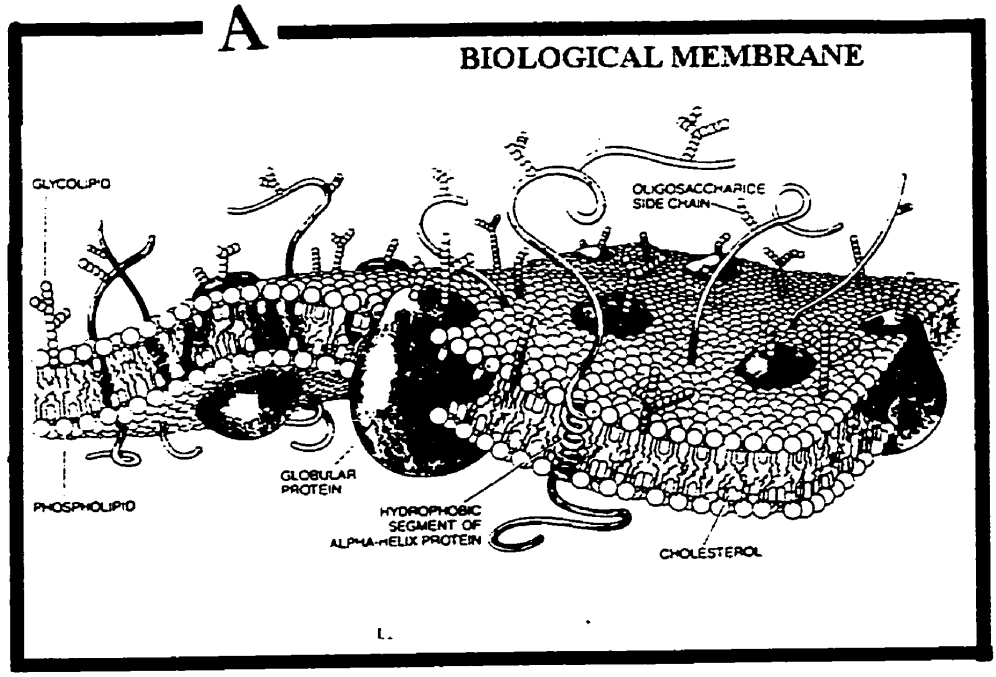
A
BIOLOGICAL MEMBRANE
GLYCOLIPID
OLIGOSACCHARIDE SIDE CHAIN
GLOBULAR PROTEIN
PHOSPHOLIPID
HYDROPHOBIC SEGMENT OF ALPHA-HELIX PROTEIN
CHOLESTEROL

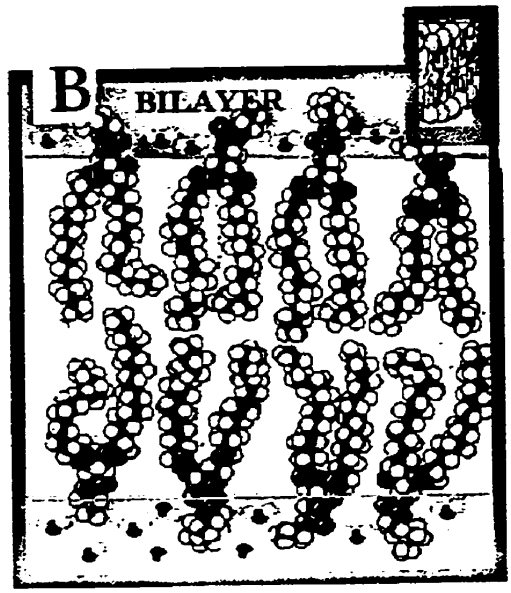
B
BILAYER

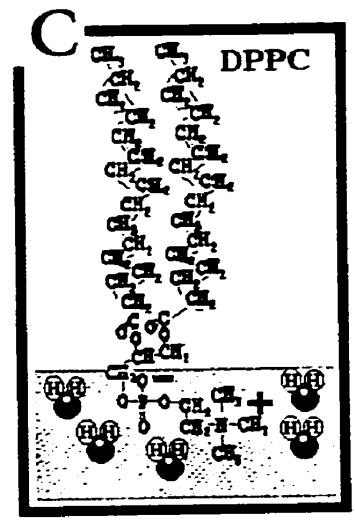
C
DPPC

around each other, in a fluid like environment (Singer and Nicholson, 1972).

2.2] Structure and Dynamics of the Biomembrane.

With the advent of some powerful biophysical and physico-chemical techniques the structure and dynamic properties of the biomembranes have somewhat emerged. Various studies of model membrane such as liposomes, black lipid membranes, planar bilayer, and monolayers at the air-water interface have led to our current understanding of the molecular structures and organization of the biological membrane.

Nuclear magnetic resonance (NMR) spectroscopic studies on mouse fibroblasts have shown that, the phosphatidylcholine (PC) and phosphatidylethanolamine (PE) phospholipid headgroups are oriented parallel to the membrane surface (Scherer and Seelig, 1987). The headgroup of phosphatidylglycerol (PG), an important constituent of *E. coli* membrane, was shown to orient about 30° from the membrane plane in such a way that the charged headgroups are accessible to divalent or monovalent cations (Mischel et al., 1987). Electron spin resonance (ESR) studies using probes indicated that water is able to partially penetrate the hydrocarbon core of the lipid bilayer in the liquid crystalline phase or when the lipids are loosely packed (Griffith et al,. 1974). Neutron diffraction methods indicated, that water penetration does not extend very far beyond the glycerol backbone of the polar groups, when the lipids are in the gel or closely packed phase (Worcester and Franks, 1976).

The *E. coli* membrane lipids, PG and PE were shown by NMR to contain a primary hydration shell of 11-16 water molecules (Boyle and Seelig, 1983). Due to this

hydration shell the lipids are fixed at their polar ends in water, and thus the bilayer structure can be maintained (Figure 2.1, B). The hydrocarbon chains of such a bilayer membrane are located facing each other, giving the membrane interior a hydrophobic environment. In most biological membranes the hydrocarbon chains of the phospholipids have one or more double bonds. Such double bonds introduce a permanent kink (see section I2.3) in the chains. When such molecules with chain kinks are packed in a bilayer, the inter-molecular mobility about the C-C bonds is high and the acyl chains can also undergo swinging motions near the kink region (Houslay and Stanley, 1983). The motions of the phospholipid chains in bilayers, with their headgroups firmly embedded in the polar media, lead to distinct thermodynamic states or phases. Restrictions in acyl chain packing due to molecular motion and kinks, in the case of biological membranes leads to the distinct physical state of loosely packed phase called the L_α or liquid crystalline phase. When the temperature of such membranes is lowered to decrease the motion of the chains, a more tightly packed or condensed phase called the gel or L_β phase occurs. The arrangement of phospholipid in the gel and liquid crystalline phases are shown in Figure 2.2 (bottom). In the gel phase the lipid chains are not fully extended, but tilted at an angle to the plane of the bilayer (Houslay and Stanley, 1983). The L_α phase is what is usually thought of as representing the bulk of the lipids in biological membranes. The fast motions of the chains in the L_α phase about their C-C bonds lasting 10^{-9} seconds, also yield smaller kinks in the chains. Other motions of the chains such as flexing in directions shown by arrows Figure 2.2 (top box), lateral diffusion of the molecules in the plane of the bilayer, and change of orientation of the

headgroups or of the whole molecule are also possible in two dimensions (Figure 2.2, box, arrows).

2.3] Phase Transitions in Bilayers

Phospholipid molecules in bilayers, when fully hydrated, can undergo phase transitions due to alterations of temperature, pressure, ionic strength and pH of the environment of the layers. These phase transitions can be indirectly detected by heating or cooling a lipid bilayer from one phase to the other, and measuring the heat absorbed during the change of phase. Figure 2.2 shows the typical phase transition and molecular arrangement occurring in a bilayer of phospholipids, and a calorimetrically measured thermal absorbtion curve which is obtained during such a change of phase. The transition from the arrangement of the lipids in the left panel to that represented on right (Figure 2.2, bottom), is called the gel to liquid crystalline (L_α) phase transition. The point where the maximum heat is absorbed during such a change of phase is called the chain melting or transition temperature denoted by the sign Tc.

The L_α phase has been shown to have two-dimensional order in the headgroup regions but considerable disorder in the acyl chains, caused by the fast molecular motions excited in the higher thermal states of the phospholipid molecules in the bilayer. In the gel or L_β phase, the molecules are packed tightly together (due to reduction of thermal motion of the chains) and are highly ordered, corresponding to an all *trans* (Figure 2.2, top) configuration in the acyl chains, similar to the ones found for the lipid molecules in dry or dehydrated pure crystals. The all *trans* configuration allows the chains to be

Figure 2.2. Illustrates the possible molecular motions of phospholipid molecules (top) and the typical arrangement of the molecules in a bilayer in the gel or L_{β} (left) and liquid crystalline L_{α} or fluid phases (right). The molecular motions (arrow marks) can be detected by various techniques such as NMR, neutron-diffraction and ESR. [The bilayer molecular structures were reprinted from Robertson, (1983), with the kind permission of the author and publisher, ©Cambridge University Press, NY.]

The temperature - heat flow plot (bottom) represents the differential scanning calorimetrically (DSC) detectable enthalpy change during the gel to liquid crystalline phase transition, and the temperature where the phase change occurs (represented by the symbol Tc). The top panel indicates the *gauche*, *cis* and *trans* isomers of the chains of the phospholipid, and some of the isomerization may occur between the chains carbon-carbon bonds during the thermally induced (at Tc) phase transition.

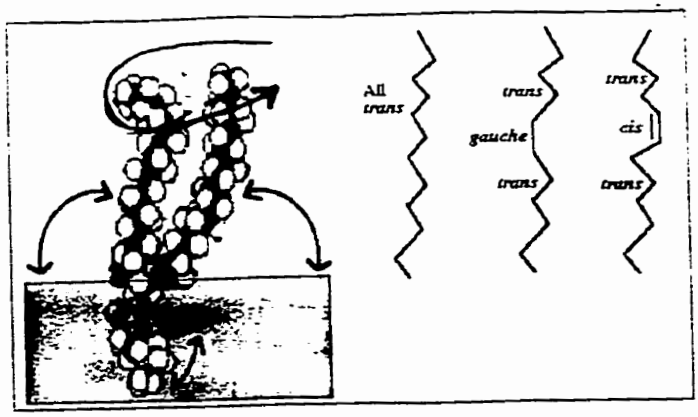
All trans
trans
gauche
trans
trans
cis
trans

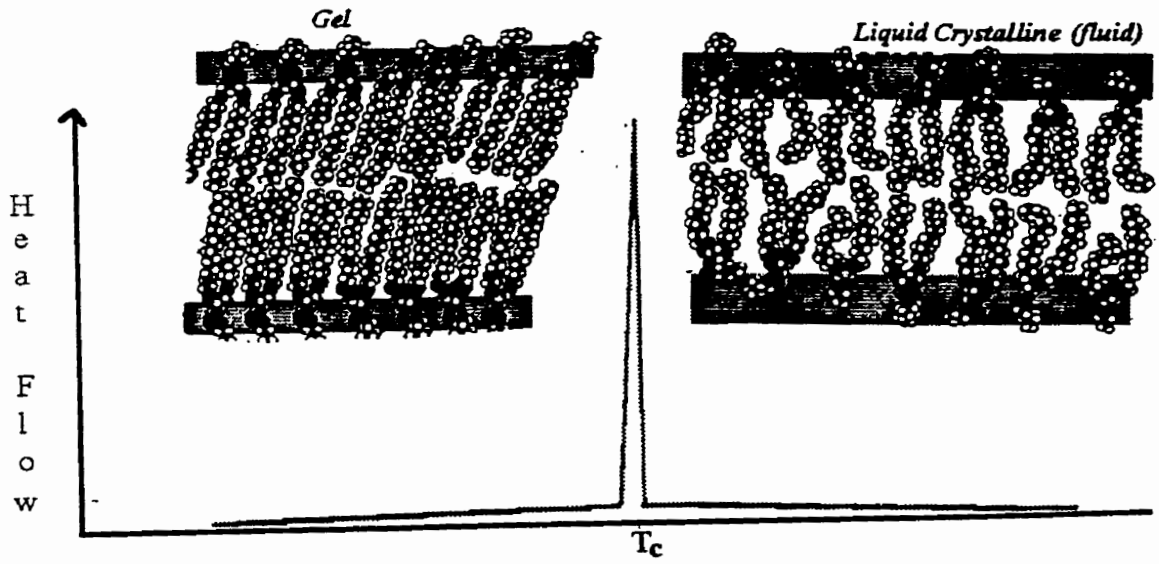
Gel
Liquid Crystalline (fluid)
Heat Flow
T_c
Temperature (°C)

maximally extended to the plane of the bilayer, whereas a *gauche* bond alters the direction or flexibility of the chains. Lipids in the liquid crystalline phase, possibly have a sequence of *trans-gauche-trans* arrangements for a C-C-C (3 carbon) bond length of the chain, resulting in kinks in the chain which effectively displace the portions of the chains above and below the *gauche* bonds (Figure 2.2, top) (Houslay and Stanley, 1983). Almost all double bonds found in phospholipids of biological membranes are *cis*, and introduce the same kind of change of direction in the chain as the *trans-gauche-trans* configuration (Gennis, 1989).

NMR studies on fully hydrated DPPC bilayers indicate that the thickness of the hydrocarbon or chain region is about 35 Angstroms (an angstrom unit or Å $=10^{-10}$ meters) in the liquid crystalline phase (Seelig and Seelig, 1980). If such DPPC chains were in the all-*trans* configuration, simple molecular dimensions or length of the molecule would give the bilayer a thickness of 45 Å, thus indicating that the chains of DPPC in the liquid crysttaline phase have different oreintation with regard to the bilayer plane, providing for the smaller thickness. The minimal cross sectional area per molecule of a diacyl phospholipid like DPPC is about 38 $Å^2$ and the chains tilted by an angle of about 30° in the gel phase would effectively increase the cross-sectional area to be compatible with that of the headgroup (Hauser et al., 1981). In the liquid crystalline phase the introduction of the *gauche* configuration increases the effective chain conformational or cross-sectional area to 50 $Å^2$ (the molecules occupy more area as shown in Figure 2.2, bottom). The effective liquid crystalline molecular areas for most diacylated phospholipids are typically in the range of 60 to 70 $Å^2$ (Gennis, 1985; Hauser

et. al., 1981). Some of cross-sectional areas of the phospholipid molecules in bilayers also can be measured by appraising the packing changes of the molecules after simply spreading them at an air-water interface in films, indicating the beauty of monolayers as models for studying biological membrane structures (Cadenhead, 1985).

2.4] Domains in Biomembranes

Due to the heterogenous composition of biological membranes, the lipids or proteins may be regionalized, or organized, into domains. The separation of the membrane lipids into compositional domains or lateral phase separation, can be due to demixing of one type of lipid with the other within a single phase or interaction of lipids with integral or peripheral proteins (Welti and Glaser, 1995). There is a large body of evidence to suggest that there are transverse and lateral regionalization of lipids or proteins or both, either in one or both leaflets (monolayers) of the bilayer, which are termed as micro- or macro- domains of membranes (Tocanne et al., 1994).

Over the last two decades structural models of the gel to liquid crystalline phase transition have predicted the co-existence of domains in bilayer membranes (Houslay and Stanley, 1983; Lee 1977). The structural model of phase transitions in gel state bilayers from various studies tend to suggest that, as the temperature approaches that of the gel to liquid crystalline phase transition (Tc), small pools of fluid lipid may form at certain regions of the gel phase (nucleation sites or areas where the lipids are slightly disorganized). These pools of fluid lipid can be essentially contained by the overall ordered lattice of the gel phase, and hence both fluid and gel phase lipid can co-exist in

the same bilayer (Houslay and Stanley, 1983). The size of these fluid pools increases as the temperature rises, leading to their coalescence or fusion, which would transform the lipids from some gel to all fluid phase in the bilayer. This event or phase transition would likely be co-operative, or of the first order, meaning one phase would grow at the expense of the other. The reverse can also occur when the fluid phase is cooled down from above its Tc. This would occur as the temperature of the fluid phase approaches the Tc of the lipids, when formation of clusters or islands of gel phase lipids would occur. The packing of the gel phase clusters may be irregular or the phase may have packing defects. Such defects may act as nucleation sites for the fluid phase, when the phase transition occurs in reversed direction (Housley and Stanley, 1983; Lee 1977).

These domains in one component lipid bilayers have never been directly observed by microscopy (during phase transitions), probably due to the small size of the domains, and the relative speed of the transition being very rapid or the co-existence of the phases occurring over very short time scale (Sankaram et al., 1992). Domain like structures in two-phase, two-component lipid bilayers have been demonstrated by electron microscopy almost two decades ago (Luna and McConnell, 1978). These workers indicated that in mixtures of DMPC/DPPC (4:1, mol/mol) band-like structure (domains) could be observed in a smooth background, when the temperature of the system approached 35°C. These domains (of one or the other lipid) or phase separation was observed since the molecules of one type of lipids in the DPPC/DMPC bilayers segregated out into these band like domains from the other lipids as the Tc of one of the lipids were approached (Luna and McConnell, 1978). By indirect measurements and studies of two component

or two phase lipid bilayers, others have also indicated the existence of domains or segregated structures in such systems (Hui, 1981; Sankaram et al., 1992; reviewed by Welti and Glaser, 1994).

In two component lipid bilayers, measurements of fluorescence recovery after photobleaching (FRAP) have indicated that gel and fluid phase domains may co-exist, one phase can form isolated domains in a "sea" or matrix of the connected or continuous other phase (Vaz, et. al., 1989). Such domains may arise caused by many factors, such as strong lateral or in plane interactions between membrane components, interaction between the membrane components and cytoskeletal elements, and on addition and removal of certain components by vesicular transport, or by combination of all or some of these factors (Thompson et. al., 1992). The average size of such lipid domains may range from a few to several thousand nanometres (Rodger and Glaser, 1991; Sankaram et. al., 1992). ESR studies on model dimyristoyl/distearoyl -phophatidylcholine (DMPC/DSPC) bilayers have indicated that domains in one phase are disconnected, and the number of lipids per domain increases linearly from a fixed number of nucleation sites as the fraction of one phase changes cooperatively or at the expense of the other (Sankaram et. al., 1992). Domains in bilayers composed of two types of lipids can be detected with relative ease, since in such systems the demixing of one lipid with the other (due to chain length and headgroup differences), leads to the process of phase segregation. At a fixed temperature one lipid component may be in gel and the other in the fluid phase, leading to each component segregating or clustering into separate phases (Sankaram et. al., 1992). Such phase segregation can also occur in bilayers of neutral

lipids mixed with acidic ones, under the influence of divalent cations, since the cation can interact with the acidic lipids headgroup and aggregate such lipids from the neutral ones or demixing the lipids from one another into domains (Kinnunen et. al., 1994). Such phase segregation in bilayers containing charged lipids can occur also under the influence of oppositely charged proteins (Kinnunen et. al., 1994 for review).

Proteins can lead to microscopic lateral heterogeneity or domain formation in bilayer lipid membranes. Integral or trans-membrane α-helical proteins (which traverse the bilayer, Figure 2.2, A) can form domains, since there may be a hydrophobic mismatch of the protein's hydrophobic (helix) length with that of the lipid bilayer or a perfect match with the lipids in the bilayer in a particular phase (Marsh, 1995). Spin label ESR measurement of the rotational diffusion of integral membrane proteins have indicated that the proteins are dissolved in the fluid phase and the lipids surrounding such proteins are motionally restricted (Marsh, 1995; Ryba and Marsh, 1992). Others have shown that binding of peripheral proteins to bilayer lipid headgroups led to re-organization of lipids in one leaflet of the bilayer or the other, depending from which direction the protein approaches the bilayer (Kinnunen et al., 1994; Tocanne et al., 1994). Using fluorescence microscopy of giant liposomal vesicles or bilayers, Glaser and co-workers have visually observed such lipid-protein domains, and have indicated that the domains can be as large as several micrometers (Haverstick and Glaser, 1987). They also indicated that domains can be formed either by divalent cations interacting with acidic lipid bilayers or by peripheral proteins such as cytochrome C with neutral lipid systems (Haverstick and Glaser, 1987, 1988; reviewed by Welti and Glaser, 1994). Such

domains were observed by inserting differently labelled fluorescent phospholipids in one leaflet of the bilayer or the other, and the segregation of one fluorescent lipid from the other, under the influence of proteins and cations (Haverstick and Glaser 1987; 1988; Welti and Glaser; 1994). The functional significance of such domains (induced in model lipid bilayers), or if such domains occur in biological membranes is not clear at present, although some speculations have been made (Davis et al., 1980, Marsh, 1995; Thompson et. al., 1992).

2.5] Monomolecular Films as Model Membranes.

"I propose to tell you of a real two - dimensional world in which phenomena occur that are analogous to those described in 'Flatland'"

Irving Langmuir, Nobel Prize in Chemistry (1932), [Langmuir (1936)].

Surfactants, most lipids, and some proteins are amphipathic molecules. Amphipathic molecules have charged or polar "water loving" groups, and hydrophobic, un-charged regions in the same molecule. When in contact with a hydrophilic-hydrophobic environment such as an air-water interface, amphipathic molecules orient themselves with the "water loving" group anchored in the polar medium (water) and the hydrophobic parts exposed to the non-polar medium (air). Such simple arrangements of amphipathic molecules were detected as early as fourth century BC by Aristotle who spoke on the subject of "spreading oil on troubled water" (quoted from Ullman, 1992). Later from the pioneering work of Lord Rayleigh, Agnes Pockels and Irving Langmuir

our understanding of the nature, physical properties and assembly of such molecules in films became more comprehensive (Reviewed by Gaines, 1966; 1995; Ullman, 1991). The amphipathic molecules, by such an arrangement at the air-water interface, formed ultra-thin, mono-molecular (one-molecule thick), surface active films termed today simply as thin films or monolayers. From several seminal works of Irving Langmuir (awarded the Nobel Prize in Chemistry, 1932), the properties of thin films of several amphipathic organic molecules were discovered. Later when such films could be transferred into solid substrates such as glass and mica, some powerful physical techniques were used to study them (Ullman, 1992). The technique of transferring thin films on to solid substrate was developed from the work of Kathryn B. Blodgett, and such transferred films are called Langmuir-Blodgett films (Blodgett and Langmuir, 1937).

Since lipids are amphipathic molecules, they easily form single molecular films at the air-water interface, and these layers are similar to the monolayer leaflets of biological membranes (mono- of the bi-layer membrane). An immense volume of work exists to date on studies of lipid films as models of biomembranes (reviewed by Birdi, 1989; Cadenhead, 1985; Ullman, 1992; 1995). Due to the simplicity with which such films can be formed and transferred, thin films have been used to study systems as diverse as synthetic optical-electronic devices, to perform molecular fabrication at nanometre scale (nanotechnology), and as models for colloids, emulsions, liquid crystals, surfactants, non-ionic detergents, polymers and pulmonary surfactants (Kuhn, 1989; Swalen et. al., 1987). The sheer volume of scientific work on and utilising thin films of organic molecules over the decades has led to specialized journals, such as Thin Solid

Films, Langmuir, Journal of Colloid and Interface Science, Colloids and Surfaces, and several textbooks on this area (i.e. Birdi 1989; Tredgold, 1994; Ullman, 1992; 1995). The study of structures of thin films of surfactant and liquid crystals at an interface, and our theoretical basis of understanding of the arrangements of molecules of liquid crystals has led to another recent Nobel prize in physics awarded to Pierre-Gilles DeGennes (DeGennes, 1991).

One of the earliest and a simplest way to measure properties of thin films was by measuring the surface tension (γ) of the air-water interface containing the film (surface activity of the material). The surface tension of an air-water interface can be detected by dipping a roughened platinum plate or paper, in the water, and measuring the force acting on the plate using a weighing balance (Adamson, 1990). Surface tension (γ) is defined as the force acting on molecules at the interface between two different materials i.e. air and water, and normally measured in units of dynes per centimetre (dyn/cm) or milliNewton per meter (mN/m). The interfacial surface tension of an air-water interface is about 72 mN/m at 22°C. When a film of material which resides at the interface is spread on such an interface, the surface tension of that interface decreases, or the force acting per unit length on a detector plate is reduced (for example the surface tension of water molecules at an air-water interface is reduced by a film since the amphipathic molecules of the films anchor at that interface). These interfacial surface forces in the presence of a film can also be represented in terms of surface pressure or π. For an air-water interface the surface tension of water (γ_w) subtracted from the surface tension of that interface with a film (γ_f) is equal to the surface pressure (π) of the film [π (mN/m)

$= \gamma_f - \gamma_w$ (mN/m)]. Further discussions on this matter can be found in a general textbook of physical chemistry (e.g. Adamson, 1990). The surface pressure can be measured directly as the force per unit of length along a barrier segment to hold the film in any given state of compression. With increasing density of the molecules or decrease in the film area, the surface pressure increases as an inverse function of molecular area of the amphipathic molecules, and at a fixed temperature, can be presented as surface pressure-area (π-A) isotherms. Figure 2.3 shows a typical surface pressure - area measuring device or surface balance (bottom), and the surface forces acting at an air-water interface with a film (top), indicating simple conceptualized models of γ and π. Surface pressure π is considered analogous to the three dimensional pressure (P) and the area of the film to volume (V) of molecules of an ideal gas. During compression of a gaseous system such as water vapour, the molecules can be compressed or condensed into a number of phases from gas to liquid to solid by decreasing the molecular motions or the energy of the system (i.e. water vapour to liquid water to ice). Analogously in thin films, by compressing the molecules in two-dimensions at a fixed temperature or increasing their surface-pressure or packing, phase transition of the molecules from one phase to another can also be achieved. The devices used for such measurements are called surface balances as shown in Figure 2.3. During compression of such films, the molecules exert an equal and opposite force on the barrier (Figure 2.3, top), which is the surface pressure (π) of the films (Adamson, 1990).

Figure 2.3 Shows the model of a modified Langmuir surface balance containing the air-water interface with a monomolecular layer of phospholipid with the surface forces (arrow marks) involved in surface tension (γ) and surface pressure (π) on such a surface (top); and the surface balance part of an epifluorescence microscopic surface balance used to observe film microstructure (bottom).

The plate in the water surface (top, shaded black) measures the force the surface tension exerts on it (downward pull, arrow), and this force can be measured in milligrams by a weighing balance (black bar) or pressure transducer (bottom). The barrier compresses the molecules laterally against the fixed walls of the container.

The water molecules at the surface have differential forces (thin arrows, top) exerted on them due to some parts of them being in contact with water proper and the rest with air, compared to the ones in the bulk. This results in a force or energy which attracts the surface water molecules towards the bulk, so that expansion of the surface requires energy or the surface is under tension. This forces the interface to be like a stretched film or under tension, and this surface tension can be measured as the force acting per unit length of a dipping plate. When molecules are placed on the water surface, these molecules decrease the surface tension by changing the forces involved in the surface water molecules (triple-arrows), and decrease the surface tension of the air-water interface. The lipid molecules when packed closely together exert an equal and opposite force on the barrier compressing them or to the fixed walls of the container, which can be measured as surface pressure (π). A detailed design of the epifluorescence microscopic surface balance is given in Figure 3.1.

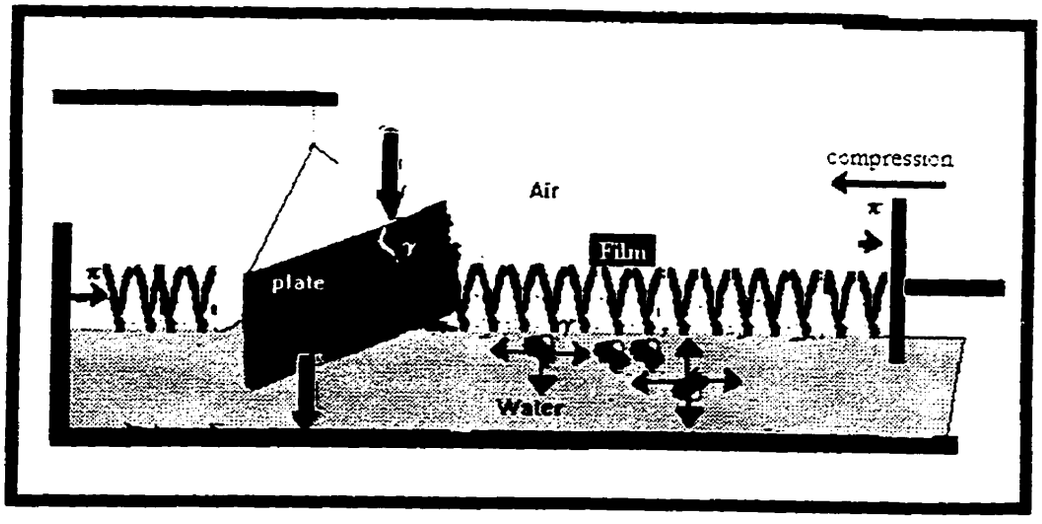
Air
compression
π
Film
plate
π
Water

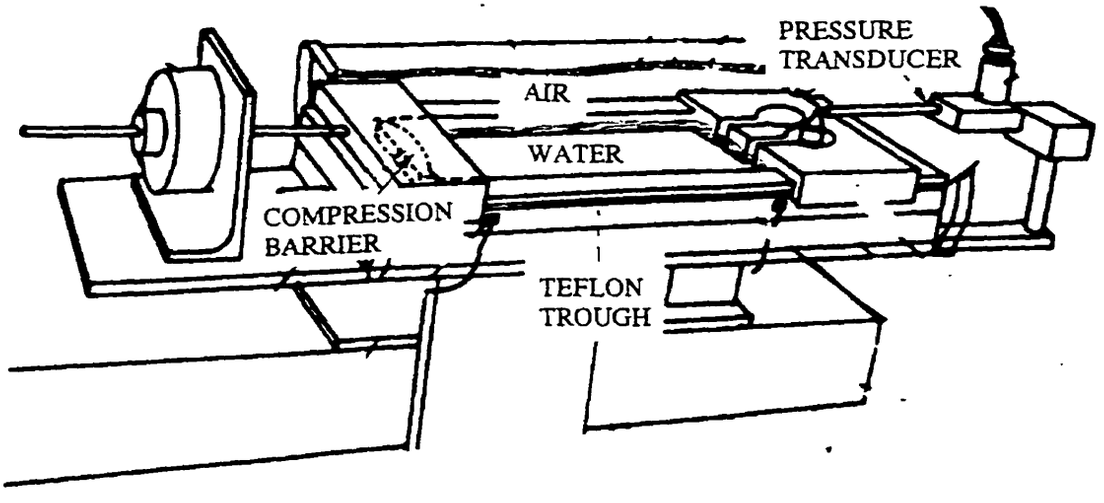
PRESSURE
TRANSDUCER
AIR
WATER
COMPRESSION
BARRIER
TEFLON
TROUGH

2.6] Phase Transition in Films

A typical surface pressure - area (π-A) isotherm of a film of phospholipid and the phospholipid packing and orientation at the air-water interface in different phases are shown in Figure 2.4. At very low packing density or surface pressure (or high area per molecule, indicated by ellipses in the Figure), the lipid chains are close to the plane of the air-water interface (panel A), the molecules are in a two dimensional gas phase (Cadenhead, 1985, Gaines, 1966). With increasing packing density or decreasing area per molecule, the chains are pushed into a more nearly perpendicular orientation to the plane of the interface (B), and as the surface pressure is increased above 0 mN/m (or γ < 72 mN/m), the molecules undergo a gas (G) to liquid expanded (LE) or fluid phase transition (panel B, C). With further packing and decrease of area per molecule (panel D) the surface pressure approaches a constant (break or plateau in the isotherm), the molecules become rigid and further extended, and undergoes transition into the liquid condensed (LC) or gel-like phase (Andelman et al., 1987). Further compression or decrease of molecular area leads to the molecules moving into an almost vertical orientation at the air-water interface, accompanied by a sharp increase of surface pressure leading the LC phase to transform into a solid-like or solid condensed (SC) phase (panel E). Further increase in packing from the end of SC phase is not permitted as the molecules reach their limiting area (or the area where one molecule would have to penetrate another to occupy the same space) and the monolayer or film collapses (C) at the air-water interface. This is seen as a plateau occurring at the high surface pressure end of the isotherms (C), where the surface pressure reaches about 72 mN/m for the

Figure 2.4 Typical packing arrangements of phospholipid molecules at the air-water interface undergoing phase transition from gas (G) to liquid expanded (LE) to liquid condensed (LC) to solid condensed phase (SC) (panels); and the typical surface pressure-molecular area isotherm observed from such transitions for DPPC are shown. The order of increasing pressure or decrease in molecular area is from the bottom panel (G) upwards. The ellipses indicate the area per molecule of the phospholipid in that particular phase. The arrow in the collapse (C) phase indicates expulsion of a molecule from the film at high packing state. In this phase (C) the monolayer is presumed to collapse or fold into multi-layers below or above the air-water interface.

The letters in the isotherm indicate surface pressures where each phase may co-exist with the next higher packed phase. The molecule in the left hand corner of each panel shows that some of the molecules in the phase co-existence region, may undergo conformations of the next higher packed phase. Using fluorescence microscopy the co-existence of such phases in phospholipid films can easily be observed by incorporating fluorescent probes which preferential partition in one phase but not the others (see next section).

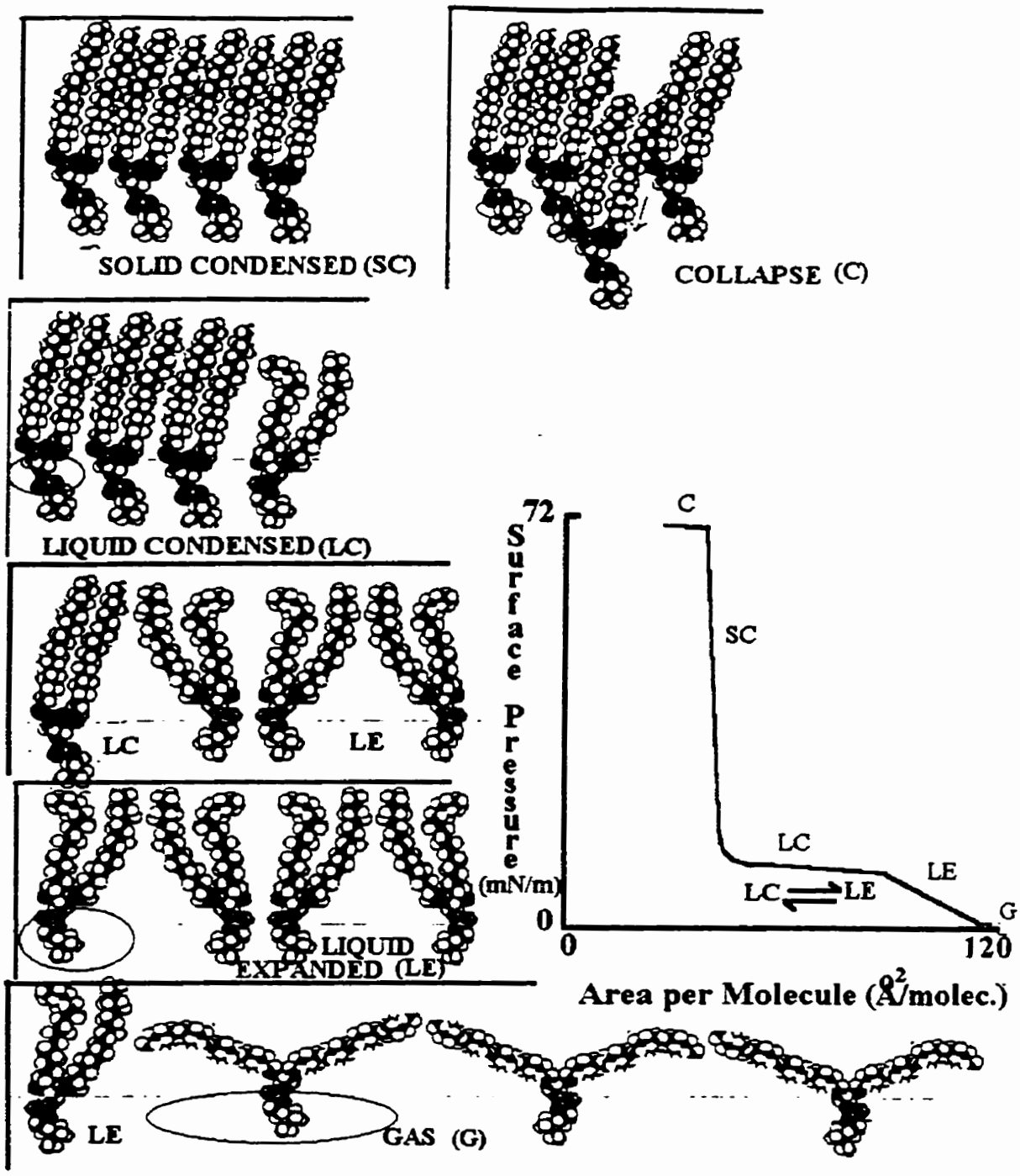
SOLID CONDENSED (SC)
COLLAPSE (C)
LIQUID CONDENSED (LC)
LC
LE
LIQUID EXPANDED (LE)
LE
GAS (G)
72
0
Surface Pressure (mN/m)
C
SC
LC
LE
LC ⇌ LE
G
0
120
Area per Molecule (Å²/molec.)

film, and the equivalent calculated surface tension of the interface approaches 0 mN/m. It has been argued that the surface pressure-surface tension relationship discussed above is not applicable for insoluble films (i.e. phospholipid films) which are at surface pressures above their "equilibrium surface pressure" (Bangham, 1987), which for most phospholipid molecules is about 45 mN/m. Others have suggested that for certain films such as those enriched in DPPC, which have long-term quasi stable properties up to collapse and appear to be in mechanical equilibrium over long time periods with the materials in the bulk phase, that the surface tension-surface pressure relationship may apply (Goerke, 1992; Keough, 1992).

At an ambient room temperature of 22°C or at the physiological temperature of most mammals (37°C), phosphatidylcholines with two saturated acyl chains of 16 carbons or higher undergo all these phase transitions. These transitions, except collapse, are reversible. The phase transition of such phospholipids from the liquid condensed to liquid expanded phase in films, is related to their chain melting transition in bilayers. By increasing the temperature of such lipids in films above their Tc, the LE-LC transition can be abolished, and such films are fluid or liquid expanded at all surface pressures up to the point of film collapse. The temperature where all the chains of the phospholipids in such films become fluid (at all states of packing) is called the critical point. This temperature (critical point) where this occurrs is the same as the lipids calorimetrically detectable gel to fluid phase transition temperatures (Tc) in bilayer. The liquid expanded (fluid) to liquid condensed (gel-like) phase transition in phospholipid films has been reported to be of the first order, like the fluid to gel transition in bilayers

(Andelman et al., 1987). The transition from LC (gel-like) to LE (fluid) phase is accompanied by increase in the number of *gauche* conformers of the hydrocarbon chain, due to each part of the chain passing from low energy to a high energy state (Georgallas and Pink, 1982; Pink, 1984). Others have compared the LC to LE transition of DPPC to the bilayer gel to fluid transition by comparing the area occupied by the molecules in the respective phases (Phillips and Chapman 1968). They recognized that below the main bilayer phase transition temperature of DPPC (Tc = 41°C) at a fixed surface pressure of 20 mN/m (presumed to be the surface pressure of the bilayer), the molecule occupied an area of 48 $Å^2$, indicating that the LC state in monolayers approximated the gel state in bilayers. In the LE state the molecules occupied a higher area compared to those in the LC phase, which was close to the molecular area in the bilayer of the phospholipid in liquid crystalline (L_α) or fluid phase (Phillips and Chapman, 1968). Peters and Beck, (1983) measured the translational diffusion of lipid probes in monolayers in the LE phase, and reported values close to the ones obtained for the same lipid in the fluid phase in bilayers. Small differences between the bilayer and monolayer molecular diffusional rates were noted, and were explained to be due to molecular density fluctuations occurring in monolayers phases or as one phase underwent transition to the other (Peters and Beck, 1983), and such density fluctuations were experimentally detected by others in films (Andelman et al., 1987; Galla et.al., 1979; Träuble and Sackmann, 1972). Although there is considerable debate on the analogy of the gel-like LC phase in films and the gel phase (L_β) in bilayers, and the equivalence of pressure in the bilayer and monolayers or the compressibility of one system versus the other, at least

the thermally induced changes in both systems are somewhat analogous (Andelman et al., 1987; Andelman and DeGennes, 1988; Cadenhead, 1985).

The LE to LC transition plateau of the of phospholipids like DPPC in films occurs at higher pressure with increasing temperature, and is finally abolished at the tri-critical point, where all chains of the phospholipid becomes fluid or liquid expanded (Albrecht et al., 1978). Bilayers of saturated phospholipid with increasing chain length from 14 carbon (DMPC) to 16 (DPPC) show an almost 18°C shift of Tc (individual Tc for DMPC is 24°C and DPPC 42°C) and the tri-critical point of these phospholipids are also shifted by similar amounts (Albrecht et al., 1978; Blume, 1979). Small differences between mono- and bi -layer phase transition may arise, since bilayers have curvature different from the flat or planar monolayers. Since the phospholipid molecules in the bilayer are localized in a spherical arrangement (in each of the leaflets of a liposome) compared to their more planar arrangements in films, the diffusional and other motions of the molecules in the bilayers can be different from those in the film (Cadenhead, 1985). Recently developed techniques such as atomic force microscopy, X-ray diffraction, neutron scattering, and some spectroscopic methods have allowed for detailed analysis of the phase transitions in films and allow for further examination of the bilayer-monolayer debate (Ullman, 1991; 1995).

The phase transition from LC to solid condensed (SC) phase is more complicated to comprehend, since this transition is continuous compared to the simple cooperative LE-LC transition. The LC to SC transition is probably a continuous phase transition since the discontinuity or break in the plateau of the isotherm between these two phases

(Figure 2.4, LC to SC) of DPPC, is not very sharp. This lack of sharp breaks or kinks in the isotherm indicates that the phase change occurring from LC to SC is continuous and no distinction between the phase depleted and the phase formed can be easily made. Controversy regarding the order of the LC to SC transition was raised due to reports indicating that the region of the isotherms between LC and SC phase is not sharp (at least for DPPC films), because of minor contaminants and methods used to spread such lipids in the surface, and is an experimental artifact (Hifeda and Rayfield, 1992; Nagle, 1980; Pallas and Pethica, 1985). By spreading DPPC from solid crystals after meticulous purification, Pallas and Pethica, (1985) reported a more discontinuous or sharper break in the isotherms between the LC and SC phase, and stated that this transition is actually of first order, as others have also recently reported (Hifeda and Rayfield, 1992). Recent reports indicate that the LC to SC transition occurs with gradual dehydration of the lipid headgroup and small changes in orientation of the glycerol backbone relative to the plane of the air-water interface (Brumm et al., 1994; Denicourt et al., 1994).

The discussion here is mainly focused on DPPC films and the phase transitions which can occur in them, since DPPC is the main phospholipid component of pulmonary surfactant and mainly this lipid was studied in combination with all other surfactant components (as discussed in the following chapters). Nevertheless it should be mentioned here that all or some of these phase transitions can also occur in films of other lipids. At room temperature cholesterol films exhibit only a gas to solid transition, and unsaturated lipids a gas to liquid expanded transition (no LC or SC phase). The differences in the phase transitions of such lipids compared to DPPC occur mainly due

to differences in their molecular structure, orientation and hence the packing of such amphiphiles at the air - water interface. It is not clear at present what the exact molecular conformations of the amphiphiles are in the very low density gas (G) and the high surface pressure collapse (C) phases.

2.7] Observing "Phenomena (or Alice !) in Flatland"

From the time of discovery of thin films, numerous attempts have been made to directly observe by eye amphiphilic films at the air-water interface. Perhaps the Japanese printers had seen such films a thousand years ago, when they reported observing oily coloured patterns floating on top of chinese ink suspensions (Kuhn, 1989). Over the last six decades numerous attempts have been made to observe the air-water interface containing films, such as observing motions of floating talcum powder, coloured dyes, floats, thin strings etc., placed in the films under different states of compression (Ullman, 1991). Although some of these attempts led to information about rigidity and viscosity of thin films under different compression states, no detailed information on micro-structures of thin films could be obtained.

Fifteen years ago for the first time, Von Tscharner and McConnell (1981) reported directly observing films of DPPC, and the LE to LC phase transition region of the films using fluorescence microscopy. They reported that the liquid expanded-liquid condensed (LE-LC) phase co-existence region of DPPC films was heterogenous and had micro-structures. Peters and Beck (1983), while reporting the translational diffusion rates of fluorophores in phospholipid films, first published fluorescence micrographs

obtained from such films from the LE-LC regions of the isotherm. They reported for films of dimyristoyl phosphatidic acid (DMPA) the LE-LC region had "black patchy" areas in a "background sea" of fluorescently labelled phase (Peters and Beck, 1983). Around the same time Lösche and Möhwald (1984a) also published a complete description of the instrument called a fluorescence microscopic surface balance, which consisted of a modified Langmuir surface balance (Figure 2.3) attached to a fluorescence microscope. Utilizing this instrument they observed most of the phase transition regions of a phospholipid film using various fluorophores, and published detailed images of such films (Lösche and Möhwald, 1984a). The principle behind the technique was simple, the various phospholipid phases in films were observed by incorporating small amounts of fluorophore-labelled lipids in the films, since such labelled-lipids (fluorescent probes) would preferentially partition in one phase and not the others, giving high contrast images from different regions of the films when observed by fluorescence microscopy. In this technique the objective of the fluorescence microscope was brought very close to the air-water interface for film observation, either from the bottom through the subphase water (Lösche and Möhwald, 1984a; 1984b) or from the top through air (Peters and Beck, 1983; Von Tscharner and McConnell, 1981). Other groups including ourselves constructed such balances to study thin films of materials of choice such as pulmonary surfactant (in our case), biological membranes, polymers and liquid crystals (reviewed by Knobler and Desai, 1992; McConnell, 1991; Möhwald, 1990; Seul and Andelman, 1995; Stine, 1994; Weis, 1991). The author constructed an epifluorescence microscopic surface balance for studies on pulmonary surfactant and its components earlier (the story

of "oils, toils and troubles" is told elsewhere in Nag, 1991, MS thesis and Nag et al., 1990). The term "epi" (in epifluorescence microscopy) means, the fluorophores in the films are excited and their emissions observed visually using the same microscope objective. Recently this technique has been refined to a point where single fluorophore molecules in phospholipid films can be detected, using laser piping through optical fibres to excite the fluorophores, and the technique is called near-field scanning optical microscopy (NSOM) (Hwang et al., 1995).

The typical images observed by epifluorescence microscopy of a DPPC film are shown in Figure 2.5. The films contained small amounts of fluorescent NBD labelled phospholipid probe 1-palmitoyl,2-nitrobenzoxadiazole-dodecanoyl phosphatidylcholine (NBD-PC) and were observed from above the air-water interface, at the surface pressures indicated in by the letters in the isotherm (A-F). The white regions in all images indicate the phase in which the fluorescent probe preferentially partitioned. The black region in image (A) represent the gas phase (G), and the white regions the liquid expanded (LE) or fluid phase. In images (C) to (F) the black regions represent the liquid condensed (LC) or gel-like phase and the white region the LE phase. The probe NBD-PC preferentially partitioned in the fluid or LE phase, giving contrast between the LC and the LE parts of the film images. The images of the DPPC film also indicate, that the LC domains had peculiar kidney bean shapes (Flörsheimer and Möhwald, 1989; Nag et al., 1991; Vanderlick and Möhwald, 1990; Weis and McConnell, 1985). The chain arrangements of DPPC in each phase are probably similar those shown in Figure 2.4.

Although fluorescence microscopy yields some qualitative information about the

Figure 2.5 Typical phase structures observed from DPPC films using epifluorescence microscopy. These structures are observed due to preferential partitioning of the fluorescent probe NBD-PC in the fluid or LE phase of the films (white regions). The surface pressure where the images were obtained are indicated in the isotherms by letters a-f. The symbols in the top right hand corner indicates the phase co-existence regions of the isotherms where such images were obtained. Scale bar is 25 μm.

The black regions in image (a) indicate the gas (G) phase in co-existence with the fluid or LE phase (white regions). The white regions in image (b) indicates the fluid or liquid expanded phase. The black regions in images (c) to (e) are liquid condensed (LC) or gel-like phase in coexistence with other phases, and in (f) SC phase in which the probe is trapped. Similar structures in pure lipid films have been observed using Brewster angle, surface plasmon and atomic force microscopy which do not require fluorescent probes to visualize such films. This indicates such structures (condensed/fluid domains) are not probe induced artifacts (see text for further details).

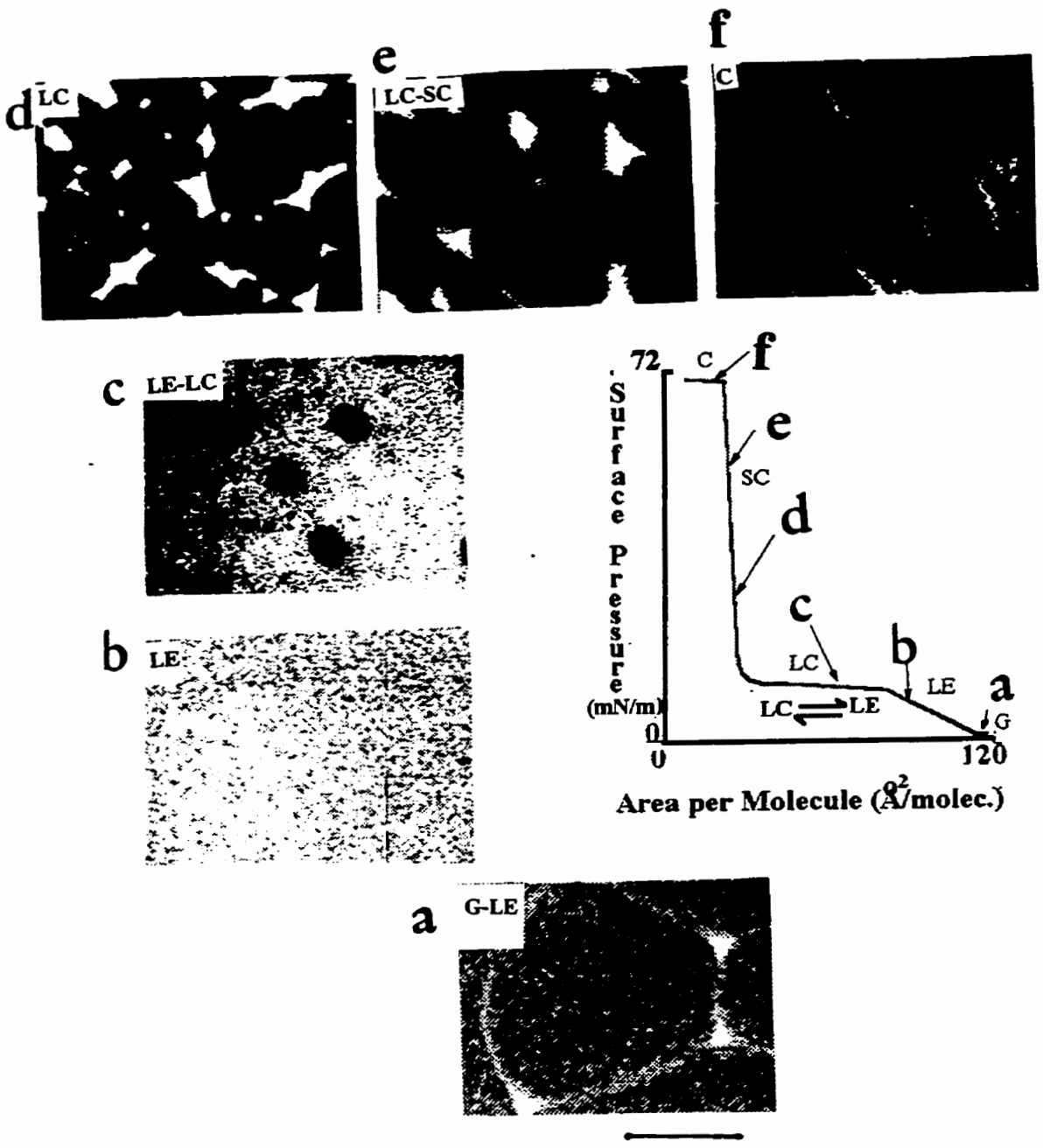
d
LC
e
LC-SC
f
C
c
LE-LC
b
LE
72
C
f
e
SC
d
c
LC
b
LE
a
G
LC ⇌ LE
Surface Pressure (mN/m)
0
0
120
Area per Molecule (Å²/molec.)
a
G-LE

phase structures of thin films, quantitative estimates are necessary to understand the process of phase transitions occurring in such films under various states of compression. At present there are three groups, which have used computer aided analysis and estimation of the phase structures (Lösche et al., 1988; Nag et al., 1990; 1991; Seul et al., 1991). Such analysis can lead to estimations of the amounts of the molecules which are in the respective phases as a function of molecular area or surface pressure. Such estimates were performed on various lipid and lipid-protein films, such as those of pulmonary surfactant components, by using digital image analysis of randomly selected images of the film at different packing densities or surface pressures (details of the computer aided image analysis are discussed in Appendix A). Such quantitative estimates of the film phases allowed us to study the interactions of lipids and proteins of pulmonary surfactant, and as models of biological membranes, as performed by others on membrane lipid-protein systems (Möhwald, 1990). Some of the quantitative information obtained in our studies is compared to the information available on similar systems in bilayers, and thus the detailed discussion of the phase transition properties of bilayers in this chapter was done.

The structures observed by fluorescence microscopy at or near the LE-LC phase co-existence regions of different lipids and their mixed films are shown in Figure 2.6. The structures indicate that not only are the LE-LC region of lipid films heterogenous, due to the coexistence of two distinct phases, but also the shapes of the LC domains (black regions) are extremely diverse. The black regions in all images in

Figure 2.6. Shapes of probe excluding (black) domains observed in various lipid films using fluorescence microscopy from the LE-LC phase co-existence regions. Scale bar is 25 μm.

A - DPPC films compressed at 0.13 Å^2/molecule/sec at π= 9 mN/m.

B - DPPC films compressed at 0.013 Å^2/molecule/sec at π= 9 mN/m.

C - DPPC + 0.2 mol % cholesterol.

D - DPPC + 2 mol % cholesterol.

E - DPPC + 4 mol% cholesterol (C-E are from similar π)

F - DPPC + 2 mol % cholesterol at a higher π than E.

G - DPPG films with calcium.

H - POPC + 40 mol % cholesterol.

Such shapes of condensed domains occur due to competition between line tension forces acting along the condensed-fluid phase boundaries and electrostatic interactions between the molecules.

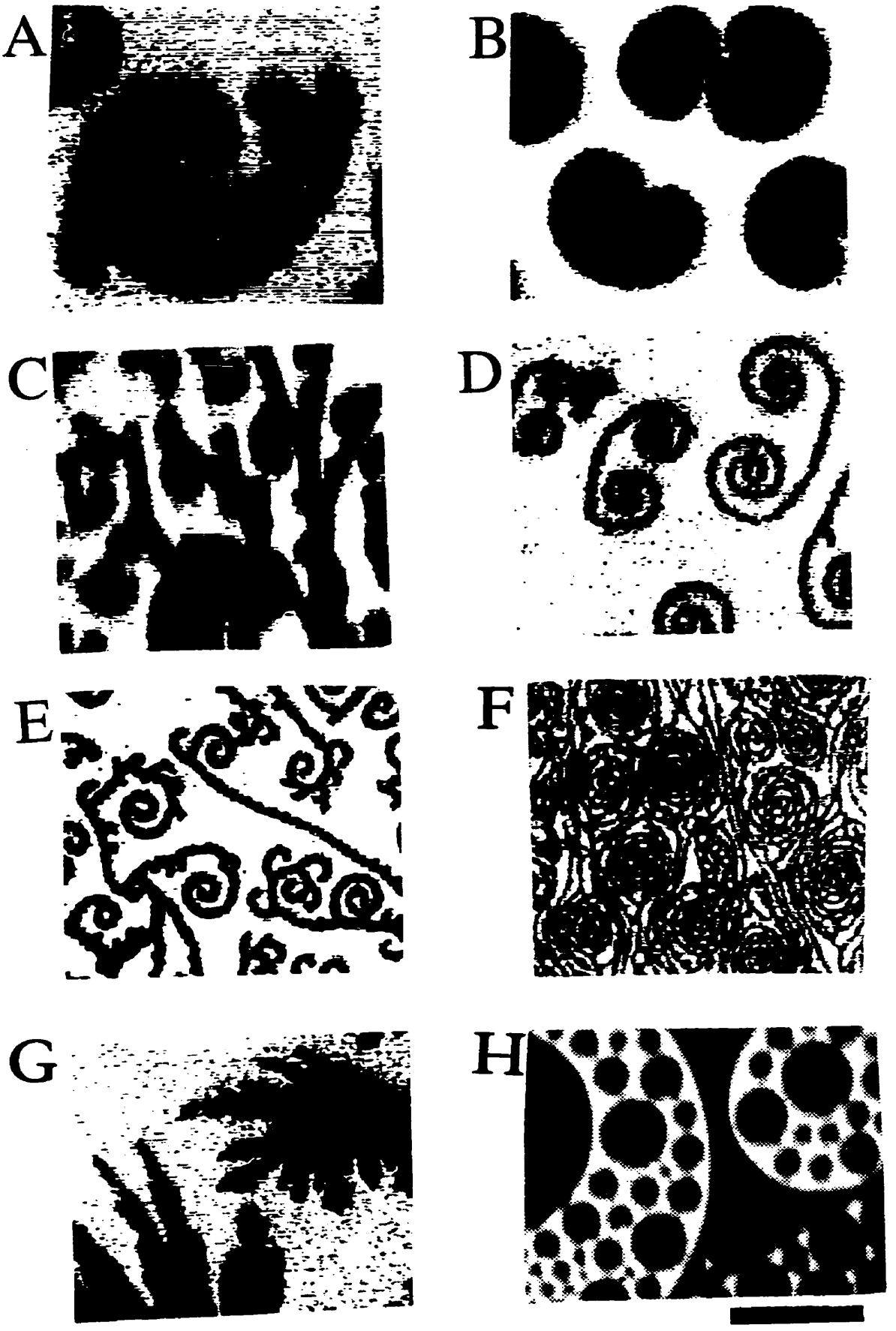
A
B
C
D
E
F
G
H

Figure 2.6 represent the liquid condensed (LC) or gel-like phase which excluded the probe. From observing such diverse LC domain shapes, the question of whether such structures really represent lipid films organization or are actually created due to fluorescent probe induced artifacts of such films arises. In the last few years others have reported observing such diverse LC domain structures in lipid films without fluorescent probes, and thus have answered the question quite conclusively. The diversity of LC domain shapes in films is real. Some of the shapes and structures of domains in lipid films as seen by fluorescence microscopy were also observed in similar films minus the fluorescent probe by Brewster angle microscopy [BAM] (Hénon and Meunier, 1991; Widemann and Volhardt, 1996), surface plasmon microscopy (Hickel et al., 1989), charge decoration electron microscopy (Fischer and Sackmann, 1984), atomic force microscopy [AFM] (Chi. et al., 1993; Mikrut et al., 1993) and time of flight mass spectral microscopy (Leufgen et al., 1996). Non imaging techniques to study films such as electron diffraction (Hui and Yu, 1993) fourier transform infrared spectroscopy [FTIR] (Hunt et al., 1989; Mendelsohn et al., 1995), polarization-evanescent illumination dichroism (Thompson et al., 1984), X-ray reflectivity (Daillant et al., 1990), X-ray diffraction and scattering (Kjaer et al., 1988; Möhwald et al., 1995) and computer simulations (Georgallas and Pink, 1982; Pink, 1984; Mouritsen et al., 1989) have also supported the existence of heterogenous phase structures in the LE-LC co-existence regions of lipid films.

Fluorescence microscopy of films has been used to study several bio-mimetic systems and processes such as lipid-protein interactions in biomembranes (reviewed by

Möhwald, 1990), enzyme catalyzed hydrolysis of phospholipids (Grainger et al., 1989; Reichert et al., 1992), receptor-ligand binding (Ahlers et al., 1989, reviewed by Stine, 1994) and interactions of pulmonary surfactant and its components at the air-water interface (Hall 1995a; 1995b; Discher et al., 1996 and chapter 3-11).

2.8] Molecular Architecture of Thin Films : Beyond Domains.

Although the studies utilizing fluorescence microscopy of phospholipid films indicate the nature and properties of the phase transitions in such systems, the diversity of shapes of the LC domains cannot be explained from such studies. The arrangement of the phospholipid molecules inside the condensed domains are not as simple as shown in Figure 2.7 (B), since such domains shape (or their molecular orientations) are drastically altered by minor changes in the system such as chirality of the lipids, composition, electro-magnetic field (Groves and McConnell, 1996; Lee et al., 1994; Rice and McConnell, 1989; Wang et al., 1996). By increasing the intensity of light on a LC (black) domain individual molecular diffusion, orientation and chain tilt can be altered, due to the incident photons effecting the chain arrangements inside such domains via electromagnetic energy dissipation (Lee et al., 1994, Wang et al., 1996). The arrangement of the molecules inside the LC domains has been recently the focus of interest of a number of groups, since techniques such as atomic force microscopy (AFM) can be used to resolve single molecule orientations inside the domains. Information obtained from some of the recent studies on molecular structure and orientations in the different domains of lipid films is discussed in the following chapters of the thesis, while

Figure 2.7 Typical fluorescence microscopic (A), three dimensional molecular arrangements (B) and atomic force micrograph (C) of phospholipid monolayers in the liquid expanded-liquid condensed (LE-LC) coexistence region. The figures in (A) and (B) are merged to show the LC-LE domains molecular arrangements. The box in (A) presents the plot of fluorescence intensity across a line in the image; and in (C) the atomic force or depth profile across the line drawn diagonally across two LC domains. [The AFM micrograph and plot in (C) was a generous gift from Dr. R. C. MacDonald of Northwestern University, and is discussed in detail in Mikrut et al., (1993), © American Physical Society]

The intensity plot in (A) indicates that the fluorescence intensity drop inside the LC domain (black) whereas it is higher in the LE or fluid regions in which the fluorescent probe partitions. The atomic force profile (vertical tip movement vs horizontal distance) in (C) indicates the height between the two LC domains (circular grey regions) decreases by a few nanometers, indicating the molecules in the LE phase have a lower height or are "softer" to the AFM tip. This would be the case if the phospholipid acyl chains (B) were in a more "fluid" or expanded conformation, and the ones in the LC phase more rigid or stretched more perpendicular to the plane of the air-water interface in the z direction. The molecules in the LE, LC or solid phase, though, are all slightly tilted from a complete perpendicular orientation, as observed in a number of studies (see text).

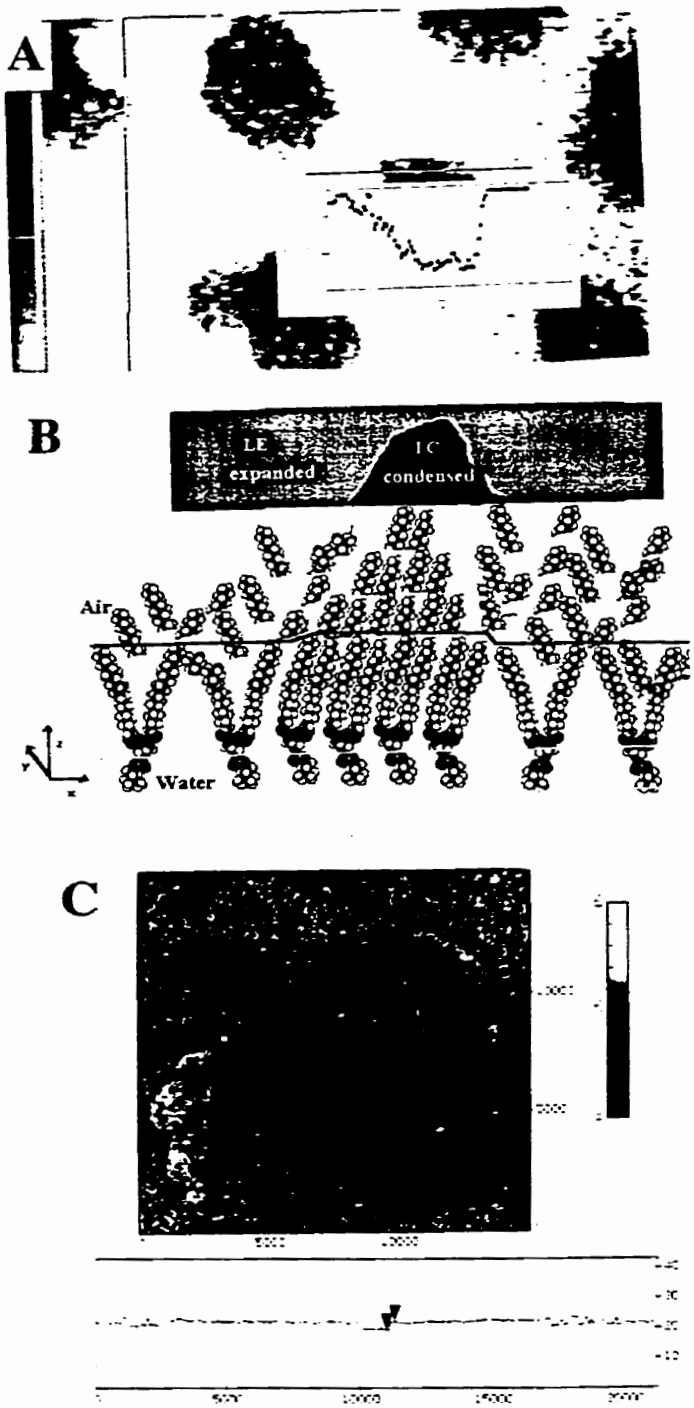

61a

discussing lipid-lipid and lipid-protein interactions of pulmonary surfactant.

Figure 2.7 shows the typical three dimensional arrangement of phospholipid molecules in films from the liquid condensed and liquid expanded phases at an air-water interface. The image in (A) of Figure 2.7 also shows a fluorescence intensity scan of image and the distribution of intensity pixel along a line across a LC domain (black) extending on both sides of the domain into the LE phase (white). The decrease in the intensity from 200 to near 0 inside the LC domain (black in A) indicated that the fluorescent probe did not penetrate this phase. The conceptualized three dimensional organization of the molecules in the LE-LC phase is shown in Figure 2.7 (B), and an atomic force micrograph from the LE-LC phase region is shown in (C). The interpretation that the molecules are more flexible in the LE phase, whereas more rigid and perpendicular to the plane of the film in the condensed or gel-like phase are indicated from studies in which "touching" the molecules of the film transferred to a solid substrate was performed by atomic force microscopy (AFM) (Mikrut et al., 1993). This art of "touching" the molecules was performed by using a one molecule thin metal tip of the AFM, to scan the LC and LE regions of the phospholipid film, and observing the movement of the tip away or into the different film phases at a nanometre resolution. The atomic tip tended to dip or penetrate more in the regions of the fluid or LE phase compared to the LC phase as shown in the vertical tip movement vs horizontal distance plot, below the AFM micrograph in (C). This dip or depression of the tip indicated that the LE regions of the film were softer or lower in height by a few nanometers compared to the LC regions. This would imply that either the molecules were tilted in the LE

phase away from a perpendicular to the film plane compared to the LC phase as shown in (B), or the LE phase was softer or less dense than the LC phase (Mikrut et al., 1993). Other studies using x-ray diffraction of films have also supported the fact that a height difference exists between the LE and LC phase (Dailliant et al., 1990). The reason why fluorescent lipid probes in films inherently prefer the fluid phase is either due to the probes chain tilt being similar to that of the phospholipid molecules in the fluid phase, or due to the bulky fluorophore region of the probe's NBD portion (shown by the grey molecules in Figure 2.7 (B)) not being allowed to pack or mix with the more rigid and tightly packed chains of the LC phase. Recent studies using Brewster angle microscopy (BAM) have shown that the arrangement of DPPC molecules inside the circular or elliptical LC domains is not uniform, but groups of the molecule are organized inside the domains (Weidemann and Volhardt, 1996). The molecules of DPPC were shown to undergo orientational (rotational and positional) changes inside the LC regions with increasing compression of the films (Weidemann and Volhardt, 1996). Comparative studies of DPPC with other phospholipids in films indicated that the tilt or orientation (or the erection) of the molecules in the LC phase is strongly dependent on the charge and size of the headgroup of the phospholipids (Weidemann and Volhardt, 1996).

The resolution of fluorescence microscopy is about 2 μm, whereas that of atomic force microscopy (AFM) can be as low a 1 Å. AFM of the films LE-LC phase structures of fatty acids and phospholipids indicate that the LE phase (which is not completely homogenously fluorescent under fluorescence microscope) has grainy structures (Chi et al., 1993; Mikrut et al., 1993). Such grains (barely visible in Figure

2.7(C) as grey spots) are considered to be the nucleation sites for condensed domains, and such structures probably makes the LE phase somewhat non-homogeneous. As previously mentioned AFM images have indicated that there is a height difference between the film's LC and LE phases, (Chi et al., 1993; Mikrut et al ., 1993). This height difference would indicate the molecules in the LE phase are more tilted towards the plane of the air-water interface compared to the ones in the LC phase.

The molecules in the LC phase of DPPC films are not completely perpendicular to the plane of the air-water interface. X-ray reflectivity of DPPC films suggests that there is also a difference in height of 3 Å between the LC phase of DPPC and the chain length of palmitic acid. This difference is the same as one would expect in the case where palmitic acid chains of DPPC were slightly tilted in the LC phase by a small angle (30°) from their position of complete perpendicularity to the plane of the air-water interface (Dailliant et al., 1990). These studies indicate that the chain arrangements and tilts of DPPC in films can contribute to differences in height between the various domains in films, and such molecular arrangement of films are reflected in the fluorescence microscopic studies in combination with other techniques can be studied quite conclusively. Other studies have shown that molecular level details of the phospholipids such as chirality (R or S enantiomers), are preserved in the shapes of the LC domains (the clockwise-anticlockwise direction of domain protrusions), indicating that the structure of this phase is far more complex than thought previously (Bringezu et al., 1996; Groves and McConnell, 1996).

Using scanning tunnelling microscopy (STM) of DMPA films it has been shown

that the individual molecules in the liquid condensed-solid condensed (LC-SC) phase coexistence region are spaced about 4.3 angstroms apart, and are organized in a hexagonal lattice (Hörber et al., 1988). This has been substantiated by x-ray diffraction methods (Kjaer et al., 1988). Using near field scanning optical microscopy (NSOM) the SC phase has been shown to be heterogenous (Hwang et al., 1995). The NSOM studies of DPPC films in the solid condensed (SC) phase indicate this phase contain filamentous networks of LC phase (Hwang et al., 1995). Surface plasmon microscopy has detected two separate phases co-existing in the SC region, and such phases consists of two distinct types of solid domains. The domains differ in their hydrocarbon chain tilts and are in equilibrium with each other (Kooyman and Krull, 1991). However charge decoration electron microscopy of DPPC films have shown that the SC phase is quite homogenous and had no domain structures (Fischer and Sackmann, 1984). Recently, the SC phase of DPPC film was indicated to be a dehydrated phase, where the phospholipids headgroup had a different conformation from those found in the LC phase (Denicourt et al., 1994), and had lost the hydration shell associated with the molecules in the LE phase (Brumm et al., 1994). Although fluorescence microscopy can not discriminate between the LC and the SC phase, since at high surface pressure the lateral mobility of the fluorescent probe decreases, or the probe gets frozen inside the solid-like phase. In the course of this thesis the black regions are considered as a condensed (gel-like) phase at all pressures and no attempt is made to discriminate the LC from the SC phase, and we consider that all probe excluding regions (black) are condensed. The molecular architectures of the gas and collapse phases are not clear at present.

It is not clear at present how some of the lipid and protein components of surfactant organize, interact and associate in films or at an air-water interface. The main objective of this thesis is to study films of various pulmonary surfactant components at the air-water interface in spread and adsorbed films using epifluorescence microscopy. By understanding the nature of the phase transitions of surfactant lipids and lipid-protein films, a semi-quantitative assessment of the packing and associations of the lipids and proteins with each other could be obtained. We first show how such packing or phase transitions occurs in simple mixtures of DPPC with unsaturated lipid (next chapter), phosphatidylglycerol (Chapter 4) and cholesterol (Chapter 5). Next, by fluorescently labelling surfactant proteins we study the phase transitions, interactions and association of the surfactant lipids with such proteins in films (Chapters 6-10). Finally we study films of pulmonary surfactant extracts obtained from porcine lungs, to correlate some of the properties of such films with the ones shown by its components in films (Chapter 11). Further interpretation of the data obtained by fluorescence microscopy of such films, presented throughout the course of this thesis, is based on some of the molecular and supra-molecular details of the phase structures discussed above.

Chapter 3.

UNSATURATED PHOSPHATIDYLCHOLINE

INTRODUCTION

Monolayers of lipids at the air-water interface have long served as models for biological membranes. Also it is generally accepted that lipid monolayers of pulmonary surfactant are responsible for the lowering of surface tension in the lung. A comprehension of the two-dimensional distribution of lipids in mixtures in monolayers is fundamental to understanding of pulmonary surfactant function, and is highly relevant to our perception of two-dimensional segregation of lipids in monolayers. In this study we employ the technique of epifluorescence microscopy of monolayers to study a set of simple mixtures of DPPC (16:0/16:0-PC) and DOPC (18:1/18:1-PC) which are relevant to our perception of how both biological systems could be organised.

Among the phosphatidylcholine species of lung surfactant about 30-40 weight percent of the lipid is mono-unsaturated (Hawgood, 1991; Kahn et al., 1995a; 1995b; Lau and Keough, 1983). One of the earliest studies on the details of chain saturation of lung surfactant PC indicated that canine surfactant PC contains about 60 % di-saturated species, whereas the rest is a mixture of monoenoic 16:0/16:1 (16 wt %) and 16:0/18:1 (10 wt%) species (King and Clements, 1972a). Currently comparative analysis of surfactant with other tissues suggests that although DPPC, an unusual molecular species, is present in other tissues, it occurs in the highest percentage in surfactant. The rest of the PC pool contains monoenoic species, such as palmitoyl-oleoyl PC (16:0/18:1-PC or POPC) and other phosphatidylcholines with the *sn-2* chains having one or two double bonds (i.e. 16:0/16:1, 16:0/18:2) (See section 1.5 for details). In various lung diseases,

the ratio of DPPC to unsaturated PC changes in pulmonary surfactant (PS), and this can alter the surface activity of the material when tested *in vitro* (Günther et al., 1995; Keough, 1984). Also, homeoviscous adaptation of animals exposed to various temperatures, altered levels of fluid components or lipids which impart increased fluidity to PS (Daniels et al., 1995; Lau and Keough, 1981). From such studies it is generally concluded that the level of fluid components of the surfactant is metabolically tightly controlled (Hawco et al., 1981b; Keough, 1984; 1992).

When compressed in monolayers, DPPC, can withstand high surface pressures of about 70 mN/m, equivalent to very low surface tensions (γ). Pulmonary surfactant contains some unsaturated lipid species, which do not withstand such high π; these have been suggested to play other roles such as facilitating adsorption and spreading of material to the interface (Bangham et al., 1979; Hildebran et al., 1979; Notter et al., 1980). DPPC can neither rapidly adsorb from an aqueous subphase nor quickly re-spread from collapsed phases of monolayers after compression.

In bilayers, DPPC shows a chain melting phase transition (T_c) near 41°C (Bashford et al., 1976; Blume, 1979; Davis et al., 1980). In PC monolayers below T_c, closely packed molecules can sustain high π, or produce very low surface tensions, at the air-water interface (Hawco et al., 1981a). The T_c of most, if not all naturally occurring unsaturated phospholipids are below 37°C and the lipids exist in a fluid or chain-melted form at that temperature. Monolayers of unsaturated lipids such as DOPC (with T_c below the measurement temperature) do not withstand very high π, and they collapse at a surface pressure near 50 mN/m (Notter et al., 1980). It has been suggested

that the unsaturated components are preferentially excluded during compression of a pulmonary surfactant monolayer, to enrich the monolayer with DPPC (Bangham et al., 1979; Egberts et al., 1989; Hawco et al., 1981a, 1981b, King and Clements, 1972b; Notter et al., 1980).

In this study we have investigated a system of mixed films of DPPC:DOPC using the epifluorescence microscopic technique. We have examined the changing sizes of condensed domains as a function of composition and surface pressure, and compared our results to the thermotropic phase behaviour of these lipid systems in bilayers (Lentz et al., 1976; Phillips et al., 1970). We have also sought evidence for the potential exclusion of one component from monolayers during a series of cycles of rapid compression to high surface pressure and re-expansion.

MATERIALS AND METHODS

1, 2-Dipalmitoyl-*sn*-glycero-3-phosphocholine (DPPC) and 1, 2-dioleoyl-*sn*-glycero-3-phosphocholine (DOPC) were purchased from Sigma Chemical, St. Louis, MO. The fluorescent probe 1-palmitoyl-2-[12-{(7-nitro-2-1, 3-benzoxadiazole-4-yl)amino} dodecanoyl] phosphatidylcholine (NBD-PC) was obtained from Avanti Polar Lipids, Birmingham, AL. The cationic probe 3,3'-dioctadecyloxacarbocyanine perchlorate (DiO) was a product of Molecular Probes Inc., Eugene, OR. Stock solutions of the probes and the lipids were prepared by dissolving them in chloroform:methanol (3:1, vol/vol). DPPC, DOPC and probe were mixed at molar ratios of 69:30:1, 49:50:1 and 29:70:1, and each individual lipid was mixed with probe at molar ratios 99:1 and stored at -20°C. Monolayers were spread on an unbuffered 0.15 M NaCl subphase with pH initially adjusted to 6.9. The saline was made with deionized, doubly-distilled water, the second distillation being from dilute potassium permanganate.

Compression and expansion of the monolayers and surface pressure - area measurements were performed on a epifluorescence microscopic surface balance whose design and schematics are described in Figure 3.1 and in detail elsewhere (Nag et al., 1990, 1991). Before spreading the monolayers the surface was repeatedly aspirated to clean the interface of contaminants. Monolayers were spread from chloroform:methanol (3:1 v/v) solutions at the air-saline interface by dropwise placing the solution at the interface from a microlitre syringe. A period of 30 minutes was allowed for solvent evaporation before compression and expansion were begun.

Figure 3.1 Schematics of the epifluorescence microscopic surface balance used to study lipid films at an air-water interface (top) and the design and parts of this surface balance (bottom, from Nag et al., 1990).

The different parts of the balance (bottom) are: A - teflon trough; B - metal base for flow of water (temperature control); C - teflon collar to minimise surface flow; D - plastic cover to minimise air-flow; E - tight fitting teflon compression barrier; F - motor for compression; G - limit switches for barrier motion control; H - Z-translator or focusing micrometer; I - vibration dampener; J - solid stone block to minimize vibrations; K - pressure transducer; L - epifluorescence filters; M - excitation light source; N - image intensifier; O - CCD camera; P -microscope eyepiece.

The films are spread at an the air-water interface in a teflon trough (top; bottom-A) and compressed or expanded using the barrier (bottom-E). The fluorescence from the film is observed by focusing the objective of the epifluorescence microscopic (bottom-M, L, P) surface balance on to the water surface. The images are observed by the eye (P) and are video recorded and analyzed using the CCD camera (N and O) and computer software. Simultaneously the surface pressure-area data obtained from measuring the surface tension of the air-water interface (K) are stored in a personal computer.

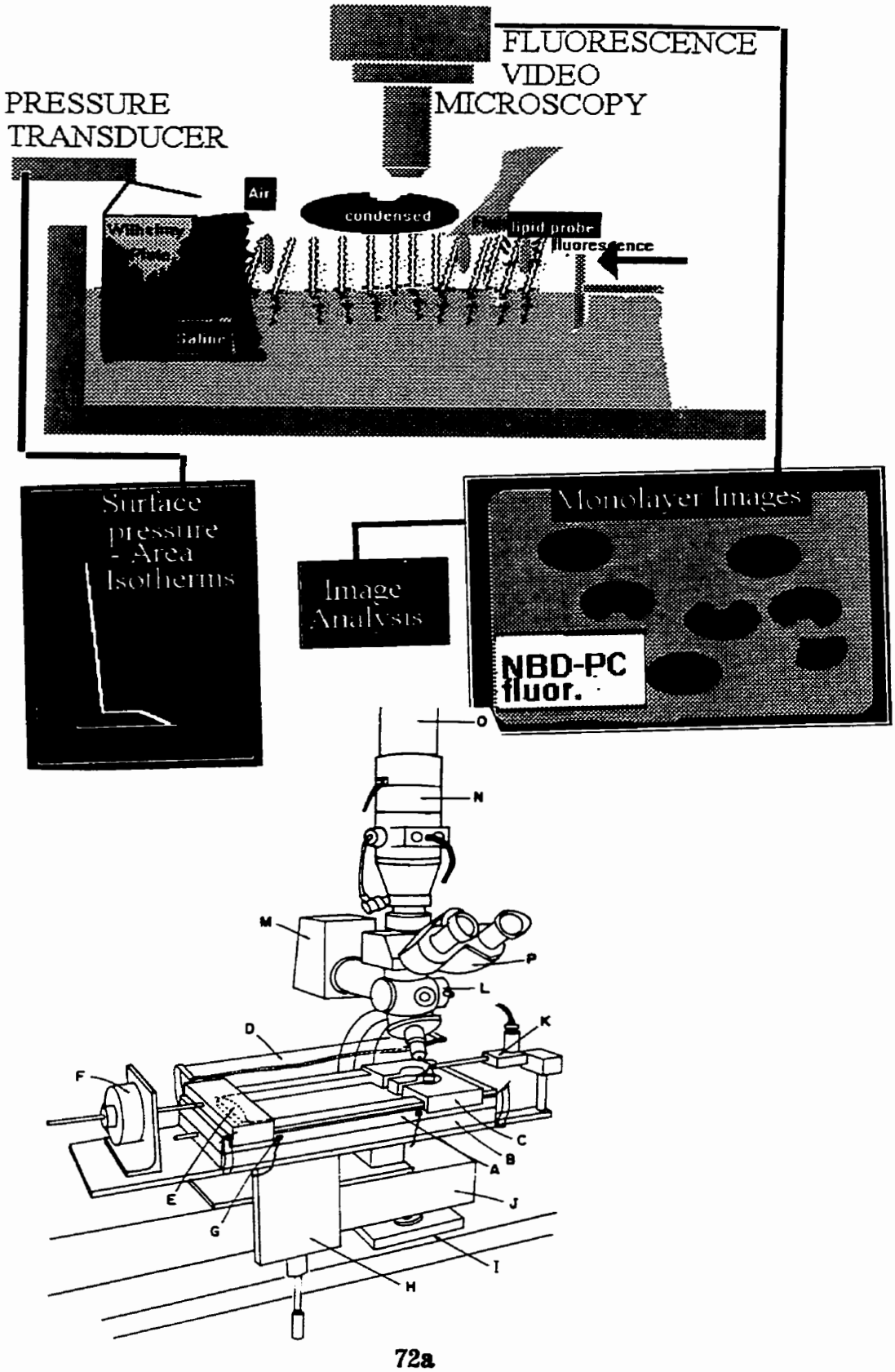
FLUORESCENCE
VIDEO
MICROSCOPY
PRESSURE
TRANSDUCER
Air
condensed
lipid probe
fluorescence
Surface
pressure
- Area
Isotherms
Image
Analysis
Monolayer Images
NBD-PC
fluor.
O
N
M
P
L
K
D
F
C
B
A
E
J
G
I
H

72a

Monolayers were compressed at two different rates of 20 $mm^2.sec^{-1}$ (slow) and 707 $mm^2.sec^{-1}$ (fast) corresponding to initial rates of 0.19 $Å^2.molecule^{-1}.sec^{-1}$ and 5.6 $Å^2.molecule^{-1}.sec^{-1}$ respectively for the usual surface loads. Isotherms of DPPC, DOPC and their mixtures were obtained using both rates of compression at a temperature of 23 $\pm$ 1°C, since instrumental limitations did not allow us to perform experiments at higher temperature. In experiments where visual observations were performed, the monolayers were compressed in 20 steps and the barrier stopped after each step for 1 minute. During about eight of these one minute periods, at selected surface pressures, video recording of monolayer appearance was performed. Processing and analysis of the recorded video images were performed using operator interactive software (JAVA; Jandel Scientific, San Rafael, CA) on a personal computer as described in appendix A.

RESULTS

When DPPC monolayers were compressed at a fast rate (700 $mm^2.sec^{-1}$) isotherms showed the onset of a LE-LC plateau at a surface pressure of ~ 7 mN/m and collapse at ~71 mN/m. DOPC monolayers compressed at the same rate showed no LE-LC plateau, and collapsed at 50 mN/m. When compressed at a slower rate of 20 $mm^2.sec^{-1}$ the DPPC and DOPC monolayers showed isotherm properties essentially the same as those obtained at the fast rate. The lipids were spread at an area per molecule of 140 $Å^2.molecule^{-1}$ ($\pm$ 5 $Å^2.molecule^{-1}$). Figure 3.2 (A) shows the isotherms obtained when monolayers of DPPC:NBD-PC 99:1, DPPC:DOPC:NBD-PC 49:50:1 and DOPC:NBD-PC 99:1 which were compressed slowly with interruptions for video recording. The inset of Figure 3.2 (A) shows the isotherms of monolayers of DPPC:DOPC:NBD-PC 29:70:1 and 69:30:1 compressed at the same rate and the typical images observed in such monolayers are shown in (B). The letters A-E, a-e, a1-e1 and a2-e2 indicates the points where visual fields were recorded for analysis. Isotherms of DOPC:NBD-PC 99:1 showed only LE phase, or no discontinuity up to the point of monolayer collapse.

The LE-LC phase transition of monolayers of DPPC:NBD-PC (99:1) under slow compression was observed visually (Figure 3.2 B). Very small probe-free condensed domains were found to appear at surface pressures of 3-5 mN/m. As surface pressure was increased to 17 mN/m the domains grew to a larger size. The domains were relatively homogenous in shape and distributed evenly over the visual fields. The domains came in contact with one another at surface pressures above 17 mN/m, but did

Figure 3.2. Isotherms of DPPC:NBD-PC (99:1, mol/mol), DPPC:DOPC:NBD-PC (49:50:1) and DOPC:NBD-PC (99:1), compressed in steps at a temperature of 23 $\pm$ 1°C. The inset shows isotherms of DPPC:DOPC:NBD-PC (29:70:1) and (69:70:1) (A). The monolayers were compressed in 20 steps at a speed of 20 $mm^2.sec^{-1}$, and at some steps (indicated by the letters) a waiting period of one minute was introduced, during which visual recording was made.

B) Typical images of monolayers of DPPC:NBD-PC 99:1 [A-E], DPPC:DOPC:NBD-PC 69:30:1 [a2-e2], 49:50:1 [a-e] and 29:70:1 [a1-e1] photographed from the video monitor at the surface pressures indicated in the isotherms in (A). The black regions represent the condensed phase and the greyish-white the expanded or fluid phase. In monolayers of DPPC:DOPC:NBD-PC 29:70:1 there were whole fields containing no condensed domains at surface pressures between 0 mN/m and 45 mN/m. The scale bar is 25 μm.

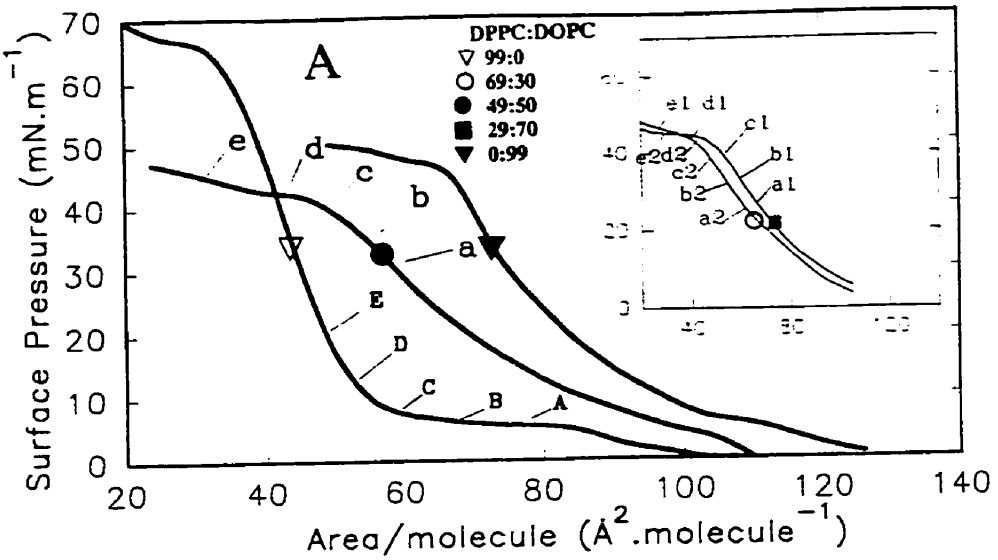
A
DPPC:DOPC
99:0
69:30
49:50
29:70
0:99
Surface Pressure (mN.m^{-1})
Area/molecule (Å^2.molecule^{-1})
a
b
c
d
e
A
B
C
D
E
a1
b1
c1
d1
e1
a2
b2
c2
d2
e2

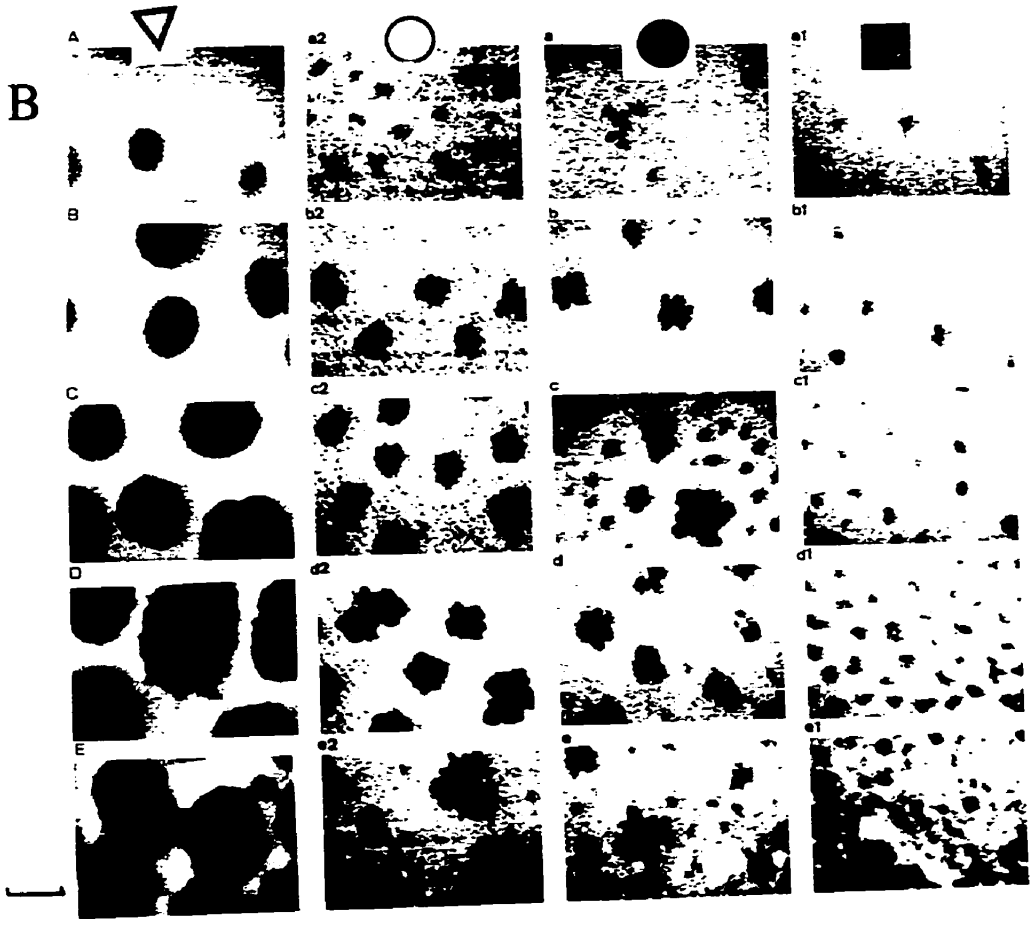
B

not appear to coalesce or fuse up to a surface pressure of 71 mN/m. This phenomenon was also observed using the cationic fluorescent probe DiO. DiO gave more intense fluorescence in the condensed regions (dark regions with NBD-PC) than in the fluid phase (fluorescent with NBD-PC). In DOPC monolayers containing 1 mol% of NBD-PC, continuous fluorescent fields, or a LE phase, were observed from low surface pressures up to the point of DOPC monolayer collapse ($\sim$ 50 mN/m). At surface pressures 2 mN/m below collapse of the DOPC monolayers, small areas ($\sim$ 2 μm in diameter) of intense fluorescence, were observed in addition to the general fluorescence of the whole field. While it is possible that the intensely fluorescent areas could be caused by aggregation of densely packed regions of probe (probe aggregates) within the monolayer, one might intuitively think that such tight packing could lead to self-quenching of the probe. Another potential explanation for the increased intensity could be the formation of multilayers (collapsed phase) where the amount of probe in the direction normal to the surface is increased without increasing the packing density.

For the DPPC:DOPC:NBD-PC (49:50:1) mixture, small condensed domains appeared at a surface pressure of 14 mN/m (Figure 3.2 B, a). The domains grew in size with increasing surface pressure up to the point (d) in the isotherm. These domains were not homogenous in shape or size, and most fields observed contained domains ranging between 50 and 250 μm^2. In all mixed monolayers at surface pressures greater than 43 mN/m, three types of regions were seen. A low fluorescent background with dark condensed regions and small spots of high intensity fluorescence was typical of the images at these surface pressures. Decreasing the DPPC content of the monolayer

resulted in a slight decrease in the domain size at equivalent surface pressures as shown in Figure 2(B), (a2 > a > a1). Similar features of the monolayers were observed using the probe DiO except at surface pressure > 43 mN/m no areas which corresponded to the small fluorescent spots seen with NBD-PC were detected.

Quantitative analysis of the appearance of the monolayer was performed on digitized recorded images. The average size and number of domains was obtained as described (Appendix A). Six to ten randomly selected frames were analyzed at each surface pressure, indicated by letters in the isotherms in Figure 3.2 A. Figure 3.3 shows the frequency distributions of domain sizes obtained from images of monolayers of DPPC:NBD-PC 99:1, DPPC:DOPC:NBD-PC 49:50:1 and DPPC:DOPC:1 69:30:1 (symbols same as in Figure 3.2). For DPPC:NBD-PC 99:1 (extreme left panel) the average size of the condensed domains increased with increasing surface pressure, as did the scatter of sizes of the condensed regions. This pattern was consistent with those observed previously with monolayers of this lipid (Nag et al., 1991). At surface pressures higher than 17 mN/m the domains began to come in contact with each other, and they could not be identified individually in order to perform a frequency distribution analysis. The frequency distributions for the mixed monolayers (Figure 3.3 middle and right panel) showed a different pattern; between π = 20 mN/m and π = 30 mN/m. The frequency distribution in the right panel for the DPPC:DOPC:NBD-PC (49:50:1) indicated a more skewed distribution of LC domains, between 27-38 mN/m. This indicated that there were possibly two separate groups of LC domains in such mixed monolayers, which probably arose from some demixing of the lipids, causing regions of

Figure 3.3 Frequency distributions of domain sizes of monolayers of DPPC:NBD-PC 99:1 (A), DPPC:DOPC:NBD-PC 69:30:1 (B) and 49:50:1 (C). The surface pressure in mN/m for each distribution is shown in the top right hand corner of each panel. Six to ten randomly - selected frames were analyzed for each surface pressure.

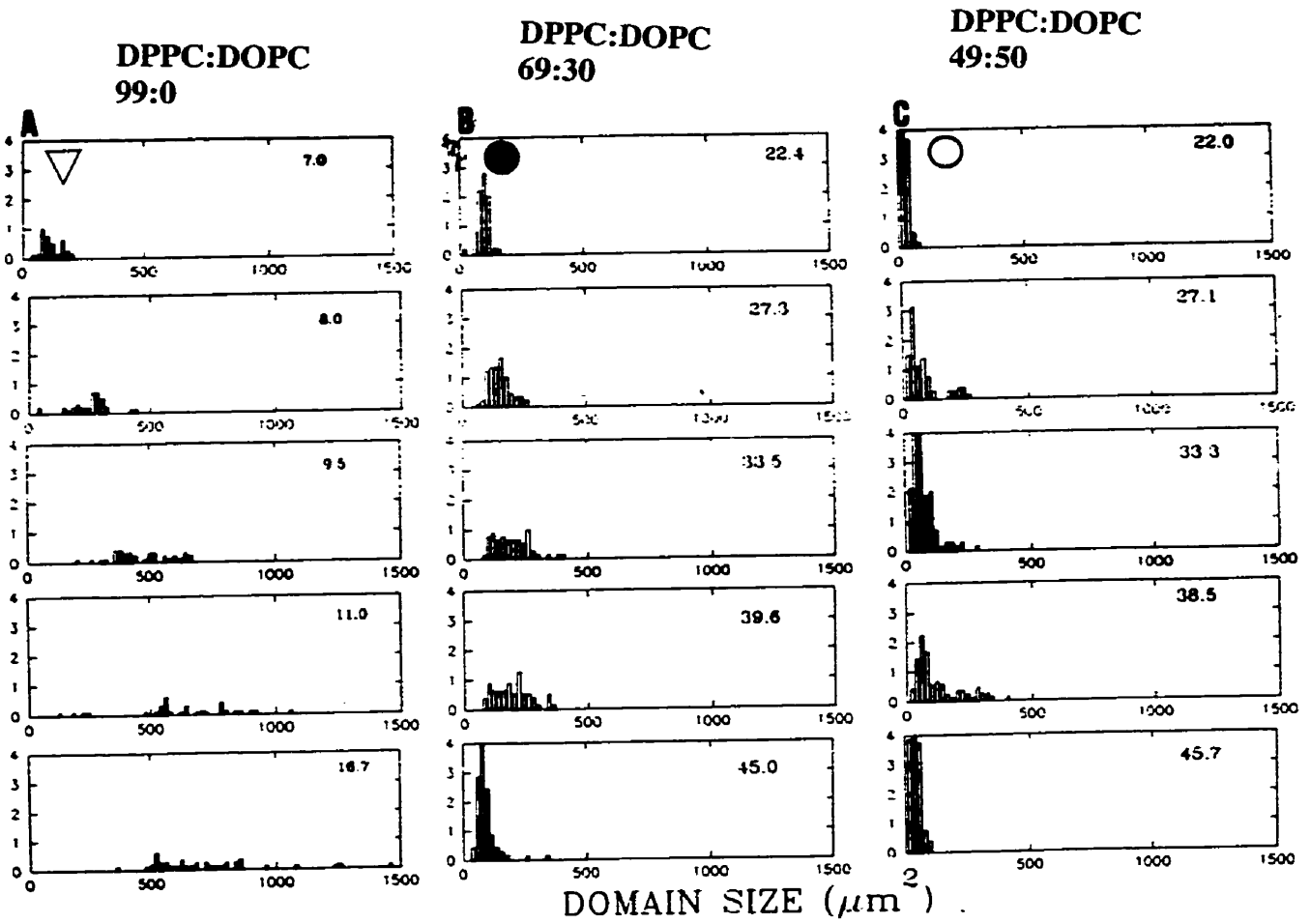
DPPC:DOPC
99:0
DPPC:DOPC
69:30
DPPC:DOPC
49:50
A
B
C
7.0
8.0
9.5
11.0
16.7
22.4
27.3
33.5
39.6
45.0
22.0
27.1
33.3
38.5
45.7
0
500
1000
1500
DOMAIN SIZE (μm^2)

the film to have large and small domains. The images Figure 3.2 (B) for this mixture also tend to indicate large and small domains present in the field of view. The heterogeneity in the size of the condensed domains increased, and above 40 mN/m they reverted to the narrower distributions observed at the low surface pressure. For mixed monolayers the range of sizes and the average size of the condensed domains was generally smaller than that seen for DPPC alone.

Figure 3.4 (A) shows the plot of average domain size as a function of surface pressure for DPPC monolayers and the three different DPPC:DOPC monolayers. The average domain size increased up to a surface pressure of 35 mN/m and then it decreased with further increase of surface pressure. For the mixed systems, the largest condensed domains were observed in the monolayers of DPPC:DOPC:NBD-PC 69:30:1. In that mixture the domains grew to about 200 μm^2 at π=35 mN/m and then decreased to 70 μm^2 at surface pressures of ~ 40 mN/m. A similar pattern in the size-pressure relationship was also observed for monolayers of DPPC:DOPC:NBD-PC 49:50:1 and 29:70:1. The sizes of condensed domains, including the maximum size at ~35 mN/m was smaller with increasing content of DOPC in the monolayers.

Figure 3.4 (B) shows a plot of the percentage of condensed lipid [(total area of the condensed domains)/(total area of the frame) x 100] as a function of surface pressure (see appendix A for a discussion on image analytical methods). For DPPC:NBD-PC 99:1 monolayers, the percentage of condensed lipid increased as surface pressure was raised, reaching a value near 80% at π= 17 mN/m. Flörsheimer and Möhwald (1989) observed similar proportion of condensed lipid in DPPC monolayers at a similar

Figure 3.4. A) Average domain size, based on six to ten images from two separate monolayers each, of DPPC:NBD-PC 99:1, DPPC:DOPC:NBD-PC 69:30:1, 49:50:1 and 29:70:1 plotted as a function of surface pressure. The error bars indicate plus or minus one standard deviation.

B) Total percentage of condensed regions per frame plotted as a function of surface pressure for DPPC:NBD-PC 99:1, DPPC:DOPC:NBD-PC 69:30:1 and 49:50:1 monolayers. Error bars indicate $\pm$ one standard deviation.

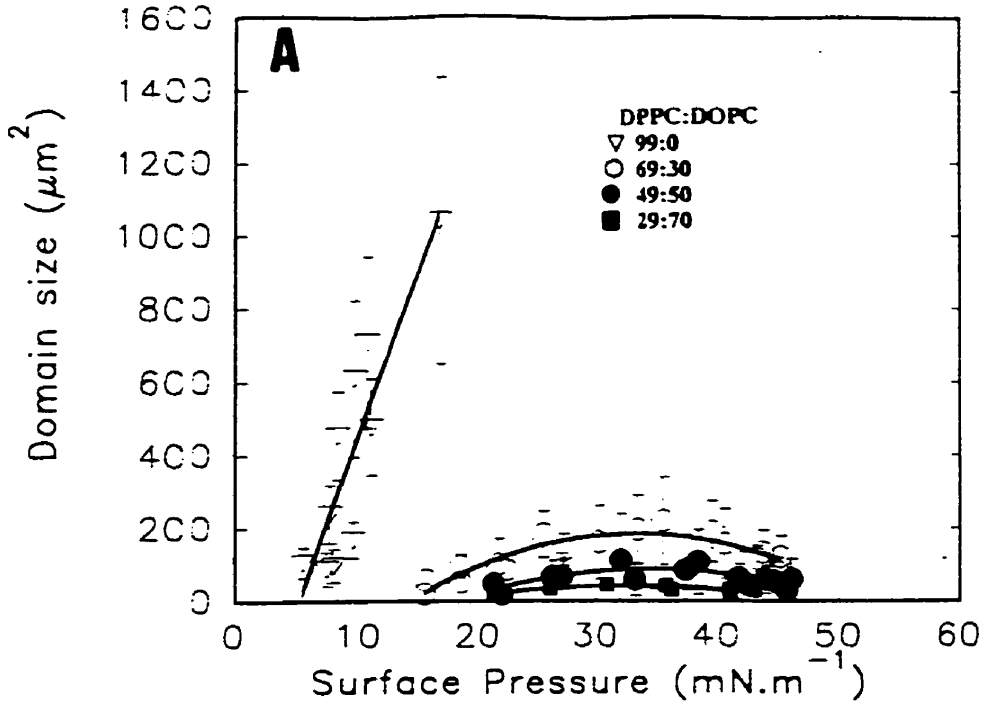
A
DPPC:DOPC
99:0
69:30
49:50
29:70
Domain size (μm^2)
Surface Pressure ($mN.m^{-1}$)
0
200
400
600
800
1000
1200
1400
1600
0
10
20
30
40
50
60

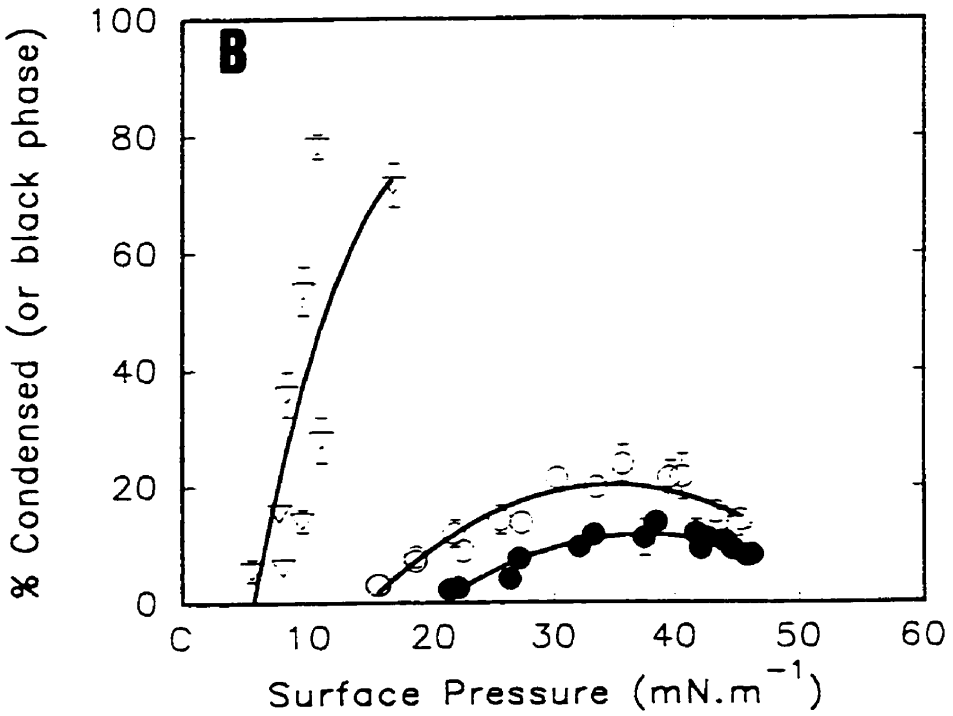
B
% Condensed (or black phase)
Surface Pressure ($mN.m^{-1}$)
0
20
40
60
80
100
0
10
20
30
40
50
60

temperature that were compressed at a lower rate and which contained a slightly lower nominal probe concentration (0.7 mol). If one assumes that the probe is primarily soluble in the liquid expanded phase, its concentration in that phase would then be approaching 5 mol%, and it would have an effect to preserve a greater amount lipid in the fluid state than would be in the case of the absence of probe. It is of interest, however, that the proportion of condensed lipids in monolayers containing DPPC:DOPC:NBD-PC 69:30:1 and 49:50:1 showed a similar pattern to the average sizes in Figure 3.4 (A). Over the range of 15 mN/m to 35 mN/m the percent condensation increased with increasing surface pressure. The percent condensation for monolayers containing DPPC:DOPC:NBD-PC 29:70:1 could not be calculated because of heterogenous distribution of images noted above. One can only estimate that the total percentage of condensed domains in the monolayer was low.

Visual observations were performed on DPPC:DOPC:NBD-PC 49:50:1 monolayers under repetitive dynamic conditions of compression-expansion re-cycling. The monolayers were spread at an initial surface load of $\sim$ 80 $Å^2$.molecule^{-1} and they were repeatedly compressed and expanded 10 times at a fast rate of 700 mm^2/sec (or an initial rate of 3.2 $Å^2$.molecule^{-1}.sec^{-1}). An 11th compression was done slowly in steps (20 mm^2/sec) and visual observation was performed for 1 min at each step. The isotherms of the fast compression- expansion cycles are shown in the inset of Figure 3.5 (A). Analysis of the images observed on the 11th compression compared to the data obtained from a initial slow compression of DPPC:DOPC:NBD-PC 49:50:1 (solid symbols) monolayers showed an increase in the percentage of condensed lipids on the eleventh

Figure 3.5 A) Percentage of condensed regions as a function of surface pressure for two DPPC:DOPC:NBD-PC 49:50:1 monolayers, one compressed slowly once at 20 $mm^2.sec^{-1}$ and the other compressed 11 times [fast (●) at 600 $mm^2.sec^{-1}$ for 10 cycles and followed by a slow compression on the 11th cycle]. The isotherms of the eleven compression - expansion cycles are shown in the inset.

B] Typical images at a surface pressure ~33 mN/m from a single slow first compression (top) and the 11th compression (bottom) of a monolayer of DPPC:DOPC:NBD-PC 49:50:1. Scale bar is 25 μm.

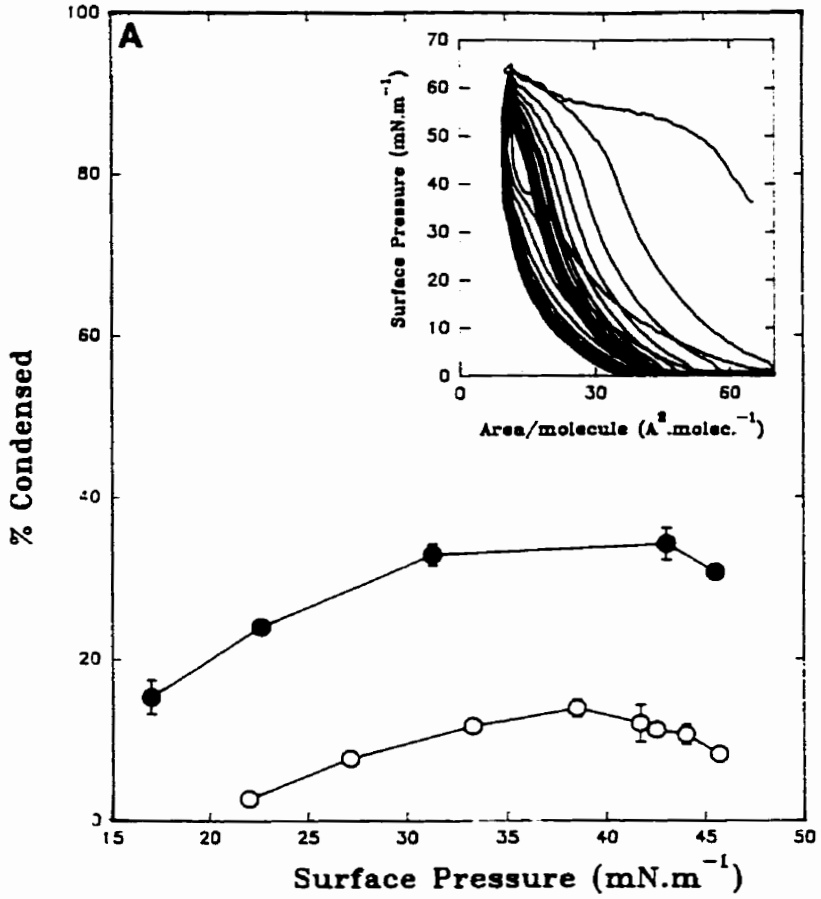
A
% Condensed
Surface Pressure (mN.m^{-1})
Area/molecule (Å^2.molec.$^{-1}$)
Surface Pressure (mN.m^{-1})

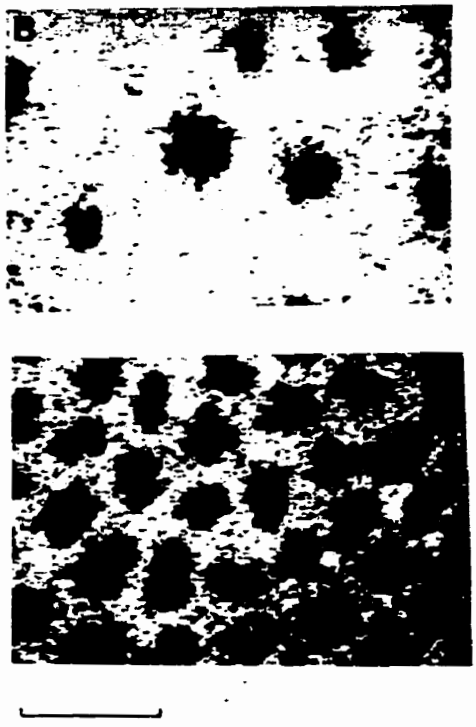
B

compression at equivalent surface pressures (Figure 3.5 (A)). The maximum percentage of condensed lipid (obtained near $\pi = 35$ mN/m) increased nearly 3-fold (from about 12% to about 35%) between the singly and the 11-times compressed monolayer. Figure 3.5 (B) shows typical images observed at $\pi \sim 33$ mN/m from a singly (top) and eleven-times compressed (bottom) monolayer of DPPC:DOPC:NBD-PC 49:50:1. While the number of condensed domains per frame was increased substantially on the 11th compression, sizes of condensed domains were not substantially changed between the first and eleventh compression.

DISCUSSION

Fluorescence microscopy has been used in studies of monolayers of various single lipids, and of cholesterol-phospholipid mixtures (Möhwald, 1990; Stine, 1994; Weis, 1991). In DPPC monolayers, studied here, there was a well defined LE-LC phase transition and formation of large condensed domains with increasing surface pressure, a behaviour consistent with that seen in previous studies (Nag et al., 1991). DOPC showed a fluid or LE phase with no LE-LC phase transition (since all chains of the lipid are fluid at this temperature), up to the point of monolayer collapse. This behaviour of DOPC in monolayers has also been reported by others using a different lipid probe in the monolayer (Yu and Hui, 1991). Electron microscopy of DOPC monolayers transferred to solid substrate showed a single homogenous phase up to the point of monolayer collapse (Tchoreloff et al., 1991).

3.41] Phase transition in DPPC/DOPC mixes.

The surface pressure - area isotherms for the monolayers of mixtures of DPPC and DOPC did not show any inflection or plateau regions at low to intermediate surface pressures where LE-LC transitions occur in pure DPPC monolayers, although collapse plateaus were observed at higher pressures. Condensed domains did form in the mixed monolayers, but the domain sizes and total amount of condensed lipid were different from those observed in monolayers of DPPC alone. In the mixed monolayers, the condensed domains did not appear until higher surface pressures were attained. Even in

monolayers containing 69 mol% DPPC the domains grew to a average maximum size of ~ 200 μm^2 at π ~ 35 mN/m compared to ~ 1100 μm^2 in monolayers of DPPC plus probe at substantially lower surface pressures (Figure 3.4 (A)). Also the percent of total condensed phase of the mixed monolayers never reached more than 20%. Since the condensed domains remained small at all pressures, we assume that the DOPC interrupts the extent to which DPPC enriched domains can grow. In the mixed monolayers it is presumed that the condensed domains are enriched in DPPC over the original proportions of that lipid. This behaviour is consistent with the broad thermal transitions of DPPC - DOPC mixtures in bilayers which show monotectic properties (Egberts et al., 1989; Phillips et al., 1970). Recently we and others (Hall et al., 1995a; 1995b; Discher et al., al., 1996), have shown that the maximum percent condensed (black) or LC phase reached by pulmonary surfactant films, was about 20-25 percent (last chapter). This study therefore would tend to indicate a direct role of unsaturated lipids in controlling the condensation of PS films (detail for discussion in chapter 11). The arrangements of DOPC in DPPC films are shown in Figure 3.6.

The monolayer properties can be related to the phase properties of bilayers of these lipids (Lentz et al ., 1976). At 23°C DOPC is well above its gel to liquid crystal phase transition temperature, whereas DPPC is well below it. Thus, monolayers of DOPC never showed condensed domains at any pressure, whereas DPPC films undergo the LE to LC transition, showing condensed domains, at relatively low pressure. The mixtures approximating DPPC:DOPC 3:7, 5:5, and 7:3 are all in co-existence region of gel and liquid crystal for bilayers at 23°C. The first of these three mixes is very close

Figure 3.6 Schematic model of mixed DPPC/DOPC monolayers at an air-water interface. The DOPC molecules occupy more area in the monolayer due to the *cis*-double bond in its oleoyl (C18:1) chains. The DOPC molecules probably prefer the fluid phase of DPPC, and may prevent some of the fluid DPPC (curved chains, top panel) from packing into the condensed phase (straight chain) upon compression, decreasing the amounts condensed phase found in such mixed films. Upon recycling of such films, DOPC may be irreversibly "squeezed out" (arrow in bottom panel) of the films into the water subphase, enriching such films with DPPC.

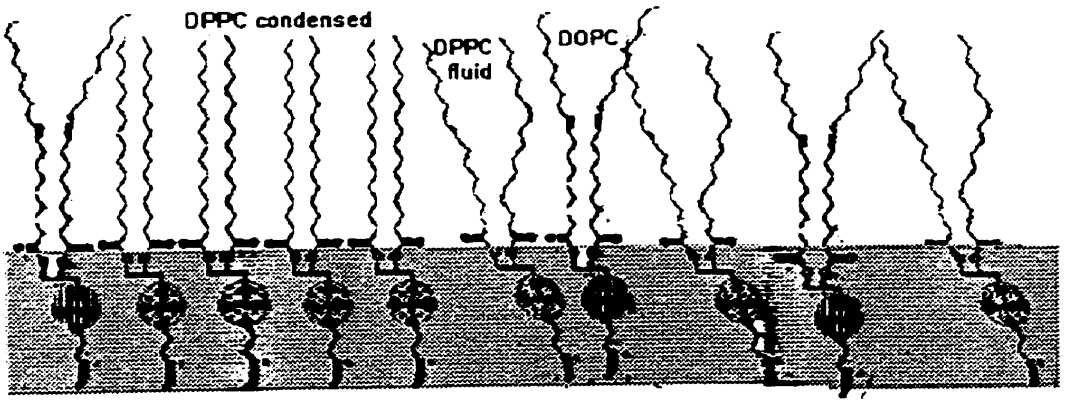
DPPC condensed
DPPC
fluid
DOPC

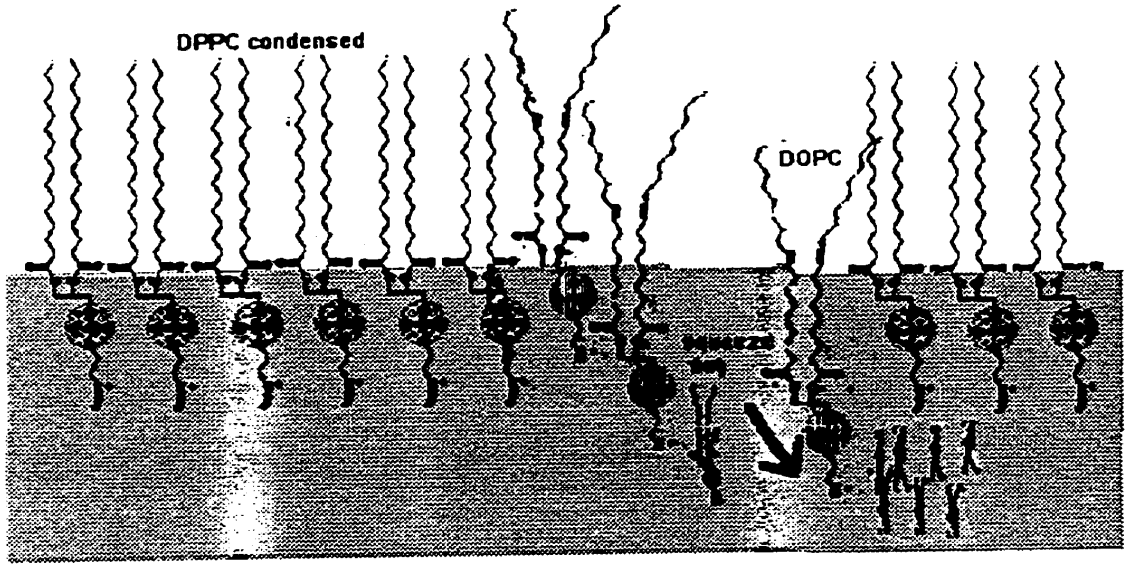
DPPC condensed
DOPC

to the liquidus of the bilayer phase diagram at 23°C, and the appearance of only very small condensed domains in the corresponding monolayer is consistent with the mixture not readily forming condensed domains. The other two mixtures show condensed domains consistent with their location in the bilayer phase diagram. The similarity of the properties of the monolayers and bilayers would suggest that it is reasonable to assume that the condensed domains in the monolayers are enriched in DPPC. Tchoreloff et al., (1991) has studied similar DPPC:DOPC monolayers by electron microcopy. They observed that in DPPC:DOPC 50:50 monolayers near collapse pressures patchy areas 10 Å thicker than those of the background monolayer could be observed (Tchoreloff et al., 1991). The patches have been suggested to be representative of rigid hydrocarbon regions coexisting with fluid areas (Tchoreloff et al., 1991).

3.42] Peculiarity of the LE-LC transition in DPPC/DOPC films.

In all the mixed monolayers studied the average size of the condensed domains increased up to a surface pressure of 35 mN/m and then decreased with higher pressure. The domain sizes and the percentages of condensed domains were also affected by the amount of unsaturated lipid in the monolayers. As would be expected, for any given π, larger condensed domains and greater total coverage with condensed domains were correlated with increasing DPPC concentration in the mixed monolayers. At surface pressures higher than 35 mN/m, the decrease in domain size and in the total condensed lipids indicates that, a more complex process of lipid mixing (particularly lipid-probe mixing), and chain reorientation may be occurring. A process of liquid ordering of

DOPC could be consistent with the observation that, above π = 35 mN/m in all the mixed monolayers, fluorescent regions with reduced intensity together with very small (2-4 μm) regions of intense fluorescence could be seen. Above pressures of 35 mN/m also, the sizes of the condensed domains decreased in the mixture with 69 and 49 mol % DPPC. As the condensed domains initially nucleate under pressure, they would be rich in DPPC. As further condensation occurs, however, sufficient DOPC may be accumulating in the condensed regions to cause the probe to be dissolved in them. Recent studies using Brewster angle microscopy (BAM) of pulmonary surfactant (lipid extract) monolayers indicate that the condensed domains also decrease in amount and size at π above 40 mN/m (Discher et al., 1996). Since BAM techniques do not require fluorescent probes in the films to visualize condensed domains, the explanation given above about solubility of probe cannot explain the phenomena of decreasing condensed phase in such films at $\pi > 40$ mN/m.

Also from results of our studies on pulmonary surfactant lipid extracts (Chapter 11), and the BAM evidence (Discher et al., 1996) it seems that the decrease of LC domains in these DPPC:DOPC monolayers is due to a more complex process, than a simple disorder-order phase transition. Others have speculated that in DPPC:DOPC bilayers, during the thermotropic phase transition there may be liquid ordered regions coexisting with the fluid phase (Bashford et al., 1976; Lee et al., 1974). It was suggested that this liquid ordering may be due to short range order in the hydrocarbon region of the fluid lipids (Bashford et al., 1976). Fourier transform infrared spectroscopy indicates that the order of the chains of DPPC in monolayers increases

during compression (Dluhy et al., 1989). Since the packing area of the lipids in a partially ordered fluid phase in DPPC:DOPC films will be less than that in the fluid phase, there may be less "need" to exclude solid DPPC into condensed domains and this may be why the dark domains decrease slightly in size above pressure of 35 mN/m. It is also possible that at higher pressures the condensed domains are fragmented to sub-micron structures which are not detectable by optical microscopy, thereby the total amount of condensed domains measured are under estimated. The details of how such processes can occur are discussed further in chapter 11.

3.43] Squeeze-out from DPPC/DOPC films.

Recycling of equimolar mixed monolayers of DPPC:DOPC for a number of cycles at a fast speed, resulted in an appearance that was consistent with a loss of unsaturated lipids from the monolayer. The percent of condensed lipids in the fields or images after 11 cycles of fast barrier movement was increased about three-fold over that of a monolayer compressed only once (Figure 3.5). A schematic diagram of such "squeeze out" process is shown in Figure 3.6 (lower panel). This evidence suggests that during cyclic compression and expansion some lipids which dissolved the probe were being excluded from the monolayer. The exclusion may involve both lipid species, but the unsaturated lipids would appear to be squeezed out to a greater extent than the saturated lipid, since the percentage of condensed domains is likely a good marker of the saturated lipid content in the monolayers. Preferential squeeze-out of the unsaturated lipid species has been suggested to occur in similar mixed monolayers under rapid

compression (Egberts et al., 1989; Hawco et al., 1981a; Notter et al., 1980), and it may be an important factor in the function of pulmonary surfactant. This finding is consistent with the presumption that pulmonary surfactant is refined in the surface by selective squeeze-out of unsaturated species (Hawco et al., 1981a; Hildebran et al., 1979; Notter et al., 1980). It is interesting to note that Schürch *et al* ., (1989), using whole natural surfactant in a captive bubble apparatus, found that one slow compression can yield bubble shapes consistent with the presence of a monolayer highly enriched in DPPC. The composition of the surfactant may lead to a much more effective selective "squeeze-out" of non-DPPC components than seen in this simple model. Such a process in natural surfactant could be promoted not only by special lipid composition, but also by the presence of unique proteins (Curstedt et al., 1987).

3.44] Fluidity of mixed PC films:Biological Relevance ?

At the usual temperature of biological organisms, membranes consist mainly of fluid and, occasionally, some rigid lipids. Such systems are complex in their phase miscibility. This study suggests that in mixed monolayers of DPPC:DOPC at pressures feasible in membranes condensed regions coexist with a partial ordered fluid phase. Such partially ordering of charged fluid lipids into small areas in single leaflets of bilayers has been observed in unilamellar vesicles by fluorescence microscopy (Haverstick and Glaser, 1989). In that case the regionally-ordered areas were induced by cytochrome c or calcium ions (Haverstick and Glaser 1987; 1988; 1989).

Pulmonary surfactant is a mixture of saturated and unsaturated lipid plus protein.

These results indicate that the amount of condensed phase which can occur if there is unsaturated lipid present is less than one expects on the basis of loss of components. In simple models of pulmonary surfactant where unsaturated and saturated components are mixed (i. e. Hawco et al., 1981a; 1981b., and this work), the small amounts of condensed regions may explain why, under slow compression, the monolayers collapse before high π is reached, since fluid lipid monolayers collapse at lower π than the ones made with rigid or condensed lipids (i.e. DPPC). Although instrumental limitations prevented us from performing experiments at 37°C, a number of species (reptiles) and their surfactant function at lower temperatures.

[** *Parts of this chapter and the figures used have been published as Nag and Keough, (1993), in the Biophysical Journal (Appendix B, No. 9). Reprinted with permission from the publisher and co-author.*]

Chapter 4

PHOSPHATIDYLGLYCEROL

AND

CALCIUM

INTRODUCTION

Phosphatidylglycerol (PG) is the major acidic lipid component of pulmonary surfactant. PG is found in significant amounts (8-10 weight%) in most adult mammalian lung surfactant, except in surfactant of the rhesus monkey, although its absence is compensated by higher amounts of other acidic lipids such as PI in such species (King, 1984; Sanders and Longmore, 1975). About 30% of the PG in surfactant is estimated to be disaturated (16:0/16:0-PG) (Adachi et al., 1989). Due to the unbalanced negatively charged phosphate group located in the PG headgroup, the phospholipid has a low (acidic) pK of 3.5-3.8 in 0.1M saline, is singly charged at the physiological pH of 7, and doubly charged at higher pH (Tocanne and Tiesse, 1990). PG is almost absent in antenatal pulmonary surfactant detected in amniotic fluid, and is the major marker for studying fetal lung maturity (Hallman et al., 1976; Hallman and Terano, 1981). Whereas phosphatidylinositol (PI) is the major acidic component in prenatal pulmonary surfactant, it is replaced by PG with lung maturity after birth (Akino, 1992; Gluck, 1995; Hallman et al., 1976; Hallman, 1992).

Phosphatidylglycerol is absent in infants with respiratory distress syndrome (RDS), and decreased in adult-RDS (ARDS). Pulmonary surfactant extracted from patients with such condition, shows altered surface activity when examined *in vitro* (Gregory et al., 1991; Hallman, 1995; 1992; Hallman et al., 1977; 1982; Hallman and Gluck, 1976). Also PG levels in surfactant are decreased in lung diseases such as transient tachypnea (Hallman, 1992) and is increased in surfactant of AIDS patients (Rose

et al., 1994). Also PG has been shown to play some immunosuppressive role in the induction of lymphocyte proliferation by surfactant (Ansfield and Benson., 1980). Re-uptake for re-cycling of pulmonary surfactant materials administered to the alveoli by type-II pneumocytes, is enhanced by the presence of PG (Rice et al., 1989; Oyarzun et al., 1980). *In vitro* assembly of tubular myelin, the highly unusual tube like non-lamellated structure of surfactant requires PG and calcium (Benson et al., 1984).

The alveolar fluid lining or surfactant subphase contains about 1-2 mM calcium, among other mono- and di- valent ions (Nielson 1986; Nielson and Lewis, 1988). Calcium possibly interacts with the acidic headgroup of PG in surfactant (and with other surfactant proteins and lipids) and allows for the formation of structures such as tubular myelin. Tubular myelin allows for rapid adsorption of surfactant to the air-alveolar fluid interface (see section 1.2). Similar concentration of calcium (2 mM) have been shown to transform normal lamellar structures of PS into tubular myelin (Benson et al., 1984). A number of *in vitro* surface activity measurements indicate that PG enhances the surface activity of PS lipids by enhancing the spreading, adsorption and re-spreading of the material at an air-water interface (Brummer et al., 1995; De Fontagnes et al., 1984; Egberts et al., 1989; Fleming et al., 1983; Fleming and Keough, 1988; Keough, 1992; Notter et al., 1980; Wojciak et al., 1985).

The phospholipid PG is unusual and specific for pulmonary surfactant, as it is not found in significant concentrations in any other eukaryotic cells, although it is present in high amounts in bacterial membranes (Gennis, 1989; Schleifer and Stackebrandt, 1983). Interestingly, acidic phospholipids such as phosphatidylglycerol in bilayers under

the influence of calcium, show some unusual thermotropic properties and fusogenic (ability to fuse vesicles) potential (Findlay and Barton, 1978; Leckband et al., 1993; Verkleij et al., 1974). To understand the properties of the acidic lipid-calcium phases, fusogenic potential of lipid bilayers, and their use as models of biological membranes, some studies using fluorescence microscopy of films of PG (Evert et al., 1994; Leckband et al., 1993) and other acidic-lipid systems have been performed to date (Eklund et al., 1988; Lösche and Möhwald, 1989; Maloney and Grainger, 1993; Möhwald, 1990). Some of these studies have indicated that cations can condense, and induce lateral phase separation in films of acidic phopholipids by strong electrostatic interactions (Evert et al., 1994; Eklund et al., 1988).

Although most of the PG species present in pulmonary surfactant are unsaturated, in order to avoid complication in interpretation because of effects of chain length and saturation in our examination of how headgroups of PG and phosphatidylcholine interact, we have studied mixtures of dipalmitoylphosphatidycholine (DPPC) and dipalmitoylphosphatidylglycerol (DPPG) films using fluorescence microscopy under the influence of small (mM) amounts of calcium. The study was also aimed at understanding the film properties of DPPC:DPPG mixtures, as a ground work for studying more complex lipid-lipid-protein (DPPC:DPPG:surfactant protein) films of PS (discussed in chapter 6).

MATERIALS AND METHODS

1, 2-dipalmitoyl-*sn*-glycero-3-phosphocholine (DPPC), 1, 2-dipalmitoyl-*sn*-glycero-3-phospho-*rac*-glycerol (sodium salt) (DPPG-Na) and 1-palmitoyl-2-(12-(7-nitro-2(1,3-benzoxadiazole-4yl)amino)-dodecanoyl) phosphatidylcholine (NBD-PC) were purchased from Avanti Polar Lipids, Pelham, AL. The lipids were found to be pure by thin layer chromatography (Silica-gel-G), and used as received.

The lipids were dissolved in chloroform:methanol 3:1 (vol/vol) and mixed in desired molar ratios. Monolayers were spread on a subphase containing 0.15 M NaCl buffered with 5 mM Tris-HCl and pH adjusted to 6.9 (with and without 1.6 mM $CaCl_2$). The salinity, pH and calcium concentration of the subphase were similar to those found in alveolar and other extracelluar fluids (Nielson and Lewis, 1988). The subphase was prepared with deionized, doubly distilled water, the second distillation being from dilute $KMnO_4$. Care was taken to obtain the deionized water completely void of any ionic contaminants, since small (nanomolar) amounts of cations can drastically alter the liquid condensed phase structures in acidic lipid films (Lösche and Möhwald, 1989). The ionic content of the doubly distilled water was checked by semi-quantitative mass spectrometry and it was found to be as free of inorganic ions as any standard mass spectroscopy grade water samples available. All experiments were performed at a temperature of 22 $\pm$ 1°C.

The experiments were performed on a epifluorescence microscopic surface balance whose design and performance is discussed in the previous chapter. The monolayers were compressed slowly at an initial rate of 0.13 $Å^2.molecule^{-1}.sec^{-1}$ (20

$mm^2.sec^{-1}$) in steps and compressions were stopped for 1 minute at each step, during which the films were visually observed and video recorded. Typical images were analyzed and the total amount of condensed (black) phase was determined as a function of surface pressure by methods discussed in Appendix A.

RESULTS

The typical surface pressure-area (π-A) isotherms of DPPC, DPPG and DPPC:DPPG (mol/mol) 9:1, 7:3, 5:5, 3:7, 1:9 plus 1 mol % NBD-PC (minus calcium in the subphase, i.e. the DPPG-Na) are shown in Figure 4.1 (top), and typical images seen in some of the monolayers at a similar π (bottom). The π-A isotherms indicate that DPPC and DPPG-Na monolayers had almost similar π-A behaviour, and all mixed monolayers could be compressed to high π of $\sim$ 70 mN/m. The liquid expanded (LE) to liquid condensed (LC) plateaus, or flat portions of the isotherms for the DPPG monolayers indicated that, the LE-LC transition for the monolayers of DPPG occurred at a slightly higher π than that for DPPC, but with increasing DPPC content this transition plateau was shifted towards that of DPPC. Also the visual features observed in all the DPPG-Na and the DPPC:DPPG-Na films were similar to those observed for DPPC films alone. The LE-LC phase transition of such films showed the formation and growth of LC domains on a fluorescent LE background, as seen for DPPC alone, except that for DPPG the LC domain were observed to appear at a slightly higher π, corresponding to the higher LE to LC plateaus in the isotherms. The sizes of the condensed domains in the DPPC, DPPC:DPPG and DPPG systems were somewhat similar. These features indicated that the lipids seemed to be quite well mixed in the condensed or expanded phase. The π-A properties of DPPG-Na and DPPC:DPPG-Na are similar to the ones previously observed by others (Bredlow et al., 1992; Pastrana-Rios et al., 1994; Rana et al., 1993; Sacré and Tocanne, 1977). Similar physical

Figure 4.1 Isotherms of DPPC, DPPG and their mixtures (DPPC:DPPG-Na 9:1, 7:3, 5:5, 3:7, 1:9; mol/mol) containing 1 mol% NBD-PC. The isotherms were constructed over a saline subphase at pH of 6.9 (top), and typical images seen in some of these monolayers at a $\pi \sim 13$ mN/m (bottom).

The black areas in the images represent the liquid condensed (LC) and the white the liquid expanded (fluid) phase. The symbols in top left of the images indicate the lipid films from which they were obtained. Scale bar is 25 μm.

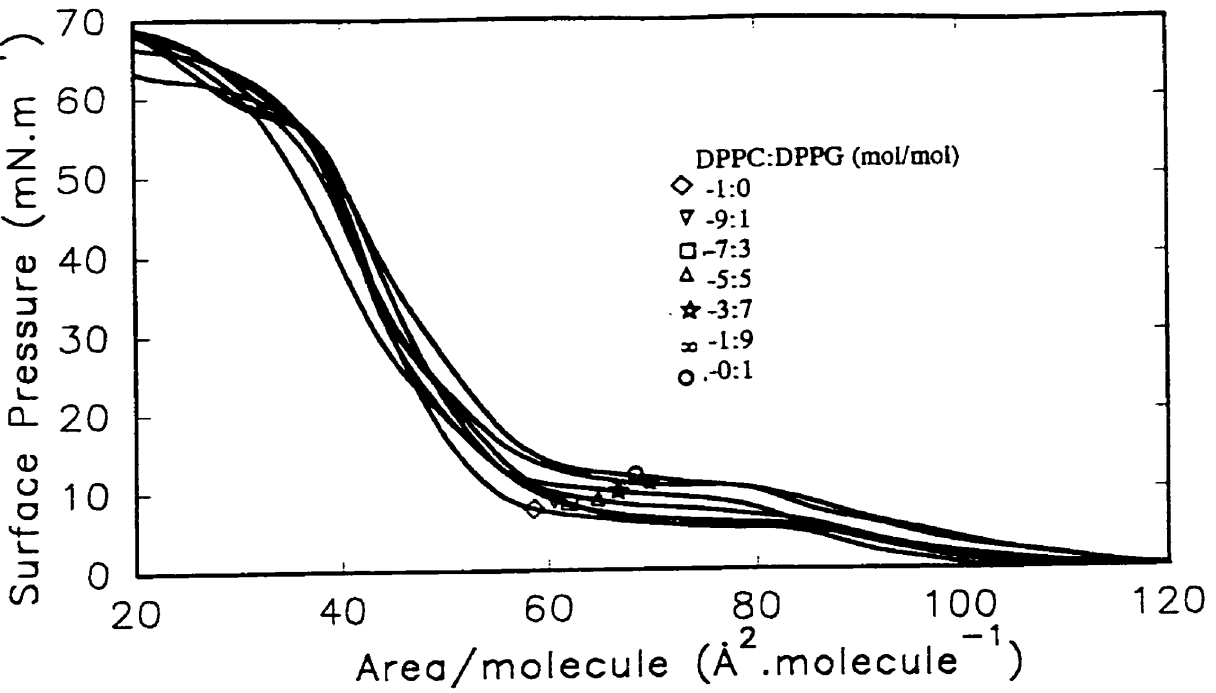
Surface Pressure (mN.m^{-1})
70
60
50
40
30
20
10
0
20
40
60
80
100
120
Area/molecule (Å^2.molecule^{-1})
DPPC:DPPG (mol/mol)
-1:0
-9:1
-7:3
-5:5
-3:7
-1:9
-0:1

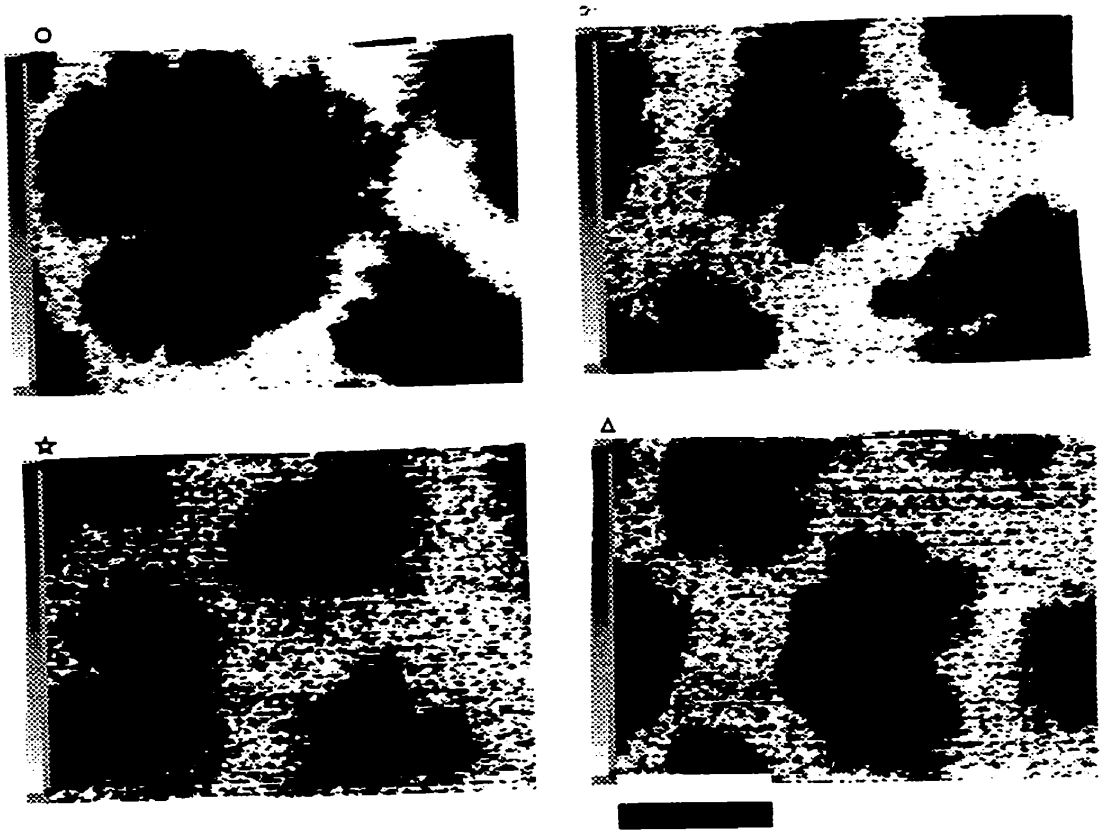
○
☆
△

properties, such as gel to liquid–crystal phase transition temperatures, have been observed previously with saturated PC and saturated PG (Findlay and Barton, 1978; Fleming and Keough, 1983; Verkeleij et al. , 1974). The lipids appear to pack in the same fashion, and so their monolayer and bilayer properties are quite similar.

The π-A isotherms of DPPG, DPPC and DPPC:DPPG (9:1, 7:3, 5:5, mol/mol) monolayers with 1.6 mM calcium in the subphase are shown in Figure 4.2 (top), and the typical images seen in some of these films at a similar π (bottom). The DPPC:DPPG-Na films showed transition plateaus corresponding to an LE-LC transition in the range 7-10 mN/m. Also all the mixed films without calcium could be compressed to $\pi \sim 70$ mN/m, showing negligible effects of DPPG on the packing of DPPC when the subphase contained only sodium ions. Isotherms of the same mixtures on a similar subphase containing 1.6 mM calcium (closed symbols) showed a reduction of the π of the LE-LC transition, and the isotherms indicated an apparent collapse of the monolayers containing DPPG-Ca and DPPC:DPPG-Ca (3:7, 5:5) at π less than 70 mN/m. Similar effects of divalent cation binding of acidic lipid headgroups on the LE-LC plateaus of the isotherms have been observed by others,. and suggested to be due to a condensing effect of these ions on the phase transition of such acidic lipids in films (Evert et al., 1994; Leckband et al., 1993; Lösche and Möhwald, 1989; Taneva and Keough, 1995).

Subsequent experiments indicated that the apparent collapse of the DPPG-Ca and DPPC:DPPG-Ca films at relatively low π, compared to that in DPPC or the DPPC:DPPG-Na films, may have been induced by the design of the fluorescence balance. The balance contained a teflon collar inserted in the area of observation and

Figure 4.2 Isotherms of DPPC, DPPG and DPPC:DPPG (9:1, 7:3, 5:5; mol/mol) monolayers constructed over a saline subphase containing 1.6 mM calcium (DPPG-Ca) (top) and typical images seen in such films at a $\pi \sim 7$ mN/m (bottom). Isotherms with open symbols represent the monolayers formed on 0.15 M Na subphase only (DPPG-Na), and those with closed symbols represent monolayers formed on a subphase containing 0.15 M Na and 1.6 mM Calcium (DPPG-Ca).

The symbols on left of the images represent the films from which the images were obtained, at a π of 8 mN/m. Scale bar is 25 μm.

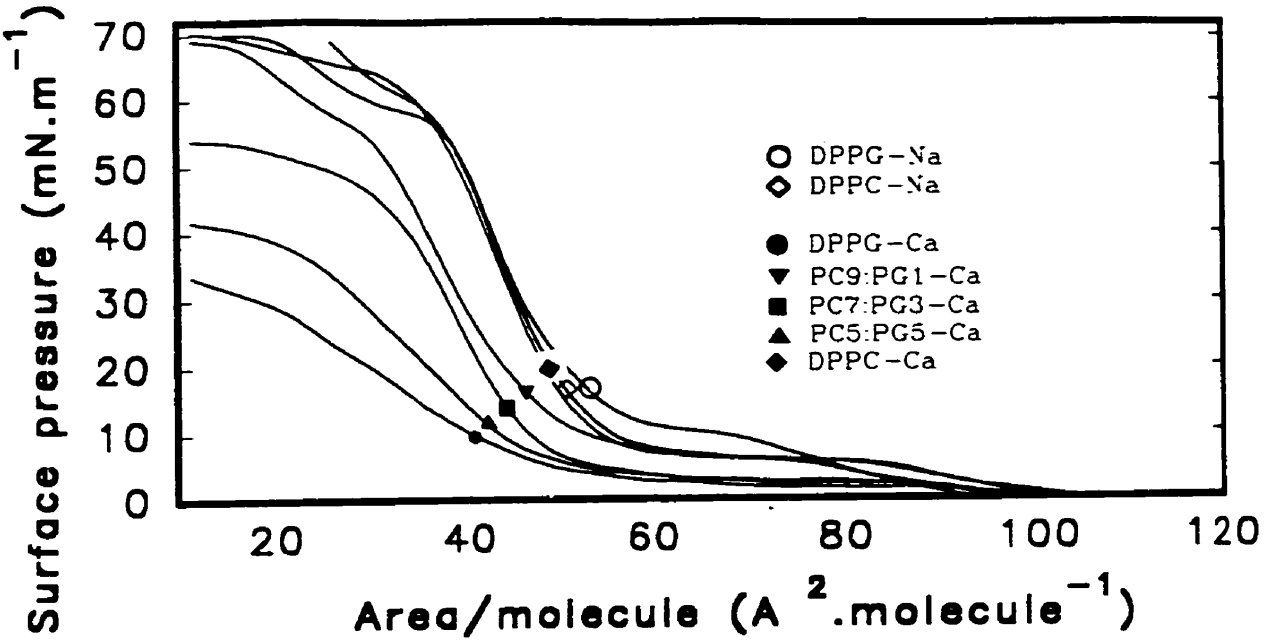
Surface pressure (mN.m^{-1})
70
60
50
40
30
20
10
0
20
40
60
80
100
120
Area/molecule (A ^{2}.molecule^{-1})
DPPG-Na
DPPC-Na
DPPG-Ca
PC9:PG1-Ca
PC7:PG3-Ca
PC5:PG5-Ca
DPPC-Ca

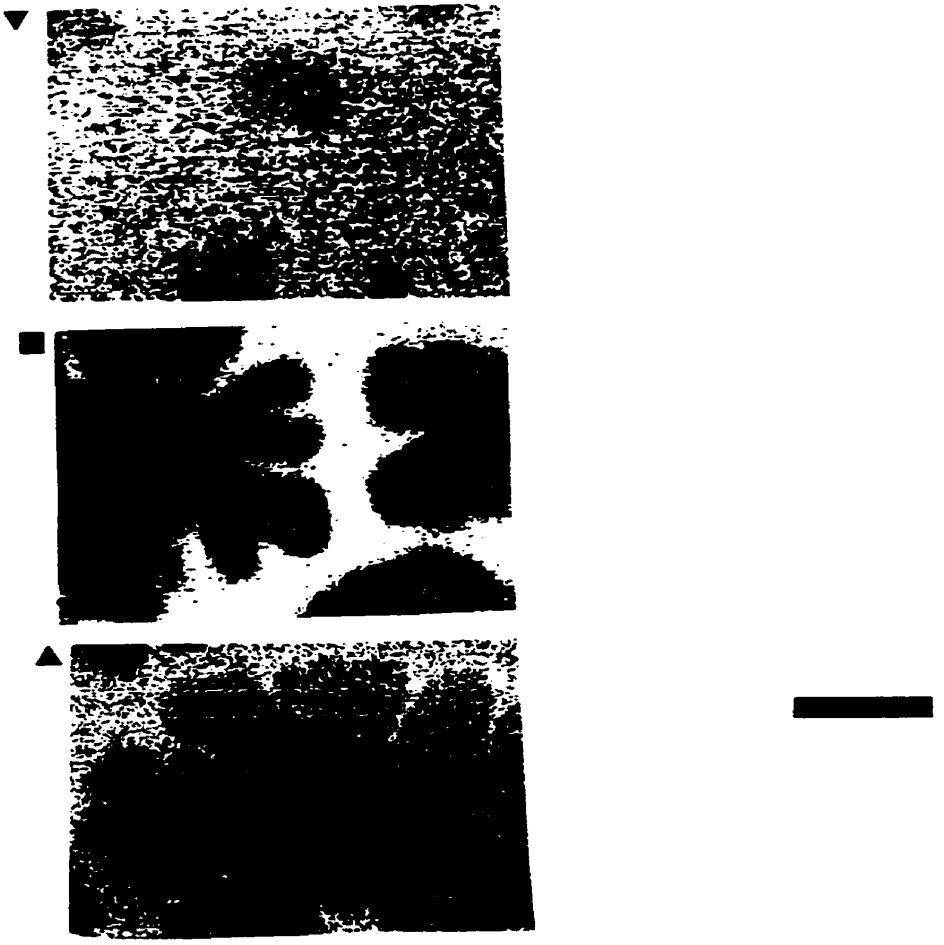

surface pressure measurement of the trough to reduce monolayer flow during visual observation. The teflon collars were connected by small canals to the main body of the trough (see Figure 2.3, bottom). The Wilhelmy plate used for measuring surface pressure is also contained in the collar region. Comparing the collapse π of the DPPC:DPPG-Ca films (shown here), with those obtained by others using a balance without the collar (Taneva and Keough, 1995), we found some discrepancies in the values of the collapse π. The DPPC:DPPG-Ca films in the latter system collapsed at a much higher π (Taneva and Keough, 1995) than seemed to be the case in this study. We interpreted, this difference to be due to the high viscosity of DPPC:DPPG-Ca films, which did not allow the packing of the DPPG-Ca molecules to reach the same state in the Wilhelmy plate dipping area (where the π is measured) as in the main parts of the film. Thus the pressure sensing plate did not pick up the change of π as rapidly as the monolayer area was changed. This occurred even though the balance was operated at a very low compression rate.

The visual features seen in the films of DPPC:DPPG-Ca (Figure 4.2) are quite different from the ones seen for DPPC and the DPPC:DPPG-Na systems. The LC domains in the DPPC:DPPG-Ca systems were larger and had "flower-like" shapes than those found in systems without calcium (Figure 4.1). Similar flower-like domains have been observed by others in acidic lipid films with divalent cations (Ca^{2+}, Mg^{2+}) (Lösche and Möhwald, 1989). This change of the shapes and sizes of the LC domains gave an indication that there were possibly strong electrostatic interactions between the negatively charged phosphate and the divalent positively charged calcium ion. Lösche and Möhwald,

Figure 4.3 Plot of percentage of the total area occupied by the condensed (black) phase plotted as a function of surface pressure (π). The symbols shown in the inset represent the isotherms containing similar DPPC:DPPG mixtures as shown in Fig. 4.1 and 4.2. Error bars indicate $\pm$ one standard deviations of an average of ten images analyzed at each π.

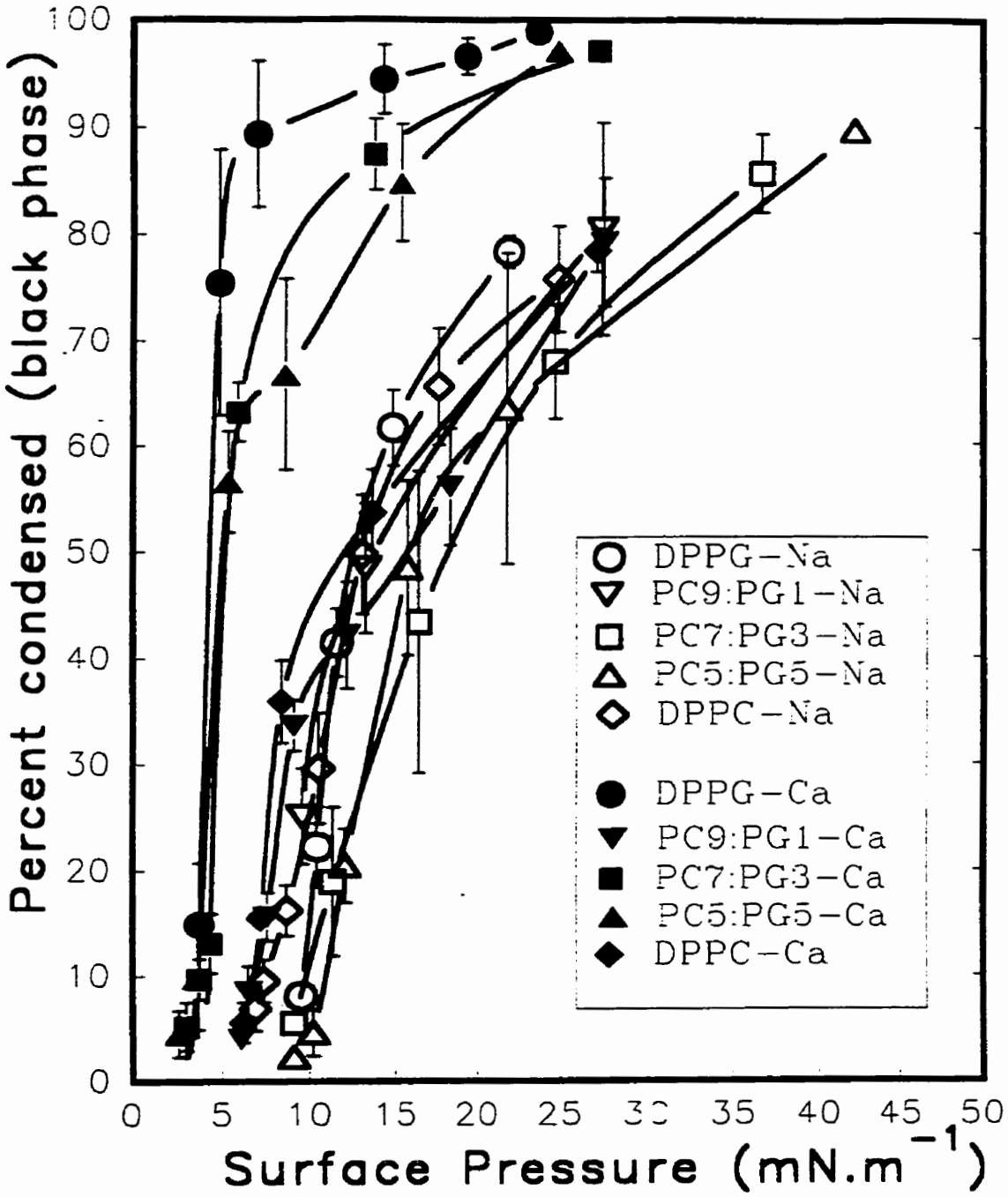
Percent condensed (black phase)
100
90
80
70
60
50
40
30
20
10
0
0
5
10
15
20
25
30
35
40
45
50
Surface Pressure (mN.m^{-1})
DPPG–Na
PC9:PG1–Na
PC7:PG3–Na
PC5:PG5–Na
DPPC–Na
DPPG–Ca
PC9:PG1–Ca
PC7:PG3–Ca
PC5:PG5–Ca
DPPC–Ca

(1989), have indicated that the cation upon binding to the acidic lipid headgroups, alters the interfacial line tension between the LE and LC phase, and thus the domains are more convoluted than the more rounded or elliptical appearance of them in systems where no such interactions occur (i.e. DPPC or DPPC:DPPG-Na).

As shown in Figure 4.3, the percentage of total area occupied by the condensed domains, or black phase, in the presence of calcium showed an increase at equivalent π, with increasing DPPG in the films. In the absence of calcium, all the monolayers gave similar results for the amount of condensed phase, indicating that there were no significant differences in the amount of condensed phase between DPPC and DPPG films at comparable π (open symbols). This may indicate that the phospholipids mixed well in either of the phases, even with the headgroup differences being present. Monolayers containing 10 mol % DPPG had similar amounts of condensed phase to those seen in the absence of calcium. In those containing more than that amount the curves of percentage of condensed phase vs π were shifted substantially to the left, indicating that a greater degree of condensation had occurred at all π in the films in the presence of calcium than in its absence. Also, the percentage of condensed domains in the monolayers containing $>$ 10% DPPG (with calcium) increased sharply between 5 and 15 mN/m compared to those without the cation. At a comparable π of 20 mN/m, DPPG-Ca films showed higher total condensed phase ($>$ 90%) compared to the DPPG-Na ($\sim$70 %) system. This indicated that calcium in millimolar amounts can increase the amounts of condensed phase of acidic lipid films and drastically affects the LE to LC transition of such films.

DISCUSSION

4.41] No phase segregation in PC/PG mixed films.

Fluorescence microscopy has been used to study in detail the ionic interactions of divalent cations with acidic phospholipid films. Divalent cations have been proposed to induce lateral phase separations or phase transitions in bilayers, as a result of specific ion-lipid interactions and this may lead to membrane fusion (Findlay and Burton, 1978; Leckband et al., 1993). Calcium induced condensation of the PG headgroups probably results from additional hydrophobicity or interaction between the domains and domain boundaries in two opposing bilayers, and induces fusion in such systems (Leckband et al., 1993). Using fluorescence microscopy of DMPC/DMPG films, below their phase transition temperature, 5 mM calcium does not induce any condensed domains at π where the films are in the LE phase, indicating miscibility of the two lipids in that phase (Leckband et al., 1993). Whereas in DLPC/DLPG systems (at 25 °C, which has only LE phase at all π) slow but gradual phase segregation or separation of probe containing and excluding domains have been observed (Leckband et al., 1993). Others have observed that more chaotic LC domain shapes are observed in acidic phospholipid films with increasing calcium concentration from the micromolar to millimolar range, and have proposed that divalent cations effect nucleation, shapes and sizes of LC domains (Lösche and Möhwald., 1989). Palmitic acid was seen to phase separate in films of DPPC, in the presence of calcium, and also cationic fluorescent dyes were found to bind to such domains (Maloney and Grainger, 1993). Others have suggested, from π-A measurements

of different chain length acidic phospholipid films, that calcium and other cations can interact with DPPG films in the gel but not in the fluid phase (Sacré and Tocanne, 1977). This study similarly suggests that calcium was able to maintain complete miscibility of the two lipids in the monolayers and influence the phase transition of such lipid systems containing small, moderate and high amounts of the acidic PG. Figure 4.4 suggests the packing of DPPC with DPPG in films at the air-water interface, and the effect of calcium on such films (bottom panel).

4.42] Calcium and dehydration of PG.

The divalent ion calcium affected the acidic DPPG and even the DPPC:DPPG (7:3) systems, but not the zwitterionic lipid DPPC. The negatively charged headgroup of PG is probably dehydrated by calcium binding to it (Figure 4.4, bottom panel). Binding of divalent cations to acidic headgroups can induce phase transitions in the case of fluid monolayers (Evert et al., 1994) or the formation of larger condensed domains (and the occurrence of high percentage condensation) at any π, such as seen in this study. The calcium ions probably bind to the phosphate headgroups and cause the intermolecular interaction of headgroups, especially those of acidic PG, to produce a more ordered phase at any given temperature. Headgroup dehydration could also lead to a change of orientation of the molecules, or straightening of the chains, as illustrated in Figure 4.4 (bottom panel). This would allow for the formation of larger condensed domains, into which the probe could not diffuse or penetrate. A higher proportion of condensed phase at lower surface pressure is associated with this tight intermolecular packing. Also,

Figure 4.4 Molecular representation of DPPC:DPPG mixed films at the air-water interface.

The top panel indicates, although there is a difference in charge and size of the polar headgroup, the molecules DPPC and DPPG accommodate each other quite well in the loosely or tightly packed phase in films. The bottom panel indicates that this accommodation of the molecules in each phase do not change under the influence of divalent calcium, but rather electrostatic interactions between the ion and the PG headgroup tilts the DPPG molecules towards the perpendicular of the air-water interface (or condenses the film).

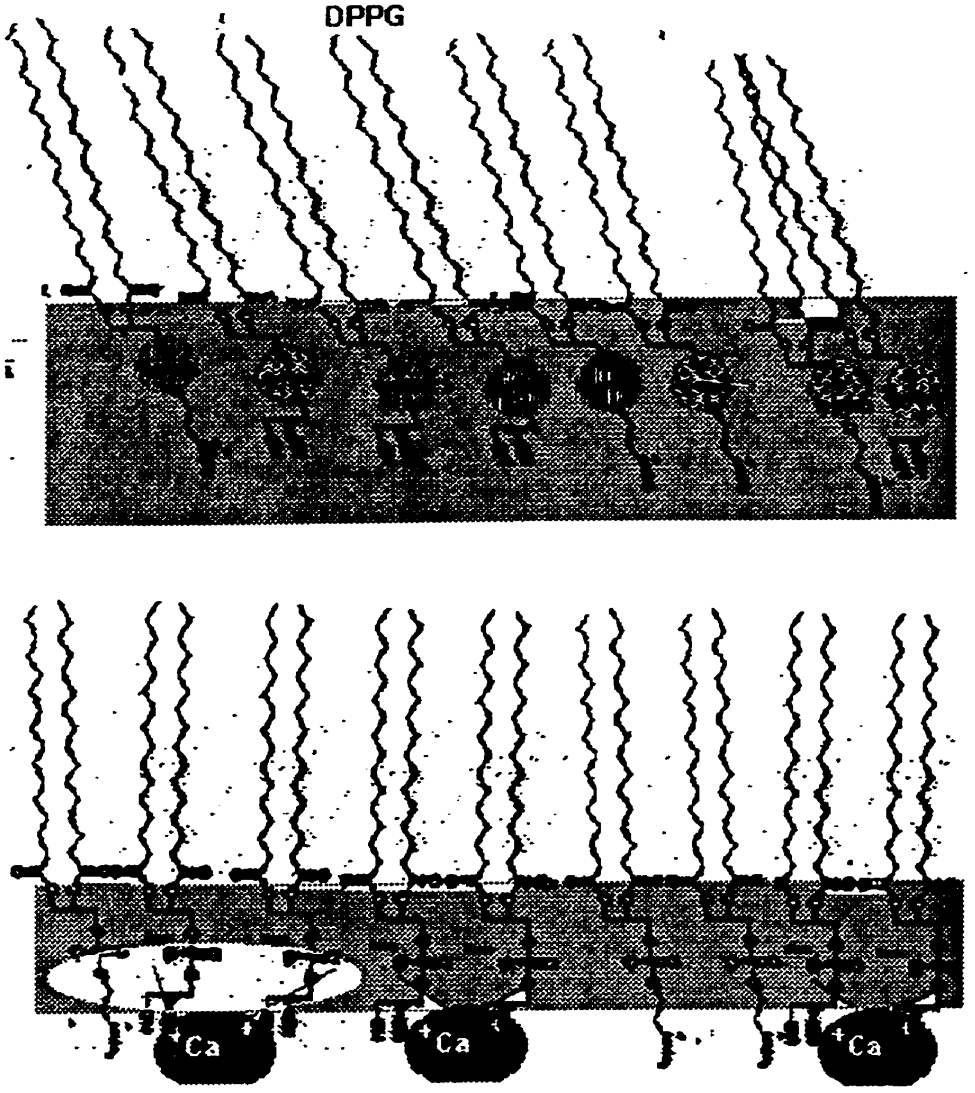
DPPG
Ca
Ca
Ca

associated with the binding of calcium, there could be a significant headgroup dehydration (Findlay and Barton, 1978; Fleming and Keough; 1992; Verkleij et al., 1974). This may promote the "squeeze out" process as suggested by others to occur in pulmonary surfactant (Egberts et al., 1989). Removal of lipids in a three dimensional structure would not require as great an energy input if the number of water molecules associated with the headgroups were reduced from that in the fully hydrated state.

4.43] Role of PG in Pulmonary Surfactant.

The dehydration process may also play a significant role in adsorption of pulmonary surfactant. From bilayer studies of phospholipids under different states of hydration, it has been shown that minimally hydrated phospholipid bilayers spread very rapidly at the air-water interface (Bangham et al., 1979; Morley et al., 1978). These authors have suggested that the spreading of lipids occurred due to the force of hydration of the phospholipid headgroups in the dehydrated bilayers, and others that minimally hydrated bilayers can have open ends or defects (Bangham et al., 1979; Keough, 1992). The adsorption process of pulmonary surfactant to the air-water interface was found to depend on its acidic lipid content and calcium. Also it has been indicated that PG containing bilayers under the influence of calcium form meta-stable phases (Lentz et al., 1982; Verkeleij et al., 1974). Non-bilayer and metastable phases have been implicated in promoting the rapid absorption of pulmonary surfactant to the interface (Keough, 1992). The PC:PG-Ca dehydrated phase observed in our study may be such a phase, which would enhance the adsorption of the materials at an air-water interface.

Films of DPPC containing small to moderate amounts of PG have been studied as models of pulmonary surfactant, since it was indicated that such films could attain high π at minimal compression and showed good spreadability. Films of DPPC containing 10 to 30 mol% unsaturated PG, can be compressed to high π, indicating that the unsaturated components may be selectively squeezed out of such films, although such films did not show any enhanced re-spreading rates compared to DPPC alone (Fleming, et al., 1983). Re-spreading after dynamic collapse though was found to be enhanced in a 90:10 (DPPC:PG, mol:mol) system by others (Notter et al., 1980a). It has been suggested that in DPPC:PG film systems containing calcium, the material may re-spread quickly from the collapse phase during dynamic compression-expansion of such films (Fleming and Keough, 1988). Recently using infrared spectroscopy (FTIR) on DPPC:DPPG (7:1) films, others have indicated that there is no squeeze-out of either component from the films at high π (Rana et al., 1993), whereas in DPPC:POPG mixtures, the unsaturated component POPG was squeezed out (Pastrana-Rios, 1994). Since some of the pulmonary surfactant PG is saturated (DPPG) (Akino, 1992; Sanders and Longmore, 1975; King, 1984) it is tempting to speculate on another role of the saturated phospholipids in surfactant, which is that DPPG enhances the stability of DPPC films at high π, as also suggested by others (Rana et al., 1993). A recent study indicates that calcium ions interact with a particular subset of phospholipids in calf lung surfactant extracts, and increase the molecular order in such extracts (Ge et al., 1995). We have also observed a similar effect of the cation on pulmonary surfactant lipid extract films at the air-water interface (Chapter 11). It is not yet clear what complex role PG plays

in the surface activity of pulmonary surfactant. This study at least indicates that PG is miscible with PC in films, and that calcium can interact strongly with such lipid in films. Also the interactions of this phospholipid and calcium with surfactant proteins (discussed in chapter 6) may further implicate other roles of PG in surfactant.

[*Small parts of this chapter was published as Nag et al., 1994 in Thin Solid Films (Appendix B, No. 6)*]

Chapter 5

CHOLESTEROL

INTRODUCTION

Cholesterol is one of the most studied components of biological membranes, whereas its role in pulmonary surfactant is only beginning to emerge. The sterol is the major neutral lipid constituent of pulmonary surfactant (PS), varying from 3 to 10 weight percent in PS from various species, and its level also varies in the PS of animals acclimatized to different temperatures (Daniels et al., 1995; Fleming and Keough, 1988; Keough, 1984; King and Clements, 1972a; Yu et al., 1983). In bovine pulmonary surfactant cholesterol is present at levels as low as 3 wt % of the total lipids (Yu et al., 1983; Yu and Possmayer, 1993; 1994), whereas in PS from rats, dogs and humans it can reach as high as 10 - 13 wt % (Daniels et al.,, 1995; King and Clements, 1972a), or in average constitutes about 15 mol% of the total lipids of pulmonary surfactant of some species (Keough, 1992).

Intratracheal administration of liposomal suspensions of cholesterol with other surfactant materials indicate that the clearance of the sterol by type-II pneumocytes occurs similarly to DPPC, indicating that the cholesterol is an integral component of PS (Pettenaizzo et al., 1989). About one percent of the surfactant cholesterol is actually synthesized by type-II cells, as most of it is cycled from unloaded material of circulating low density lipoprotein to the type-II pneumocytes (Haas and Longmore, 1980). Cholesterol enhances the spreadability, re-spreadability and adsorption of pulmonary surfactant lipids, and alters the stability of surface films of PS (Fleming and Keough, 1988; Hildebran et al., 1979; Notter et al., 1980b; Taneva and Keough, 1995; Yu et al.,

1983). Recently it has also been indicated that surfactant protein-A (SP-A) and calcium affect the ability of cholesterol to alter the PS films stability (Yu and Possmayer, 1993; 1994).

Cholesterol is present in an abundance of around 20-40 wt % of lipids in most biological membranes, and is an extremely important regulator of biomembrane fluidity (Gennes, 1989; Yeagle, 1985; 1993). Mammalian cell membranes may utilize endogenous or exogenous sources of cholesterol for regular maintenance of membrane structure and growth, and cholesterol determines certain physical properties of biological membranes such as fluidity or permeability (reviewed by Yeagle, 1993; 1985). Model phospholipid bilayer studies with 0 -50 mol % of cholesterol have indicated that the sterol can laterally segregate into cholesterol-rich or cholesterol-poor domains. In such systems the phase diagrams are complicated and contain a host of lipid phases beyond the simple gel or liquid crystalline phases seen in most phospholipid systems (Estep et al., 1978; Smutzer and Yeagle, 1985).

Numerous studies on interaction of cholesterol with phospholipid films have been performed as models of biological membranes (reviewed in Cadenhead, 1985) and over the last decade utilising fluorescence microscopy (Benvegnu and McConnell, 1993; Heckl et al., 1986; 1988; Hirschfeld and Seul, 1990; Hwang et al., 1995; Mattjus, 1995; Mattjus and Slotte, 1994; Seul, 1990; Slotte, 1995; Slotte and Mattjus, 1995; Subramanium and McConnell, 1987; Weis and McConnell, 1985). The interest in studying such phospholipid/cholesterol systems in films has grown for many reasons. Films of cholesterol/phospholipid in addition to being models of biological membranes,

can also be used as models of lipoprotein particles (Lund-Katz et al., 1988; Smaby et al., 1994). Lipoprotein particles have phospholipid and cholesterol molecules packaged into various density particles which have a spherical outer monolayer shell made of lipids and apoproteins, and these particles transfer cholesterol among different body tissues using the circulatory system (Chao et al., 1988; Yeagle, 1993). Also the other advantage of studying cholesterol in films is that high amounts ($>$ 50 mol %) of cholesterol can be accommodated in phospholipid surface films which are not possible in liposomes or bilayers, since bilayers with high amounts of the sterol ($>$50 %) are extremely unstable (Collins and Phillips, 1982; Estep et al., 1978). Various phospholipid/cholesterol films, with low to intermediate amounts of the sterol have been studied in detail by us (Worthman et al., 1996) and others using fluorescence microscopy (Hirschfeld and Seul, 1990). The phase diagrams and miscibility of the lipids in films were derived using surface pressure-area profiles, and the phase structures observed have been correlated by fluorescence microscopy (Hirschfeld and Seul, 1990; Lee et al., 1994). Although cholesterol amounts used in such studies rarely exceeded the critical miscibility limit of the lipids in monolayers or bilayers, film studies have been performed with higher ($\geq$ 30 mol%) cholesterol in different phosphatidylcholine systems (Mattjus and Slotte, 1994; Merkel and Sackmann, 1994; Slotte, 1995; Slotte and Mattjus 1995; Worthman et al., 1996).

In this study we employed fluorescence microscopy to study DPPC monolayers with low amounts of cholesterol (2-10 mol percent), to comprehend the properties of such films as models of pulmonary surfactant.

MATERIALS AND METHODS

The lipids 1, 2-dipalmitoyl-*sn*-glycero-3-phosphocholine (DPPC), and cholesterol were purchased from Sigma Chemicals [St.Louis, MO]. Cholesterol was recrystallized from ethanol before use. The fluorescent lipid probe 1-palmitoyl-2-{12-[(7-nitro-2-1,3-benzox- adiazole-4yl) amino] dodecanoyl}-*sn*-glycero-3-phosphocholine (NBD-PC), were purchased from Avanti Polar Lipids (Pelham, AL). The purity of the DPPC and probe were confirmed by thin layer chromatography (TLC). The concentrations of the lipid samples were determined by a modified version (Keough and Kariel, 1987) of an analysis of organic phosphorus described by Bartlett, (1959). The lipids and the probe were dissolved in chloroform:methanol (3:1 vol/vol) and mixed in desired molar proportions (DPPC:cholesterol 99:0, 97:2, 94:5, 89:10, 0:99 mol/mol containing 1 mol% NBD-PC) and stored at -20°C. A solution of saline of 0.15 M NaCl, pH-6.9, made with doubly distilled water, was used as the subphase on which the monolayers were spread. The doubly distilled water had the second distillation performed with dilute $KMnO_4$.

Monolayers were spread on the epifluorescence microscopic surface balance and all experiments were performed at a temperature of 21 ± 2°C. The monolayers were compressed at a very slow initial rate of 20 $mm^2.sec^{-1}$, in steps, and a wait period of 10 minutes was introduced at each step, leading to a final compression speed of 0.022 $Å^2.molecule^{-1}.sec^{-1}$. This relatively very slow rate of compression was chosen to allow for the condensed domains to attain near equilibrium or quasi-equilibrium shapes or states, as discussed by others previously (Weis and McConnell, 1985). During the last

minute of the waiting period the monolayer features were video recorded and analyzed by methods described in Appendix A.

RESULTS

The typical isotherms of DPPC monolayers containing 0-10 (mol%) and 99 mol % cholesterol (plus 1 mol% NBD-PC) are shown in Figure 5.1 (top), and the typical images observed in such films at a $\pi \sim 11$ mN/m (bottom). The DPPC isotherm showed the typical LE-LC phase transition as indicated by the plateau region at $\pi \sim 8$ mN/m, which was slightly shifted to higher pressures by the addition of 2-10 mol % cholesterol. The cholesterol monolayer showed no detectable change of the initial surface pressure of 0 mN/m up to an area per molecule of 46 $Å^2$.molecule^{-1}, and then a sharp increase of surface pressure occurred. The cholesterol film collapsed at a π of 42 mN/m, which was lower than the collapse π of the DPPC of 72 mN/m. The cholesterol isotherm indicated that the lipid underwent a phase transition from highly expanded gas (G) phase to a solid condensed (SC) phase, in agreement with previously reported studies on such systems (Cadenhead, 1985). The typical images from the DPPC/cholesterol films indicated that with increasing cholesterol content, the shapes of LC phase of DPPC were drastically altered. The typical kidney shaped condensed domains of DPPC became spiralled or convoluted into thin filamentous structures. These drastic changes of domain shapes were not accompanied by any significant changes in the π-A isotherms of these systems. The pure cholesterol monolayer (plus 1 mol% NBD-PC) showed a black, almost homogenous single phase, with few small regions of intense fluorescence (last image in Figure 5.1) at all π. This black phase was probably the solid condensed (SC) phase of cholesterol, and such features indicated that the probe NBD-PC was excluded

Figure 5.1 Typical π-A isotherms of DPPC, cholesterol and DPPC + cholesterol (mol%) films containing 1 mol% of NBD-PC are shown (top), and the typical images observed in such film at a $\pi \sim 9$ mN/m (bottom). The films were compressed on a non-buffered subphase of 0.15 M NaCl (pH-6.9) in 20 steps, at a final rate of 0.20 $Å^2$.molecule^{-1}.sec^{-1}. The scale bar is 25 μm.

The black regions in the first four images indicate the liquid condensed phase and the white the liquid expanded phase. In the last image observed from a typical pure cholesterol film, the black region may be a solid condensed (SC), probe excluding phase.

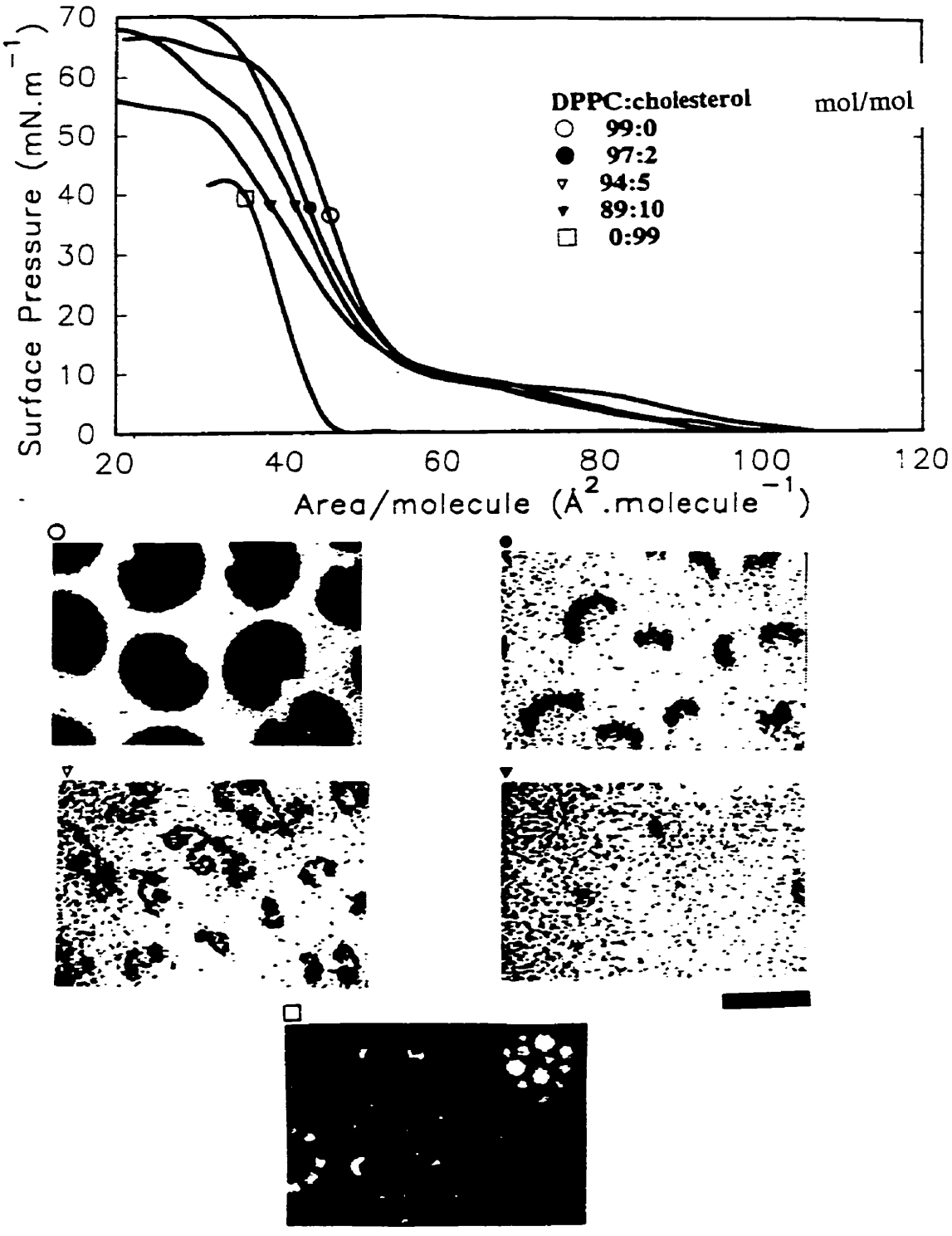
Surface Pressure (mN.m^{-1})
70
60
50
40
30
20
10
0
20
40
60
80
100
120
Area/molecule (Å^2.molecule^{-1})
DPPC:cholesterol
mol/mol
99:0
97:2
94:5
89:10
0:99

Figure 5.2 Typical images observed in films of DPPC + 2 mol% cholesterol compressed in 50 steps (under the same conditions in the last figure, except slowly) showing the evolution of the condensed spiral domains. The final compression rate of the film was 0.022 $Å^2$.molecule^{-1}.sec^{-1}. The surface pressures (π in mN/m) are indicated at the bottom of each image. The scale bar is 25 μm.

The condensed domains grew in length rather than in sizes (circular or elliptical) as seen in films of pure DPPC. The width of the filaments decreased with increasing π. The length of the filaments increased, and spiralled into highly convoluted patterns at π ~ 16 - 18 mN/m.

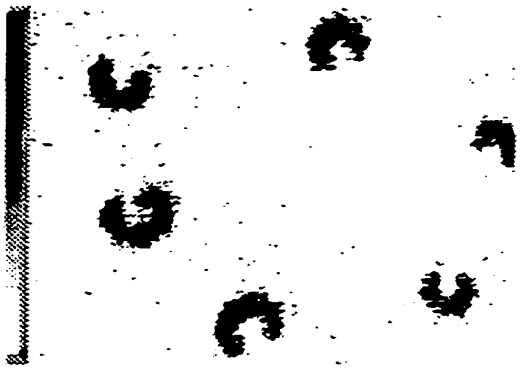

π = 9 mN/m

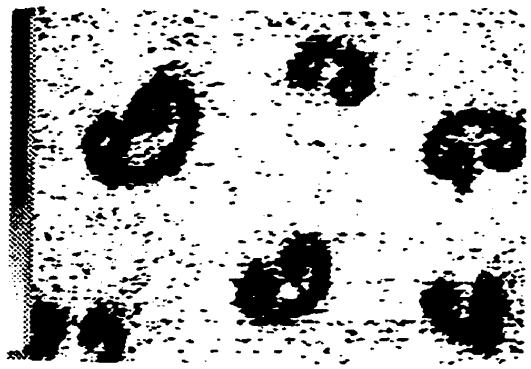

11 mN/m

13 mN/m

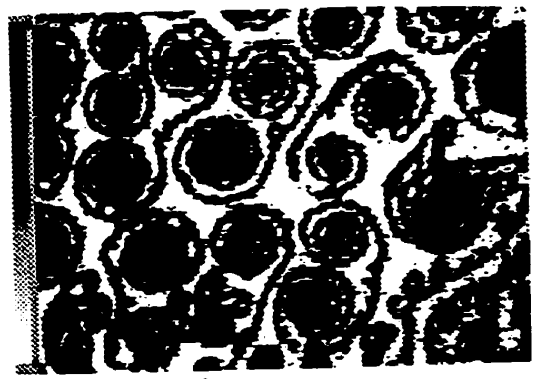

14 mN/m

16 mN/m

18 mN/m

out of the SC phase.

The evolution of LC domain shapes with increasing surface pressure in films of DPPC with 2 mol % cholesterol (plus 1 mol % NBD-PC) is shown in Figure 5.2. Up to a π of 7 mN/m, the monolayer showed a single homogenous LE phase (not shown), and at a π of 9 mN/m nucleation of small comma like LC domains (black) was observed. With increasing π between 9 and 18 mN/m, these comma-like LC domains increased in length and became thinner, and became spiralled. Such spiral LC domains have been previously observed in DMPA/cholesterol and DPPC/cholesterol films (Heckl et al., 1988, Weis and McConnell, 1985). It has been suggested that cholesterol acts as an "line active impurity" between the LC-LE domain boundaries of the phospholipids, and alters the shapes of the typical kidney shaped domains of DPPC (Weis and McConnell, 1994).

The plot of total amount of black or condensed phase plotted as a function of π for films of DPPC with cholesterol is shown in Figure 5.3. The plots indicated that small amounts of cholesterol do not drastically effect the amounts of condensed phase at surface pressures of 5-20 mN/m, although at higher π the total amount of LC phase is decreased from those found in DPPC films at equivalent π. This indicated that small amounts of cholesterol slightly perturbs films of DPPC, especially at higher π, and is consistent with previous reports (Slotte, 1995). The cholesterol monolayer had 75-84 % black phase at all π, although the black phase in pure cholesterol films may be a solid phase and not the liquid condensed (LC) phase seen in phospholipid films. Using the NBD-PC probes partitioning, this solid-like phase cannot be discriminated from the LC

Figure 5.3 Percentage of the black phase plotted as a function of surface pressure of DPPC-cholesterol films. The error bars indicate $\pm$ one standard deviation for 10 images analyzed at each π.

For films of pure cholesterol an almost homogenous or continuous black phase was observed, although about 10-15 % of the films area was occupied by the fluorescent probe. This black phase may be a solid condensed (SC) phase, and may be different from the liquid condensed (LC) phase (which also appear as black or probe excluding) observed in all the other systems.

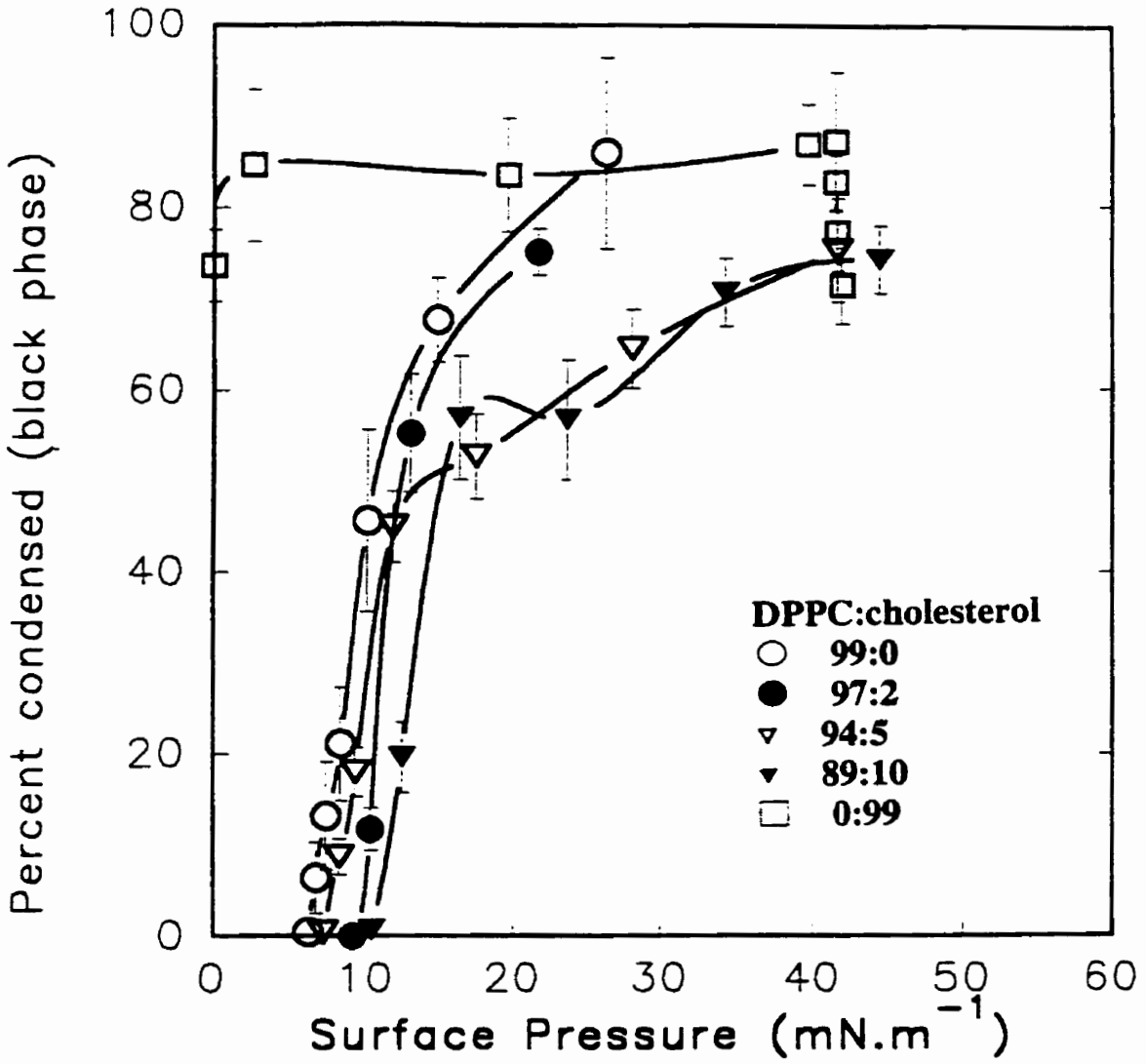
Percent condensed (black phase)
100
80
60
40
20
0
0
10
20
30
40
50
60
Surface Pressure (mN.m^{-1})
DPPC:cholesterol
99:0
97:2
94:5
89:10
0:99

phase such as seen in DPPC films, but our results at least indicate that this phase is tightly packed and excludes the probe. These results indicate that although small amounts of cholesterol perturbs the packing of DPPC films at high π, the sterol has a far greater effect on shapes of condensed domains of the phospholipid.

5.41] Cholesterol alters phase properties of DPPC films.

The effect of increasing molar concentrations of cholesterol in phospholipid films has been studied extensively (Albrecht et al., 1981; Chapman et al., 1969; Ghosh and Tinoco, 1972; Müller-Landau and Cadenhead, 1979; Phillips and Chapman, 1968; reviewed by Cadenhead, 1985). Over the last decade fluorescence microscopy has been used in such studies (reviewed by Weis, 1991, McConnell, 1991). Visualization of the DPPC film has indicated that the LE to LC phase transition at ~ 7 mN/m coincides microscopically with an exclusion of the probe from the regions of high packing or condensed (black) phase to regions of high fluidity or low packing or expanded (white) phase (Meller, 1988; Nag et al., 1991; Weis and McConnell, 1985). The LC domains of DPPC also show quasi-equilibrium "kidney bean" shapes (Nag et al., 1991; Weis and McConnell, 1985). The typical images in the DPPC/cholesterol films shown in Figure 5.1, and the increase in amounts of fluid or expanded (white) phase with increasing cholesterol in such films (Figure 5.3) tends to indicate that cholesterol probably partitioned mostly in the fluid phase of such films. This is consistent with the fact that the structure of cholesterol was not being accommodated in the tightly packed LC domains of DPPC, although cholesterol molecules pack very well by themselves as indicated from the films of pure cholesterol (Figure 5.1). Figure 5.4 shows a cartoon of the potential arrangements of cholesterol in films of DPPC at the air-water interface. In films, cholesterol by itself probably orients at the air-water interface with its terminal

Figure 5.4 Typical arrangements of cholesterol in films of DPPC at the air-water interface. Cholesterol molecules are probably oriented with their hydroxyl group in the water and the sterol rings in the air.

Cholesterol occupies mostly the fluid phase of DPPC films, and alters the shapes of LC domains by binding as a "line active impurity" to the LC domains edges (adapted from Weis and McConnell, 1985).

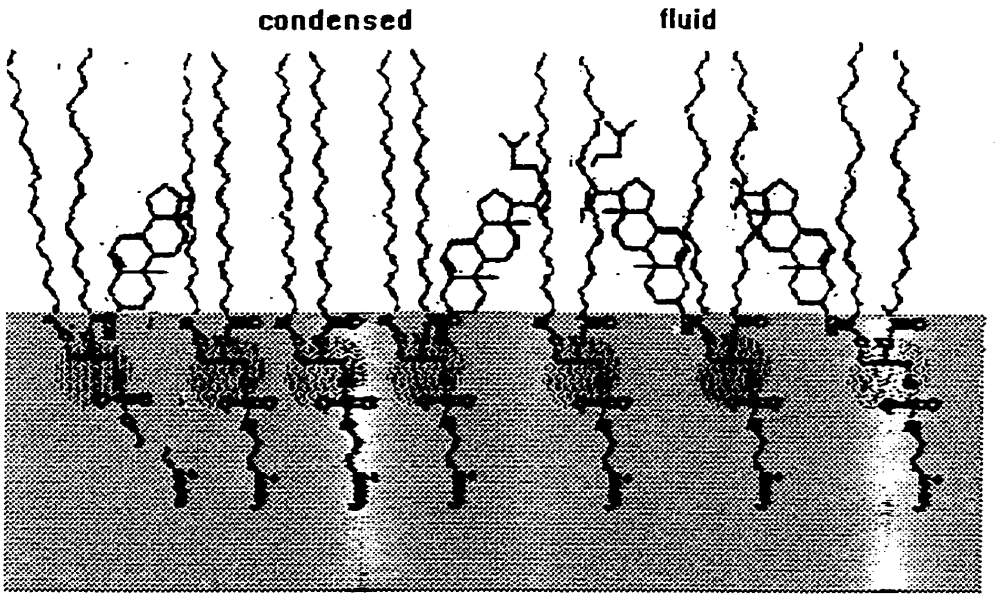
condensed
fluid

polar hydroxyl group in water and the rigid or inflexible sterol rings oriented towards the air, and forms a tightly packed solid or solid condensed (SC) phase at π above 0 mN/m. The partitioning of cholesterol mostly in the LE or fluid phase of DPPC could be due to the rigid molecule (sterol rings) not being accommodated well in the DPPC tightly packed LC phase. As seen from the isotherms of pure cholesterol films, the rigidity of the molecule is inherent since such films undergo a single phase transition from gas to solid. The images of such films indicate the existence of a single mostly homogenous, continuous solid-like phase. Such solid-like phase is continuous and do not have any domain boundaries or shapes, compared to those seen for liquid condensed domains of DPPC in films. Recently Lee et al., (1995), have shown that cholesterol in fluid DMPC films can be segregated out of the fluid phase by applying an electrostatic field, confirming the localization of most of the molecules in the fluid phase.

5.42] Shape changes of DPPC condensed domains.

It was interesting to note in this study that, although cholesterol (in low amounts) did not substantially alter the π-A isotherms of DPPC, it had a drastic effect on the shapes of LC domains of DPPC. Such shape changes have been termed as "shape transitions" in analogy to phase transitions occurring in thin films (McConnell, 1991; Seul and Andelman, 1995), and studying such transitions reveals somewhat the molecular arrangements of the phospholipids inside such domains. The probe-excluded phase which we associate with LC or liquid condensed domains of DPPC exhibits circular or "kidney bean" shapes due to a "competition between line tension and electrostatic forces acting

on the phospholipid molecules" (McConnell, 1991). Line tension can be described as the tension or force acting along the boundary of the condensed phase with the fluid, which allows the LC phase to be isolated into units as separated elliptical or circular domains (Groves and McConnell, 1996; McConnell, 1995). The line tension prevents the domains from fusing. It arises from different dipole orientations of the molecules in the LE and LC phase. The phospholipid molecules at an air-water interface are considered as single molecular dipoles and arise from the orientation of the headgroup in the water. The shapes of the phospholipid domains occur through a competition between the dipole orientation, line tension and the culombic or electrostatic forces between the molecules (the concepts of dipole orientation of lipids and resulting shapes of domains have been discussed in McConnell, 1991). Weis and McConnell (1985) observed the effect of cholesterol on the LC domains of DPPC with the introduction of 2-4 mol% cholesterol in such films, and reported for the first time that the LC domains of such systems were thin and filamentous, and that the direction of the filamentous growth depended on the chirality of the phospholipid molecule. They suggested that cholesterol acted as a line active impurity at the LC domain boundary, and induced electrostatic instabilities which deform the circular domains to more longitudinal spiral shapes, or allow the domains to grow in one direction or axis and not the others. It was suggested that cholesterol in low amounts concentrated from the fluid phase around the edge of the LC phase of DPPC with an increase in packing density of the films, and destabilised the condensed-fluid domain interfaces as an "line active impurity". Others have shown that increasing amounts of cholesterol from 2 to 20 mol% in DMPA films

will systematically decrease the thickness of the spiral domains, and above 25 mol% cholesterol, the LE/LC phase transition is no longer detectable by fluorescence microscopy (Heckl et al., 1986, 1988). Also such drastic changes of condensed domains shape in phospholipid-cholesterol films are not reflected in their π-A isotherms. Such studies including ours, suggest that studies of π-A isotherms of lipid-cholesterol films need further re-evaluation of molecular details in light of fluorescence microscopy results.

5.43] Possible role of cholesterol in pulmonary surfactant.

Only a few reports on cholesterol/phospholipid films as models of pulmonary surfactant have appeared over the last decade or more (see Keough, 1984; 1992 for review), and the role of the lipid in pulmonary surfactant is only beginning to emerge (reviewed by Daniels, 1995; Keough, 1984). These reports indicate that cholesterol in low amounts enhanced the adsorption, re-adsorption and spreading of some PS components in films (Fleming and Keough, 1988; Taneva and Keough, 1995), but the sterol decreases the stability of some phosphatidylcholine films at high π (Yu and Possmayer, 1993; 1994; Taneva and Keough, 1995). Other studies have indicated that cholesterol can impede the surface activity of mixed surfactant lipid films at high surface pressure (Fleming and Keough, 1988). In this study, the amount of condensed phase of DPPC was affected at high π, indicating that cholesterol affects the DPPC films packing more at high π (or low γ). Also since the fluidizing effect of the sterol on DPPC films seems to occur at high π, cholesterol is possibly present in such films at those π or it is

difficult to "squeeze - out" from such films. This would tend to indicate that cholesterol is detrimental to some of the surface activity of DPPC films or ability of such films to lower surface tension (γ) to very low values, at high compression. Since pulmonary surfactant films are far more complex than the mixtures studied here, and are adsorbed instead of solvent spread to the air-fluid interface, the function of cholesterol in PS may be more complex. In pulmonary surfactant cholesterol may help in the mechanism of adsorption of particular phospholipids to the films at the air-alveolar fluid interface. Yu and Possmayer (1993; 1994) have indicated that although cholesterol decreased the stability of surface films of some surfactant phospholipids, in adsorbed films surfactant protein - A (SP-A) and calcium could remove such instability. They suggested that the protein by some unknown mechanism prevents cholesterol in PS from reaching the surface-films during adsorption, thus removing any detrimental affect the sterol has on stability of PS films at high π. The fluidity imparted by cholesterol to the DPPC films can thus be implicated to be conducive of an imperfection of the DPPC packing in bilayer structures, allowing them to adsorb rapidly. In the case of the more complex pulmonary surfactant system, selective adsorption of DPPC to the surface and prevention of cholesterol from reaching such films by proteins, may remove any detrimental effect of this lipid on the films stability.

Fluorescence microscopy has also been used in studying solvent-spread films of lipid extracts of pulmonary surfactant at the air-water interface (Hall et al., 1995a; 1995b), and some definitive effect of the sterol on such films have been found (Korcakova et al., 1996). The studies by Hall and co-workers have indicated that

removing the neutral lipids such as cholesterol from the lipid extracts produced significant alteration of the amounts of condensed phase formed in such films. In our study we observed that, cholesterol perturbed the packing and fluidized films of DPPC, and was probably difficult to squeeze-out of such films. The studies by Hall and co-workers, and the more simpler system studied here indicate that the sterol probably plays some important role in the fluidity, stability and organization of pulmonary surfactant films at the air-water interface.

[*The study of complete range of cholesterol in phospholipid films and the discussions of such films as model of biomembranes is given in Worthman et al., (1996); Appendix B, No. 2*]

Chapter 6

SURFACTANT PROTEIN - C

(SP-C)

INTRODUCTION

Pulmonary surfactant (PS) contains small amounts (2-5 wt%) of specific proteins, among which the smallest is a hydrophobic protein called surfactant protein-C (SP-C). The protein is under intensive scrutiny in order to comprehend its functional role in pulmonary surfactant. Porcine SP-C is a 4.2 kDa, dipalmitoylated, 35 residue peptide, of which 23 residues are hydrophobic (Beers and Fisher, 1992; Curstedt et al., 1990; Hawgood and Shiffer, 1991). The processing and synthesis of SP-C occurs in type - II pneumocytes, and its post-translational processing takes place in the acidic environment of the lamellar bodies, which can be altered by changing the pH of the pneumocytes internal environment (Beers, 1996). Figure 6.1 shows the typical gene from which the SP-C peptide is translated and transcribed, and the typical orientation of the protein in phospholipid bilayers. A recent high resolution NMR study showed that SP-C in an apolar solvent has a 37 Å long α-helix between residues 9 to 34 (Johansson et al., 1994b). Other studies have indicated that SP-C has about 60 % α-helical conformation in lipid bilayers (Pastrana et al., 1991; Vandenbussche et al., 1992b) or monolayers (Creuwels et al., 1993) and has a trans-bilayer orientation similar to integral membrane proteins (Morrow et al., 1993b). The larger precursor protein from which mature SP-C is formed was suggested to contain a trans-membrane α-helical region, which may be embedded in the membrane of type-II cells, with the N-terminal of this precursor located in the cytosol (Keller et al., 1991).

Hydrophobic proteins of surfactant, SP-B and SP-C, together make up about 2

Figure 6.1 The gene, mRNA and the processing of surfactant protein - C (SP-C) and the secondary structure of the matured, dipalmitoylated protein. [From Weaver and Whitsett, (1991), reprinted with the permission of the authors and publisher, © The Biochemical Society & Portland Press, UK]

The protein in its mature form is an α-helix and has dipalmitoylated cystine residues near its C-terminal.

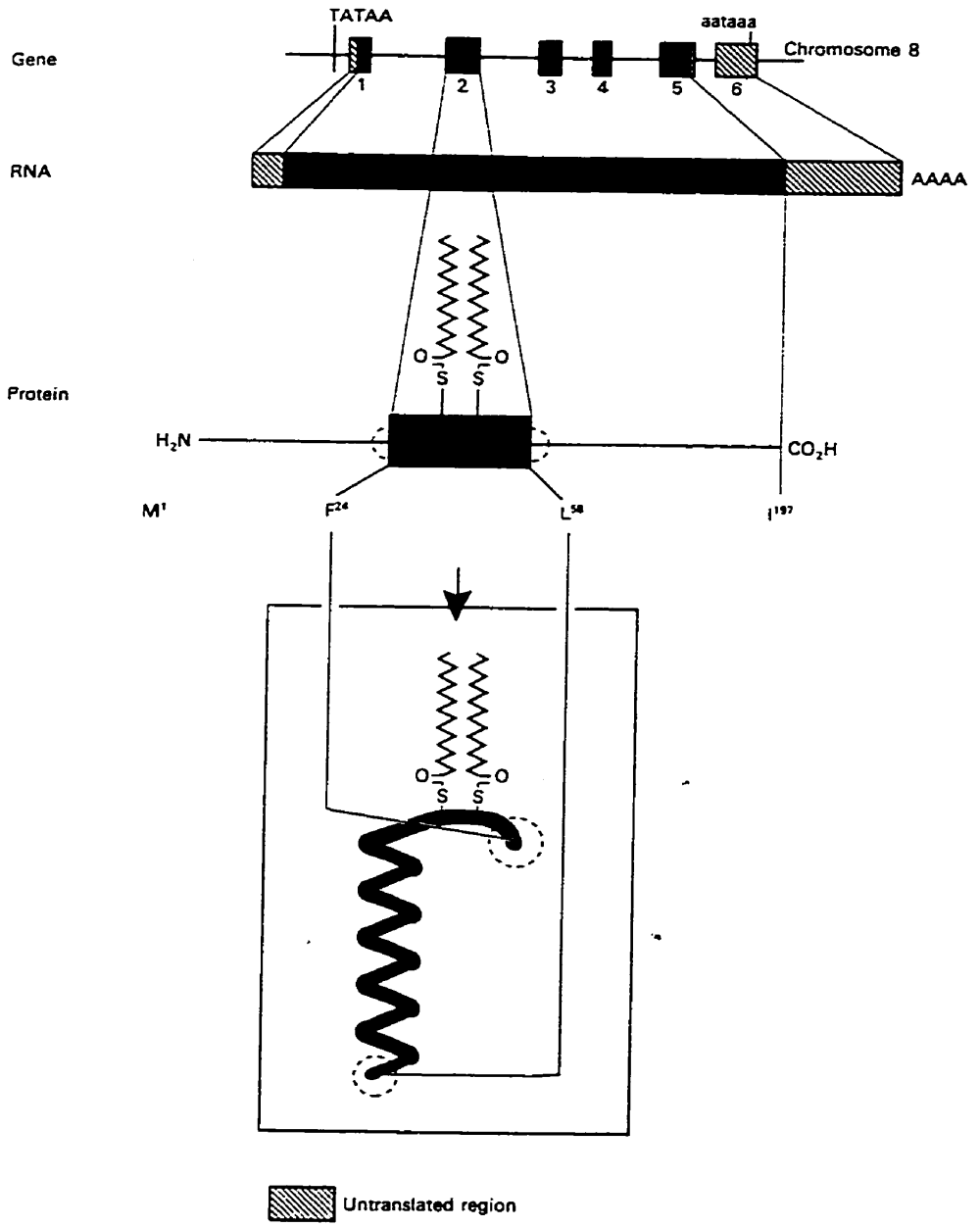
TATAA
aataaa
Gene
Chromosome 8
1
2
3
4
5
6
RNA
AAAA
Protein
S
S
S
S
H_2N
CO_2H
M^1
F^{24}
L^{58}
I^{197}
Untranslated region

weight percent of the lipids, although the exact amounts of each has not yet been determined with certainty. The precise amount of the proteins which may be associated with the films at the air-water interface is even less well defined, although recent experiments suggest that at least SP-C can adsorb into the layer (Chapter 7), and small amounts can remain in the film even under high compression (Taneva and Keough, 1994; 1994a; 1994b; 1995). *In vitro* studies have shown that SP-C facilitates PS lipid adsorption into an air-water interface (Hall et al., 1992; Notter et al., 1987; Perez-Gil et al., 1992b; Takahashi and Fujiwara, 1986; Yu and Possmayer, 1988), mediates lipid insertion into preformed lipid monolayers (Creuwels et al., 1993; Oosterlaken-Dijksterhuis, et al., 1991a) and facilitates re-spreading of lipids from collapsed phases of monolayers (Taneva and Keough, 1994). SP-C also can alter the elasticity and viscosity of lipid monolayers (Pastrana et al., 1991). Some of these processes were enhanced in the presence of anionic lipids and calcium. Porcine SP-C has positively charged residues near its N-terminal and these may interact with anionic phospholipids (Shiffer et al., 1992; 1993). Neutralization of the positive charge of SP-C in lipid vesicles alters functional properties of the protein, such as inducing the binding of the vesicles to phospholipid monolayers (Creuwels et al., 1995a). Also palmitoylation and pH alter some of the functional properties of SP-C in studies *in vitro*, such as increasing adsorption rates of phospholipid vesicles to an air-water interface (Johansson et al., 1995; Quanbar and Possmayer, 1995). Although studies have indicated roles for SP-C in pulmonary surfactant dynamics, only recently have investigations indicated how SP-C may structurally interact with some PS lipids (Horowitz et al., 1993; Johansson et al.,

1994a; 1995; Krill and Gupta, 1994; Morrow et al., 1993b; Pastrana et al., 1991; Panaiotov et al., 1996; Shiffer et al., 1993; Simatos et al., 1990; Vandenbussche et al., 1992b).

Monolayers of lipid-protein systems have long served as models of biological membranes (Cadenhead, 1985; Cŝerhati and Sžogyi, 1994; Möhwald, 1990), and as models of serum lipoprotein particles (Ibadah et al., 1988; Krebs and Phillips, 1983; Krebs et al., 1988). This study of SP-C with lipids in monolayers is relevant to lipid-protein interactions of integral membrane proteins in model membranes, as well as to the interactions of the components in surfactant monolayers and bilayers. Using epifluorescence microscopy, the influence of proteins on lipid monolayer phase packing, and the transition from liquid expanded (LE) to liquid condensed (LC) phase has been semi-quantitatively assessed (Heckl et al., 1987; Möhwald, 1990; Perez-Gil et al., 1992a; Peschke and Möhwald, 1987). The influence of ions or anionic lipids (Evert et al., 1994; chapter 4) and lipid-protein (Heckl et al., 1987) monolayers has also been studied by this technique. Similarities of surface pressure-induced monolayer changes with bilayer lipid systems undergoing thermal phase transitions have been noted (Möhwald, 1990; Nag et al., 1993). In a previous collaborative study we found SP-C caused lipid packing re-arrangements and affected isothermal phase properties of DPPC in spread monolayers (Perez-Gil et al., 1992a) and bilayers (Keough et al., 1992). In this study we show directly how fluorescein-labelled SP-C (F-SP-C) is organized in spread monolayers of DPPC, DPPC:DPPG (dipalmitoylphosphatidylglycerol) (7:3 mol/mol), under the influence of calcium. Although the amounts of the surfactant proteins used in

this and following studies (3-30 wt%) exceeds the amounts present in pulmonary surfactant, the studies could be compared to other studies done in bilayers using similar high amounts of proteins. Also these model studies required high amounts of proteins to detect any saturation of interactions of the proteins with the lipids.

6.21] Materials.

1,2-dipalmitoyl-*sn*-glycero-3-phosphocholine(DPPC), 1,2-dipalmitoyl-*sn*-glycero -3-phospho-*rac*-glycerol (sodium salt) (DPPG-Na) and 1-palmitoyl-2-{12-[(7-nitro-2-1,3-benzoxadizole-4-yl)amino] dodecanoyl} phosphatidylcholine (NBD-PC) were purchased from Avanti Polar Lipids (Pelham, AL). The lipids were found to be pure by thin layer chromatography and used as received. Fluorescein isothiocyanate (FITC) was purchased from Molecular Probes (Eugene, OR). The subphase buffer for the monolayers was 0.15 M NaCl and 5 mM Tris dissolved in deionized doubly-distilled water, the second distillation performed from dilute $KMnO_4$ containing 1.6 mM calcium ions when required. The pH was adjusted to 6.9 with 0.1N HCl. Pulmonary surfactant protein SP-C was isolated from porcine lungs by the method of Curstedt et al., (1991), by Dr. Jesus Perez-Gil of the University of Madrid and is discussed elsewhere (Perez-Gil et al., 1993).

6.22] Fluorescent labelling of SP-C.

Purified and native SP-C was fluorescently labelled by Antonio Cruz and Jesus-Perez Gil (University of Madrid) by the following method. The pH of a solution of 200 μg of purified SP-C in 2 ml of chloroform:methanol (2:1 vol/vol) was adjusted to 7.8 by addition of appropriate amounts of 50 mM Tris in methanol. Fluorescent labelling was achieved by incubating the SP-C solution with 20 μl of 10 mM fluorescein isothiocyanate

(FITC), at 4°C overnight. The pH of the solution was re-adjusted to 2 and the proteins eluted from a LH-20 Sephadex (Pharmacia LKB, Sweden) column to remove the unreacted FITC. The chromatographic profile of the LH-20 effluent was followed by absorbency at 250 nm (unreacted SP-C) and 450 nm (fluorescein labelled SP-C). Fluorescein labelled SP-C (F-SP-C) showed a single band on SDS-gel electrophoresis around 5000 Da and was not further purified.

Native and labelled SP-C (F-SP-C) were scanned by Matrix Assisted Laser Desorption/Ionization (MALDI) spectrometry by Mr. Lorne Taylor at the department of Chemistry, University of Waterloo (Ontario, Canada), to determine their respective molecular weights by procedures discussed by Hillenkamp et al. (1991). A similar type of Matrix Assisted Plasma Desorption spectrometry has been used previously by Curstedt et al., (1990) to determine the molecular weight of SP-C and the analytical procedures are given in detail by these authors.

SP-C and F-SP-C were quantitated by amino acid analysis. DPPC, DPPG and NBD-PC were assayed by estimating the total amount of phosphorus in the lipids by a modified of method of Bartlett (1959) as described elsewhere (Keough and Kariel, 1987).

6.23] Monolayer formation and observation.

The lipids, NBD-PC (fluorescent lipid probe) and protein F-SP-C (fluorescein-labelled SP-C) were dissolved in chloroform:methanol (3:1 vol/vol) and mixed in desired weight proportions. One mol% of NBD-PC was included in DPPC and DPPC:DPPG

(7:3 mol/mol) mixtures. No lipid probe was used when F-SP-C (3, 6 and 12 wt% or 0.5, 1.07 and 2.14 mol%) was present in lipid monolayers since fluorescence emission from F-SP-C was found to be sufficient to observe the monolayers. Monolayers were spread on a buffered saline subphase from the chloroform:methanol (3:1 vol/vol) solution in the epifluorescence microscopic surface balance described above. All experiments were carried out at a temperature of 21 $\pm$ 1°C. The monolayers were compressed in steps at a rate of 20 mm^2/sec or an initial rate of 0.13 $Å^2$.molecule^{-1}.sec^{-1}, compression stopped for one minute and monolayer images obtained during the minute using the video camera and recorder of the epifluorescence balance. The images were analyzed using digital image processing by methods discussed in details in Appendix A. The percentage of condensed phase was estimated as (total area of black regions per image/the total area of the image x 100).

6.24] Quantitative Estimation of lipid-SP-C Association.

Estimates of the distribution of F-SP-C in the liquid expanded and liquid condensed phase were performed using a procedure of Heckl et al., (1987). In this procedure the percentage of black or condensed phase is converted to degree of crystallization and plotted as a function of area/molecule of the lipid, and this plot can be used to give an estimation of the area of the protein in each phase. The degree of crystallization ϕ was calculated by the methods of Heckl et al., (1987), where $\phi = 1 - (1 - X).A/A_{fl}$, where X = the ratio of the dark (condensed) area to the total area; A = the observed area per lipid molecule; A_{fl} = the area of the lipid molecule in the fluid

region just below the liquid expanded to liquid phase transition region. The percentage of dark phase gives the proportion of the total area which is in the condensed phase whereas the degree of crystallization gives the proportion of the lipid molecules which are in that phase.

RESULTS

The MALDI mass spectra of SP-C (top panel) and its fluorescein-labelled analogue F-SP-C (bottom panel) are shown in Figure 6.2. As shown in the top panel of Figure 6.2 native SP-C produced a main peak at 4213 Da, and minor ones at 4023 and 8081 Da. The F-SP-C spectrum in the bottom panel showed a major peak at 4117 Da and smaller ones at 3747, 4007 and 4360 Da. The formula weights (FW) of SP-C from amino acid analysis are 4186 Da (+ 2 palmitates), 3948 (-1 palmitate) and 3710 (-2 palmitates). Curstedt et al. (1990) using similar mass spectrometry of SP-C have shown that the native protein had spectral peaks at 4210 Da (+ 2 palmitates), 3971 Da (-1 palmitate) and 3733 Da (- 2 palmitates), the main peak of SP-C (4210 Da) being close to our SP-C peak at 4213 Da. The difference in MALDI spectrometrically determined molecular mass and the formula weight (FW) of SP-C may be due to sodium adjuncts of various forms of SP-C being detected spectrometrically, as has been discussed by Curstedt et al. (1991). The spectrum in Figure 6.2 (top panel) indicates that SP-C is mainly in its dipalmitoylated, native, monomeric form (4213 Da), with minor amounts of SP-C in other forms such as SP-C dimer (8081 Da) and monopalmitoyl SP-C (4023 Da). Similarly, the F-SP-C spectrum can be explained as displaying some deacylated form of SP-C from the peak at 3747 Da [4213 Da - 476 Da (FW of 2 palmitates) = 3737 Da], and a main peak at 4117 Da which corresponds to this deacylated form labelled with one mole of fluorescein per mole of protein [3737 Da + 376 Da (FW of fluorescein) = 4113 Da for F-SP-C]. The other peaks in the F-SP-C spectra indicate

Figure 6.2 MALDI mass spectra of porcine SP-C (top panel) and fluorescein-labelled deacylated F-SP-C (bottom panel).

The main peak at 4213 Dalton (top panel) is from the dipalmitoylated monomer of the protein and the one at 4117 Da (bottom panel) is from the deacylated, fluorescein-labelled protein (F-SP-C). The other minor peaks are for various forms (see main text) of SP-C present in the extracted protein.

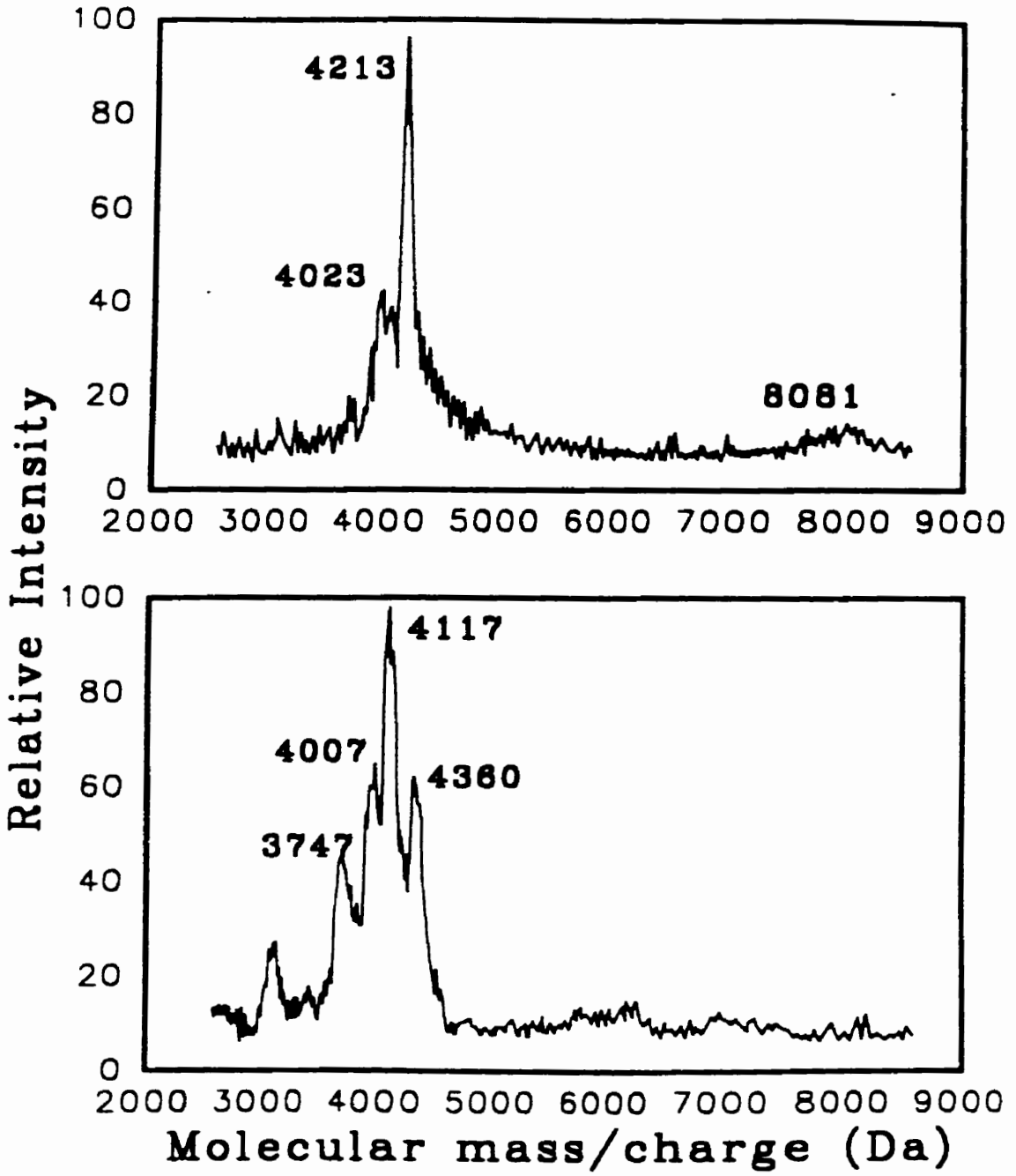
100
80
60
40
20
0
4213
4023
8081
2000 3000 4000 5000 6000 7000 8000 9000
100
80
60
40
20
0
4117
4007
4360
3747
2000 3000 4000 5000 6000 7000 8000 9000
Relative Intensity
Molecular mass/charge (Da)

minor amounts of SP-C at its various levels of acylation.

Figure 6.3 shows the surface pressure - area per molecule (π-A) isotherms of DPPC monolayers containing 0, 3, 6, and 12 wt% or 0, 0.5, 1.07 and 2.05 mol% of F-SP-C (top), and the typical images obtained from a monolayer containing 3 wt% F-SP-C are shown in the figure (bottom). The isotherm in the inset of Figure 6.3 (top) is for pure F-SP-C. The monolayer without F-SP-C contained 1 mol% of the fluorescent lipid probe NBD-PC. The letters near the isotherms (arrows) indicate the π at which the images (bottom) in the film were obtained. The liquid expanded (LE) to liquid condensed (LC) phase transition for DPPC + 0 - 6 wt % F-SP-C monolayers occurred between 5 - 7 mN/m as indicated by the plateau regions in the isotherms in Figure 6.3. The protein isotherm (top inset) showed behaviour similar to native SP-C monolayers studied previously (Perez-Gil et al., 1992a; Taneva and Keough, 1994b). The lipid-protein isotherms also showed a levelling at $\pi \sim 50$ mN/m corresponding to the exclusion of F-SP-C-lipid units or monolayer collapse, similar to the values found previously in the case of pure SP-C (Taneva and Keough, 1994).

The typical images in Figure 6.3 (bottom) of a monolayer of DPPC + 3 wt% F-SP-C showed that LE (bright regions) and condensed phase (dark regions) of DPPC, could be visualized from the fluorescence of the fluorescein-labelled protein. Image A in Figure 6.3 shows mainly LE or fluid phase for the lipid monolayer and suggests that F-SP-C is in that phase. Image E indicates that F-SP-C (light regions) remained in the monolayer at high surface pressures (π = 64 mN/m). Recently, Panaiotov et al., (1996) using atomic force microscopy have shown similar architecture of films of DPPC/SP-C,

Figure 6.3. Typical surface pressure - area per molecule (π-A) isotherms of DPPC containing 0 - 12 weight percent (0.5 - 2.05 mol %) of fluorescently labelled SP-C (F-SP-C), and 100% F-SP-C (inset) (top) and the typical images obtained from a DPPC monolayer containing 3 wt% F-SP-C at various π (bottom). The monolayers of DPPC only, contained 1 mol% NBD-PC. The letters A to E indicated in the isotherms (top) represent the π at which the images (bottom) were obtained. The light areas in the images represent the LE phase and were observed from the emission of the fluorescently-labelled protein or F-SP-C. The scale bar is 25 μm.

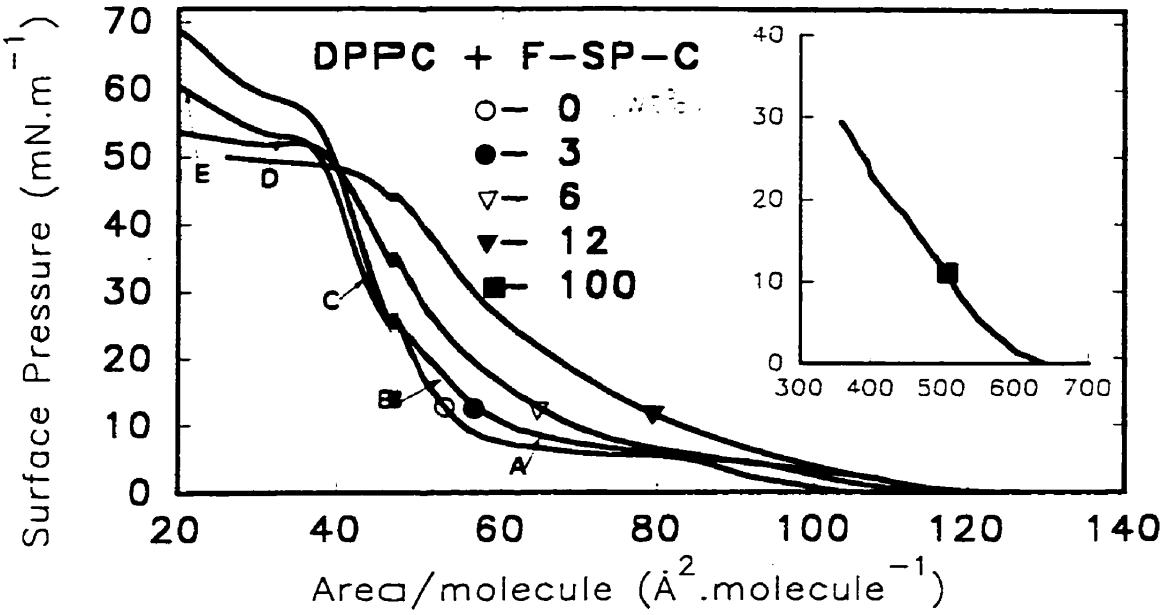
DPPC + F-SP-C
0
3
6
12
100
Surface Pressure (mN.m^{-1})
Area/molecule (Å^2.molecule^{-1})
A
B
C
D
E

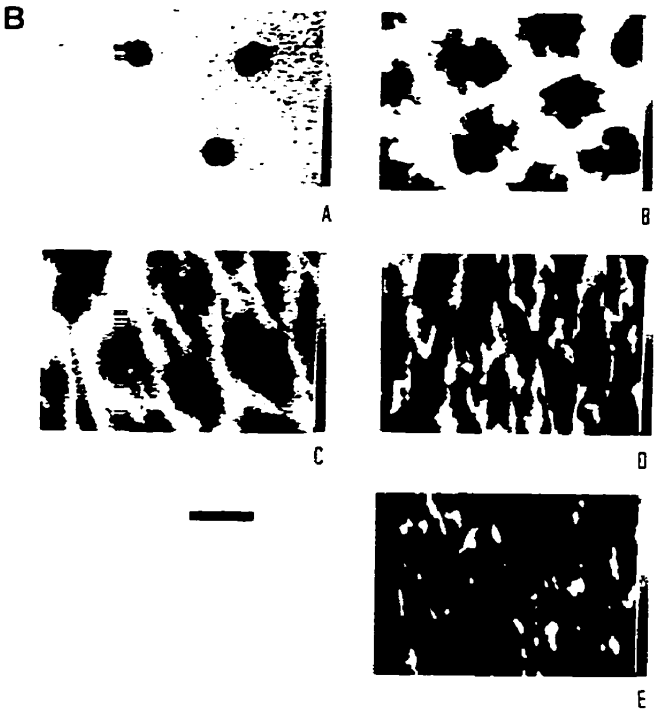
B
A
B
C
D
E

especially the ones observed here at high surface pressure (image E). The bright regions in image E may be residual fluid phase containing protein or regions of excluded protein (plus or minus small amounts of adherent lipids). Image B indicates that the shape of the LC domains of DPPC + 3 wt% F-SP-C films had small protrusions at the LE/LC boundaries and were different from more elliptical or kidney-bean shapes generally observed in pure DPPC monolayers (Möhwald et al., 1988; Nag et al., 1991).

The isotherm of F-SP-C (Figure 6.3, top, inset) indicated that the protein occupied molecular areas of 640 $Å^2$.molecule^{-1} at "lift off" π, and 380 $Å^2$.molecule^{-1} at a π of 25 mN/m. These values are in agreement with ones previously found for α-helical lipoproteins (Krebs et al., 1988) and close to those seen with native acylated SP-C (Taneva and Keough, 1994; 1994b). Others have shown by circular dichroism and infrared spectroscopy that SP-C has a high amount of α-helix in DPPC monolayers (Oosterlaken-Dijksterhuis et al., 1991; Pastrana-Rios et al., 1995). The isotherms in Figure 6.3 can be recalculated in terms of π versus area per molecule of DPPC only (as opposed to the average area per molecule of DPPC plus protein as in Figure 6.3, top). Then the apparent change in area of a DPPC molecule that is induced by the protein can be calculated by subtraction of the recalculated isotherms of DPPC plus protein from the isotherm of DPPC alone (Heckl et al., 1987). Such a presentation is made in Figure 6.4. The change of area of the lipid-protein monolayers from that of DPPC (open circles, Figure 6.4) was non-linear between 83 $Å^2$.molecule^{-1} and 40 $Å^2$.molecule^{-1} of DPPC. This difference in area was low at higher areas per molecule of lipid, reached a maximum at 55 $Å^2$.molecule^{-1} (π = 5 mN/m), and then declined to become negligible

Figure 6.4. The nominal change in the area per molecule of DPPC induced by the protein plotted as a function of the area per molecule of DPPC. The change of area was obtained by subtracting the area per molecule of pure DPPC from the nominal area per molecule of DPPC in the presence of the proteins at six different surface pressures. The symbols correspond to systems containing DPPC plus 0 wt % (○); 3 wt% (●); 6 wt% (▽) and 12 wt % (▼) of F-SP-C.

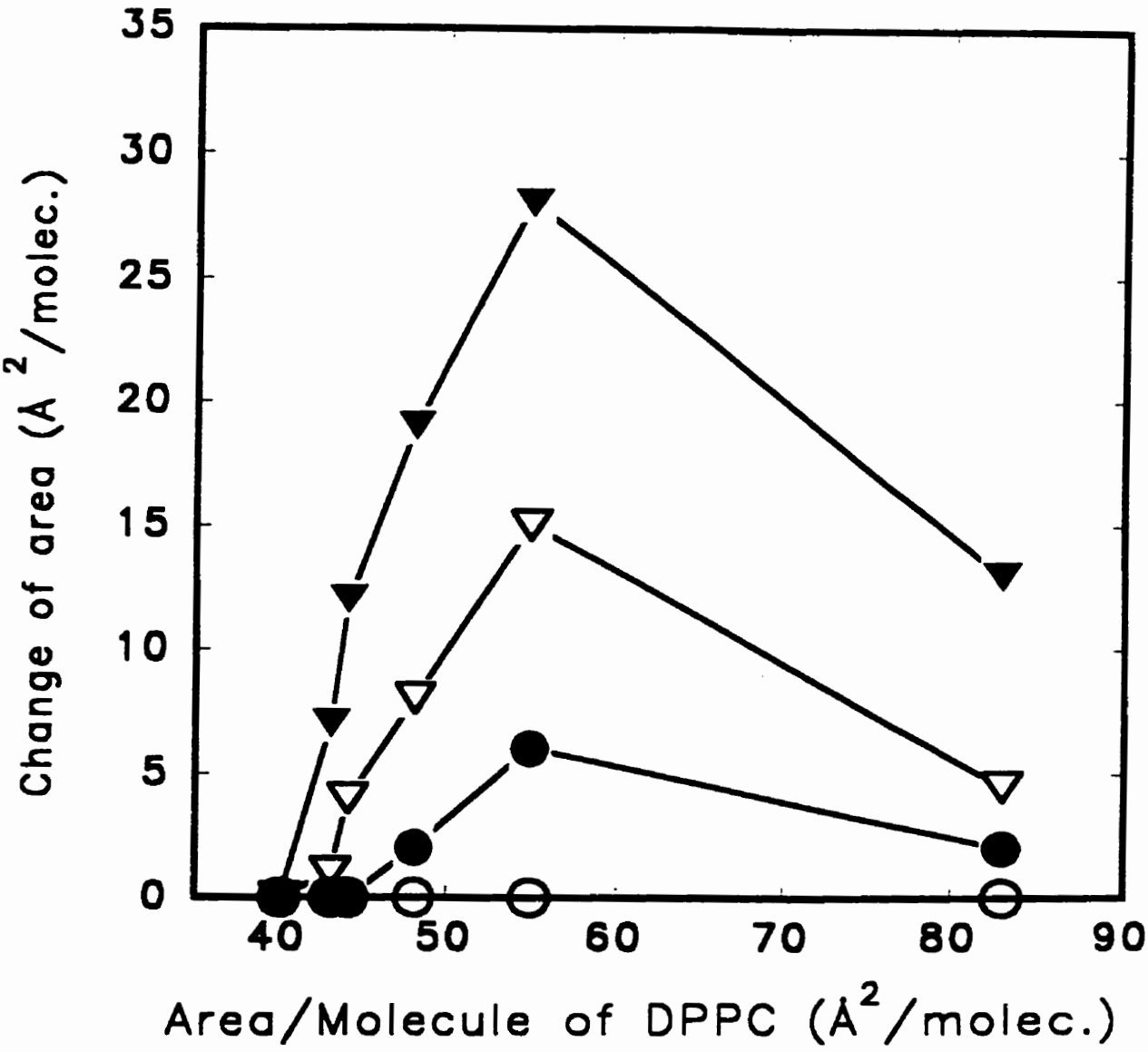
35
30
25
20
15
10
5
0
40
50
60
70
80
90
Change of area (A 2/molec.)
Area/Molecule of DPPC (Å2/molec.)

at 40 $Å^2$.molecule^{-1}, for all concentrations of the protein. The change of the area of the isotherms of lipids containing protein can be used to approximate the partial molar areas of the protein at the different areas per molecule of DPPC in the lipid-protein systems, by dividing the area change by the molar amount of protein in the monolayers. This assumes that all the area difference is due to the presence of the protein.

The average nominal area of the protein at 5 mN/m (which corresponds to an area of DPPC of 83 $Å^2$.molecule^{-1}) so calculated from the change of area at different protein concentrations was 512 $\pm$ 103 $Å^2$.molecule^{-1}, an area close to that of the protein observed from the isotherm of the pure protein at that π (Figure 6.3, top, inset). This would indicate that, at least at low π the protein at all concentrations in the phospholipid monolayers occupied the same area as it would in the pure protein monolayer. At a higher π of $\sim$ 25 mN/m (corresponding to 55 $Å^2$.molecule^{-1} area for DPPC) where the change of area induced in the protein-DPPC isotherms was maximum (Figure 6.4), the nominal area of the protein molecule in the mixed films was determined as 1306 $\pm$ 100 $Å^2$.molecule^{-1}, whereas the protein only had an area of 370 $Å^2$.molecule^{-1} in the pure protein monolayer (Figure 6.3, inset). This implies that the protein had a greater partial area at the higher π in the mixed films than it would occupy in a monolayer of the protein alone. It is also possible that the protein probably alters lipid packing at a given surface pressure and a substantial part of the apparent change in lipid area probably is a reflection of the lipid state. It has been shown recently by ellipsometry and infra red spectroscopy (Post et al., 1995, Pastrana-Rios et al, 1995) that native acylated SP-C in lipid films undergoes possible conformational changes at the air-water interface between

10-25 mN/m, and possibly a change of orientation of the alpha-helix occurs. While such changes might be responsible for an increase in partial area, the size of the change estimated from the surface data is large and it is difficult to envisage how changes of such a magnitude would accompany the conformational and orientational effects noted by Post et al., (1995) and Pastrana-Rios et al., (1995). It is possible to interpret the data in Figure 6.4 to indicate that at low areas per molecule of DPPC, where the lipid is in the liquid expanded phase, the protein and the lipid effect limited perturbation of each other. At higher pressures where more lipid would be in the liquid condensed phase, more protein would be excluded into liquid expanded phase, causing greater perturbation of packing of lipid in these domains, and an apparent increase in the calculated protein area because of the initial assumption that the area change is all due to proteins in the system.

Figure 6.5 (top) shows typical π-A isotherms of DPPC:DPPG (7:3 mol/mol) containing 0, 3, 6 and 12 wt% of F-SP-C (DPPC:DPPG/F-SP-C) without calcium, and the typical images observed in such monolayers at a π of 15 mN/m (bottom) (symbols represent the amounts of protein in the films). In the absence of calcium DPPC:DPPG/F-SP-C monolayers displayed isotherms similar to those obtained for the DPPC/F-SP-C system (Figure 6.3, top), except that the LE-LC plateau occurred at a slightly higher π of 8-9 mN/m. The isotherms in Figure 6.5 (top) in the inset are for similar DPPC:DPPG/F-SP-C monolayers in the presence of 1.6 mM $CaCl_2$ in the subphase (DPPC:DPPG-Ca). The tendency for the isotherms obtained with these mixtures in the presence of calcium to show plateaus around 50 mN/m could be partly

Figure 6.5 Typical π-A isotherms of DPPC:DPPG (7:3, mol/mol) containing 6-12 wt % of F-SP-C as in Figure 6.3, with (inset) and without 1.6 mM calcium in the subphase (top), and typical images seen at $\pi \sim 15$ mN/m in such monolayers without calcium (bottom). The letters A - D in the bottom right of each image indicate direction of increasing concentration (from 0-12 wt%) of protein. Scale bar is 25 μm.

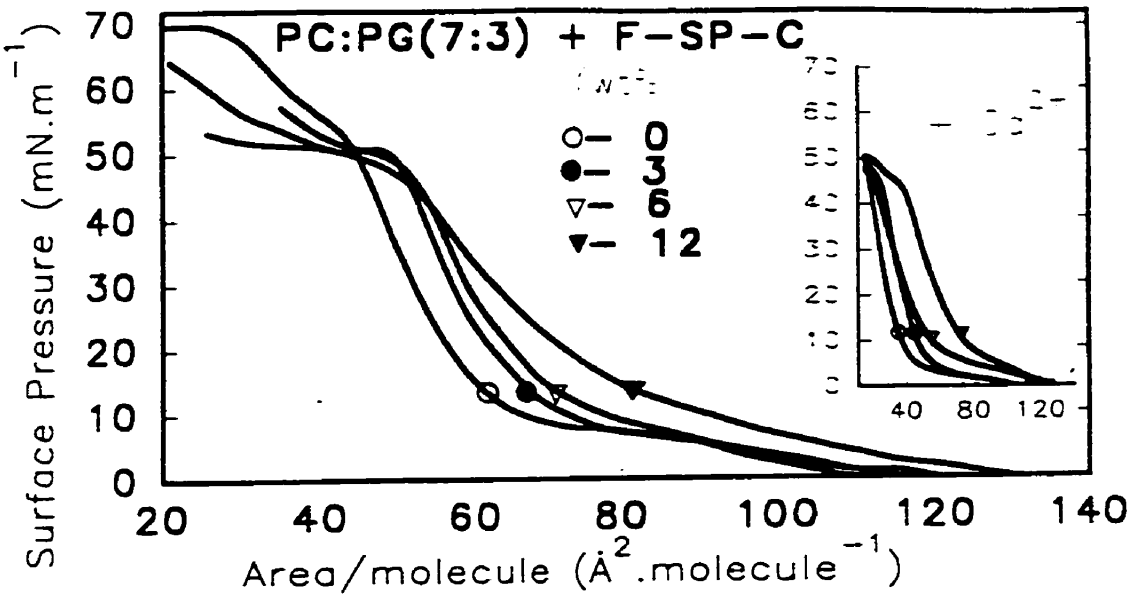
PC:PG(7:3) + F-SP-C
0
3
6
12
Surface Pressure (mN.m^{-1})
Area/molecule (Å^2.molecule^{-1})
70
60
50
40
30
20
10
0
20
40
60
80
100
120
140
40
80
120

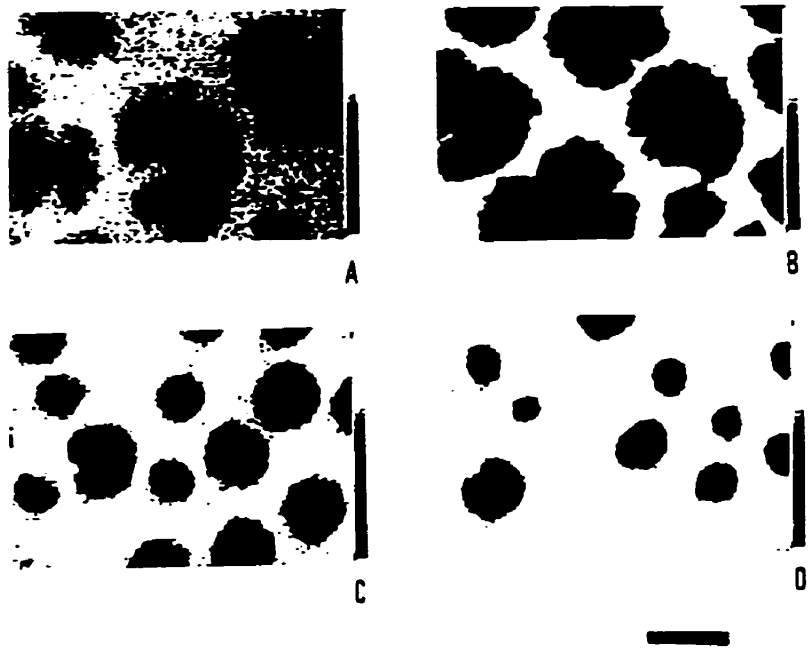
A
B
C
D

due to the design of the balance and the high viscosity of these monolayers at high π (see chapter 4, for details). The balance was designed with a channel between the main surface and the observing regions (Nag et al., 1990; Peters and Beck, 1983). For highly viscous monolayers (DPPC:DPPG-Ca) the channel produced an apparent reduction of π in comparison to that observed in such monolayers on a balance of different design (Taneva and Keough, 1995). The effect was ascribed, likely improperly, by us to monolayer collapse when such systems were first studied in this balance (Nag et al., 1994, chapter 4).

The DPPC:DPPG/F-SP-C isotherms obtained in the presence of 1.6 mM calcium (inset of Figure 6.5) showed LE to LC phase transition plateaus at a lower π compared to the monolayers without calcium. This behaviour of DPPC:DPPG monolayers under the influence of calcium was consistent with similar anionic lipid monolayer systems studied previously (Flach et al., 1993; Lösche and Möhwald, 1989; Nag et al., 1994; Taneva and Keough, 1995, chapter 4). Images in Figure 6.5 (bottom) indicated that with increasing amounts F-SP-C (A to D) the average size of the LC domains of the lipids decreased. This pattern of decreasing size of LC domains with increasing amounts of protein in the monolayer, was also observed in the DPPC/F-SP-C system and previously in DPPC monolayers containing a native, unlabelled and acylated SP-C (Perez-Gil et al., 1992a).

The total amount of condensed phase as a percentage of the total monolayer (% condensed) for DPPC/F-SP-C (top panel) and DPPC:DPPG/F-SP-C (bottom panel) monolayers without calcium plotted as a function of π are shown in Figure 6.6. At

Figure 6.6 Percentage of the monolayers in condensed phase (% condensed) as a function of π for DPPC (top) and DPPC:DPPG (bottom) containing F-SP-C in the absence of calcium. The symbols correspond to systems containing the phospholipids plus 0 wt % (○); 3 wt% (●); 6 wt% (▽) and 12 wt % (▼) of F-SP-C. Error bars represent $\pm$ one standard deviations of ten frames analyzed at each π from an individual monolayer.

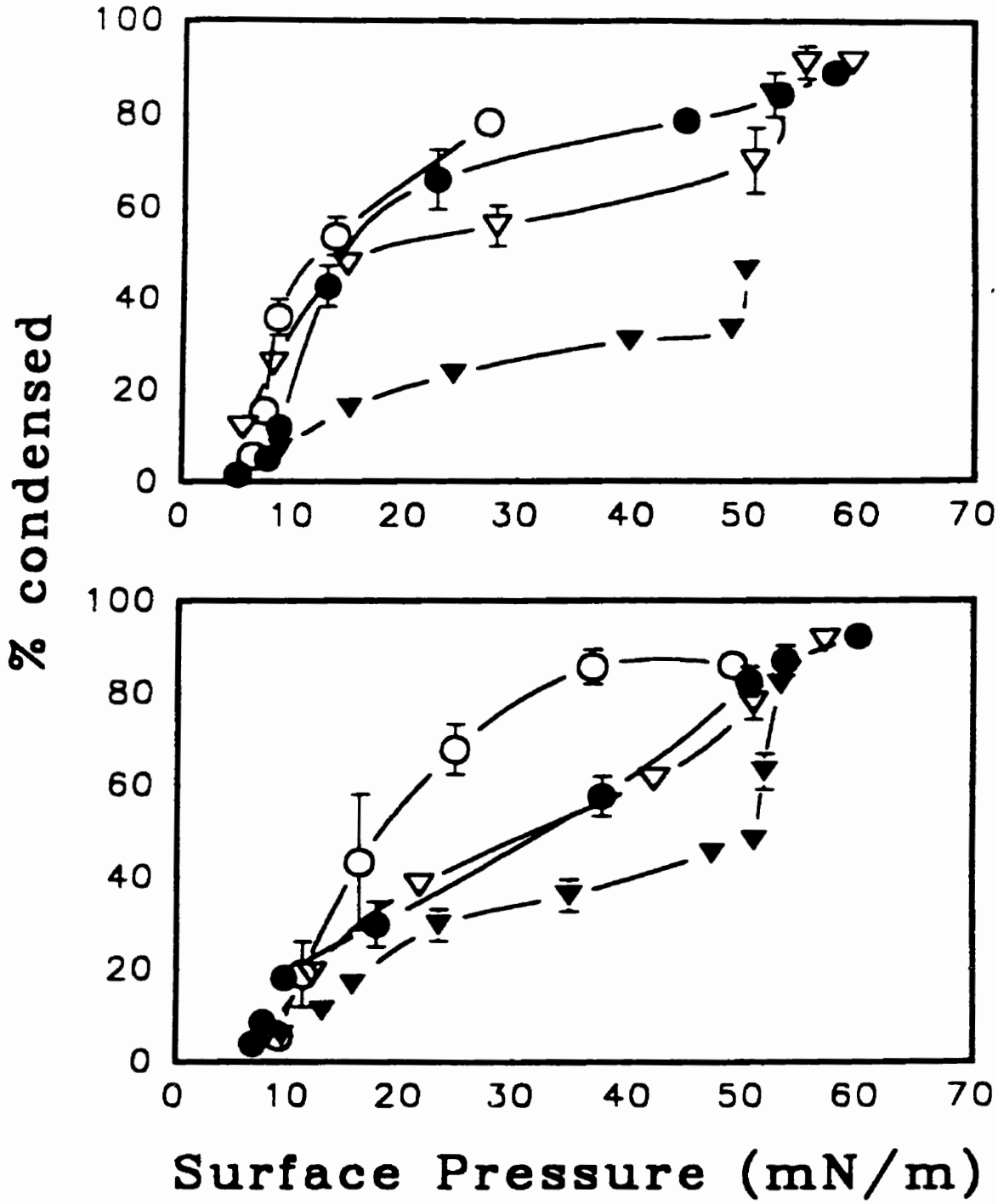
% condensed
100
80
60
40
20
0
0
10
20
30
40
50
60
70
Surface Pressure (mN/m)

comparable π increasing amounts of F-SP-C decreased the total amounts of condensed phase for both DPPC and DPPC:DPPG monolayers. It can be observed in Figure 6.6 (top panel), that although up to 6 wt% of F-SP-C caused smaller condensed domains, it did not substantially reduce the amount of condensed phase of DPPC monolayers, whereas 12 wt% of F-SP-C did reduce that total amount. In a previous study (Perez-Gil et al., 1992a) a similar perturbation of DPPC monolayers by native SP-C was observed. The total amounts of condensed phase in DPPC:DPPG monolayers were reduced by F-SP-C.

Figure 6.7 shows the relative amounts of condensed phase (left panels) and the degree of crystallization ϕ (right panel) plotted as a function of molecular area of the lipids. Both forms show a difference in the influence of 12 wt% protein as compared to that of 3 and 6 wt%. The degree of crystallization plots (right pane, Figure 6.7) can be used to estimate the area occupied by the lipid in the gel or crystalline (condensed) phase and in the fluid phase, by extrapolating the linear portions of the plots to ϕ of 1 or 0 respectively, as previously discussed by Heckl et al, (1987). For the pure DPPC monolayers (open circles in 6, right panel) an area per molecule of 75 $\pm$ 2 $Å^2$.molecule^{-1} [95 % confidence limit] (ϕ = 0) was obtained for the lipids in the fluid phase, and 46 $\pm$ 2 $Å^2$.molecule^{-1} (ϕ = 1) for the lipids in the gel or condensed phase, and the values were very close to those for the mixed DPPC/DPPG monolayers. These values are in close agreement with those found previously for DPPC by others (Heckl et al., 1987; Möhwald, 1990). The plots of the degree of crystallization are linear up to ϕ = 0.9, and for monolayers containing 0, 3 and 6 wt% of F-SP-C they converge to a similar area per

Figure 6.7 Percentage of condensed phase as in Figure 6.6 (left panel) and degree of crystallization or ϕ (right panel) plotted as a function of molecular area of the lipids. Top panels are of DPPC and the bottom ones are for DPPC:DPPG systems containing 0 wt % (○); 3 wt% (●); 6 wt% (▽) and 12 wt % (▼) of F-SP-C.

The degree of crystallization was obtained by converting the percentage condensed (Figure 6.6) to amount of gel phase by methods used previously by Heckl, et al (1987) (see text for details), to estimate partial molar areas occupied by the protein in the monolayers.

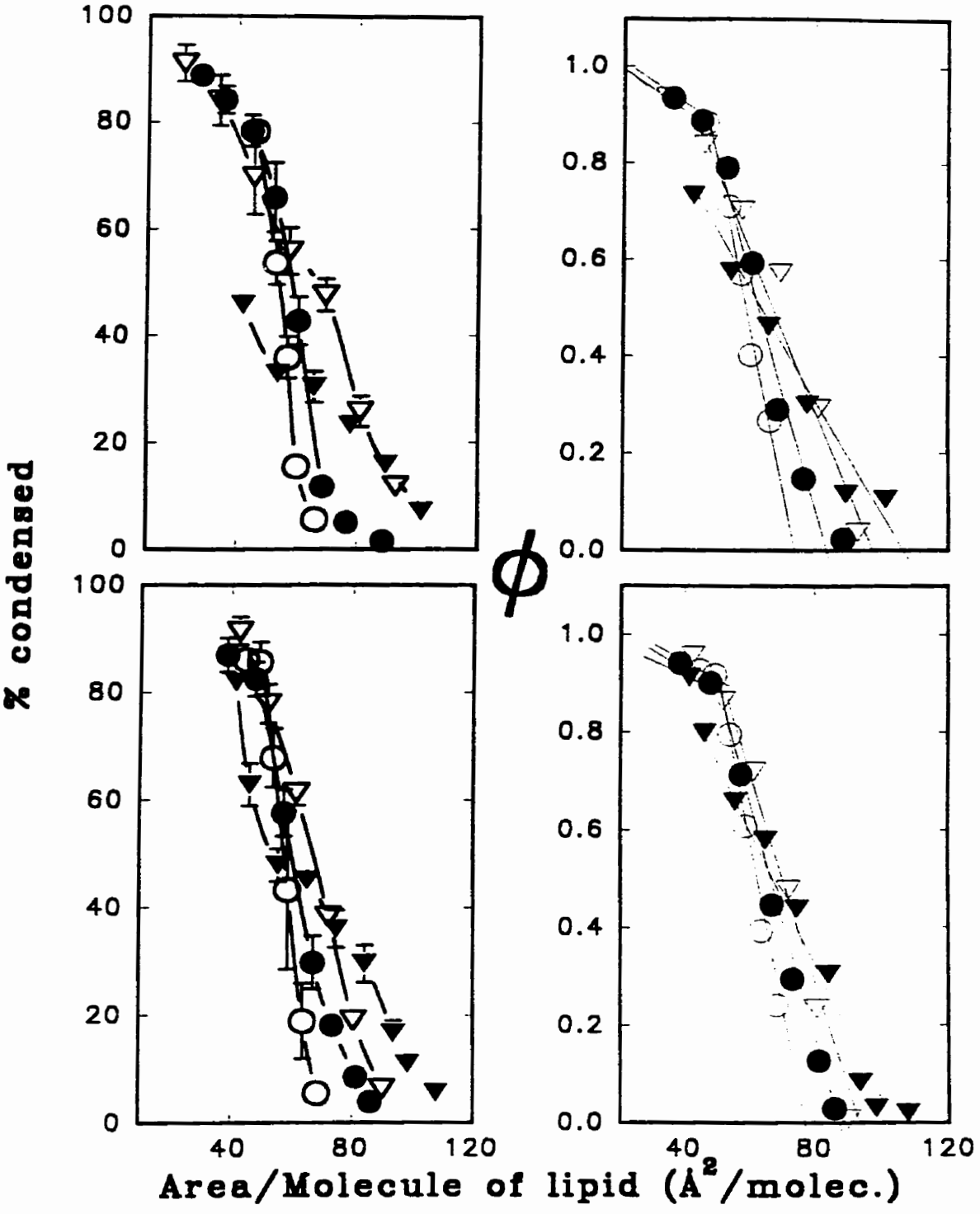
% condensed
100
80
60
40
20
0
1.0
0.8
0.6
0.4
0.2
0.0
ϕ
40
80
120
Area/Molecule of lipid (Å²/molec.)

molecule (or ~ 55 $Å^2$.molecule^{-1}) of lipid at that ϕ. Beyond this point there is a change of slope in most of the systems, except in the lipid monolayers containing 12 wt% F-SP-C. The slope change is observed for lipids with and without protein possibly indicating that there was no effect of the protein on the gelation patterns above ϕ of 0.9. This would be consistent if the protein were essentially squeezed out of the condensed lipids above $\phi \sim 0.9$. In contrast when the plots were extrapolated to $\phi = 0$, the indication was that with increasing protein concentrations the area of the lipids in the fluid or expanded phase increased by about 10 $Å^2$.molecule^{-1}, with each increment of protein added. This indicates that the proteins changed the area of the lipids, and presumably their packing modes in the expanded or fluid phase. Extrapolation of the initial linear lines to the upper axis of $\phi = 1$ (for 0-6 wt% protein), revealed a value of 45 $\pm$ 2 $Å^2$.molecule^{-1} (95% confidence), which suggests that the partial molar areas of the lipids in the gel phase for the pure lipids and lipid-protein systems are similar. This would suggest that the protein, up to 6 wt %, did not affect the gel phase. The systems with the 12 wt% protein showed lower slopes of the ϕ vs area plots which did not extrapolate to real areas per molecule at $\phi = 1$, behaviour which suggests that, at the high protein concentration, the gel phase packing could be influenced by the protein. The percentages of condensed phase as a function of surface pressure of DPPC:DPPG monolayers in the presence of 1.6 mM calcium are shown in Figure 6.8 (top), and typical images observed in such monolayers at $\pi = 8$ mN/m are in the bottom. The calcium produced higher amounts of condensed phase in DPPC:DPPG monolayers at any given π compared to the ones without calcium, but the F-SP-C continued to induce a

Figure 6.8 Percentage of condensed phase plotted as a function of π for DPPC:DPPG/F-SP-C monolayers in the presence of 1.6 mM $CaCl_2$ (top); and typical images from such monolayers obtained at a π of 8 mN/m (bottom). The symbols correspond to systems containing the DPPC:DPPG plus 0 wt % (○); 3 wt% (●); 6 wt% (▽) and 12 wt % (▼) of F-SP-C. The letters A-D in the bottom right of each image indicates the direction of increasing concentration of F-SP-C, (0-12 wt% F-SP-C). Scale bar is 25 μm. Error bars indicate standard deviations of ten images analyzed at each π from an individual monolayer.

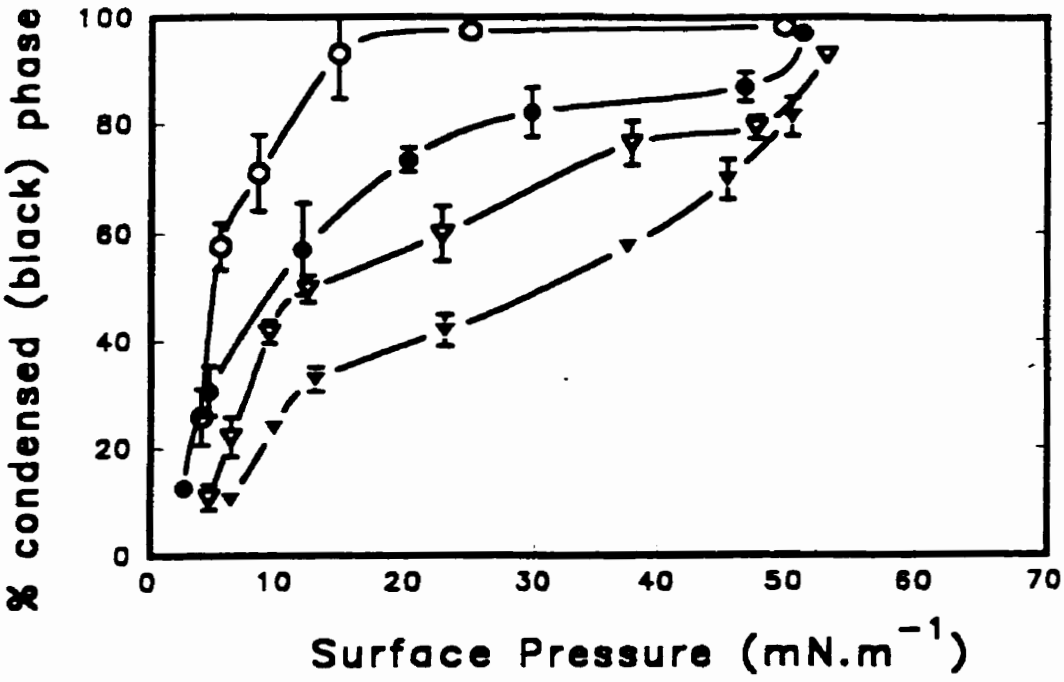
% condensed (black) phase
100
80
60
40
20
0
0
10
20
30
40
50
60
70
Surface Pressure (mN.m^{-1})

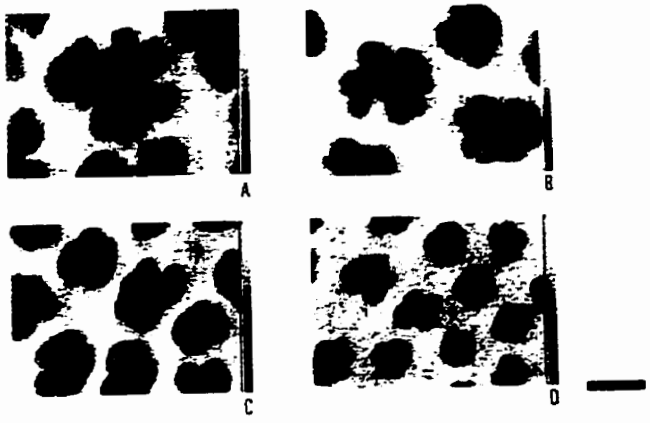
A
B
C
D

decrease in the size of condensed phase domains. The images in Figure 6.8 (bottom) also indicated that the LC domains in DPPC:DPPG monolayers had a different shape (flower-like) in the presence of calcium (± F-SP-C) compared to the ones seen in DPPC or DPPC:DPPG systems without calcium (Figure 6.3 and 6.5, bottom panels). Flower-like LC domains have been observed previously in anionic lipid monolayers containing divalent cations (Lösche and Möhwald, 1989) and by us as shown in chapter 4. In the presence of calcium increasing amounts of F-SP-C decreased the amounts LC phase of DPPC:DPPG monolayers (Figure 6.8), as had been seen in the systems without calcium (Figure 6.5).

6.41] Characterization of SP-C.

Pulmonary surfactant protein SP-C is difficult to isolate and study due to its extremely hydrophobic nature and insolubility in polar solvents usually employed in structural characterization of proteins (Beers and Fisher, 1992; Keough, 1992). Extracted native SP-C was found to contain forms which differed in their levels of acylation, truncation and dimerization, which were easily detected by MALDI type mass spectrometry (Curstedt et al., 1990). In this study MALDI analysis of SP-C and F-SP-C was used to determine the degree of acylation, dimerization and fluorescent labelling of the protein. During the fluorescent labelling process the protein underwent partial deacylation along with labelling with 1 mole of fluorescein (F-SP-C) per mole of SP-C. This partially deacylated, fluorescein-labelled F-SP-C was found not to exhibit any significant differences in its surface pressure-area monolayer characteristics (Figure 6.3, inset), and its interaction with DPPC in monolayers from properties observed with native SP-C studied previously (Perez-Gil et al., 1992a). Recently it has also been shown that, in the absence of calcium the level of SP-C acylation does not significantly alter its function in lipid adsorption and insertion to preformed monolayers (Creuwels et al., 1993). In another study F-SP-C was found to increase the rate of adsorption of DPPC to an air-water interface similar to native, non-labelled SP-C (Chapter 7). In that same study, evidence was obtained that spread films and those adsorbed from liposomes displayed similar surface textures and domain distributions. Nevertheless, it is noted that

the solvent-spread films of simple systems used here may not totally reflect the adsorbed film of pulmonary surfactant which may potentially have more complex composition *in situ*.

6.42] Effect of SP-C on DPPC/DPPG films

Proteins like glycophorin (Jones and Davis, 1987), bombilitin III (Signor et al., 1994) and cytochrome C (Peschke and Möhwald, 1987) were found to cause changes in the isotherms of lipid monolayers. Up to a π of 30 mN/m, F-SP-C produced a slight expansion of the monolayers compared to that expected for ideal mixing of lipids and proteins, irrespective of the lipid and ionic conditions used. Assuming all the nominal change in the area to be due to the area occupied by the protein, the data in Figure 6.4 could be interpreted to indicate that the protein occupied a partial molar area of $\sim$ 512 $Å^2$.molecule^{-1} in the lipid-protein monolayers at low π and at all protein concentrations, whereas at higher π its calculated partial molar areas appeared to increase. This change in the partial molar area of the protein at higher π, may be suggestive of a change of conformation or alignment of the protein in the monolayers, or a change of lipid area or both. The area changes of the DPPC monolayers induced by SP-C at lower π, are however, smaller than the ones seen in water soluble cytochrome protein, which was also found to insert in the fluid phase of DPPC (Heckl et al. 1987), indicating that hydrophobic SP-C may have a different organization in phospholipid monolayers than the water soluble proteins. Recently, Post et al. (1995) showed by ellipsometry of DPPC/SP-C monolayers that a change of thickness of the lipid-protein monolayers

occurred between 10 to 25 mN/m in the presence of SP-C, possibly indicative of some change of molecular alignment of this protein in monolayers occurred between those π. SP-C is insoluble in aqueous systems so that it can be spread in monolayers in pure form (Figure 6.3, inset). Monolayers of pure protein formed through spreading from solvent do not show an increase in partial molar areas with compression. So while it might be possible that the lipid causes a large change in the area of the protein, it seems more likely that the assumption that the lipid is unaffected by the protein at the higher pressure (and lower areas per lipid molecule) is not warranted, and that SP-C perturbs the lipid packing especially of the liquid expanded phase.

6.43] Association of SP-C with the fluid phase of DPPC/DPPG films.

The typical orientation of SP-C in bilayers (top) and in monolayers (bottom) at low (A) and high (B) surface pressures are shown in Figure 6.9. This study showed that F-SP-C occupied the LE or fluid phase of all the phospholipid monolayers studied, as shown in the images in Figure 6.3, 6.5, 6.8 (bottom panels). Previous studies have shown that fluorescently-labelled cytochrome c inserted into the LE phase of lipid monolayers (Peschke and Möhwald, 1987; Möhwald, 1990). In lipid bilayers, bactereorhodopsin and calcium ATPase have been shown by electron microscopy to be excluded from the gel phase of lipids and distributed in the fluid phase (Kleeman and McConnell, 1976; Cherry et al., 1980). Recent studies on the amphipathic helical peptide bombilitin-III in DPPC monolayers also indicate that the protein is excluded from the LC phase of lipids (Signor et al., 1994). Horowitz et al. (1993) have recently shown

Figure 6.9. Possible orientation of the α-helix of SP-C in a phospholipid bilayer (A) and in monolayers at low (B) and high (C) surface pressures (bottom).

The image (A) indicates that the orientation of the α-helix of SP-C in lipid bilayers is similar to many trans-membrane proteins, the hydrophobic stretch of the helix located in the hydrocarbon regions inside of the bilayer. The polar amino acid residues of the protein are probably located near the headgroup of the lipids, and the dipalmitoyl chains embedded into the bilayer interior to anchor the protein to the layer.

SP-C is localised in the liquid expanded or fluid phase (green regions of the films) of the phospholipid monolayers (bottom). In monolayers, the helix of SP-C may lie close to the plane of the air-water interface (B), whereas with increasing π or packing of the phospholipids the helix may orient or tilt toward the perpendicular plane of the interface (C).

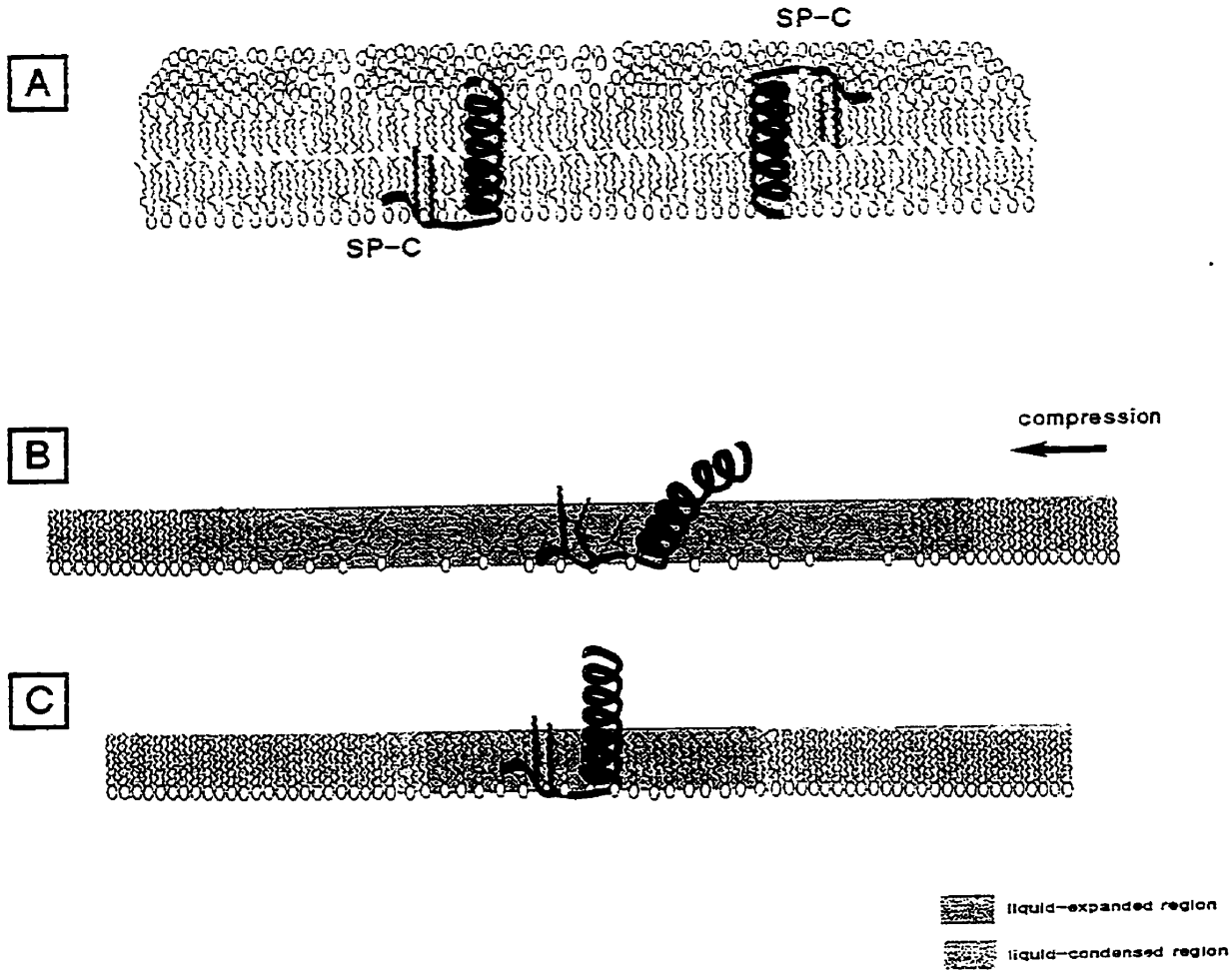
SP-C
A
SP-C
compression
B
C
liquid-expanded region
liquid-condensed region

by fluorescence energy transfer methods that SP-C is excluded from the gel phase of DPPC:DPPG bilayers, and the exclusion prompts the protein to self-associate in the fluid phase. The preference of F-SP-C for the fluid phase thus seems to be a general property of proteins to occupy loosely packed regions of bilayers or monolayers. The pattern of plots of degree of crystallization as a function of molecular area (Figure 6.7) also supports the idea that F-SP-C occupied the fluid phase, as the area per molecule of the lipids were changed in the expanded or fluid phase ($\phi = 0$), whereas the change at 100 per cent gelation ($\phi = 1$) was only minimal. This may also indicate that F-SP-C (up to 6 wt%) does not penetrate the gel or condensed phase and does not perturb the molecular areas of the lipids in that phase significantly. At 12 wt%, the lipid-protein packing appears to follow a different pattern where the F-SP-C does somehow or other influence the gel phase packing also. This is consistent with previous results for high amounts of non-fluorescent SP-C in DPPC monolayers (Perez-Gil et al., 1992a). Recently atomic force microscopy (AFM) of DPPC/DPPG films containing native SP-C has shown that the protein occupies the LE phase of the films, and that the protein molecules are organized as long strips or strands in that phase (Amrein et al., 1995). Others recent studies using AFM of SP-C in DPPC films have indicated that the organization of the LE-LC phase in such films are exactly similar to the ones observed here by fluorescence microscopy (Panaiotov et al., 1996).

6.44] Packing changes of the lipids induced by SP-C.

F-SP-C altered the packing of monolayer phases as indicated by the decrease in

domain size and amount of the condensed phase shown in Figures 6.7 and 6.8, a behaviour consistent with that seen for native SP-C in DPPC monolayers reported previously (Perez-Gil et al., 1992a). Pastrana et al. (1990) have shown by FTIR that SP-C alters the packing of DPPC:DPPG bilayers so that the lipids in lipid/SP-C mixtures exhibit more fluid characteristics than the lipids alone. In bilayers of saturated lipids, increasing amounts of SP-C broadened the range of the gel to fluid transition, decreased the co-operativity and caused a reduction in the calorimetrically detectable enthalpy of the transition in a concentration dependent manner (Shiffer et al., 1993; Simatos et al., 1990; Vandenbussche et al., 1992b). These studies indicate that SP-C can alter lipid packing in bilayers. A decrease of co-operativity of the gel to fluid transition is associated with the protein "removing" a certain number of lipids which take part in that transition or modifying the way in which the overall chain melting occurs. As seen in this study F-SP-C affected the condensed phase formation and growth in DPPC and DPPC:DPPG monolayers in a concentration dependent manner (Figure 6.6 and 6.8). Higher surface pressures were required to reach similar amounts of condensed phase lipid with increasing amounts of protein in the lipid monolayers. Figure 6.6 shows that 12 wt% F-SP-C in DPPC and DPPC:DPPG monolayers decreased the percent condensed lipid from 80% to 30% at a π of 30 mN/m. As discussed previously the appearance of more numerous and smaller LC domains in the presence of protein is likely due to a competition between the disrupting effect of SP-C on the packing and the need to pack into condensed phase caused by increasing applied pressure, resulting in more nucleation sites which grow in size with increasing π (Perez-Gil et al., 1992a). These experiments

provide direct evidence for the location of SP-C in the LE phase, something which could only be implied in the previous work (Perez-Gil et al., 1992a), and is supported by recent AFM observations (Amrein et al., 1995; Panaiotov et al., 1996).

The LC domain shapes seen in the DPPC/F-SP-C monolayers (Figure 6.3, B) showed protrusions on their boundaries, and were different from the more circular or elliptical ones found in pure DPPC monolayers. This is also consistent with the presence of lipid-protein association in the monolayers studied. Similar LC domain shapes (with protrusions) have also been observed by others in lipid-protein monolayers, and have been suggested to be due to protein mediated instabilities occurring at the LC/LE domain boundaries (Möhwald et al., 1988). The qualitative effects of F-SP-C on DPPC and DPPC:DPPG systems were similar in both the presence and absence of calcium, that is, the protein produced more, smaller LC domains in all cases. This suggests that the interaction of SP-C with the lipids in these systems is primarily governed by hydrophobic forces as implied from studies with native SP-C (Taneva and Keough, 1994a; Taneva and Keough, 1995).

Pulmonary surfactant is presumed to provide a DPPC-rich monolayer at the air-alveolar fluid interface, which reduces surface tension of that interface. In the lung alveoli the surface tension has been directly measured to be very low (corresponding possibly to very high surface pressures) at low lung volumes (Schürch et al, 1976), and it is currently believed that the alveolar fluid interfacial surface pressure due to the PS monolayer varies between 40-70 mN/m during normal breathing (Goerke and Clements, 1986). Other PS components such as SP-C may be squeezed out of such monolayers

during compression to maintain a low surface tension (or high π) at the air alveolar-fluid interface. It is hard to estimate from this study the exact amounts of F-SP-C present in the monolayers at very high π, due to difficulty in obtaining quantitative estimates of the highly irregular fluorescently labelled areas at these pressures. The results however indicate that some SP-C may be present in the monolayers at high π (see, for example, Figure 6.3, D and E) and support other studies which also indicated that small amounts of protein could be associated with the films at high surface pressures (Taneva and Keough, 1994; 1994a; 1994b). Above the collapse π of pure SP-C, the monolayer images indicated (Figure 6.3, E) that F-SP-C was mostly excluded out of the LC phase into aggregated (highly fluorescent) regions, but at least some of it may be still present in the interface. This fact is also reflected in the percent condensed plots in Figure 6.6, where about 90 % of the monolayer area was occupied by the condensed phase above the collapse π of SP-C. These results are consistent with those of Taneva and Keough (1994b) which suggest that small amounts of SP-C remain in the monolayer up to very high π, but that at high SP-C concentrations exclusion of some SP-C-lipid units occurs. The α-helix of SP-C can have preferred orientations in monolayers depending on the π (Creuwels et al., 1993). With increase in π (from 10 to 30 mN/m), the α-helical axis could change from being parallel to the plane of the monolayer to being perpendicular to it as shown in Figure 6.9 (Creuwels et al., 1993). F-SP-C may be following a similar course with the more perpendicular orientation allowing for some protein to remain in such monolayers at high π (above the collapse π of the protein). The presence of the protein at high π may also support a functional role for SP-C in rapidly re-spreading

lipids from compressed monolayers as suggested elsewhere (Taneva and Keough, 1994b).

6.45] Electrostatic interactions of SP-C ?

A recent ^{2}H-NMR study indicated that the charged N-terminal of SP-C is located at the surface of the DPPC bilayer, near the polar head-group region (see Figures 6.1 and 6.9) of the lipid (Morrow et al., 1993b). SP-C was found to order the bilayer membrane surface of DPPC:DPPG (7:1 mol/mol), partially immobilizing the lipid headgroups (Horowitz et al., 1992). Since the N-terminal region of SP-C also contains the cationic residues arginine and lysine, the protein has the potential for electrostatic interactions with anionic lipids (Shiffer et al., 1993). Our monolayer data do not allow us to confirm that such an association occurs but the percent condensed-π plots (Figure 6.6, bottom panel) may indicate some interaction of F-SP-C with the anionic headgroup of DPPG. At 12 wt% F-SP-C, the percent condensed phase profile of DPPC:DPPG in Figure 6.6 (bottom panel), indicates a slightly higher amount of gel phase formation in such monolayers compared to DPPC at similar π. This observation could also be interpreted in terms of SP-C inducing a slight ordering effect on DPPC:DPPG monolayers in comparison to DPPC. In Figure 6.8 a similar ordering effect of pure DPPC:DPPG monolayers under the influence of calcium can be seen, as higher amounts of condensed phase were reached at a lower π compared to the calcium free system. Bilayers of DPPG plus 4-10 mol% SP-C have been shown to exhibit chain melting transitions at temperatures (T_c) 20-25°C higher than DPPG alone (Perez-Gil et al., 1994; Shiffer et al., 1993). The higher T_c of the bilayers indicate that they are more densely

packed and ordered than those in the absence of protein. Thus F-SP-C may have some electrostatic interactions with anionic lipid monolayers but they cannot be isolated in this study, possibly because of hydrophobic lipid-protein interactions overshadowing the electrostatic interactions.

Fluorescence microscopy of anionic lipid monolayers has shown that calcium can condense or increase the amount of LC phase of phosphatidylglycerol (Evert et al., 1994; Leckband et al. 1993; Nag et al., 1994, and Chapter 4) and other anionic lipids (Lösche and Möhwald, 1989), compared to its effect on DPPC. This condensation was observed as an increase in formation and growth of LC regions of such monolayers at lower π compared to DPPC (Evert et al., 1994; Lösche and Möhwald, 1989; Nag et al., 1994). Our observations of DPPC:DPPG-Ca monolayers are similar to those found in the previous studies. As shown in Figure 6.8, higher amounts of condensed phase were found in all DPPC:DPPG and DPPC:DPPG/F-SP-C monolayers in the presence of calcium compared to the monolayers without calcium (Figure 6.7, bottom panel). Also the shapes of the LC domains in all DPPC:DPPG/F-SP-C monolayers in the presence of calcium (Figure 6.8, bottom panel) showed flower-like structures, and were different from those seen in monolayers without calcium. These structural changes in DPPC:DPPG/F-SP-C condensed domains may indicate that calcium-mediated effects on the lipid packing persist in monolayers containing the protein. The condensation of the acidic lipids in monolayers is possibly due to dehydration of the anionic lipid headgroups by calcium which leads to an ordering of the lipid acyl chains at low π (Flach et al., 1993). The occurrence of a calcium induced lateral phase segregation of PG-rich LC

phase may also be possible (Leckband et al., 1993), where the total LC phase is a mixture of segregated DPPG-Ca rich phase plus the normal surface pressure induced LC phase.

The plots of percent condensed phase versus π for DPPC:DPPG monolayers in the presence of calcium (Figure 6.8) showed that 95 % condensed phase is reached at π of 15 mN/m compared to a requirement for twice the π (30 mN/m) to reach similar amounts of condensed phase in the monolayers in the absence of the cation (Figure 6.6). For the most part, inclusion of F-SP-C in DPPC:DPPG-Ca monolayers caused relatively larger reductions in the percent condensed then it did in DPPC:DPPG monolayers [Compare Figures 6.6 (bottom panel) and 6.8 (top panel)]. This observation suggests that the protein partially overrides the condensing effect of calcium and continues to perturb the monolayer lipid packing. Alpha helical peptides have been suggested to interact with an air-water or lipid-water interface according to their hydrophobicity (Krebs and Phillips, 1983), and the highly hydrophobic F-SP-C even disrupted the monolayer packing of a highly condensed (by ions) monolayer. The perturbing effects of the protein over the condensing effect of cations demonstrated a predominance of hydrophobic forces over electrostatic ones in the lipid-protein interactions.

Recent studies on mellitin in lipid films have shown that a dehydration of the lipid headgroups is associated with the protein assuming a different secondary structure in the lipid environment (De Jongh et al., 1994). Creuwels et al. (1993) have shown that, with increase in π the α-helix of SP-C undergoes an orientational change from a parallel to perpendicular orientation relative to the monolayer plane. Since calcium can dehydrate

the DPPG headgroup, F-SP-C possibly might have had a different orientation in the DPPC:DPPG monolayers when calcium was present, and perturbed the packing in such monolayers differently from that of DPPC or PG systems without the cation.

SP-C can induce packing re-arrangements (increase fluidity or decreased condensed phase formation) in neutral and anionic lipid arrays. Fluid lipid bilayers have higher rates of adsorption to the air-water interface compared to gel state bilayers. SP-C may enhance the capacity of lipids, neutral or anionic, to adsorb at an air-water interface, by causing packing perturbations and increasing fluidity in monolayers or it might provide sites of dislocation in bilayers so that cooperative lipid transfers to the interface might be initiated. When calcium was present the relative perturbation of the anionic lipid system by SP-C seemed to increase consistent with enhanced adsorption and lipid insertive processes seen previously by others (Creuwels et al., 1993). This study indicates that the α-helical protein SP-C is dispersed in the fluid (LE) phase and confirms the prediction of a previous study (Perez-Gil et al., 1992a). It also confirms that such proteins may remain in the monolayer at high surface pressure, in regions laterally-excluded from the condensed phase. Although the protein studied here was mainly deacylated, currently it is not known what the function of the acylation of the protein is, and if such acylation would alter the surface activity of the protein.

[*This chapter and the figures have been published as Nag et al., 1996 in the Biophysical Journal (Appendix B, No. 5); and reprinted with permission of publisher and co-authors*].

Chapter 7

ADSORPTION

INTRODUCTION

Although lipids are easily spread in monolayers and yield some information on biological membranes, lipid-protein monolayers are difficult to assemble (Schindler, 1989) because of the insolubility of most proteins in volatile non-polar solvents. Monolayers formed by adsorption from lipid-protein vesicles can have proteins incorporated in them (Schindler, 1989). Planar lipid-protein bilayers formed from adsorbed monolayers have served as tools in studying biomembrane lipid-protein and lipid-lipid interactions (Lawrie et al., 1996; Pattus et al., 1981; Schürholz and Schindler, 1991). Adsorbed monolayers have also been used in studying processes such as biomembrane assembly (Gershfeld, 1989), lipid exchange between membranes (Jähnig, 1984), antibody-antigen recognition (Fischer et al., 1993) and pulmonary surfactant biophysics (Goerke and Clements, 1986; Keough, 1992). Monolayers spontaneously formed from vesicles may be similar to their solvent-spread counterparts (Gershfeld, 1976; Schindler, 1989), but limited direct experimental evidence exists on this issue (Salesse et al., 1987). There has been a continuous interest in the equivalency of spread and adsorbed films, especially in the field of pulmonary surfactant, since the films in the lung alveoli are adsorbed and not solvent spread. In studying adsorption processes of some pulmonary surfactant components, we have found direct evidence for equivalence or similarities in monolayers formed by adsorption or spreading from volatile solvents.

Fluorescence microscopy of solvent-spread lipid and lipid-protein films but not adsorbed ones have been used to visually observe monolayer structures at the air-water

interface as discussed in the preceding chapters (Möhwald, 1990; Stine, 1995). Using fluorescence microscopy, Heyn et. al. (1990) showed that films formed by adsorption of lipid vesicles show LE or LC phases during isothermal compression. These films were formed from vesicular suspensions that had been transferred by a "wet bridge" on to an air-water interface to yield films without attached vesicles (Heyn et al., 1990). In this chapter we report on the phase characteristics as a function of time and changing surface pressure (π) of monolayers of DPPC and DPPC/SP-C that were formed by adsorption from vesicles injected below the air-water interface. Some of these films were compared to the properties of films spread from organic solvent. The location of the protein SP-C in the adsorbed DPPC films was determined with fluorescently-labelled protein (F-SP-C), the property of which was discussed in solvent-spread films in the last chapter. Although the adsorption of surfactant films in the alveoli may occur via more complex processes (tubular myelin, reservoir), this study at least shed some light on adsorption of simple components of surfactant at the air-water interface.

7.21] Materials.

DPPC and F-SP-C were obtained as discussed in Chapter 6. The fluorescent probe N-lissamine-rhodamine-B-sulphonyl-1,2,hexadecyl phosphatidylethanolamine (R-PE) was obtained from Molecular Probes (Eugene, OR).

The vesicle solvent and monolayer subphase buffer was prepared by dissolving 0.15 M NaCl, 10 mM MOPS (3-[N-morpholino] propane-sulphonic acid) (Sigma, MO) and 5 mM $CaCl_2$ in doubly glass distilled water, the second distillation being performed with dilute $KMnO_4$, and the pH adjusted to 6.9 with 0.1N HCl.

7.22] Preparation of vesicles.

Liposomal suspensions of DPPC and DPPC plus F-SP-C were prepared by two methods to yield multilamellar vesicles (MLV) and sonicated vesicles (SV). DPPC, F-SP-C and the probe R-PE were individually dissolved in chloroform:methanol 3:1 (vol/vol) and mixed in desired proportions. The solvents were dried down under a stream of nitrogen in small 1 ml chromosulphuric-acid cleaned glass vials. Sonicated vesicles (SV) were prepared by resuspending the dried materials in 0.9% buffered saline and sonicating the suspensions on ice. Sonication was performed with 60 individual bursts lasting 1 sec at medium-power with a microprobe sonicator (Bronson Ultrasonics, ON, CAN.). MLV were made by incubating the re-suspended material at 45°C for 30 minutes (above T_c of DPPC) and vigorously vortexing the suspensions until a milky

homogenous suspension was achieved. These methods and their liposomal type yields are discussed in detail by Woodle and Papahadjopoulus, (1989).

7.23] Epifluorescence microscopic adsorption apparatus.

Adsorption was observed on a modified version of the epifluorescent microscopic surface balance. Modification was done by attaching an adsorption chamber to the original balance. The adsorption apparatus was made of teflon and contained two circular chambers connected by a short channel to maintain subphase and monolayer continuity. Diagrams of the adsorption balance (top), and the adsorption chamber (bottom) are shown in Figure 7.1. The total volume of the subphase was 10 ml and the total surface area 15 cm^2. The vesicles in desired amounts (0.04-0.06 mg/ml final concentration) were injected into the buffer under the air-buffer interface at the centre of the channel linking the two chambers. Surface fluorescence was monitored by epifluorescence microscopy from one of the circular chambers and surface pressure in the second chamber using a Wilhelmy dipping plate suspended from a pressure transducer.

7.24] Monolayer formation and visual observation.

Vesicular suspensions of DPPC or DPPC + F-SP-C were injected under the air-buffer interface of the surface balance discussed above. The change of surface pressure (π) during adsorption from vesicles was monitored using a roughened platinum Wilhelmy dipping plate attached to a pressure transducer (Figure 7.1, top) connected to

Figure 7.1 Diagrams of the epifluorescence microscopic adsorption apparatus (top) and a cross section of the adsorption chamber (bottom) are shown. The adsorption chamber (bottom) was made from a solid teflon block with two cylindrical cups cut into the block, and the cups were connected by a channel or canal. Smaller circular wells or grooves (2 mm in depth) were cut into the bottom of each of the cups to hold a magnetic stirrer. The complete volume of the chamber was 10 ml.

This chamber was fitted into the cavity of the larger epifluorescent microscopic surface balance used for compression of solvent spread films. The surface tension of the clean buffer poured into the chamber was measured by a platinum dipping plate in one of the circular cups, converted into surface pressure by the computer, and plotted as a function of time. After injection of vesicles under the air-water interface through a small hole in the middle of the canal, the surface was immediately brought into focus in the microscope. The features of the surface or the films formed was observed over 1 hour, and typical images were video recorded and analyzed.

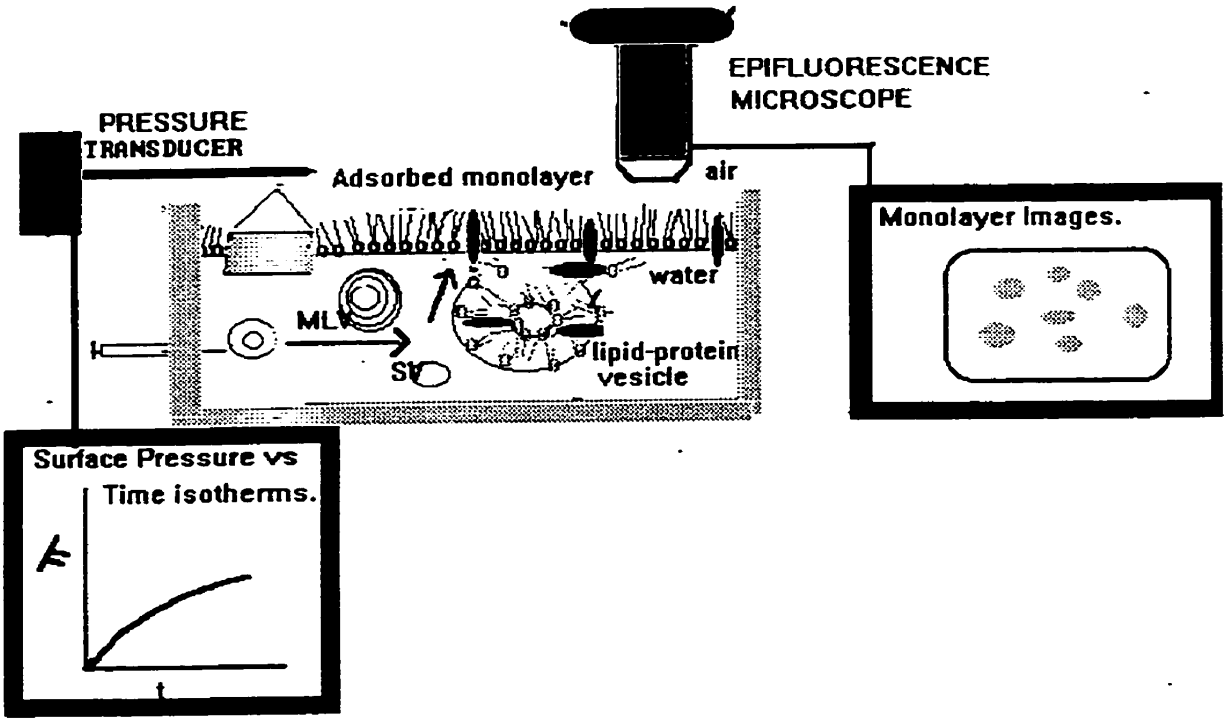
EPIFLUORESCENCE
MICROSCOPE
PRESSURE
TRANSDUCER
Adsorbed monolayer
air
water
ML
SV
lipid-protein
vesicle
Monolayer Images.
Surface Pressure vs
Time isotherms.
π
t

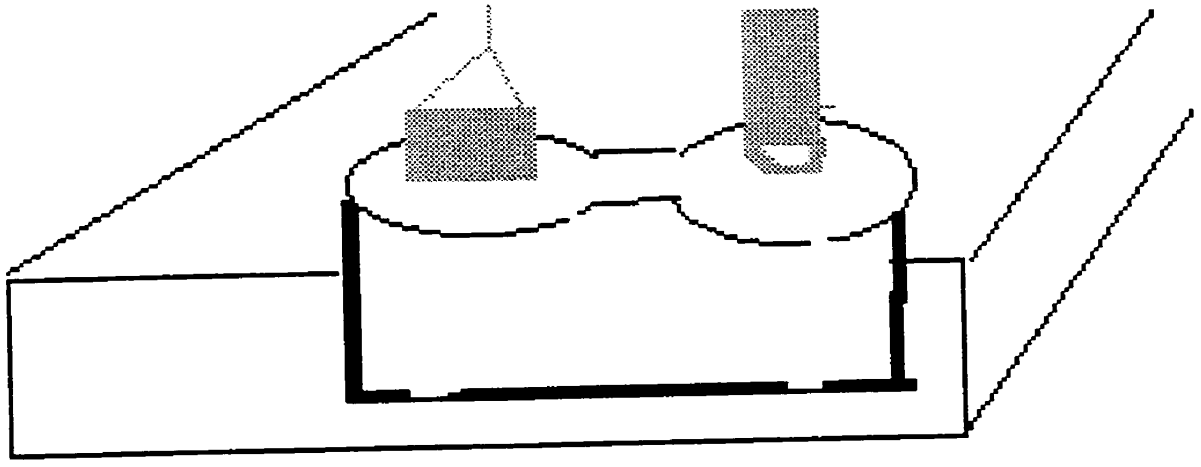

a personal computer, as discussed above. Experiments were performed at a temperature of 22 $\pm$ 2°C. After injection of vesicles under the buffer interface, the surface of the solution was brought into focus in the epifluorescence microscope. The formation of the monolayer was observed from R-PE or F-SP-C fluorescence emission. Typical monolayer images were recorded on a video tape and analyzed as discussed above (Chapter 2 and Appendix A).

Although the apparatus had capabilities for stirring the subphase with magnetic stirrers (Figure 7.1, bottom), the vesicular subphase was not stirred, as stirring (30-50 cycles/minute) aggregated the monolayer phase domains, and made the monolayers extremely inhomogeneous in visual appearance. The general shapes of the condensed domains forming the aggregates though were the same in stirred and un-stirred systems.

7.31] Adsorption from lipid vesicles.

Surface pressure versus time (π-t) isotherms of DPPC + 1 mol% R-PE formed by adsorption from vesicles are shown in Figure 7.2 (top) and typical images observed at the π indicated by letters in the isotherms are displayed (bottom). Sonicated vesicles (SV) of DPPC adsorbed more rapidly (reaching a $\pi \sim 9$ mN/m in 30 min) than multi-lamellar vesicles (MLV) (0.1 mN/m in 30 min). As shown in Figure 7.2 (bottom), image (A), the surface monolayer initially formed by adsorption from MLV had gas phase domains (dark areas) coexisting with fluorescent liquid expanded (LE) phase (light areas). Typical images of adsorbed monolayers formed from SV are shown in Figure 7.2 (bottom; (B), (C) and (D)). These images show distinct liquid condensed (LC) domains (dark areas) coexisting with the fluorescent liquid expanded (white regions) phase. Images (B) and (C) are taken from a monolayer formed by adsorption from a SV suspension containing 0.04 mg/ml of DPPC and image (D) is from monolayer adsorbed from SV at 0.06 mg/ml. The bright areas indicated by arrow marks in images (C) and (D) might be fluorescent vesicles attached to or near the surface monolayer.

It is apparent from images in Figure 7.2 that DPPC monolayers undergo gas to LE to LC phase transitions because of increasing surface pressure during adsorption. Gas and LE phase domains which were seen previously in highly expanded solvent-spread DPPC monolayers at $\pi \sim 0$ mN/m also appear in the spontaneously adsorbed ones (Figure 7.2, bottom, (A)) at similar π. The increase in surface pressure during

Figure 7.2 Surface pressure - time (π-t) isotherms of DPPC + 1 mol% R-PE adsorbing from vesicles (top) and typical images from the surface monolayers formed (bottom). Letters A-D represent the π at which the images in the lower panel were obtained. The light regions indicate the LE phase into which the probe R-PE partitioned. The bright areas indicated by the arrow marks in the lower panel (C and D) may be vesicles in close proximity to the interface. Scale bar is 25 μ.

MLV (0.06 mg/ml) of DPPC (∇) adsorbed only to a $\pi \sim 0.1$ mN/m in 30 minutes and the surface monolayer formed showed gas phase (dark) domains coexisting with LE phase (A). Sonicated vesicles ($\bullet$) (0.04 mg/ml) of DPPC adsorbed more rapidly than MLV, but slowly enough to show typical kidney bean shaped LC phase (dark) domains (B), which increased in size with time and come in contact around $\pi \sim$ 9 mN/m (C). Sonicated vesicles (SV) of DPPC ($\bigcirc$) at 0.06 mg/ml adsorbed to reach a similar π as in C but in shorter time, and showed smaller and more numerous LC domains (D).

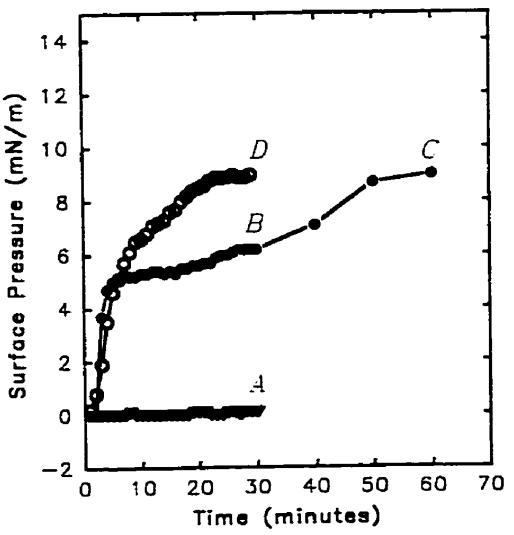
Surface Pressure (mN/m)
Time (minutes)
A
B
C
D

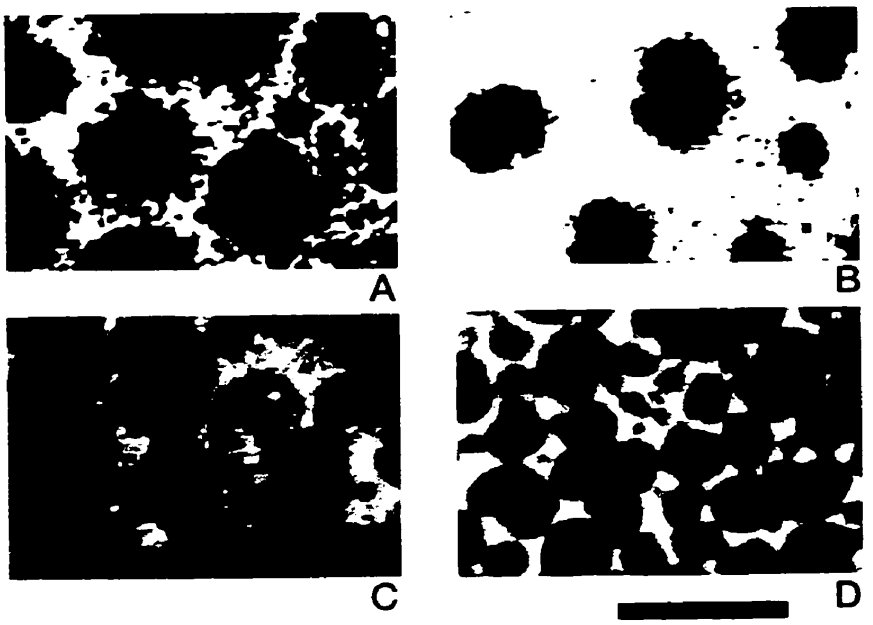
A
B
C
D

adsorption (between points B and C in Figure 7.2, top) occurred due to increased packing density of the lipids, and is equivalent to the increase in π seen during compression of solvent spread monolayers. The LC domains of DPPC in solvent-spread monolayers that have been compressed relatively slowly display a kidney bean shape (Flörsheimer and Möhwald, 1989; McConnell, 1991; Nag et al., 1990; Weis and McConnell, 1985), and these are seen at similar π in the adsorbed monolayers (Figure 7.2, bottom, B).

Spread monolayers of DPPC and of other lipids, when compressed relatively rapidly showed a different LC domain distribution compared to that seen in slowly-compressed ones (Chi et al. 1993; Nag et al, 1991; Shimomura et al., 1992; Weidman and Volhardt, 1996). Fast compression leads to large numbers of small-sized LC domains compared to those seen in monolayers which have been slowly compressed to equivalent π (Nag et al. 1991; Shimomura et al. 1992). This pattern of dependency of size and number of condensed domains on compression rates is also seen here in adsorbed monolayers. The condensed domains in Figure 7.2, C (slower adsorption) are larger in size and less numerous per image compared to those shown in D (faster adsorption). The monolayer formed from the higher concentration of lipid in the subphase (D) had more material adsorbed at a shorter time (analogous to fast compression of a spread monolayer) than the one seen in C (analogous to slow compression of spread monolayers).

Schindler (1979) proposed a model sequence for adsorption from lipid vesicles which agrees with our experimental observations. A diagram of the adsorption process from dry lipids, large and small vesicular structures and bilayer forms to form surface

monolayers is shown in Figure 7.3 (Lawrie et al., 1996). Schindler's (1979) model proposes that bilayer vesicles disintegrate at an open air-water interface at $\pi \sim 0$ mN/m. This disintegration leads to monolayer formation at the interface and an initial rapid increase in π. Once the monolayer is formed no further vesicular disintegration occurs due to the absence of an open interface and a layer of vesicles can form under the monolayer, which may come in contact with the monolayer (Schindler, 1979). Slow exchange of material then occurs between the outer leaflet of the bilayer vesicles and the surface monolayer with more material moving from the bilayer to the monolayer than in the opposite direction. The exchange occurs because of exclusion of free water between monolayer and vesicles (or dehydrated headgroup regions) as polar lipid head-group contacts are transiently formed. This absence of free water decreases the free energy, and allows the hydrophobic chains to transfer from one layer to the other, until a steady-state or equilibrium surface pressure is reached. DPPC vesicular adsorption seems to follow this sequence. A surface monolayer was formed relatively quickly (a rapid rise in π in the first few minutes). Once the initial DPPC monolayer was formed possible transfer of material from the bilayer occurred more slowly (a decreased slope in the π-t curve after 10 minutes), and was accompanied by growth of LC domains. LC domains grew relatively slowly, allowing for tilt and orientational order to set in, thus producing the shapes and sizes of LC domains that are typical of a slowly-formed condensed monolayer (Figure 7.2, (C)). With the higher concentration the rate of transfer was greater and the condensed monolayer was achieved faster (Figure 7.2, (D)). Once the condensed monolayers were formed (as evidenced by the high amounts of LC phase

Figure 7.3 Diagram of the adsorption of lipids to an air-water interface, from various vesicular and aggregated forms [Reprinted from Lawrie et al., (1996), with the kind permission from the author and publisher, ©Elsevier Science Ireland Ltd., Ireland].

Dry lipids (a) (anhydrous) can disperse at an air-water interface to form films. Different bilayer forms such as uni-lamellar or multi-lamellar vesicles which can be prepared by dispersing such lipids in water, adsorb at different speeds to an air-water interface to form monolayers ((b) and (c)). Some of the lipids in the films or in their anhydrous bulk forms (a), can "sink" or "squeeze-out" of the films to form other structures in the bulk phase (myelinic and liposomal structures).

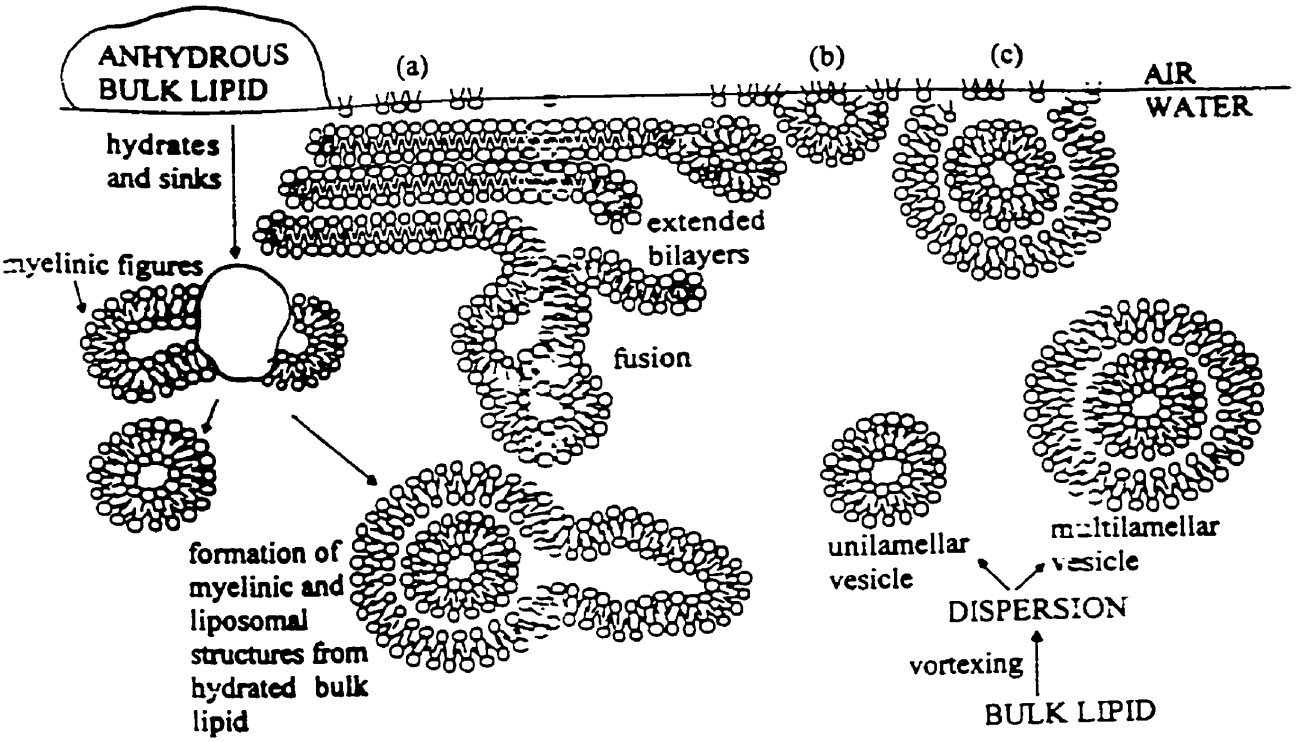
ANHYDROUS
BULK LIPID
(a)
(b)
(c)
AIR
WATER
hydrates
and sinks
extended
bilayers
myelinic figures
fusion
formation of
myelinic and
liposomal
structures from
hydrated bulk
lipid
unilamellar
vesicle
multilamellar
vesicle
DISPERSION
vortexing
BULK LIPID

lipids in Figure 7.2, (C) and (D)), the bilayer-monolayer lipid transfer process appeared to be approaching directional equivalence or a steady-state.

7.32] Adsorption from lipid-protein vesicles.

Monolayers made by adsorption of vesicles containing lipids and proteins from biological membranes have been used to study lipid-protein interactions and protein functions (Pattus et al., 1981; Schindler, 1989; Schurholz and Schindler, 1991). The lipid-protein ratios of such adsorbed monolayers were found to be close to those of the vesicles from which they were formed (Pattus et al., 1981; Schürholz and Schindler, 1991). Such adsorbed monolayers have been used to form black lipid (or lipid-protein) membranes (BLM) by special techniques (Schindler, 1989). Ion channel proteins in such reconstituted BLM were found to be functionally fully active (Schindler, 1989). Formation of such adsorbed lipid-protein monolayers has shown that the adsorption of lipids was enhanced in the presence of membrane proteins. The transbilayer parts of most membrane proteins are α-helical in their structure and some of these proteins can be incorporated into the monolayers (Pattus et al. 1981; Schindler, 1989). Pulmonary surfactant protein SP-C is mainly α-helical in lipid environments (Morrow et al., 1993b) and promotes the adsorption of lipids to the air-saline interface (Curstedt et al., 1987; Simatos et al., 1990; Takahasi and Fujiwara, 1986; Yu and Possmayer, 1990). Incorporating 3 and 7 wt% of fluorescently labelled SP-C (F-SP-C) in MLV of DPPC, enhanced the rate of adsorption of DPPC as shown in Figure 7.4 (top). The surface monolayers formed by adsorption from DPPC/F-SP-C vesicles after 30 min are shown

Figure 7.4 Surface pressure - time (π-t) isotherms obtained from adsorption of MLV of DPPC and DPPC + F-SP-C (top), and typical images from the surface monolayer formed (bottom) at π indicated in the isotherms. MLV (0.06 mg/ml) of DPPC (■) or DPPC plus 3 wt% (●) and 7 wt% (○) of F-SP-C were used. Error bars indicate plus one standard deviation from three sets of experiments. The scale bar is 25 μm.

The bright part of the images (bottom) represents the fluorescence observed from the labelled protein obtained at points A and B noted on the adsorption isotherms shown on top. The highly fluorescent regions (arrow mark) in image (B) indicate possible protein aggregates. These were not likely vesicles, as the fluorescence intensity in these spots was much higher than that seen in DPPC vesicles adsorbing to or near the surface monolayer (Figure 7.2, arrow marks in (C) and (D)).

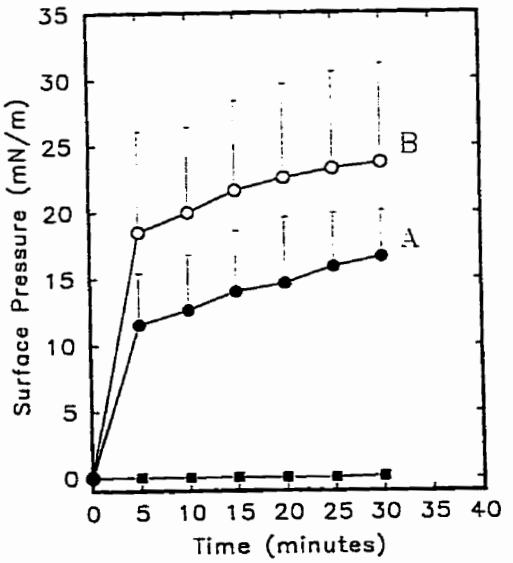
35
30
25
20
15
10
5
0
Surface Pressure (mN/m)
B
A
0 5 10 15 20 25 30 35 40
Time (minutes)

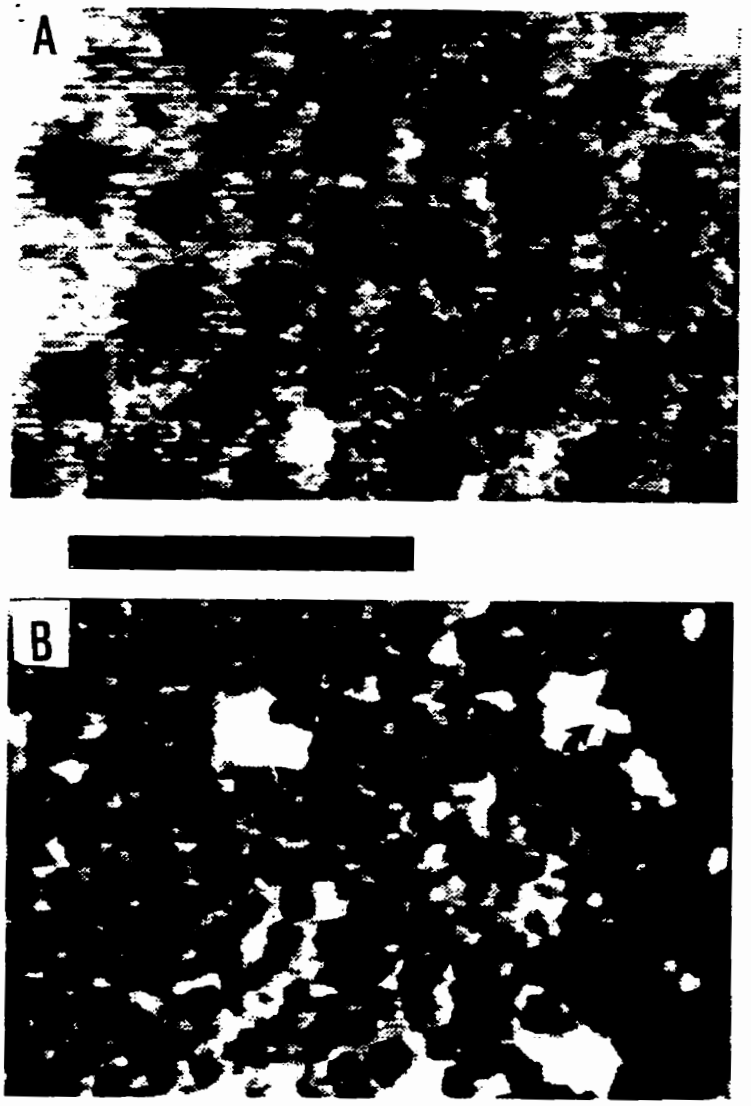
A
B

181a

in Figure 7.4 (bottom). The fluorescent (light) part of the images in Figure 7.4 reflect F-SP-C emission, and indicate that the protein accompanies the lipid into the monolayer at the air-water interface and it is in the LE or fluid phase of the monolayer.

Increasing amounts of F-SP-C not only enhanced the rate of adsorption of DPPC (A to B in Figure 7.4, top), but also decreased the average size of LC domains in the corresponding monolayers ((A) to (B) in Figure 7.4, bottom). The fact that F-SP-C induced a decrease in the size of condensed domains is consistent with previous results from spread monolayers of DPPC that contained similar amounts of non-labelled SP-C (Keough et al., 1992; Perez-Gil et al., 1992a), and in solvent-spread systems discussed in chapter 6.

SP-C has been reported to produce discoidal structures in certain lipid dispersions (Williams et al., 1991). Defects produced in the bilayer structure or the presence of the discoidal structures may promote rapid monolayer formation. Also SP-C seems to behave in a lipid environment in a similar fashion to some transmembrane proteins (Pattus, et al., 1981; Schürholz and Schindler, 1991) in enhancing monolayer formation over that seen for pure lipid vesicles.

7.33] Spread and adsorbed monolayers.

To further analyze the similarities between solvent-spread and adsorbed monolayers, films of DPPC + 3 wt% F-SP-C were spread from solvent and compressed at a rate to achieve the same π over the same time as a monolayer adsorbed from MLV of a similar mixture (e.g. Figure 7.4, top). Figure 7.5 (top) shows typical images from

Figure 7.5. Typical images observed in monolayers formed by solvent spreading (0.014 mg) and adsorption from vesicles (0.06 mg/ml) each containing DPPC + 3 wt% F-SP-C (top) and the percentage of LC phase observed in such monolayers at $\pi \sim 12$ and 15 mN/m (bottom). Image (A) is from an adsorbed monolayer and (B) from a solvent-spread monolayer compressed to a $\pi \sim 15$ mN/m. The white scale bar at the bottom of image B is 25 μm.

In the plot (bottom) the bars indicate the types of monolayers analyzed as adsorbed (black) and spread (white). The total percentage of condensed domains was calculated by estimating the total amount of LC phase observed per image. An average of ten images were analyzed at each π from both types of monolayers and the error bars indicate plus one standard deviation.

A

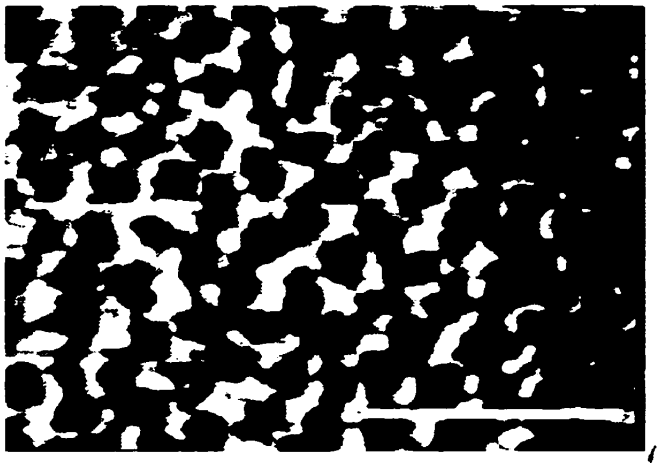

B

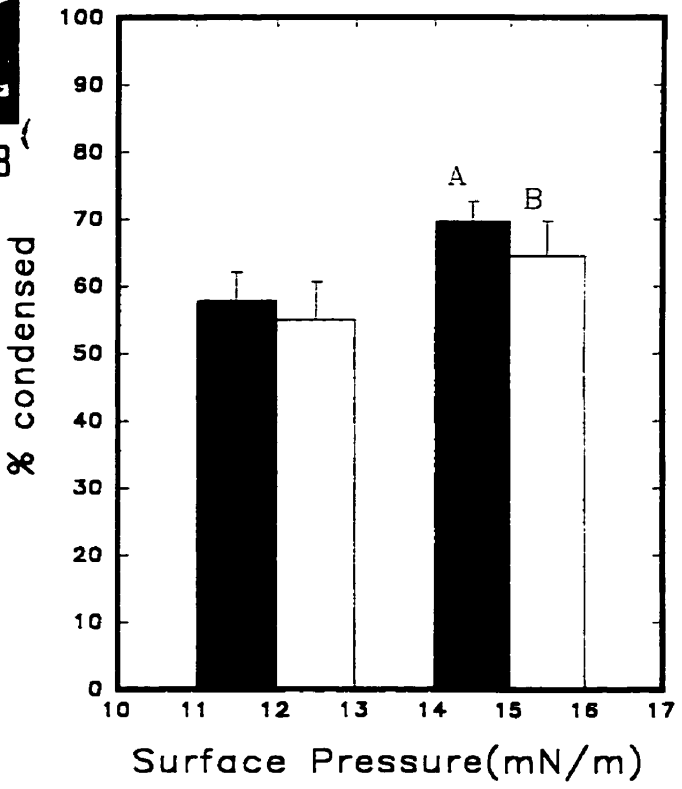
100
90
80
70
60
50
40
30
20
10
0
% condensed
A
B
10
11
12
13
14
15
16
17
Surface Pressure(mN/m)

an adsorbed monolayer (A) at a $\pi \sim 15$ mN/m and a solvent-spread monolayer (B) after compression to the same π. The shapes of LC domains were similar in both monolayers. The total amounts of LC phase (black areas in the images) at $\pi = 12$ and 15 mN/m for such monolayers are shown in Figure 7.5, (bottom). The relative amounts of condensed phase in adsorbed and spread monolayers of DPPC + F-SP-C were similar, suggesting that the process by which monolayers were formed lead to similar distributions at the interface.

Hydrophobic proteins of pulmonary surfactant alter the π-A isothermal characteristics of some spread lipid monolayers (Longo et al., 1993; Perez-Gil et al., 1992a; Taneva and Keough, 1994a, 1994b; last chapter). SP-C has been shown to expand spread DPPC monolayers (Perez-Gil et al., 1992a; Taneva and Keough, 1994b), and broaden the range of the gel to liquid crystalline melting temperature (T_c) of the DPPC bilayers (Shiffer et al., 1993; Morrow et al., 1993b). This is consistent with a decrease in the co-operativity of the bilayer gel to fluid phase transition (Gershfeld, 1976; Simatos et al., 1990). Adsorption of fluid lipid bilayers at an air-water interface is more rapid than that from gel state bilayers (Gershfeld, 1976, 1989; Heyn, et al. 1990). F-SP-C may increase adsorption of DPPC bilayers by "fluidizing" the chain packing of such lipids or producing defects in the packing of the system. In spread monolayers of DPPC containing similar amounts of SP-C to those in this system, the protein increased the amount of LE phase at any given π in comparison to that in pure DPPC (Keough et al. 1992; Perez-Gil et al., 1992a), and in systems with F-SP-C as discussed in chapter 6. In adsorbed monolayers the decreased size of the condensed (LC) domains (Figure 7.3,

bottom, A to B) seen when the amount of F-SP-C was increased is consistent with a decrease in the co-operativity of an isothermal phase transition.

The results of the direct visualization presented here, taken together with previous findings in other systems, suggest that these adsorbed and solvent spread monolayers are equivalent or at least have striking similarities in the phase structures observed in both systems. The protein SP-C enhanced monolayer formation, and is excluded from the liquid condensed regions of adsorbed DPPC monolayers, as also seen in the solvent spread-ones. Establishing the equivalence of adsorbed and spread monolayers reinforces the use of either system to study monolayer characteristics as they pertain to pulmonary surfactant or as models for biological membranes.

[*This chapter and the figures have been published as Nag et al., 1996 in Biophysical Journal (Appendix B, No. 4); and reprinted with permission from the co-authors and the publisher*]

Chapter 8

SURFACTANT PROTEIN - B

(SP-B)

INTRODUCTION

Surfactant protein B (SP-B) was first recognized in lipid extracts of pulmonary surfactant (PS) as another hydrophobic protein which co-isolated with SP-C. Figure 8.1 (a) (top) shows the gene, RNA, SP-B and the active form of the protein in a lipid bilayer (box) (Weaver and Whitsett, 1991). The active 79 amino acid SP-B peptide is produced by the proteolytic cleavage of a pro-SP-B (Figure 8.1, a, top), generating a peptide containing 7 cysteines, and having a molecular weight of 8.7 kDa. The 7 cysteine residues allow the active SP-B peptide to form inter- and intra- molecular disulphide bridges (S-S bonds) that ultimately form oligomers of 17 kDa (dimer), 26 kDa (trimer) and 35 kDa (tetramer). Amino acid sequences of the protein in surfactant of different mammalian species show that SP-B is extremely well conserved (Bruno et al., 1995; Glasser et al., 1987; Hawgood et al., 1987; Whitsett et al., 1995). The protein was found to enhance the surface activity of PS lipids when tested *in vitro*. Targeted disruption of the SP-B gene *in vivo* caused altered surfactant homeostasis and rapid respiratory failure in newborn rats, indicating the functional significance of the protein in pulmonary surfactant (Clark et al., 1995), as was also found for SP-C.

Figure 8.1 (b) shows the secretory pathway of SP-B in type II cells (top) and the localization of the protein in mono and bilayers (bottom) (Whitsett et al., 1995). SP-B is found in the lamellar bodies, secreted into the air-alveolar fluid interface, and is also possibly present in tubular myelin (Figure 8.1 (b), top). Mature SP-B can form amphipathic helixes (cylinders with + signs in Figure 8.1 (b), bottom) due to a number

Figure 8.1 Gene, mRNA and the pre-protein form of SP-B (from which the active peptide is cleaved) and the 8.7 kDa active peptide possible localization in a lipid bilayer (box) are shown (a). The secretory pathway of the protein in the type - II cell (top), and the possible localization of the amphipathic helices of SP-B in mono and bilayers in (bottom) are shown in (b). [Reprinted with permission of the authors and publishers, (a) from Weaver and Whitsett, (1991), © The Biochemical Society & Portland Press, UK; and (b) from Whitsett et al., (1995), © American Physiological Society]

The helical (coil) parts in (a) or cylindrical structures in (b, bottom) indicate the amphipathic helices of SP-B. These helices are proposed to localize in the headgroup regions of the phospholipids in mono- or bi- layers.

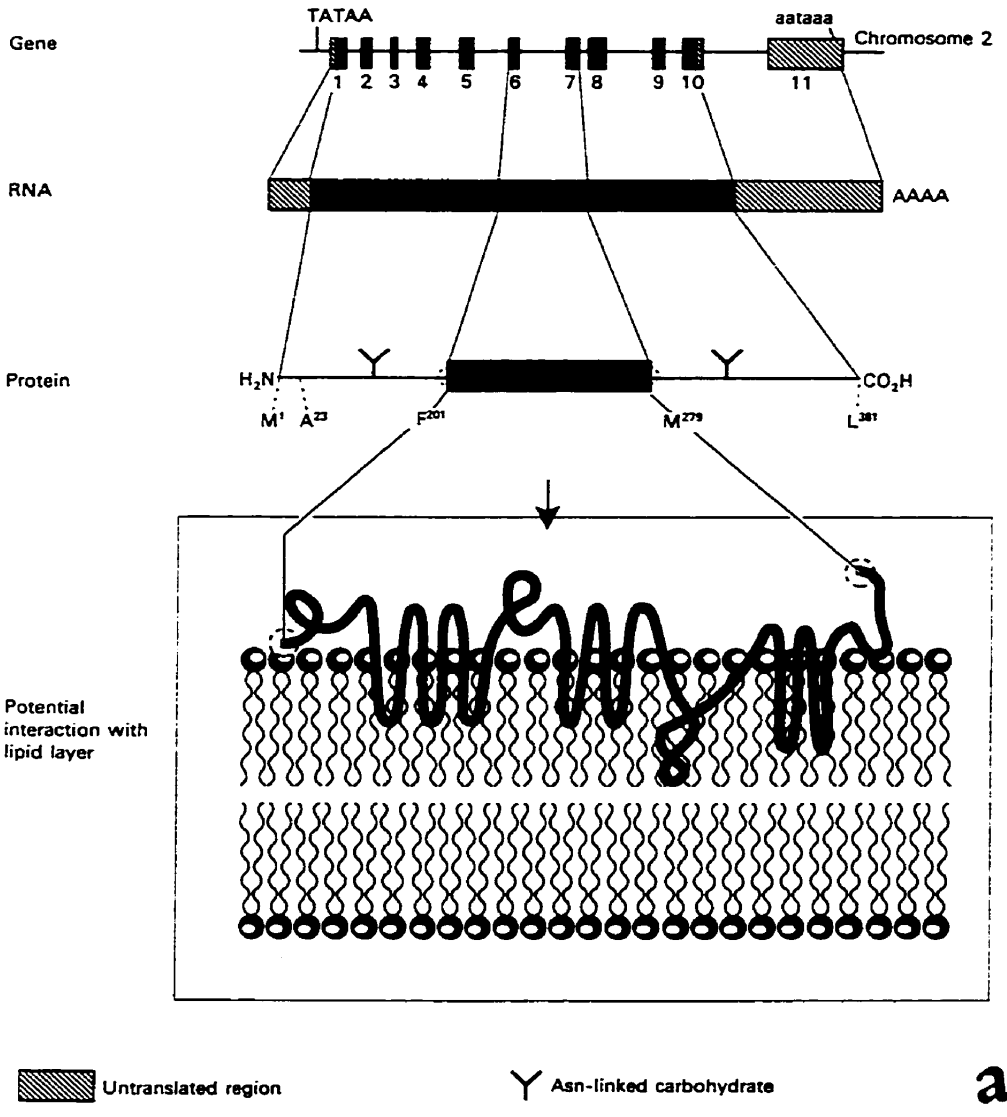
Gene
TATAA
aataaa
Chromosome 2
1 2 3 4 5 6 7 8 9 10
11
RNA
AAAA
Protein
H_2N
CO_2H
M^1
A^{23}
F^{201}
M^{279}
L^{381}
Potential interaction with lipid layer
Untranslated region
Asn-linked carbohydrate

a)

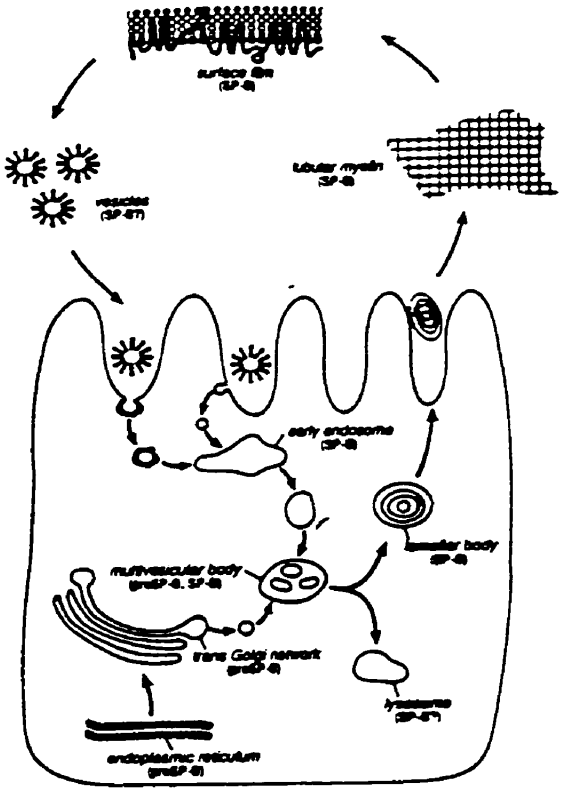

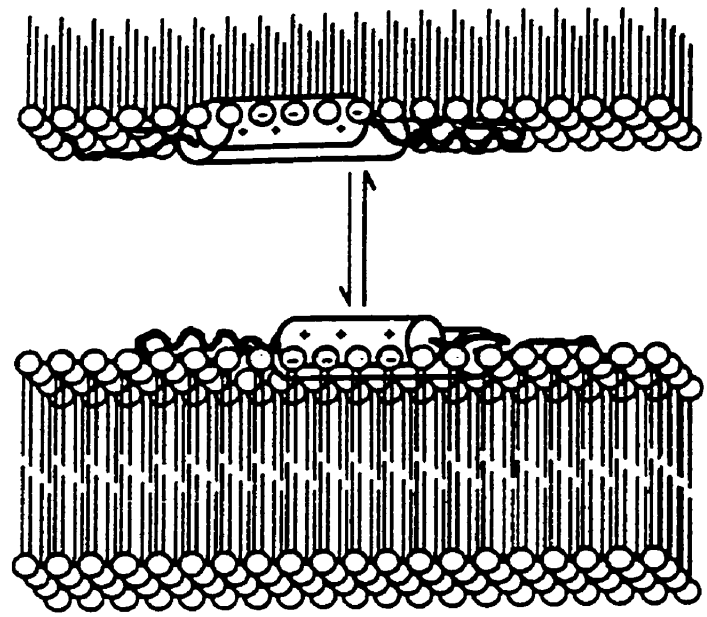

b)

of charged amino acids dispersed throughout its sequence. The hydrophobic face of the first helix contains leucine, valine and isoleucine and imparts the protein its hydrophobicity. In lipid bilayers as shown in Figure 8.1 (a), (bottom) such amphipathic helices are suggested to be located near the lipid headgroups or the membrane surface (Baatz et al., 1991; Gustafsson et al., 1996; Keough, 1992; Morrow et al., 1993a; Waring et al, 1989). This is a distinctly different arrangement than the ones seen from the transmembrane α-helix of SP-C (see Figure 6.9, A). The structure of SP-B exhibits about 40-50 % of α-helical motifs (Figure 8.1, box) inter-connected by some β-turn and random coil secondary structure (Cruz et al., 1995; Waring et al. 1989; 1994). Also the proteins sequence suggests, it has kringle domains. Kringle domains or structures posses disulphide bonds between their first and last cysteine residues, and SP-B has some sequence homology with other proteins containing kringle domains such as fibronectin and haptoglobin (Johansson et al., 1991).

The protein facilitates interfacial adsorption of PS lipids (Takahasi and Fujiwara, 1986; Yu and Possmayer 1990), re-adsorption and re-spreading of DPPC in monolayers (Taneva and Keough, 1994), and insertion of lipids to pre-formed monolayers (Oosterlaken-Dijksterhuis et al., 1991a; 1991b). Also synthetic peptides from various structural domains of SP-B together with DPPC can reproduce some of the surface properties of native PS *in vitro* (Gustafsson et al., 1996; reviewed by McLean and Lewis 1995). Although most of the structure-function studies of SP-B to date have been performed in solvent and lipid vesicles or dispersions (Morrow et al., 1993a; 1993b; Shiffer et al., 1993), recently similar studies have also been performed in monolayers

(Cochrane and Revak 1991; Longo et al., 1993; Oosterlaken-Dijksterhuis et al. 1991a; Pastrana-Rios et al., 1995; Taneva and Keough, 1994a). Some studies with synthetic segments of SP-B in lipid films suggest that the amphipathic α–helices interact with the anionic lipid headgroups, which allows the films to attain high π (Longo et al. 1993), and such segments are possibly oriented mostly at the polar interfacial area of the films (Cochrane and Revak 1991; Gustafsson et al., 1996; Lipp et al., 1996).

Fluorescence microscopy of films containing native, porcine SP-B in DPPC monolayers was performed in this study. By quantitatively analyzing the visual features observed in the DPPC/SP-B monolayers under different π, and protein concentration, the packing changes induced by the proteins on the lipid could be determined. In the next chapter we report comparative studies between fluorescently labelled SP-B and SP-C in DPPC films, and a mixture of both proteins in such films. Therefore this study with unlabelled, native SP-B was performed to get a preliminary understanding of the interactions of this hydrophobic protein of pulmonary surfactant with DPPC, and its comparison with unlabelled SP-C in DPPC films (Perez-Gil et al., 1992a).

MATERIAL AND METHODS

DPPC and NBD-PC were obtained and checked for purity as discussed in the previous chapters. Porcine SP-B was isolated and purified by Dr. Jesus Perez-Gil, University of Madrid, by modification of the method of Curstedt et al.(1987) discussed by him elsewhere (Perez-Gil et al. 1993).

The SP-B and DPPC was dissolved in chloroform:methanol (3:1 vol/vol) and mixed in desired weight proportions. The proportions were, DPPC plus 10, 20 and 30 wt% of SP-B (or 0.6, 1.03 and 1.9 mol% of SP-B respectively based on the molecular weight of SP-B monomer). The higher concentration range of SP-B was chosen after preliminary observations that SP-B in 2-10 weight percent did not show any significant effects on DPPC films (isotherms), compared to native SP-C used in previous experiments in similar concentration range (Perez-Gil et al., 1992a). The mixtures were spread on a 150 mM NaCl solution made with doubly distilled water, buffered to a pH of 6.9 with 5 mM Tris-HCl, in the epifluorescence microscopic surface balance. All experiments were performed at an ambient room temperature of 22 $\pm$ 1°C. The monolayers were compressed slowly in steps at an initial rate of 0.13 $Å^2.mol^{-1}.sec^{-1}$ (20 $mm^2.sec^{-1}$), the surface pressure - area (π - A) monitored and the images of the monolayers were video recorded and analyzed as discussed above.

RESULTS

The surface pressure-area (π-A) isotherms of DPPC monolayers containing 0 to 30 wt % SP-B are displayed in Figure 8.2 (top), and typical images observed from such films from NBD-PC fluorescence at a π of 12 mN/m are shown (bottom). The plateau region in the isotherms of DPPC at $\pi \sim$ 7-10 mN/m, indicated the phase transition of DPPC from a liquid expanded (LE) to a liquid condensed (LC) phase, whereas in the ones with 20 and 30 % SP-B, this plateau was not very distinct. The change in slope at the higher π of 43 mN/m in the DPPC plus 30 wt % SP-B isotherms (Figure 8.2, top) arose from the characteristic "squeeze out" of the protein. These characteristic plateaus were previously seen in DPPC monolayers containing similar amounts of SP-B (Taneva and Keough, 1994a). This squeeze-out plateau of SP-B in DPPC films occurred at a lower surface pressure than those seen for equal amounts of SP-C in such films (Taneva and Keough, 1994a; 1994b; 1994c). The typical images observed in such monolayers (Figure 8.2, bottom) with increasing amounts of SP-B indicate that the protein decreased the size of the LC domains at equivalent π, as was previously seen with SP-C (Perez-Gil et al., 1992a) and with fluorescent labelled SP-C (Chapter 6).

Figure 8.3 shows the average size (A), number (B) and total amount (percentage) (C) of liquid condensed (black) phase seen in monolayers of DPPC plus 0-30 wt% of SP-B. The protein changed the distribution of condensed domains of DPPC. Increasing amounts of SP-B decreased the average size and amount of LC phase in the DPPC films, whereas the number of domains in the films (with 20 and 30 wt% of SP-B) was

Figure 8.2. Typical surface pressure - area (π-A) isotherms of DPPC plus 1 mol% NBD-PC films containing 0 - 30 weight % SP-B (top) and the typical images observed from such films at a π of 12 mN/m (bottom).

The black regions in the images represent the liquid condensed phase and the white regions the fluorescent (from NBD-PC) liquid LE phase.

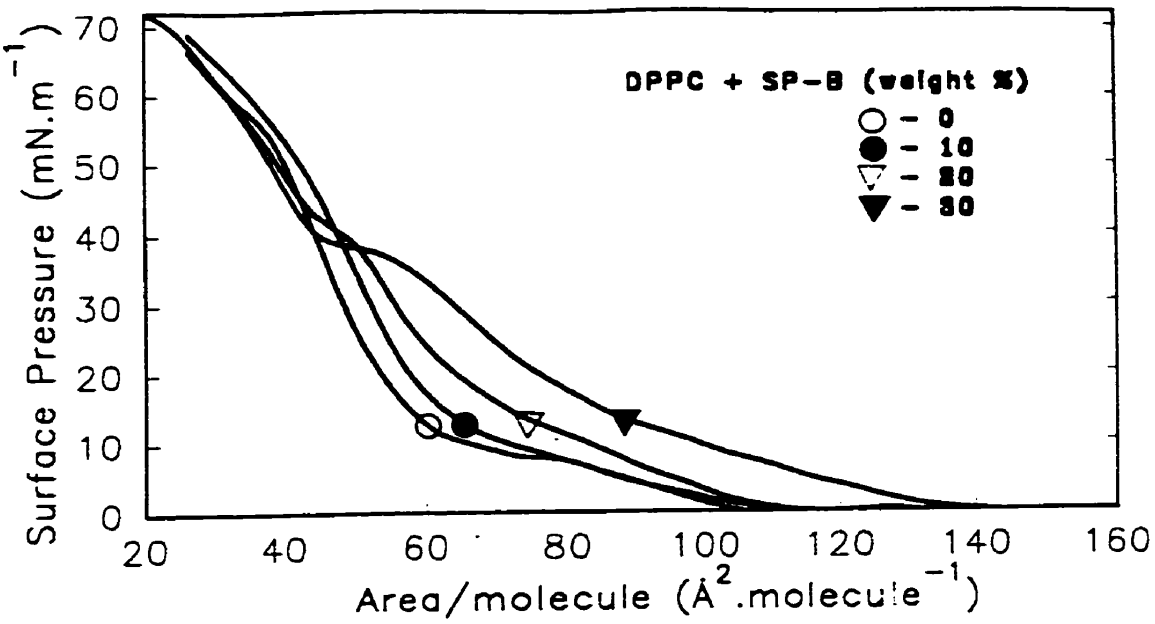
DPPC + SP-B (weight %)
○ - 0
● - 10
▽ - 20
▼ - 30
Surface Pressure (mN.m^{-1})
0
10
20
30
40
50
60
70
20
40
60
80
100
120
140
160
Area/molecule (Å^2.molecule^{-1})

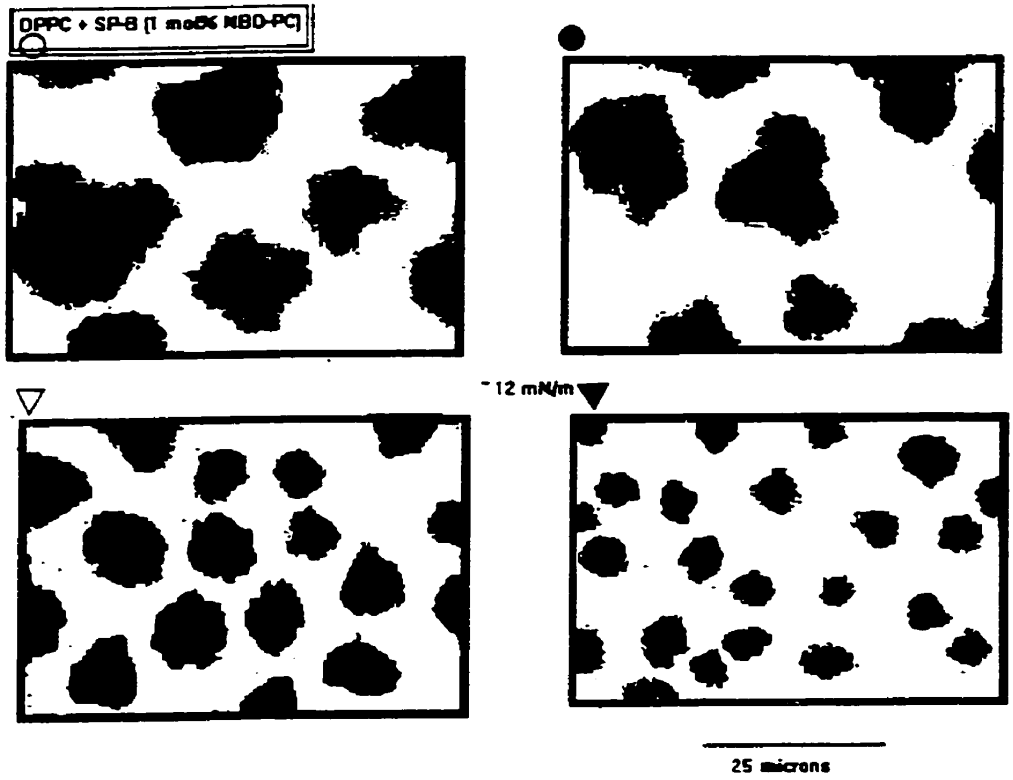
DPPC + SP-B (1 mol% NBD-PC)
~12 mN/m
25 microns

Figure 8.3 The size (A), number (B) and percentage (C) of condensed (black) phase in the films of DPPC plus 0 - 30 wt % SP-B. The error bars indicate $\pm$ one standard deviation for 10 images analyzed at each surface pressure.

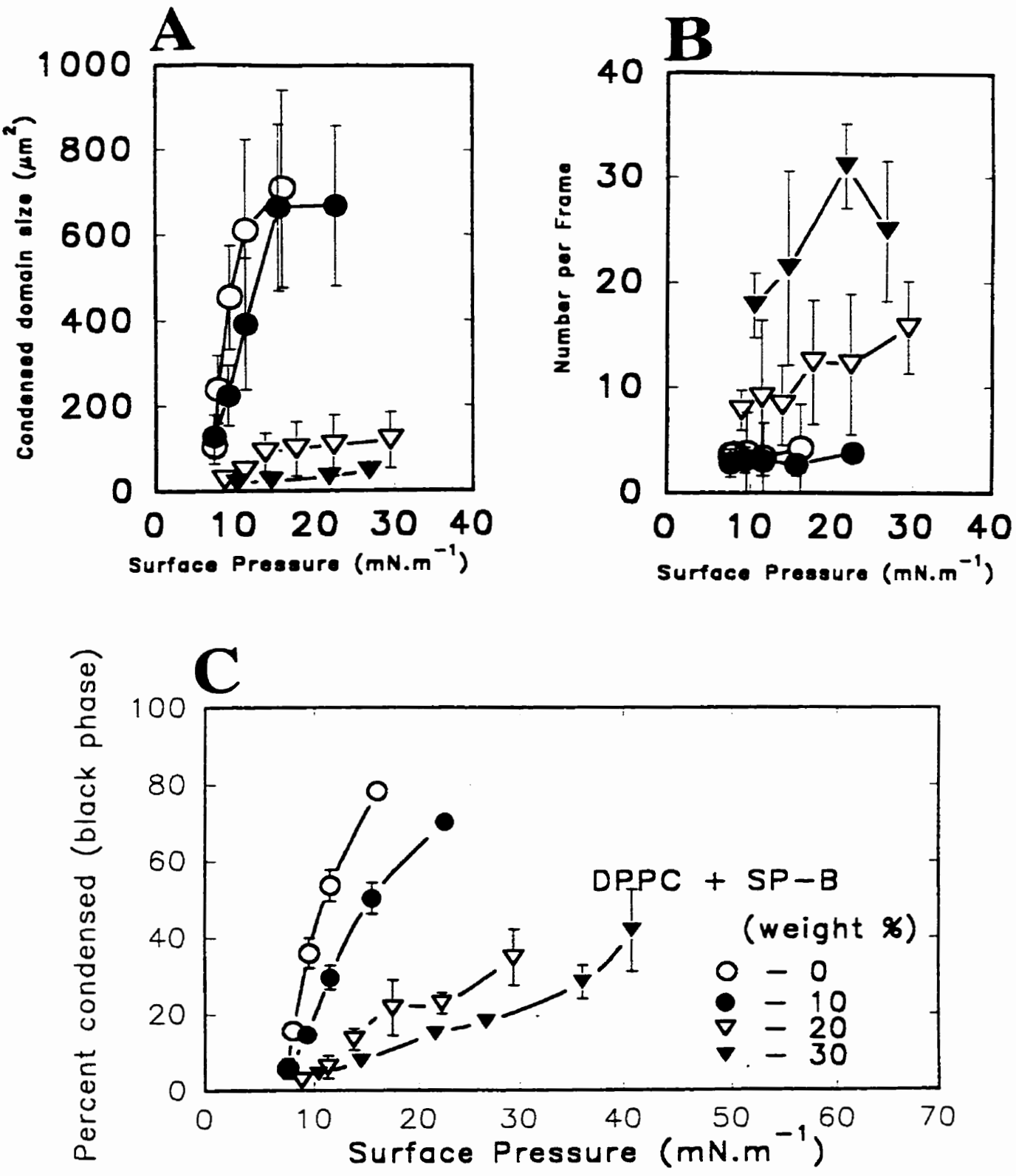
A
Condensed domain size (μm^2)
1000
800
600
400
200
0
0 10 20 30 40
Surface Pressure ($mN.m^{-1}$)
B
Number per Frame
40
30
20
10
0
0 10 20 30 40
Surface Pressure ($mN.m^{-1}$)
C
Percent condensed (black phase)
100
80
60
40
20
0
0 10 20 30 40 50 60 70
Surface Pressure ($mN.m^{-1}$)
DPPC + SP-B
(weight %)
○ – 0
● – 10
▽ – 20
▼ – 30

increased. These results indicated that the packing of DPPC films was perturbed by SP-B since, at equivalent π smaller amounts of condensed phase were formed in the DPPC/SP-B films compared to those of the lipid alone.

DISCUSSION

SP-B affected the liquid expanded (LE) to liquid condensed (LC) phase transition of DPPC films in a concentration dependent manner, and altered the amount of lipids which could pack into the LC phase at any given π. In other words higher surface pressures was required to attain similar amounts of condensed phase with increasing amounts of protein. In DPPC bilayers, SP-B have been shown to reduce the calorimetrically detectable gel to fluid chain melting transition. This suggests that the protein "removed" some acyl chains from undergoing transition to the gel phase, and our results complement those studies (Shiffer et al. 1993). This packing perturbation induced by the protein in bilayers has been suggested to enhance the adsorptivity of DPPC (by creating defect in packing of gel phase DPPC) to an air-water interface (Haagsman 1994; Keough 1992; Perez-Gil et al., 1992b). Antibodies directed against SP-B inhibit rapid adsorption of pulmonary surfactant, confirming the role of the protein in the adsorption process (Suzuki et al., 1986). Protein-induced monolayer packing changes may also enhance the adsorption of further lipids from the bulk subphase as suggested by others (Haagsman 1994; Oostarlaken-Dijksterhuis et al., 1990). Figure 8.4 shows the possible localization of SP-B dimer in a phospholipid bilayer (A) and in monolayers in (B) and (C).

The studies presented here indicate that SP-B perturbed the packing of DPPC in films, probably differently than did SP-C, and the reason could probably be the localization of SP-B near the phospholipid headgroup region (Figure 8.4 (B)). The

Figure 8.4 Possible arrangement of a SP-B dimer in bilayers (A), and monolayers (B and C). [Figure was graciously provided by Dr. Jesus Perez-Gil of University of Madrid].

SP-B is probably localized in the headgroup region of the phospholipids (small circles in (A)) although some parts of the protein may penetrate the chain region. In monolayers at low surface pressure (B) some parts of SP-B (hydrophobic regions) are probably localized at or near the hydrocarbon region of the phospholipid (due to low packing density of the phospholipid). At high surface pressure, the protein may be easily squeezed-out of the films into the water subphase, due to the highly polar nature of its amphipathic helices and their close localization to the air-water interface or the lipids headgroup (C).

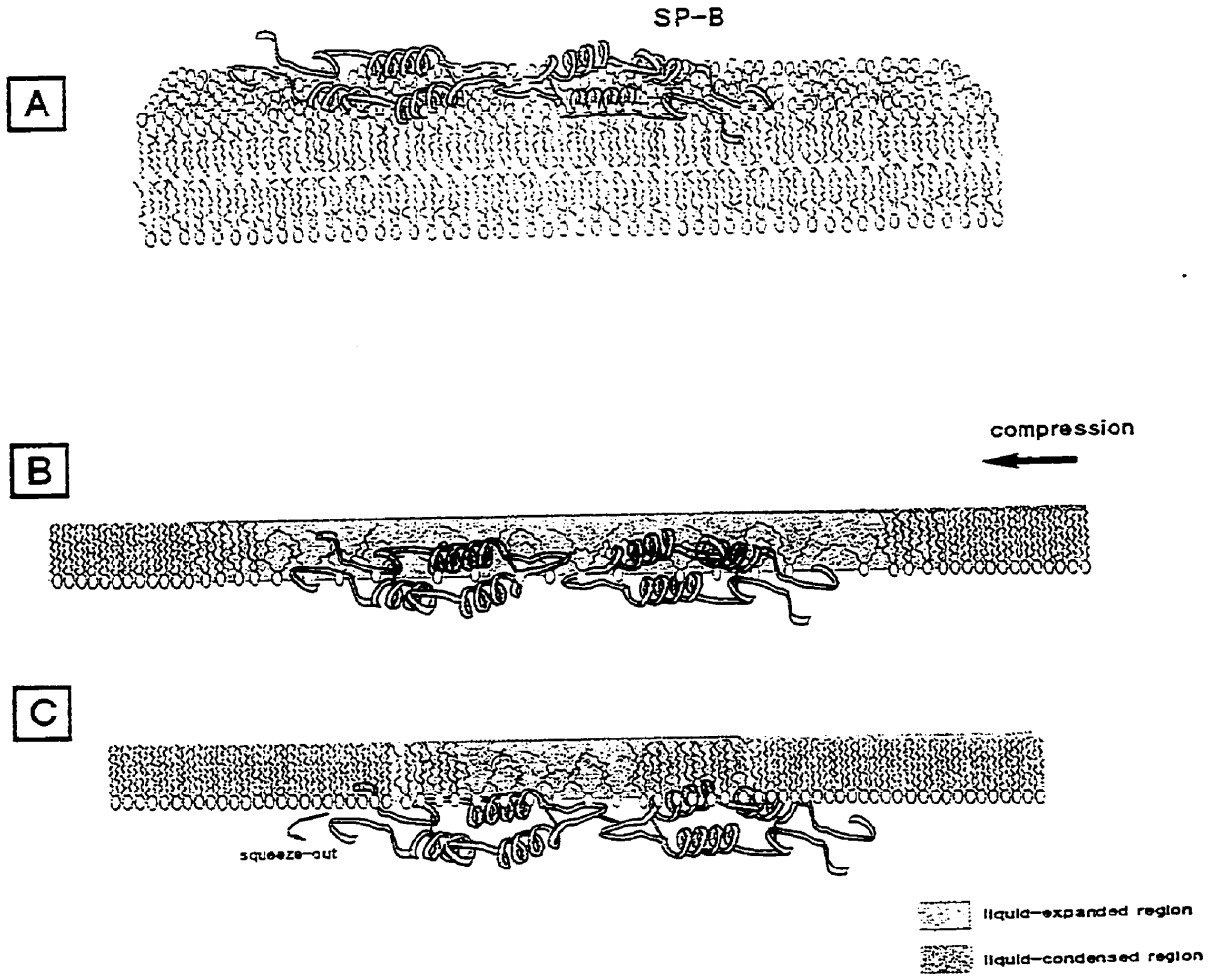
SP-B
A
B
compression
C
squeeze-out
liquid-expanded region
liquid-condensed region

higher amounts of SP-B required to perturb the DPPC films and the difference in "squeeze-out" surface pressure of DPPC/SP-B films (Figure 8.2) compared to DPPC/SP-C films, may be an indication of such a lipid-protein association. Previous studies on SP-B/phospholipid bilayers have indicated that the protein, having a number of positively charged residues spread over the entire polypeptide chain, can make several electrostatic interactions with anionic phospholipid headgroups (Johansson et al., 1994a). About 11 wt% of SP-B only minimally affected the acyl chain mobility as detected from the first moments of ^{2}H NMR spectra in DPPC bilayers (Morrow et al., 1993a), and by fluorescence anisotropy measurements in DPPC:PG systems (Baatz et al., 1990). Fluorescent antibody, directed against SP-B, bound to surfaces of giant bilayer vesicles, indicates that the protein was localized in the polar or headgroup region of the phospholipid bilayers instead of being deeply embedded in the hydrocarbon interior (Longo et al., 1992; Vincent et al., 1991; 1993). Others have indicated by electron microscopy that SP-B in combination with DPPC and PG can form bilayer discs (Williams et al., 1991). The localization of SP-B in such a situation is probably around the edges of the discs where the hydrophobic faces of SP-B can associate with the acyl chains and the polar parts with the lipid headgroups (Morrow et al., 1993a). The current structural model of SP-B from several such studies suggests that SP-B associates with phospholipids in bilayers by a combination of electrostatic interaction with the headgroups and hydrophobic interactions with the acyl chains, and does not appear to be embedded deep within the hydrophobic core (Vandenbussche et al., 1992a). In case of bilayer discs, parts of the protein may associate with the edges of the discs (Morrow et

al., 1993a). A combination of both lipid-protein arrangements may also occur.

Functionally, SP-B is more effective in inducing bilayer fusion and lipid insertion into preformed monolayers containing the protein, than SP-C (Osterlaken-Dijksterhuis 1991a, b). Taking into account the observations of others on SP-B-lipid association, it is tempting to speculate from our results that since the squeeze-out π of SP-B in lipid films is lower than SP-C, and that since SP-B localized near the lipid headgroups which are in water, it is easily squeezed-out of the films on minimal compression (Figure 8.4, C) (Taneva and Keough, 1994a). Although the DPPC/SP-B film studies presented here may not clarify any possible DPPC headgroup-SP-B interactions or the proteins localization in the films, the study does provide some indication that SP-B and SP-C may have different modes of interaction with DPPC in films. This possibility is explored in the next chapter using fluorescent labelled hydrophobic proteins individually and in combination in DPPC films.

Chapter 9

SP-B AND SP-C : A COMPARATIVE STUDY

INTRODUCTION

Although DPPC films can withstand high surface pressure (π) or low surface tension (γ), the rate of surface adsorption from DPPC dispersions to form films and the spreadability of the lipid at an air-water interface is low compared to natural pulmonary surfactant (PS) (Notter et al., 1980b; Snik et al., 1978). Hydrophobic proteins SP-B and SP-C enhance these surface properties of DPPC (Curstedt et al., 1987; Takahasi et al., 1990; Yu and Possmayer 1990), and some lipid/protein systems can reproduce many of the surface properties of native PS *in vitro* (Notter et al., 1987; Revak et al. 1991; Sarin et al., 1990; Smith et al., 1988; Suzuki et al., 1986; Tanaka et al., 1986). Also synthetic peptides from various structural domains of SP-B and SP-C in conjunction with DPPC can reproduce many of the surface properties of native PS (see McLean and Lewis 1995, for review). Such lipid-protein mixtures have potential for use as artificial surfactants in PS replacement therapies (Smith et al., 1988; Suzuki et al., 1986; Tanaka et al., 1986) and can be used for treating patients with surfactant related disorders or deficiencies, such as Respiratory Distress Syndrome (RDS). Targeted disruption of the genes of the hydrophobic proteins have been shown to alter pulmonary surfactant homeostasis and cause respiratory failure in newborn animals (Clark et al., 1995), indicating the critical role these proteins play in the normal respiratory dynamics of the lungs. From dynamic cycling experiments of monolayers containing DPPC and SP-B or SP-C *in vitro*, it was suggested that the such films can easily attain low γ or high π. The proteins get "squeezed out" of the monolayer at high π, and since small amounts of

proteins may remain in the monolayers at high π the film could rapidly re-spread from highly compressed states (Takahasi and Fujiwara 1986; Taneva and Keough, 1994a; Yu and Possmayer 1986). Recently infra red spectroscopy of the proteins in DPPC monolayers indicated differential orientation and lipid association between SP-B and SP-C at the interface (Pastrana-Rios et al., 1995). Due to structural differences of the proteins, it is feasible to assume that SP-B and SP-C probably interact and associate with DPPC films differently, although little direct experimental evidence exists to date (Pastrana-Rios et al., 1995).

Epifluorescence microscopy of lipid-protein monolayers has become a convenient tool for studying protein distribution and lipid-protein interactions at the air-water interface (Ahlers et al., 1991; Möhwald, 1990; see Stine 1995 for a review). By labelling proteins with different fluorophores, individual partitioning of lipids or protein in the condensed or expanded phases of the films, or in the subphase can be visually observed (Ahlers et al., 1991; Dietrich et al., 1993; Heckl et al., 1987; Möhwald, 1990). The differential distribution of the proteins in lipid monolayers occurs because of different electrostatic and hydrophobic interactions between the proteins and the lipids (Heckl et al., 1991; Möhwald, 1990). Protein-induced effects on lipid packing can be measured by estimating the amounts of each phase as a function of protein concentration at different monolayer lipid packing states (Heckl et al., 1987; Peschke and Möhwald 1987; Perez-Gil et al, 1992). Although most of these lipid-protein monolayers were studied as models of biological membranes under quasi-equilibrium conditions of compression (Möhwald, 1990), our epifluorescence balance allows studies of such

monolayers under dynamic conditions (fast compression and expansion and multiple π-A cycling) relevant to studies of PS *in vitro* (Nag and Keough 1993). Using this system we have studied SP-B and SP-C labelled with different fluorophores (separately and in some combinations) in spread DPPC monolayers under conditions of dynamic compression-expansion cycling. By quantitatively analyzing the visual features observed in the individual protein-DPPC films under similar conditions of temperature, concentrations, and compression speed, some comparative estimates of the interaction of each protein with DPPC films could be determined. This study (compared to the other studies, chapters 3-9) was performed under fast dynamic conditions (probably non-equilibrium nor quasi-equilibrium) to obtain information about whether or not the proteins behave in a similar manner to those in more slowly compressed film studies (Chapters 6 and 8).

9.21] Materials.

DPPC was purchased from Sigma Chemical Co. (St. Louis, MO), and fluorescein-5-isothiocyanate (FITC) and Texas-Red® sulphonyl chloride (TR) from Molecular Probes Inc. (Eugene, OR). SP-B and SP-C were isolated from porcine lung by Dr. Jesus Perez-Gil (JPG), University of Madrid, by a modification of the method of Curstedt et al.(1987), discussed elsewhere (Perez-Gil et al. 1993). The saline subphase on which the monolayers were spread, was made with doubly glass distilled water, the second distillation performed from dilute potassium permanganate.

9.22] Fluorescent labelling of SP-B and SP-C.

Isolated SP-B and SP-C were labelled by JPG and Antonio Cruz at University of Madrid, with TR and FITC respectively by the following procedures. About 300 μg of SP-B or SP-C in 2 ml of chloroform:methanol (2:1 vol/vol) was adjusted to a pH of 7.8 by adding appropriate amounts of 50 mM Tris in methanol. These SP-B and SP-C solutions were then incubated overnight with 10 mM solutions of TR or FITC respectively in chloroform: methanol 2:1 (vol/vol) at 4°C. The pH of the solutions was re-adjusted to 2 by adding appropriate amounts of 0.2 N HCl, and concentrated under a stream of N_2 to give a final solvent volume of 0.5 ml. The solutions were then applied onto a LH-20 column (Pharamacia LKB, Sweden) to remove the un-reacted probes, and the chromatographic profiles followed by measuring absorption at 250 nm (protein) and

450 nm (fluorescein) or 520 nm (TR). The amounts of labelled proteins were estimated by quantitative amino acid analytical procedures, discussed elsewhere (Perez-Gil et al. 1993).

9.23] Mass spectrometry of proteins.

Matrix Assisted Laser Desorption/Ionization (MALDI) mass spectrometry was performed by Mr. Lorne Taylor, University of Waterloo on a VG TofSpec spectrometer (Manchester, UK) on a cyano-4-hydroxy cinnamic acid matrix by methods of Hillenkamp et al., (1991). External calibration of the spectrometer was performed with recombinant eglin-C or trypsinogen by methods of Hillenkamp et al. (1991). Typically, 100 picomoles of R-SP-B or F-SP-C in chloroform:methanol (3:1 vol/vol) were mixed with the cinnamic acid solution in 1:1 (vol/vol), and 2 μl of the mixed solution placed on a stainless steel support. About 20 laser shots were averaged over a mass/charge range of 2000 - 10,000 Da for F-SP-C and 6000 - 20,000 Da for R-SP-B.

9.24] Dynamic π-A measurements of monolayers.

The R-SP-B and F-SP-C in chloroform:methanol (3:1 vol/vol) were mixed with DPPC in the same solvent in desired weight proportions of DPPC plus 10 or 20 wt% of R-SP-B (0.6 and 1.03 mol% respectively, based on MW of SP-B dimer) or F-SP-C (1.9 and 4.19 mol%, MW of SP-C monomer) and DPPC + 10 wt% of each protein.

The mixtures were spread on a 150 mM NaCl solution containing 2 mM $CaCl_2$ at a pH of 6.9. Monolayers of the same DPPC-protein mixtures were tested

simultaneously by Dr.Svetla G. Taneva on a teflon ribbon-barrier surface balance (Taneva and Keough, 1994) which allows for prevention of leakage at high π, and in our epifluorescence balance. The "leak-free" balance had a rectangular teflon tape which enclosed the films on all sides, and the film's compression and expansion was achieved by decreasing or increasing the area enclosed by this rectangle. Such "leak free" balances have been used previously by us (Taneva and Keough, 1994) and others (Notter et al., 1980b) to study high compression or low surface tension (or high π) regimes of surfactant films, where the leakage of the films behind the teflon barrier is problematic in the normal Langmuir type balances (Goerke, 1992; see Nag, 1990).

All experiments were performed at an ambient room temperature of 22 $\pm$ 2°C, in both balances. The monolayers were compressed up to a surface pressure (π) of ~ 65 mN/m and expanded to 0 mN/m for four cycles at an initial rate of 333 mm^2/sec (0.64 $Å^2.mol^{-1}.sec^{-1}$) in both surface balances, and the surface pressure-area (π-A) data collected using a Wilhelmy dipping plates attached to force transducers (Nag et al., 1990). The surface pressure was plotted as a function of area per amino acid residue of the proteins, as 35 residues for F-SP-C and 79 for R-SP-B. The details of such measurements have been discussed previously (Taneva and Keough, 1994a). In the epifluorescence balance the monolayers were compressed or expanded in 20 steps, and 5 seconds was introduced in each step to video record the visual features of the films.

9.25] Visual observations and analysis of monolayers.

The observations of the monolayers by epifluorescence microscopy were achieved

by switching fluorescence filter combinations, which allowed for observing fluorescence emissions from either R-SP-B at 590 nm, or F-SP-C at 520 nm. This technique has been previously used by us and others to observe various fluorophores simultaneously in lipid monolayers (Maloney and Grainger 1993; Montero et al. 1991). The stored images were processed and analyzed as discussed above, and an average of 5 images was analyzed at each individual π. The data were represented as percent condensed (black phase) as a function of π or area per molecule. The percentage of black phase was also converted to degree of crystallization or gelation, ϕ, by methods of Heckl et al., 1987, to estimate any deviation of areas of the lipid molecules induced by the proteins in the different phases of the lipid/protein monolayers from that of the lipid alone (as discussed in chapter 6).

RESULTS

Figure 9.1 shows the MALDI spectra of fluorescently labelled SP-B (top panel) and SP-C (bottom panel). The SP-B spectra showed a major peak at 8777 Da corresponding to the FW of SP-B monomer (8.7 KDa) (Curstedt, et al 1990). This peak might arise because of fragmentation of the SP-B in the MALDI process, or it may come from the dimer with two excess charges instead of one. SDS gels of this material indicated that it was essentially in the native, dimeric form. The minor peak at 9329 Da corresponds to FW of labelled SP-B (8700 Da + 625 (Texas-Red-sulphonyl) ~ 9329 Da) and the one at 17463 Da to the dimer of the protein (8700 Da x 2 = 17400 Da). The SP-C spectra (bottom panel) showed sharp peaks at 3744 Da and 4225 Da, corresponding with the formula weight (FW) from amino acid analysis of SP-C (3.7 kiloDalton) and dipalmitoylated SP-C (4.2 kDa) (Curstedt et al., 1990). The minor peak at 4609 Da indicates the presence of the fluorescein-labeled form of the protein F-SP-C [4200 Da (native) + 376 Da (fluorescein) ~ 4609 Da]. The other diffuse smaller peaks at higher molecular weights are possibly SP-C labelled with more than one mol of fluorescein [Note the difference of this acylated, minimally labelled F-SP-C with the one previously discussed in chapter 6, where F-SP-C was de-acylated]. The molecular weights of SP-B and SP-C are in close agreement with the ones previously reported by Curstedt et al. (1990) using a similar MALDI type technique or plasma desorption mass spectrometry. SDS gels and the MALDI spectra indicated that the proteins were minimally labelled and intact, SP-C predominantly in its monomeric form and some SP-B

Figure 9.1 Typical MALDI mass spectrum of Texas Red-SP-B (R-SP-B, top panel) and Fluoresceinated-SP-C (F-SP-C, bottom panel) plotted as relative intensity as a function of molecular weight in Dalton (or mass/charge ratio). The peaks at 8777 and 17463 (top panel) comes from the unlabelled form of SP-B and that at 9329 Da from the labelled R-SP-B. The peak at 4226 Da (bottom panel) arises from the unlabelled and acylated form of SP-C, 4609 Da from the labelled F-SP-C and 3744 Da from the deacylated protein. The other minor peaks indicate the presence of different forms of the labelled or unlabelled proteins (see text for details).

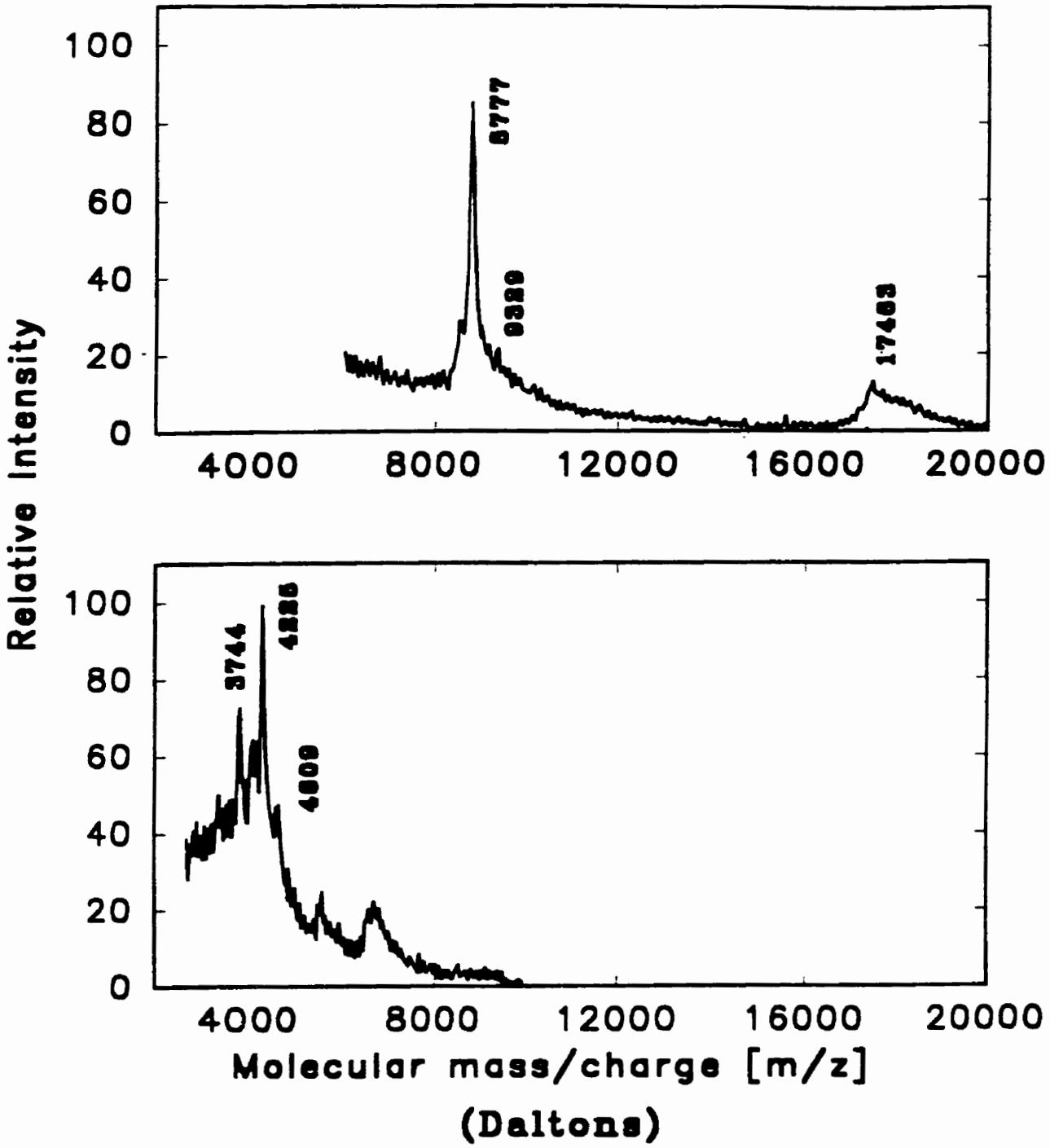
100
80
60
40
20
0
8777
9389
17403
4000
8000
12000
16000
20000
Relative Intensity
100
80
60
40
20
0
3744
4235
4000
4000
8000
12000
16000
20000
Molecular mass/charge [m/z]
(Daltons)

was in dimeric form.

Typical surface pressure - area per residue of the proteins (π-A) isotherms of monolayers of DPPC plus 10 weight % of R-SP-B (top panel) and F-SP-C (bottom panel) are displayed in Figure 9.2 (left panel) and the typical images observed from such monolayers are shown (right panel, R-SP-B in the top and F-SP-C in the bottom panel). The dashed lines in the isotherms in Figure 9.2 indicate the fourth compression-expansion cycle. The letters in isotherms indicate the surface pressure (π) at which the images in from R-SP-B fluorescence (top right) and F-SP-C fluorescence (bottom right) were obtained, from the first compression-expansion cycles. The plateau regions in all the isotherms at lower π (7-10 mN/m) indicate the phase transition of DPPC from a liquid expanded phase (LE) to a liquid condensed (LC) phase. The change in slope at the higher π of 43 mN/m in the DPPC/R-SP-B and the plateau area at 55 mN/m in the DPPC/F-SP-C isotherms arise from the characteristic "squeeze out" of the proteins. These characteristic plateaus were previously seen in DPPC monolayers containing similar amounts of native SP-B or SP-C (Taneva and Keough, 1994a and chapters 6 and 8), indicating that the labelled proteins behaved in a manner similar to the native ones.

The typical images observed in such monolayers (Figure 9.2, right panel, top for R-SP-B and bottom for F-SP-C) showed distinct LC domains (dark regions) of DPPC (A, A') in a homogenous fluorescent background of the proteins, indicating that the R-SP-C or F-SP-B partitioned in the liquid expanded (LE) or fluid phase of the DPPC. Increasing π from 14 mN/m to 63 mN/m (A or A' to C or C' in Figure 9.2, left), resulted in the LC domains growing in size and amount, and deforming from more

Figure 9.2 Surface pressure (π) plotted as a function of area per protein residue (π-A) isotherms of DPPC plus 10 weight % R-SP-B (top left) and 10 wt % F-SP-C (bottom left); and the typical fluorescence images seen in such monolayers at π indicated by letters A-E and A′-E′ in the isotherms in the right panels are shown in (top) for R-SP-B and (bottom) for F-SP-C. A lipid molecule is considered as one "residue" in this calculation. The long dashed lines (associated with the solid lines) in the isotherms indicate the fourth compression-expansion isotherms. The small dashed lined isotherm in the top panel is from a film of DPPC (plus 1 mol % NBD-PC) compressed and expanded at the same rate.

The bright regions in images indicate the fluorescence from the labelled proteins and the dark areas the condensed phase of DPPC. The scale bar is 25 μm.

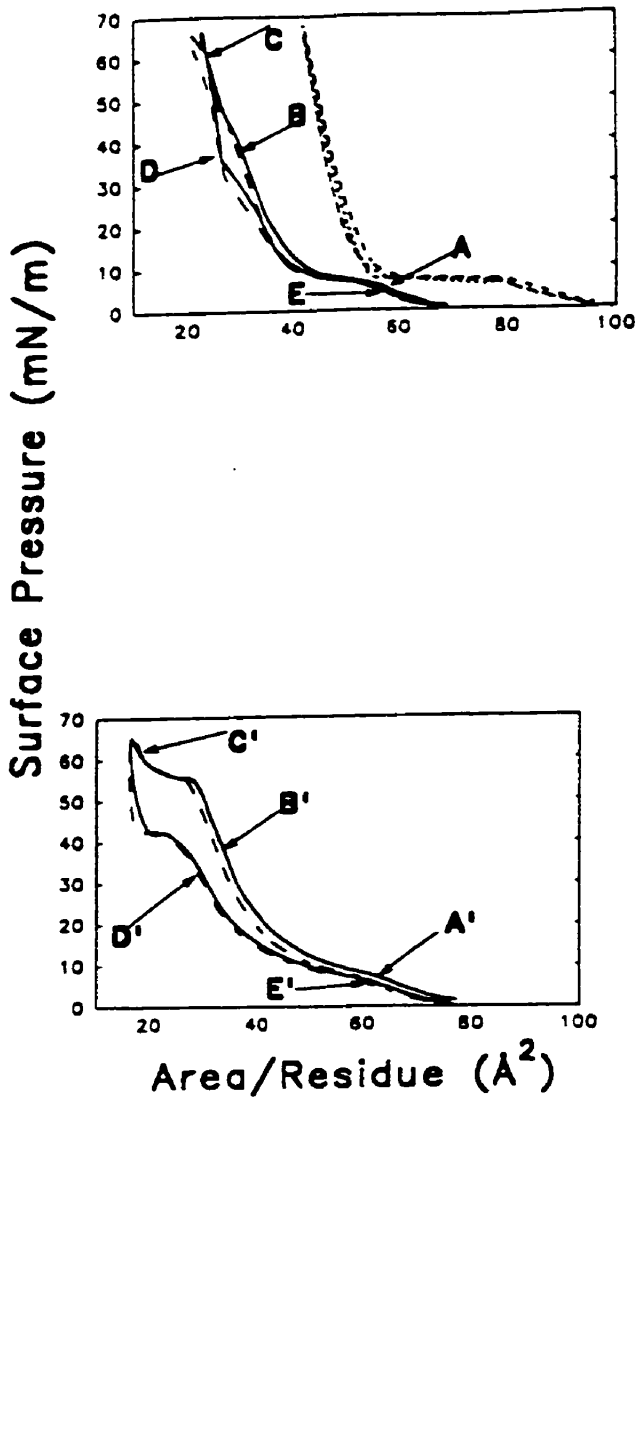
Surface Pressure (mN/m)
Area/Residue (Å²)
A
B
C
D
E
A'
B'
C'
D'
E'

circular to elongated shapes. The images also indicated that some of the proteins remained in or very near the monolayers at high $\pi \sim 63$ mN/m (C, C′). The typical collapse π of the native SP-B or SP-C are around 37 - 40 mN/m (Oosterlaken-Dijksterhuis et al., 1991b; Taneva and Keough, 1994a; 1994b) with "squeeze out" effects appearing in the isotherms, but the images in C ($\pi > 60$ mN/m) indicated that some amount of the proteins remained associated with DPPC above the collapse pressures of pure SP-B or SP-C films. This conclusion was also reached by Taneva and Keough, (1994 a; 1994b) based upon behaviour of the isotherms of DPPC containing small amounts of native, unlabelled SP-B and SP-C. Upon expansion of the film, with resulting decrease in π (C to E and C′ to E′), the proteins were found to re-distribute or re-disperse in the expanded phase, indicating reversibility of protein distribution in the LE phase during the compression-expansion process, since images at A and A′ were similar to those at E and E′. Visual features of the monolayers on the fourth cycle (dashed isotherm in Figure 9.2, left) were similar to those shown for the first cycle, suggesting that only minor changes occurred in the lipid-protein distribution in those monolayers from cycle to cycle. Also the visual features did not indicate any significant difference between R-SP-B and F-SP-C distributions in DPPC monolayers at the different π, both proteins being associated with the fluid or LE phase.

Figure 9.3 shows the amounts (percentage) of condensed phase or black regions seen in monolayers of DPPC, and DPPC containing 10 wt% and 20 wt% of R-SP-B (top panel) and F-SP-C (bottom panel) as a function of π, during the first cycle compression (closed symbols) and expansion (open symbols). The data were obtained by analyzing

Figure 9.3 Total amount of condensed phase plotted as a function of surface pressure for monolayers of DPPC + 1 mol% NBD-PC (■), DPPC + 10 wt% (▼) and 20 wt% (▲) of R-SP-B (top panel) and F-SP-C (bottom panel). The open symbols indicate data obtained from the expansion of these monolayers. The error bars indicate ± one standard deviations of five images analyzed at each π.

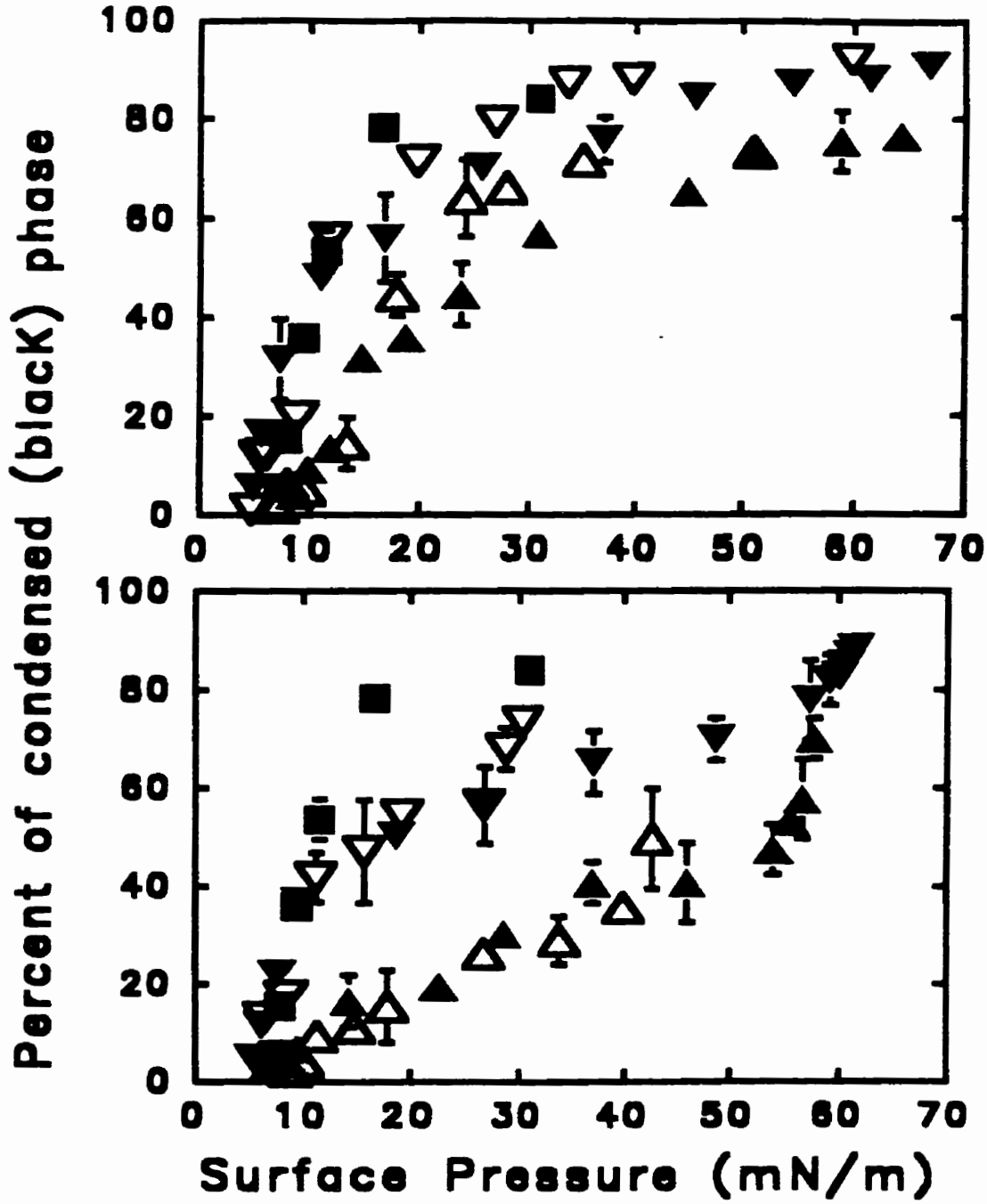
Percent of condensed (blacK) phase
100
80
60
40
20
0
0
10
20
30
40
50
60
70
Surface Pressure (mN/m)

five randomly selected typical images at each π. The DPPC monolayer without fluorescent protein was observed by using low amounts (one mol%) of a fluorescent lipid probe 1-palmitoyl,2-nitro-benzoxadiazole-phosphatidylcholine (NBD-PC), and the DPPC data are shown for comparative purposes. The condensed phase packing of DPPC was perturbed by both proteins since at equivalent π, smaller amounts of condensed phase were formed in the lipid-protein films compared to those of the lipid alone. A similar pattern of perturbation of condensed phase of DPPC films by native, acylated SP-C has been previously observed (Perez-Gil et al., 1992a), by and with native non-labelled SP-B (Chapter 8). Increasing amounts of the proteins from 10 to 20 weight percent decreased the total amounts of condensed phase. This indicated that both proteins perturbed the packing of DPPC in monolayers, and with higher protein content higher π was required to reach similar amounts of DPPC condensed phase or higher packing states, although this decrement in DPPC/R-SP-B monolayers (top panel) was less than the ones seen for F-SP-C (bottom panel). Also in the DPPC/F-SP-C monolayers (bottom panel) almost similar amounts of condensed phase were observed at comparable π during compression (closed symbols) and expansion (open symbols), indicating that during these processes similar lipid-protein distributions occurred at comparable π. In the monolayer containing R-SP-B however the amount of dark or condensed phase seen on expansion (open symbols, top panel) seemed to be consistently somewhat higher than on compression (solid symbols). These results indicate that both proteins perturbed the condensed phase packing of DPPC, SP-C more than SP-B, and the packing of DPPC may be different in the presence of equal amounts of each protein.

Figure 9.4 Total amounts of condensed phase plotted as a function of surface pressure for DPPC monolayers containing 10 wt% of R-SP-B (●) or F-SP-C (⬣) from the fourth compression cycle (dashed lines) and the first cycle (solid lines ○, ◇). The error bars indicate ± one standard deviations of five images analyzed at each π.

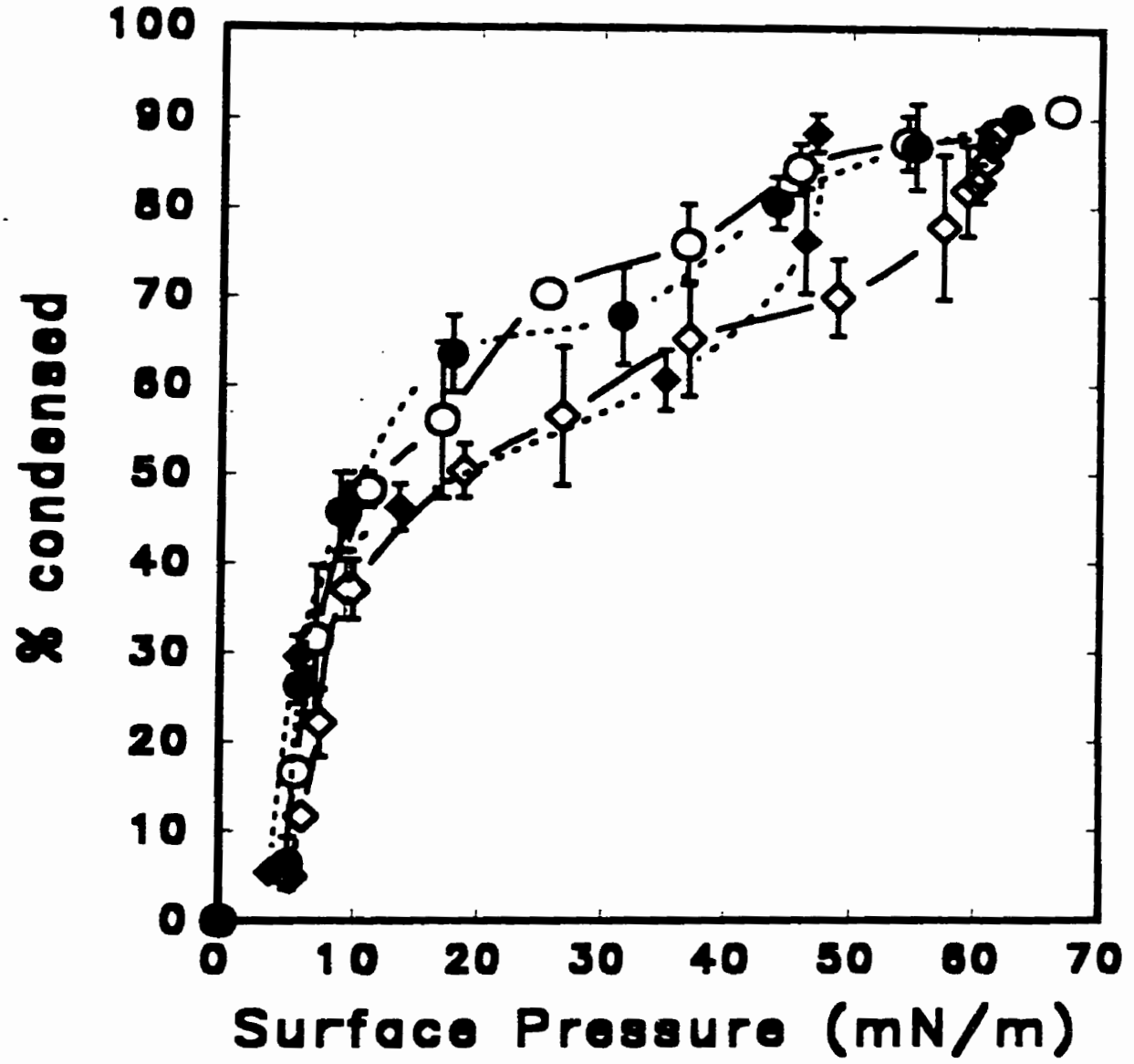
100
90
80
70
60
50
40
30
20
10
0
% condensed
0
10
20
30
40
50
60
70
Surface Pressure (mN/m)

Figure 9.4 shows the amounts of condensed phase seen in DPPC monolayers containing 10 wt% of either protein from the first (solid lines) and the fourth compression (dashed lines). The percentage condensed between the first and the fourth cycle were very similar indicating that the distribution of lipid and protein are similar at similar π between successive cycles. Since there was no drastic change of the amounts of condensed phase between the first and the fourth cycle, it seems that negligible irreversible loss of materials from the monolayers to the subphase occurred between successive cycles as long as the monolayers were not over-compressed (to a $\pi \sim 72$ mN/m) into the collapsed state.

Figure 9.5 displays the amount of condensed or black phase (left panel) and the degree of crystallization or gelation, ϕ (right panel) of DPPC, and DPPC plus R-SP-B (top panel) and F-SP-C (bottom panel) plotted as a function of area per molecule of the lipid. The percentage of condensed phase plots (left panel) indicate that the amounts of that phase formed at equivalent area per molecule of the lipid is increased from that of the lipid alone, between 60 $Å^2$.molecule^{-1} and 90 $Å^2$.molecule^{-1}. Below 60 $Å^2$.molecule^{-1}, the percentage of condensed phase decreased for the monolayers containing 20 wt% of the proteins, albeit more for F-SP-C (lower panel) than for R-SP-B (upper panel). This suggested that the DPPC molecules could not pack to form equivalent amounts of condensed or gel phase in the presence of the proteins.

As noted above, degree of crystallization or ϕ (see experimental procedures) *vs* area per molecule plots of lipid-protein systems can be used to give quantitative estimates of the area occupied by the lipids in the different phases, and whether or not the proteins

Figure 9.5 The total amounts of condensed phase (left panel) and the degree of crystallization ϕ [see text for details] (right panel) plotted as a function of area per molecule of the lipid, for monolayers of DPPC and DPPC plus R-SP-B (top panel) and F-SP-C (bottom panel). The data is from DPPC films containing 0 wt% (■), 10 wt% (▼) and 20 wt% (▲) protein or similar lipid-protein ratios as in Figure 9.3.

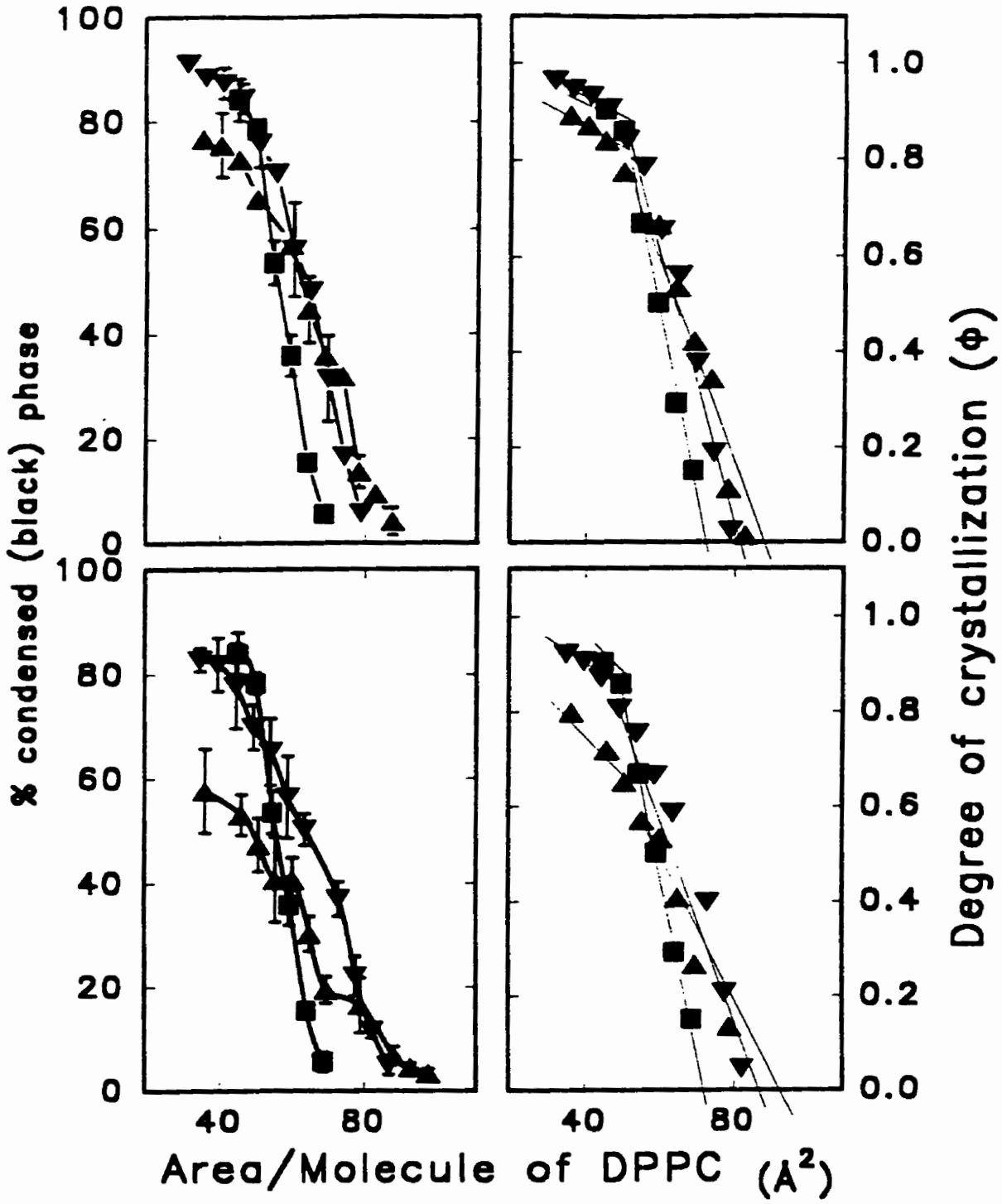
100
80
60
40
20
0
% condensed (black) phase
1.0
0.8
0.6
0.4
0.2
0.0
Degree of crystallization (Φ)
40
80
Area/Molecule of DPPC (Å²)

alter the areas of the lipids in such phases (Heckl et al, 1987; Möhwald, 1990). The degree of crystallization patterns of DPPC plus F-SP-C and R-SP-B indicated that the crystallization or gelation of DPPC and DPPC/protein monolayers is linear between 70 to 90 $Å^2$.molecule^{-1} (Figure 9.5, right panel). Below this area per molecule the slopes changed at $\phi \sim 0.9$ for the monolayers of lipid alone and the ones with 10 weight % of either R-SP-B (top panel, right) or F-SP-C (bottom right). The degree of crystallization plots for DPPC are similar to the ones seen previously by Heckl et al., (1987). The change of slope at $\phi \sim 0.9$ for the DPPC monolayer implied that the crystallization or gelation which occurred in this system is altered at or near the limiting areas of DPPC ($\sim$ 40 $Å^2$.molecule^{-1}), and is an indication that the molecules in the condensed phase undergo some form of re-orientation or phase transition to a "solid-like" phase, as suggested by others (Möhwald, 1990). In our systems this process occurred for DPPC and seemed not to be affected by 10 wt% of either protein, indicating the proteins did not substantially affect the crystallization of DPPC, at least at that protein concentration. By extrapolating the linear portion of the lines to $\phi = 1$, the area of the DPPC in the monolayers and the ones containing 10 wt % of either protein gave an area 44 $Å^2$.molecule^{-1} which is very close to the limiting areas of the lipid (40 $Å^2$.molecule^{-1}; see Chapter 2, section 2.3), and was not changed significantly by 10 wt % of R-SP-B and F-SP-C. By extrapolating these lines to $\phi = 0$, an estimate of the change of the area of the lipids in the fluid phase occupied by the proteins could be performed. This gave 74 $\pm$ 2 $Å^2$.molecule^{-1} for pure DPPC and 82-90 $\pm$ 2 $Å^2$.molecule^{-1} in the presence of 10 wt% of the proteins and indicated that the proteins indeed changed the area of the lipids

in the monolayer in the fluid phase. These results suggest that the proteins occupying the fluid phase changed the area of the lipid in that phase, but could not penetrate the gel or crystallized phase and thus change the area of the lipids in that phase. This is only possible if the proteins get substantially "squeezed out" of the monolayer. In monolayers containing 20 wt % F-SP-C, the change of slope (bottom right, up triangle) occurred at a lower ϕ of 0.6, implying that higher concentrations F-SP-C perturbed the crystallization of DPPC. These studies suggests that their might be some possible differences between R-SP-B and F-SP-C interactions with the lipid phases.

The π-A isotherms of DPPC plus 10 wt% of R-SP-B plus 10 wt% F-SP-C are shown in Figure 9.6 (a). Typical images seen in such monolayers from fluorescence of R-SP-B (left panel) or F-SP-C (right panel) are shown in Figure 9.6 (b), and the percentage of condensed phase as a function of π in 9.6 (c) (the symbols from monolayers containing 20 wt % of either protein are shown for comparison). The fourth cycle isotherms are shown as dashed lines in (a) and the letters indicate the surface pressures at which the images in (b) were obtained. The first cycle isotherm in (a) indicated that although small "squeeze out" plateaus at $\pi \sim$ 43 mN/m for R-SP-B and at $\pi \sim$ 55 mN/m for F-SP-C could be observed (as with the individual protein shown in Figure 9.2) they were smaller than the ones seen in DPPC monolayers plus equal amounts of the individual protein (Figure 9.2). The images in Figure 9.6 (b) indicated that both proteins partitioned into the expanded phase of DPPC monolayers and mixed homogenously in that phase at all π (A, A'), they were present to some degree at high π (B, B'), and re-inserted back into the monolayer upon expansion (C, C'). The plot of

Figure 9.6 Surface pressure plotted as a function of area per residue of protein (and lipid) for monolayers of DPPC + 10 wt% R-SP-B + 10 wt % F-SP-C, from the first (solid line) and the fourth compression-expansion cycle (dashed lines) (a); the typical images seen from R-SP-B (left panel, A-C) and F-SP-C fluorescence (right panel, A′-C′) in (b); and the percentage of condensed phase plotted as a function of π for the above monolayer (●, ○), and the ones containing 20 weight % of R-SP-B (△) or F-SP-C (▲) (c). The letters in (a) represent the π at which images in (b) were obtained. The open symbol (○) in (c) represent the data from the expansion cycle of the DPPC film containing both proteins. The scale bar in (b) is 25 μm. The error bars represent $\pm$ one standard deviation of 5 images analyzed at each π.

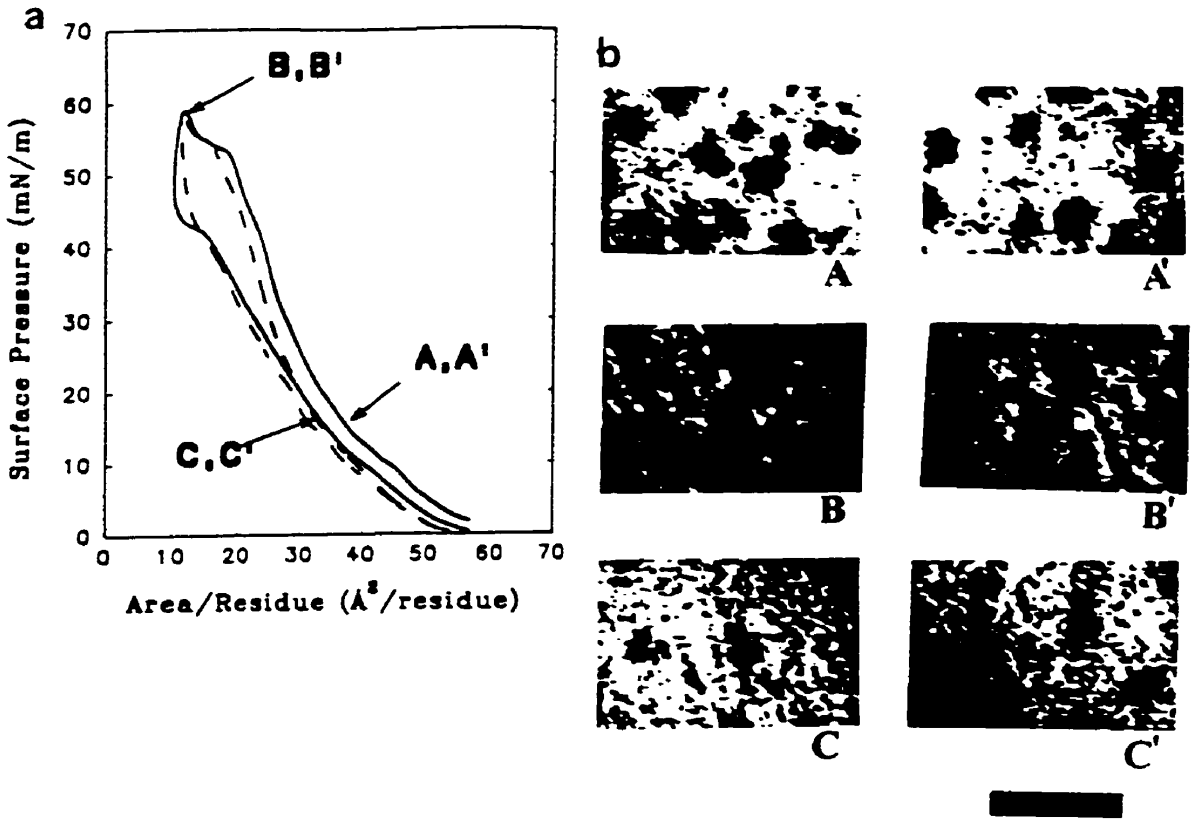
a
b
Surface Pressure (mN/m)
Area/Residue (Å²/residue)
B,B'
A,A'
C,C'
A
A'
B
B'
C
C'

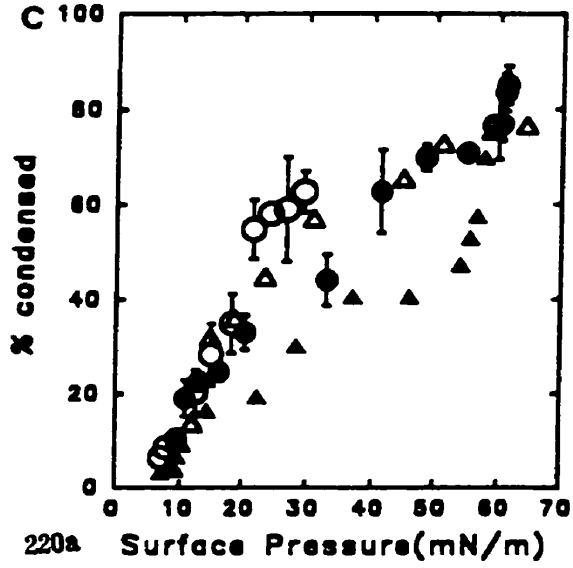
c
% condensed
Surface Pressure(mN/m)

condensed phase as a function of π in Figure 9.6 (c) compared to the ones with 20 wt % of either protein suggested that the proteins perturbed the monolayer condensed phase in a additive manner.

9.41] Significance of SP-B and SP-C in pulmonary surfactant films.

Pulmonary surfactant (PS) undergoes a number of transformations in the alveolar fluid and possibly in the alveolar air-fluid interface, such that during normal respiratory cycling a surface film is formed which is enriched in one component (DPPC) over others. *In vitro* dynamic cycling of extracted PS shows that the material undergoes transformation from heavy to light subtypes which can be separated by density gradient centrifugation (Gross, 1995a). The lighter subtypes are thought to be material eliminated from the interfacial PS monolayer, and do not contain any surfactant proteins (Gross, 1995a). To maintain low surface tension at the interface, the monolayers are enriched in DPPC by surface refining where the unsaturated lipid or the other components are possibly squeezed out of the monolayer (Goerke and Clements 1986; Keough 1992). Clements (1977) found evidence for a DPPC rich material at the air-alveolar interface, since the temperature dependence of the surface component of transpulmonary pressure-volume relationship during lung deflation closely resembled that of the chain melting of transition of DPPC and not that of extracted PS. It was also shown that the surface tension at the air-alveolar fluid interface was near 0 mN/m (or $\pi \sim 70$ mN/m) at low lung volumes (Schürch et al., 1978), and the only component of PS that could reach such values upon compression is DPPC, which suggests that it could be present in high amounts in the PS surface films (Clements, 1977; Hawco et al., 1981a; 1981b). The models proposed for such DPPC enrichment of PS films from *in vitro* studies usually

involve the selective elimination of unsaturated and other non-DPPC lipids at intermediate π during compression of monolayers (Notter et al., 1980b; Snik et al., 1978), or after a number of cycles (Nag and Keough, 1993). Other models suggest that DPPC can be adsorbed in collective packets during expansion of PS monolayers (Schürch et al., 1994), or be replenished in the monolayer from highly compressed states (Notter et al., 1981b; Taneva and Keough, 1994). Some of these models have implicated the role of the hydrophobic proteins in aiding such biophysical processes. This study suggests that SP-B and SP-C can be present in small amounts in DPPC monolayers at high π (Figure 9.2), and the proteins are accommodated in or near the DPPC monolayers at such π (or low surface tension). Also the films were enriched with DPPC at high π, as seen through the high amounts of condensed phase formed in such films, from probable squeeze out of some of the hydrophobic protein (Figure 9.3 and 9.5). An advantage of having some of the proteins embedded in, or associated with, the DPPC matrix at high π may be to aid in rapid re-spreading and replenishment of the monolayer with that lipid upon expansion (Taneva and Keough, 1994). Such proteins in the monolayers might also allow rapid adsorption of collective units from the subphase as suggested in the model discussed by Schürch et al., (1994). The adsorption model may be further supported by the fact that SP-B and SP-C in preformed monolayers can induce the rapid transfer of phospholipid from vesicles in the subphase (Oostarlaken-Dijksterhuis et al., 1991). Whichever may be the case our studies suggest that the hydrophobic proteins SP-B or SP-C or both can remain associated with DPPC monolayers under various stages of dynamic compression or expansion, and such monolayers can be

compressed to high π, observations which support these suggestions made in a previous study (Taneva and Keough, 1994c).

9.42] Comparative effects of SP-B and SP-C on DPPC packing in films.

This study indicates that both proteins affected the expanded to condensed phase transition of DPPC monolayers in a concentration dependent manner and thus altered the amount of lipids which could pack into the condensed phase at any given π or area per molecule (Figure 9.3 and 9.5). In other words higher pressures or compression states of the lipid were required to attain similar amounts of condensed phase or degrees of gelation with increasing amounts of protein. In DPPC bilayers SP-B or SP-C have been shown to reduce the calorimetrically detectable gel to fluid chain melting transition, indicating that they "removed" some acyl chains from undergoing into the gel phase, results which complement this study (Shiffer et al. 1993; Simatos et al., 1990). In monolayers since both proteins occupied the expanded or fluid phase, and reduced the ability of the molecules to interact with each other in that phase, the proteins prevented the lipid from undergoing a phase transition to the more ordered condensed phase.

The influence of F-SP-C on lipid packing appeared to be greater than that of R-SP-B as seen from the percent condensed and the degree of crystallization patterns. For the 10 wt% F-SP-C system (Figure 9.3, bottom) the amount of condensed phase increased steeply with π up to 50 mN/m where the squeeze out of F-SP-C plus lipids probably began, whereas in the 20 wt% F-SP-C system a more gradual increase of condensed phase was observed until the squeeze out π was reached. In case of R-SP-

B/DPPC system there was somewhat less sharp increase of the condensed phase with π, for both concentrations of protein. The patterns of degree of crystallization (Figure 9.5) also displayed similar characteristics. For 20 wt % of F-SP-C there was a change of slope at around $\phi \sim 0.6$ whereas for R-SP-B there was no noticeable change at that ϕ, indicating possibly that the proteins perturbed the packing of DPPC molecules differently. Also the area per molecule calculated by extrapolating the lines to $\phi = 0$, (Figure 9.5, right panel) were higher in case of F-SP-C than those for equivalent amounts of R-SP-B. This would indicate that F-SP-C perturbed the fluid phase DPPC molecules more than an equivalent amount of R-SP-B. Previously others have shown in a different lipid-protein system (cytochrome b-DPPC) that the change of slope at lower ϕ, is a possible indication of "squeeze out" process being detected (Heckl et al, 1987), and also a possible indication that the proteins perturbing the packing of the lipids not only in the fluid but also in the gel or crystalline phase. In our system it seems that F-SP-C perturbed the gel phase packing somewhat more than an equivalent amount (20 wt%) of R-SP-B. This provides some evidence that equal amounts (weight %) of SP-C perturbed the DPPC monolayers more than SP-B, correlating well with previous bilayer studies on such lipid-protein systems (Shiffer et al., 1988; 1993). A recent study using fluorescence energy transfer of labelled SP-B and SP-C in DPPC bilayers showed that SP-C is excluded out of the gel phase phospholipid and aggregates in the fluid phase, whereas SP-B has little or no preference for either phase (Horowitz 1995). This would be consistent with SP-B being placed at or near the surface of the bilayer or monolayers at high surface pressures.

Previous studies on SP-B/phospholipid bilayers have indicated that the protein having a number of positively charged residues spread over the polypeptide chain can make several electrostatic interactions with anionic phospholipid headgroups (Johansson et al., 1994a; see Figures 8.1 and 8.4), whereas SP-C has an arrangement similar to transmembrane α-helical peptides (Horowitz et al., 1992; Morrow et al., 1993a; see Figure 6.9). Although SP-C has a few positive charges localized at the N-terminal, the highly hydrophobic α-helical C-terminal region and the dipalmitoyl chains allows the protein to orient in bilayers with the α-helical axis parallel to the acyl chains, as most trans-membrane proteins do (Clercyx et al., 1995; Horowitz et al. 1992; Johansson et al., 1995; Morrow et al., 1993a; Vandenbussche et al., 1992b). Also functionally SP-C is less effective in inducing bilayer fusion and lipid insertion to preformed monolayers of the protein than SP-B (Osterlaken-Dijksterhuis 1991a, b). Thus SP-C could affect the lipid packing in bilayers and monolayers through different mechanisms than SP-B as indicated in this study from differences in the perturbation patterns of the films.

9.43] Squeeze-Out, stability and possible orientation of SP-B and SP-C.

The structural orientation of SP-C monomers or dimers (deacylated) in monolayers studied by circular dichroism showed that the proteins have a high amount of α-helical structures with the helix axis oriented parallel to the air-water interface (Creuwels et al., 1995b; Oosterlaken-Dijksterhuis et al. 1991a; 1991b; Pastrana-Rios et al., 1995). Our MALDI data indicates that SP-C was mainly monomeric and acylated, and similar to the proteins studied by these authors (Creuwels et al., 1995a; 1995b;

Oosterlaken-Dijksterhuis et al. 1991b). Recent studies of SP-C indicate that the protein had less α-helix in solvents of increasing degrees of polarity (decreasing acetonitrile/water ratios) (Cruz et al. 1995). Also ellipsometric studies with DPPC/SP-C monolayers indicate that there is an slow increase of monolayer film thickness between 10 and 50 mN/m, and then an abrupt increase with increasing π (Post et al. 1995). Our data on condensed phase as a function of π in F-SP-C/DPPC monolayers (Figure 9.3) also indicates some possible orientational changes occurring in such monolayers with increase in π. The amount of condensed phase as a function of π showed abrupt changes at around 50 mN/m. Also the π-A isotherms shown in Figure 9.2 (bottom panel) showed a distinct plateau at around 50 mN/m, assumed to be the squeeze-out of the proteins from the monolayers possibly accompanied by some lipids (Taneva and Keough, 1994b). Pastrana et al. (1991) had suggested that SP-C packing in a lipid matrix is very stable even with large compression, so that the protein may not be squeezed out, but undergo some type of structural changes. Others have suggested from collapse-plateau ratio measurements and IRAAS studies of such lipid-protein monolayers that although most of the protein gets squeezed out, some may remain lipid-associated above the collapse π of the protein (Pastrana-Rios et al., 1995; Taneva and Keough, 1994). Recent neutron diffraction studies indicate that DPPC headgroups in monolayers undergo conformational changes and dehydration at $\pi >$ 30 mN/m (Brumm et al., 1994). Others have indicated a change of orientation of DPPC around those π, inferred from antraloxy-stearic acid probe orientation studies in such monolayers (Denicourt et al. 1994). The degree of crystallization patterns of DPPC (Figure 9.5) also show a change in slope of the lines at

or near the limiting molecular areas of the lipid, where 100 percent gelation or crystallization is to be expected. Also pure SP-C film's isotherms show a distinct plateau region around 20 - 25 mN/m (Creuwels et al., 1995b; Perez-Gil et al., 1992a; Taneva and Keough, 1994a), which has been suggested to be an orientation change of the pure protein in the monolayer (Creuwels et al., 1995b). Thus a combination of lipid-protein orientational changes may be involved in accommodating the protein in the lipid matrix at high π.

The structure of native SP-B in monolayers is about 47 percent α-helical, the helix axis oriented parallel to the interface (Oosterlaken-Dijksterhuis et al., 1991b). Due to charged amino acid residues distributed throughout its sequence, an amphipathic-helical conformation has been suggested for SP-B (Bruni et al., 1991; Cochrane and Revak, 1991; Johansson et al., 1991; Longo et al., 1993; Takahasi et al., 1990; Waring et al., 1989). The positively charged synthetic amino-terminal peptide of SP-B, interacts strongly with negatively charged phosphatidic acid in monolayers, increasing the collapse π of such monolayers (Longo et al. 1993). No significant secondary structural change from the predominant α-helical ($\sim$40 %) conformation of the SP-B was observed in a DPPC bilayer environment by fourier transform infrared spectroscopy (Pastrana-Rios et al., 1995; Vandenbussche et al. 1992), indicating that the protein probably has stable orientations in mono- or bi-layers in its native structural form. The N-terminal domain of SP-B has been suggested to contain amphipathic helical sections in membrane-mimetic bilayer or monolayer systems (Fan et al., 1991). The R-SP-B/DPPC isotherms (Figure 9.2) and the percentage of condensed phase - π plots (Figure 9.3, top panel) show, that

at $\pi \sim 40$ mN/m there was only a small plateau and the amount of condensed phase increased with π in a different pattern from that seen in the F-SP-C/DPPC system (Figure 9.3, bottom panel). There was no abrupt increase of the condensed phase at any π (as was seen in the F-SP-C/DPPC films), suggesting that the minimal perturbation of DPPC condensed phase by R-SP-B was constant as a function of π, also indicating possible different associations and orientation of the protein compared to SP-C in DPPC films.

Recent infra-red spectroscopy studies of DPPC/SP-B or DPPC/SP-C films suggest that SP-B may not re-adsorb back into films after compression as efficiently as SP-C (Pastrana-Rios et al., 1995), and the lipid-protein structures formed at high π or collapse phases may differ between these two proteins. In our study, during expansion of R-SP-B/DPPC monolayers higher percentage of condensed phase was observed (Figure 9.3, top panel, open symbols) in such monolayers at comparable π than observed from compression (closed symbols), possibly indicating that more DPPC was present in the films at equivalent π during expansion than during compression. This may indicate that upon expansion SP-B spreads less rapidly back into the monolayer than SP-C. As spreading of phospholipids to an air-water interface is dependent on hydration, it is tempting to speculate that R-SP-B may be indirectly "hydrating" the DPPC headgroups, after they have been dehydrated due to compression (Denicourt et al. 1994; Dietrich et al., 1993). Such hydration may be due to the amphipathic helices having some water associated with them laying near the headgroup regions of the lipids, or by other electrostatic interactions of the protein charged residues and the lipids headgroup. Thus

the orientation of SP-B in the headgroup or polar region of the phospholipid in films may be of significance to previous findings that SP-B was more effective in inserting phospholipid to preformed monolayers than SP-C, and SP-B containing vesicles adhere to each other more than SP-C containing ones (Oosterlaken-Dijksterhuis et al., 1991a; 1991b).

9.44] Association of SP-B with SP-C in DPPC Films

The study of the monolayers containing both R-SP-B and F-SP-C (Figure 9.6) showed that the proteins mixed with each other quite homogenously in the fluid or expanded phase of DPPC. With the amounts of protein used, both proteins also reduced the ability of DPPC to form condensed phase. A previous study on similar lipid-protein mixtures showed that the proteins and some accompanying lipids were separately squeezed out of the monolayer, SP-B at ~ 43 mN/m and SP-C ~ 55 mN/m, indicating independent behaviour of the proteins in the presence of each other (Taneva and Keough, 1994a). The percentages of condensed phase in the monolayers of DPPC + 10 wt% R-SP-B + 10 wt% F-SP-C (Figure 9.6c) are roughly intermediate between those obtained for DPPC monolayers containing 20 wt% of either protein alone. This indicated that the proteins may perturb the DPPC monolayers in an independent and additive fashion. However some of both proteins remained associated with the DPPC monolayer at high π as seen in the images B, B′ in Figure 9.6 (b), and both were located in the same regions of the monolayers (fluid phase) under all conditions of compression and expansion (Figure 9.6b).

These monolayer results may have significance to pulmonary surfactant function and dynamics at the air-alveolar fluid interface. Instillation of such lipid-protein mixtures into the alveoli has been reported to improve lung function in PS-deficient experimental animals (Smith et al. 1988; Suzuki et al. 1986; Tanaka et al. 1986; see McLean and Lewis, 1995, for a review). The hydrophobic proteins individually perturbed the monolayer packing of DPPC by dispersing in the expanded phase of the monolayers, but some remained in or near the monolayers at high π. These factors may allow for replenishment of DPPC in to the surface monolayer (Taneva and Keough 1994), and after monolayer collapse on over-compression at high π, since some of the protein remain associated with the lipids to enhance re-spreading. Transfer of DPPC from surfactant secreted complexes to a preformed monolayer (Haagsman, 1994; Oosterlaken-Dijksterhuis et al., 1991a), or movement of collective units of lipids from the subphase to the interface (Goerke and Clements, 1986; Schürch et al., 1994), without interfering with DPPC monolayers reaching high π or low surface tension may be accomplished by the presence of the proteins. Also by increasing the fluidity of the DPPC monolayers, the proteins may enhance oxygenation of the air-alveolar fluid interface as suggested previously (Taneva and Keough, 1994b), since highly packed monolayers (i.e. DPPC at high π) exhibit greater resistance to gas exchange than fluid or expanded ones (Birdi, 1989). The results presented and discussed here are quite consistent with the role ascribed to these proteins *in vivo*, and with their potential positive benefit of their inclusions in synthetic surfactant. [*This chapter has been submitted for publication in the Biophysical Journal, (Appendix B, No. 1)*].

Chapter 10

SURFACTANT PROTEIN - A

(SP-A)

INTRODUCTION

Pulmonary surfactant protein - A (SP-A) belongs to the lectin family of water soluble glycoproteins. As detected by gel chromatography, the monomeric molecular weight (MW) of SP-A is around 28,000 - 36,000 Da, depending on the protein's levels of glycosylation. Native SP-A in association with surfactant lipids isolated from lung lavage is an octadecamer (18 monomers) of MW ~ 700,000 Da. Figure 10.1 shows the assembly and structure of human SP-A from its genomic (chromosome 10), pre-translational to post translational to its mono-, tri- and final octadeca- meric (18 monomers) stage (Weaver and Whitsett, 1991). The protein is associated with the more dense fraction of lavaged surfactant lipids which mainly consist of lamellar bodies and tubular myelin (Wright et al, 1984). The amino acid sequence of SP-A is highly conserved from species to species, and human SP-A consists of 248 amino acids (White et al., 1985). Two dimensional polyacrylamide gel electrophoresis (PAGE) of rat SP-A showed bands of around 38, 32 and 26 kDa, and each of these units were found to be cross-linked by disulphide bridges (Katyal and Singh, 1981). The monomer of SP-A contains near its N-terminal, collagenous domains of 24 repeating triplets of Gly-X-Y, similar to the ones found in other collagenous proteins (King, et.al. 1989). In SP-A, X is any amino acid and Y is hydroxyproline in 13 of the 24 repeats. This collagenous domain of SP-A can form a collagen-like triple helix (as found in tropocollagens of keratinous tissue), aligning the monomers to form a trimer. At 80 residues from the N-terminus of SP-A, the collagenous domain terminates, and is followed by a sequence of

Figure 10.1 Proposed protein structure of human SP-A.

The SP-A gene is encoded by 5 exons (filled boxes) on chromosome 10, has a 2.2 kilo base mRNA which gives rise to a post-translational protein with a 20 amino acid signal peptide. Post translational modifications of the pre-protein such as cleavage, inter- and intra- chain disulphide bond formation, glycosylation and the hydroxylation of proline residues leads to the formation of a tropocollagen like helix in a SP-A trimer (tape like region, in the trimer). Mature and non-denatured SP-A consists of six trimer linked by disulphides to form the flower bouquet-like octadecamer (18 monomers) of molecular weight ~ 700,000 Da. [Reprinted from Weaver and Whitsett, (1991), with the kind permission of the author and publisher, © The Biochemical Society and Portland Press, UK].

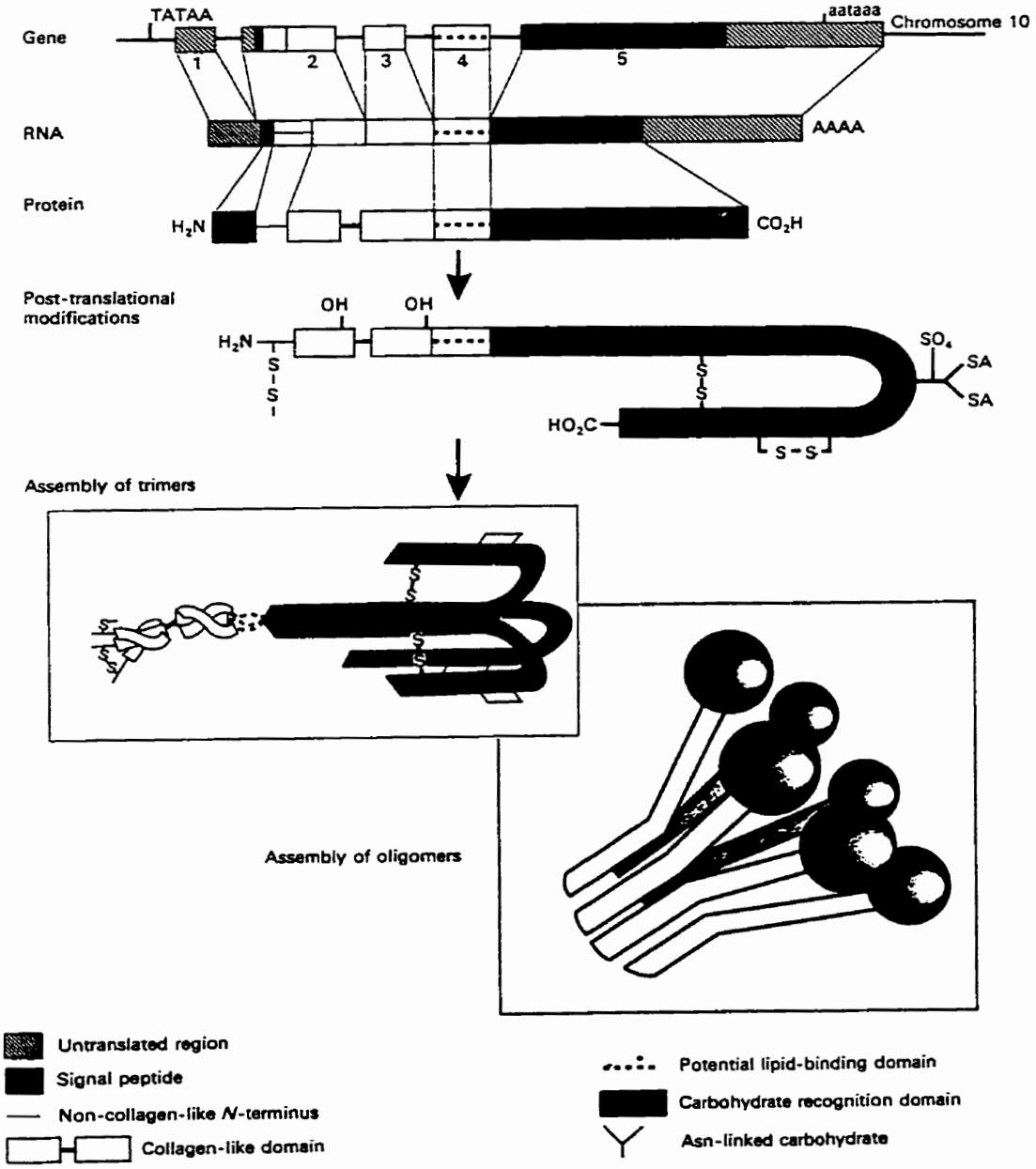
Gene
TATAA
aataaa
Chromosome 10
1
2
3
4
5
RNA
AAAA
Protein
H_2N
CO_2H
Post-translational modifications
OH
OH
H_2N
S
S
S
S
S
S
SO_4
SA
SA
HO_2C
S-S
Assembly of trimers
Assembly of oligomers
Untranslated region
Signal peptide
Non-collagen-like N-terminus
Collagen-like domain
Potential lipid-binding domain
Carbohydrate recognition domain
Asn-linked carbohydrate

30-40 amino acids which form the lipid binding domain of SP-A (Ross et al., 1986). After the 120th amino acid in the sequence of the SP-A monomer, the C type lectin domain occurs, and this domain stretches up to the carboxyl terminal residue. The lectin region of SP-A, called the carbohydrate recognition domain (CRD), contains a triple-antennae oligosaccharide chain linked to the asparagine-187 residue (Munakata et al., 1982). Each of the triplets can combine to form a 18 subunit octadecamer of molecular weight around 700,000 dalton (King at.al. 1989), 6 trimers being linked to each other by inter-chain disulphide bonds. The huge 20 nm x 20 nm, SP-A octadecamer can be seen by electron microscopy to form a "flower bouquet", those being similar to ones seen in other collectins such as mannose binding protein (Van Golde, 1995). The quaternary structure of SP-A indicates that the protein is globular (prolate ellipsoid) with a Stokes radius of 110 Å, and sedimentation coefficient of 14 Svedberg (King et.al. 1989). The structure of SP-A has been reviewed and discussed in detail by Hawgood, (1992).

SP-A plays important roles in physio-chemical, metabolic and host-defence functions of pulmonary surfactant. The protein enhances the rate of adsorption of surfactant hydrophobic lipid extracts to an air water interface (Schürch et al., 1992b; Yu and Possmayer, 1990), and helps in the surface sorting of such lipids to enrich pulmonary surfactant interfacial films with DPPC (Schürch et al., 1992b). Surfactant lipid-protein reconstitution studies *in vitro* indicate that SP-A is required along with DPPC, PG, SP-B and calcium ions to form tubular myelin (TM) (Suzuki et al., 1989), and that SP-A is localized at the corners of the square lattices of the TM (Voorhout et al., 1991). As TM is considered to be a reservoir for, or precursor to, the alveolar

surfactant films, SP-A plays important roles in structural transformation of PS from its secretory stages in lamellar bodies to surface film. SP-A has been found to have altered activity in its interactions with surfactant lipids, and lipid binding ability, under the influence of mono- and di-valent (calcium) ions (Efrati et al., 1987). Also the protein removes the inhibitory effect of several plasma proteins on pulmonary surfactant *in vivo* (Yukitake et al., 1995) and *in vitro* (Venkitaraman et al., 1990). Other than the roles SP-A play in pulmonary surfactant transformations, the protein inhibits the secretion and stimulates the metabolic re-uptake (or clearance) of surfactant lipids by type -II pneumocytes (Kuroki et al., 1996; Wright, 1990; Ueda et al., 1995). One of the first non-surface active roles of pulmonary surfactant protein detected was from studies indicating that SP-A plays some part in the immune host-defence functions of the lungs. The protein stimulates chemotaxis and oxy-radical generation in alveolar macrophages, which are required for macrophages to remove bacteria from the alveoli (reviewed by Van Golde, 1995). There is still some controversy regarding how SP-A elicits such responses in macrophages, although there is evidence to suggest that the process occurs via binding of SP-A to specific receptors on the macrophage surface (Pison et al.,1992) leading to a cellular response via the phosphoinositide/calcium signalling pathway (Ohmer-Schröck et al., 1995). SP-A and SP-D are now considered to belong to the family of proteins called collectins, proteins which can selectively recognise carbohydrates that are present on the cell walls of pathogenic bacteria or viral surface proteins (reviewed by Van Golde, 1995).

Studies by King and co-workers have shown that SP-A affects the gel to liquid

crystalline phase transition of DPPC in bilayers, and that the protein binds to the phospholipids in the gel phase (King and Macbeth, 1979; King et al. 1986). Later others have shown that the lipid binding of SP-A was cation dependent, and limited and specific to long chain phosphatidylcholines such as DPPC (C 16:0:16:0) or DSPC (C 18:0:18:0), but not to similar chain length phosphatidylethnolamine (PE) or phosphatidylglycerol (PG) (Kuroki and Akino, 1991). Also recent studies on binding of liposomes to isolated type-II pneumocyte membranes have suggested that by binding to DPPC of pulmonary surfactant *in vivo*, SP-A directs the lipids to the type-II pneumocytes for uptake and recycling (Kuroki et al., 1996). Specific studies on the interaction of SP-A with DPPC in films are limited, but a recent study by Taneva et al., (1995), have indicated that SP-A enhances the re-spreading of lipid films compressed beyond collapse, and small amounts of the protein remains in the lipid films at high surface pressure. Others have shown that SP-A either causes the selective adsorption of DPPC into the interface or has a compression-independent mechanism for removal of non-DPPC components from monolayers of pulmonary surfactant, enriching the films with DPPC (Schürch et al., 1992a).

As lipid films observed by fluorescence microscopy can easily show the surface pressure dependent separation of two dimensional phases, we have utilized the technique to study the distribution of fluorescent labelled SP-A in DPPC films, and thereby the association and interaction of SP-A with the two-dimensional lipid phases. Some limited studies on the interaction of SP-A with DPPC:DPPG (with and without calcium) and with SP-B in such films were also performed, since such lipid-protein combinations are

required for formation of tubular myelin. Since SP-A is water soluble, the methods used to study lipid-protein film in this study were somewhat different from the ones used to study hydrophobic proteins. SP-A was adsorbed from a buffered subphase into the DPPC monolayers, instead of spreading the protein in conjunction with the lipids at an air-water interface as done by Taneva et al., (1995).

10.21] Materials.

DPPC, DPPG-sodium salt (DPPG-Na) and NBD-PC were purchased from Avanti Polar Lipids (Pelham, AL) and checked for purity by TLC as above. Texas-Red isothiocyanate (TR-ITC), fluorescein isothiocyanate (FITC) and concanavalin A-rhodamine conjugate were purchased from Molecular Probes (Eugene, OR), and used as received.

10.22] Isolation and labeling of SP-A.

The isolation, purification and labelling of SP-A and some of the experiments were performed in collaboration with our colleagues in Spain, Dr. Jesus Perez-Gil (JPG), Miguel L. F. Ruano (MLFR) and Christina Casals (Department of Biochemistry and Molecular Biology, University of Madrid). Porcine SP-A was isolated, purified and labelled with Texas-Red by MLFR using methods of Casals et al., (1993), and this protein gave a single broad band between 32-36 kDa. Details of such methods are discussed in Ruano et al., (1996). The labelled R-SP-A was dissolved in a buffer (0.15 M NaCl, 5 mM Tris-HCl, pH-7.4) and stored in 10 μg/ml aliquots at - 20°C, and analyzed using MALDI mass spectrometry at University of Waterloo, by Mr. Lorne Taylor. SP-B was isolated and labelled with fluorescein by JPG by methods discussed in the last chapter.

10.23] Video microscopy of dual labels in lipid films.

Figure 10.2 Schematic diagram of the epifluorescence microscopic surface balance method of studying fluorescent labelled SP-A (R-SP-A) adsorbed on to lipid monolayers.

For clarity, to show details of the instrumentation and to fit the diagram in the same page the lipid (DPPC) and the protein (SP-A) sizes are not drawn to scale [1 lipid molecule = 40-80 $Å^2$; whereas 1 SP-A molecule = 40,000 $Å^2$]. The colours represent the fluorescence observed by eye from the lipid probe (green) and the fluorescent protein (red) respectively. The images were video recorded in black white for image analysis due to the limitation of our charge coupled device (CCD) video camera to record in colour. They were subsequently coloured in the figures based upon their examination by eye.

A Wilhelmy plate was used to measure surface tension of the air-saline interface, which was converted to surface pressure (π) to obtain π-A isotherms. The monolayer images were observed at individual π independently by switching excitation-emission filters between NBD-PC (emission-green) and R-SP-A (Texas-Red, emission-red). The individual excitation colour of each fluorophore (blue and green) is shown by the small coloured bars in the monolayer images.

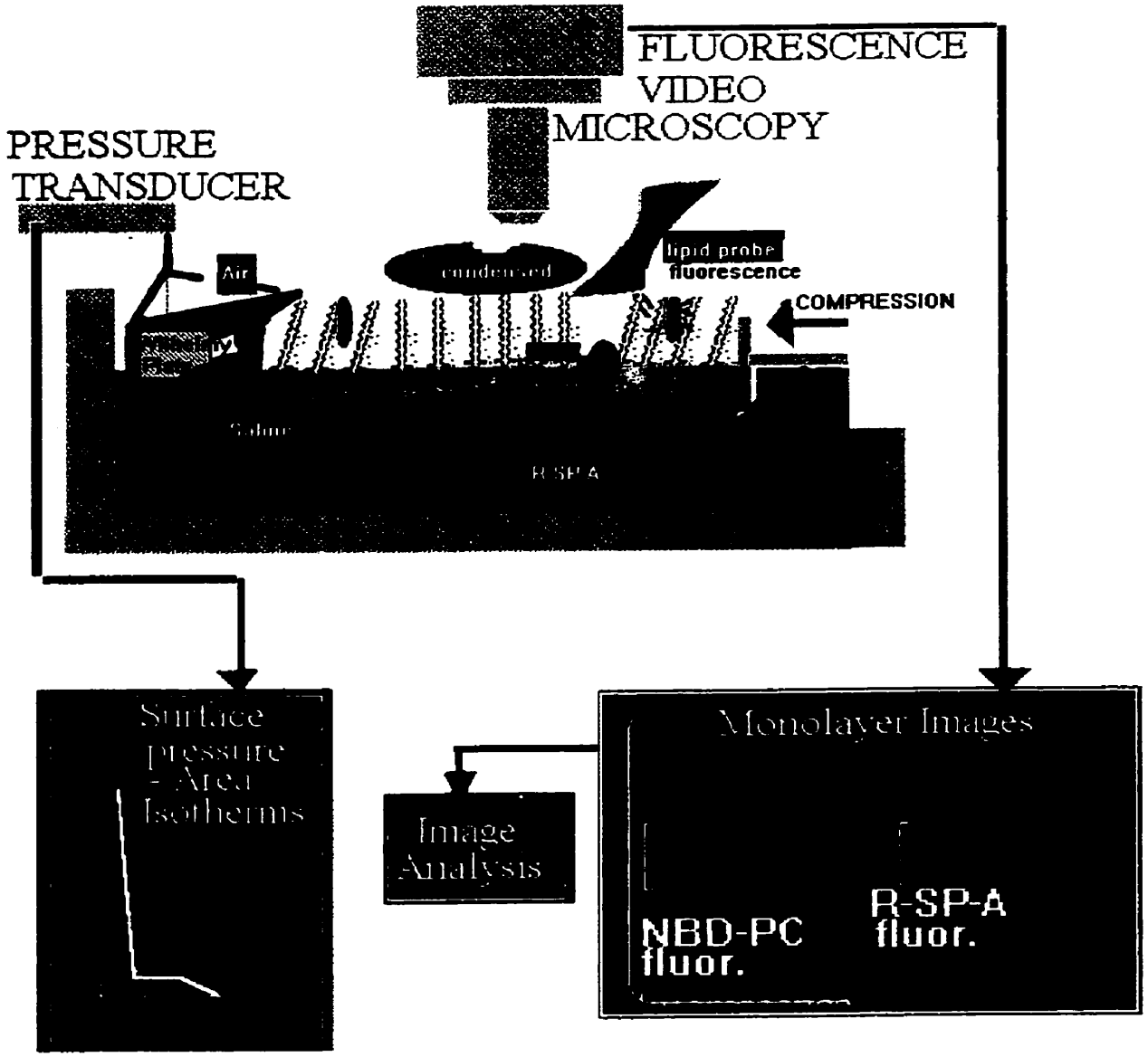
FLUORESCENCE
VIDEO
MICROSCOPY
PRESSURE
TRANSDUCER
Air
lipid probe
fluorescence
COMPRESSION
Surface
pressure
- Area
Isotherms
Image
Analysis
Monolayer Images
R-SP-A
fluor.
NBD-PC
fluor.

The Texas-Red labelled SP-A (R-SP-A) was dissolved in a 150 ml subphase buffer (0.15 M NaCl, 5 mM Tris-HCl, pH-7.4 and 4.0), made with doubly distilled deionized water. Amounts of 0, 10, 20 and 40 μg of R-SP-A were dissolved in 150 ml of the buffered subphase giving a final concentration of 0, 0.06, 0.13 and 0.26 μg/ml. Control experiments were performed using 0.13 μg/ml of fluorescently labelled concanavalin A in the subphase. The lipids (20 nanomoles) containing 1 mol% of lipid probe NBD-PC were spread from chloroform:methanol (3:1, vol/vol) solutions on top of the subphase containing R-SP-A in the epifluorescence balance. Such an arrangement of lipid film with protein in the subphase in the epifluorescence microscopic surface balance is shown in Figure 10.2. The final lipid:protein molar ratios in the experiments using monomeric MW of R-SP-A (35 kDa) were approximately 80:1, 40:1 and 20:1, assuming all the protein molecules in the subphase associated with the lipid films. All experiments were performed at a room temperature of 22 $\pm$ 1°C.

After spreading the lipid monolayers, a one hour wait period was allowed for the R-SP-A to equilibrate with and adsorb onto the lipid films before compressing the films at a rate of 20 $mm^2.sec^{-1}$ (or 0.13 $Å^2.mol^{-1}.sec^{-1}$) in steps. Monolayers were observed visually from the fluorescence of the lipid probe (NBD-PC) (green = 540 nm, Figure 10.2) and then by switching the filter combination to that for R-SP-A (red = 610 nm, Figure 10.2). The images were video recorded in black and white, due to the inability of the video camera to acquire colour images, and later false-coloured in 16 colour levels using a Windows 3.1 software (Microsoft) to display the image as they seem to the eye. The black and white video recorded images were analyzed using methods discussed

above and in Appendix A.

10.24] Video microscopy of SP-A and SP-B: Fluorescence energy transfer.

Aliquots of DPPC and fluorescent F-SP-B in chloroform:methanol (3:1 vol/vol) were mixed in a weight proportion of 10:1 (DPPC:F-SP-B). The mixed solutions were spread on the buffer solution described above, the subphase being with and without 0.13 μg/ml of R-SP-A. The monolayers were compressed in steps at a rate of 20 $mm^2.sec^{-1}$ and fluorescence observed from either F-SP-B (540 nm emission, green) or R-SP-A (610 nm, red).

Since the excitation wavelength of the Texas-Red label on R-SP-A had maximal absorbency at $\sim$ 589 nm (greenish-yellow), this wavelength falling in the tail end of the range of the broad emission spectrum of the fluorescein label on F-SP-B (500-600), experiments were designed to see if there was any resonant energy transfer between the fluorophores. The optics (cut-off filters) of the microscope were modified to excite the fluorescein label in the F-SP-B and to observe (without switching filters) the emission from R-SP-A (615 nm maximal emission; red). If the fluorophores (and thus the proteins SP-B/SP-A) were located very close to each other, then fluorescein would transfer its emission energy to excite the Texas-Red via resonance energy transfer.

RESULTS

The MALDI mass spectrum of Texas-Red labelled porcine SP-A is shown in Figure 10.3. The three major peaks shown at 28,220, 33,954 and 37,438 Dalton indicated the deglycosylated, glycosylated and the Texas-Red labelled forms of SP-A (R-SP-A), respectively. The other smaller peaks (i. e. 29,832; 35,080; 38,308 Da) indicated the protein with different levels of labelling and glycosylation. The peak at 37,438 Da indicates the native glycosylated, monomer of SP-A (MW ~ 36,800, from PAGE analysis) labeled with one mol of Texas-Red (36,800 Da + 625 (MW of Texas-Red) = 37,425 Da). The native monomeric form of this porcine SP-A as seen by PAGE showed a small band around 28,000 Da, and a broad band between 33,000-37,000 Da, since the extracted porcine SP-A reduced to its monomeric form, was a mixture of isoforms with different levels of glycosylation as discussed elsewhere (Ruano et al., 1996). Katyal and Singh (1981) had reported that rat SP-A prepared by detergent solubilization and immuno-affinity chromatography showed bands at 38, 32 and 26 kDa by SDS-PAGE, the 38 kDa band being the richest in its amount of attached polysaccharide. The peaks in the mass spectrum in our porcine R-SP-A indicated that the protein was a mixture of monomeric deglycosylated, glycosylated and Texas-Red labelled isoforms.

Typical images seen in DPPC monolayers with adsorbed R-SP-A (0.13 μg/ml dissolved in the subphase) are shown in Figure 10.4 (a) (pH-7.4) and (b) (pH-4.5), and from a DPPC monolayer spread over similar amounts of labeled concanavalin-A in buffer

Figure 10.3. Matrix-assisted laser desorption/ionisation (MALDI) mass spectrum of fluorescently labelled SP-A in buffer (0.15 M NaCl, 5 mM Tris-HCL, pH-7.4).

The plots indicates that R-SP-A was mainly in its deglycosylated ~ 28 kDa, glycosylated ~ 33-36 kDa, and fluorescent labelled (> 37 kDa) forms.

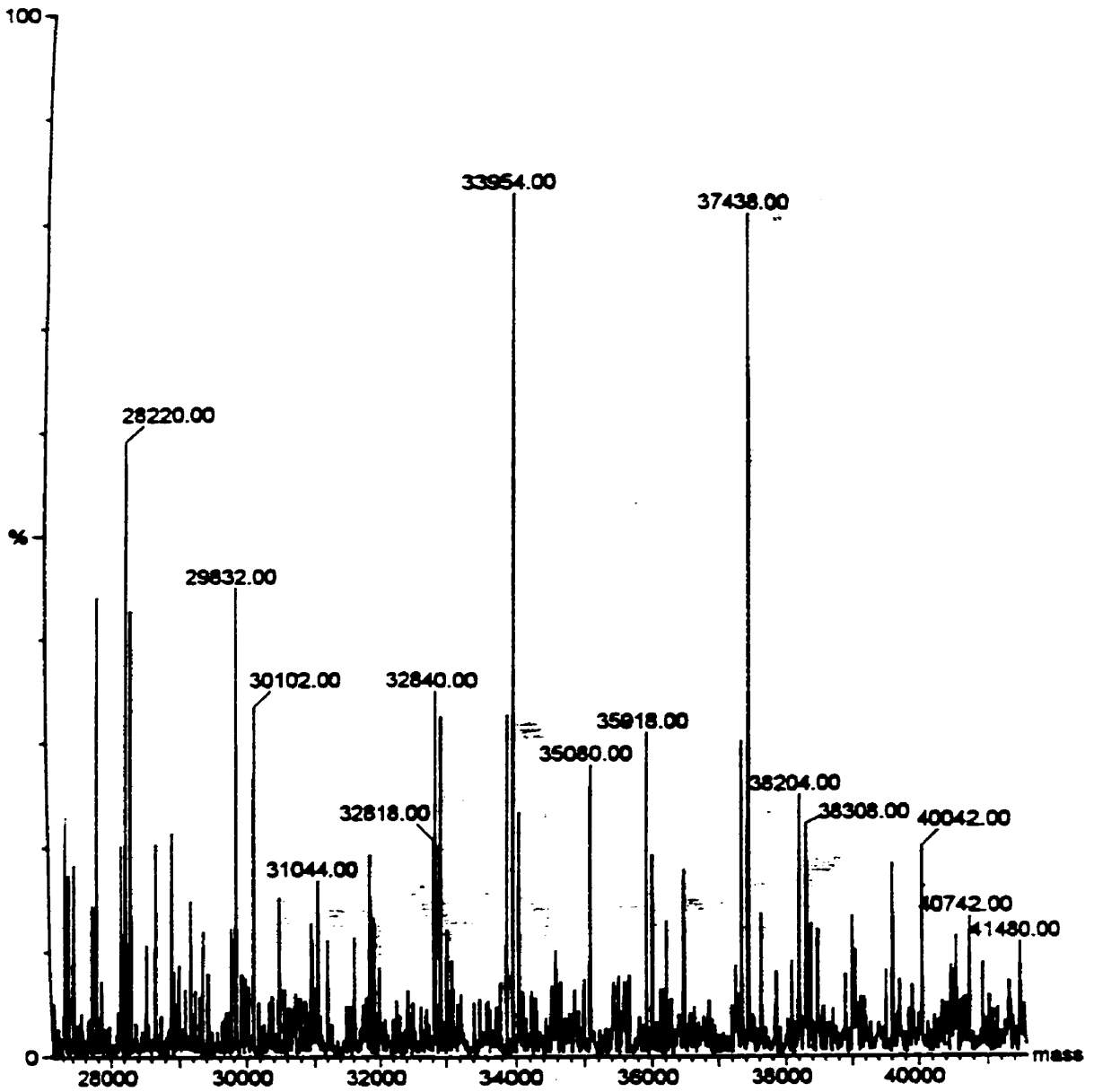
100
%
0
28220.00
29832.00
30102.00
31044.00
32818.00
32840.00
33954.00
35080.00
35918.00
37438.00
38204.00
38308.00
40042.00
40742.00
41480.00
28000
30000
32000
34000
36000
38000
40000
mass

(pH-7.4) in Figure 10.4(c). The left panels of Figure 10.4 (a-c), indicate false coloured images observed from fluorescence of NBD-PC (green) and the right, from the proteins (red). The black regions of the images indicate the liquid condensed (LC) and the coloured regions the liquid expanded (LE) phase. The fluorescence observed from the protein (bright red, right panel) indicated that the R-SP-A aggregated between the condensed (gel-like) and expanded (fluid) phase boundaries at both pH. Although Con-A looked as though it may have aggregated at LC-LE boundaries, and that it was not present in the LE phase, it had a different arrangement than the aggregates of R-SP-A at either pH. This indicated that DPPC/SP-A interactions may be specific. At the lower pH of 4.5 (Figure 10.4b), there was more R-SP-A present at the LE-LC boundaries compared to the amounts observed at the higher pH (Figure 10.4 a). R-SP-A was somewhat regularly distributed all around the condensed phase, as the outlines of individual condensed domains (kidney shaped) could clearly be observed from protein fluorescence. The images of DPPC/R-SP-A (pH 7.4) at intermediate π between 10 to 20 mN/m some protein was also found to be dispersed in the fluid phase (dull-red). This indicated that some R-SP-A was probably dispersed in the fluid or LE phase of the lipid films at the higher pH. The bottom right images of the DPPC/R-SP-A system (Figure 10.4a and b) observed at $\pi \sim 61$ mN/m, indicated that some protein was present in or near the films at high π.

Figure 10.5 shows the isotherms of DPPC plus 0, 0.06, 0.13 and 0.26 μg/ml of R-SP-A films (total lipid/total protein ratio of 100:0, 80:1, 40:1 and 20:1, assuming all the dissolved protein was associated with the lipid film) on a buffered subphase (pH-7.4)

Figure 10.4 Typical images seen in monolayers of DPPC spread over a subphase buffer containing 0.13 μg/ml of R-SP-A, at buffer pH of 7.4 (a) and 4.5 (b), DPPC films containing Texas-Red labelled Con-A in a similar buffer of pH 7.4 (c). The images in the left panel were observed from NBD-PC fluorescence and the right panel from R-SP-A (or Con A in (c)) at the π shown at the corners of the images. The black regions represent the LC phase and the coloured regions the LE or fluid phase. The scale bar is 25 μm.

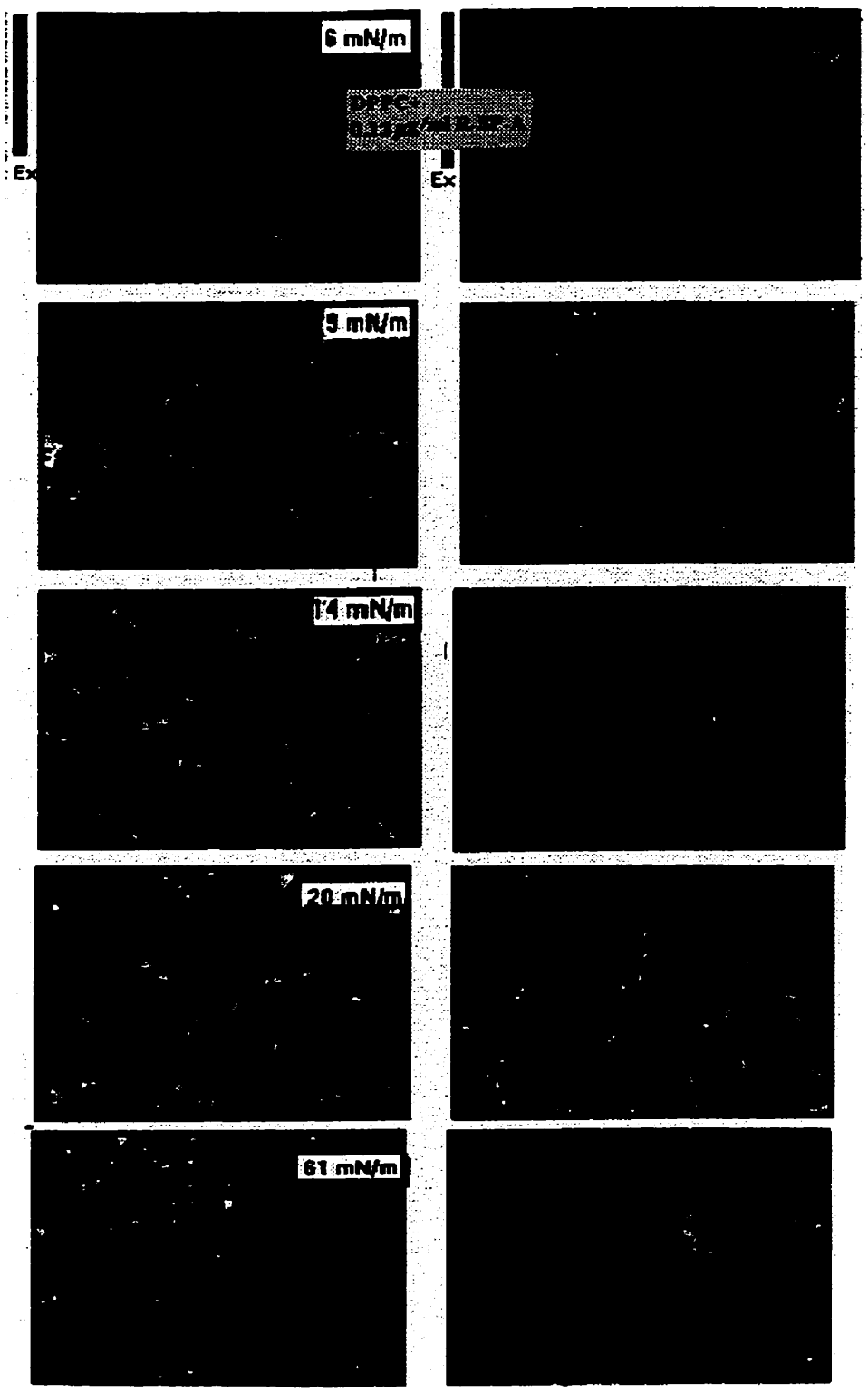

(a)

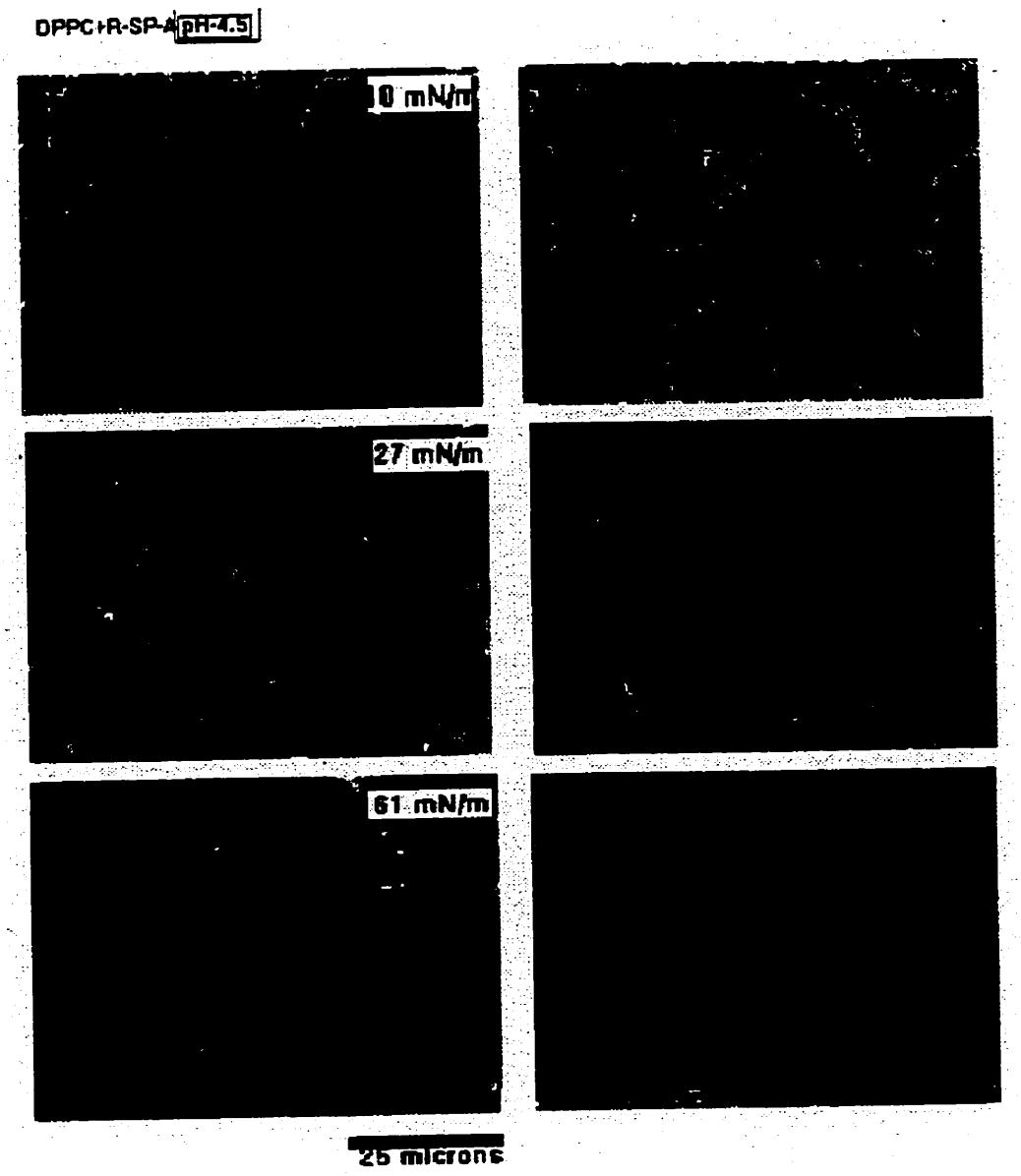

(b)

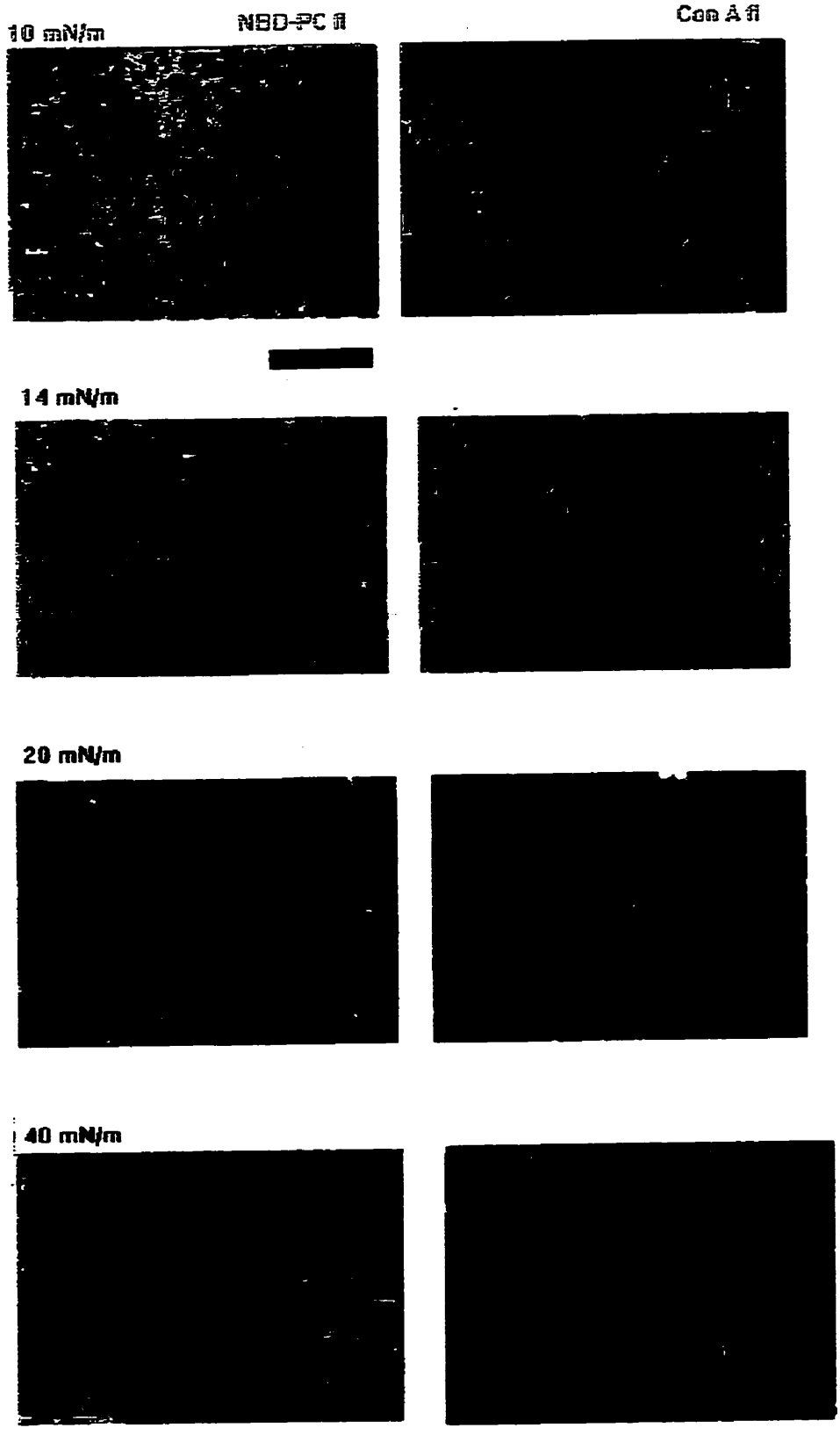

246c

(c)

Figure 10.5 Typical surface pressure - area per molecule of the lipid (π-A) isotherms of DPPC films containing 0 - 0.26 μg /ml of R-SP-A dissolved in the subphase (top), and typical images observed in such monolayers at $\pi \sim 12$ mN/m (bottom). The black in the images indicate the liquid condensed and the grey regions the fluid phase. The images are represented in black and white as observed through the CCD camera and video recorded from the NBD-PC fluorescence. The scale bar is 25 μm.

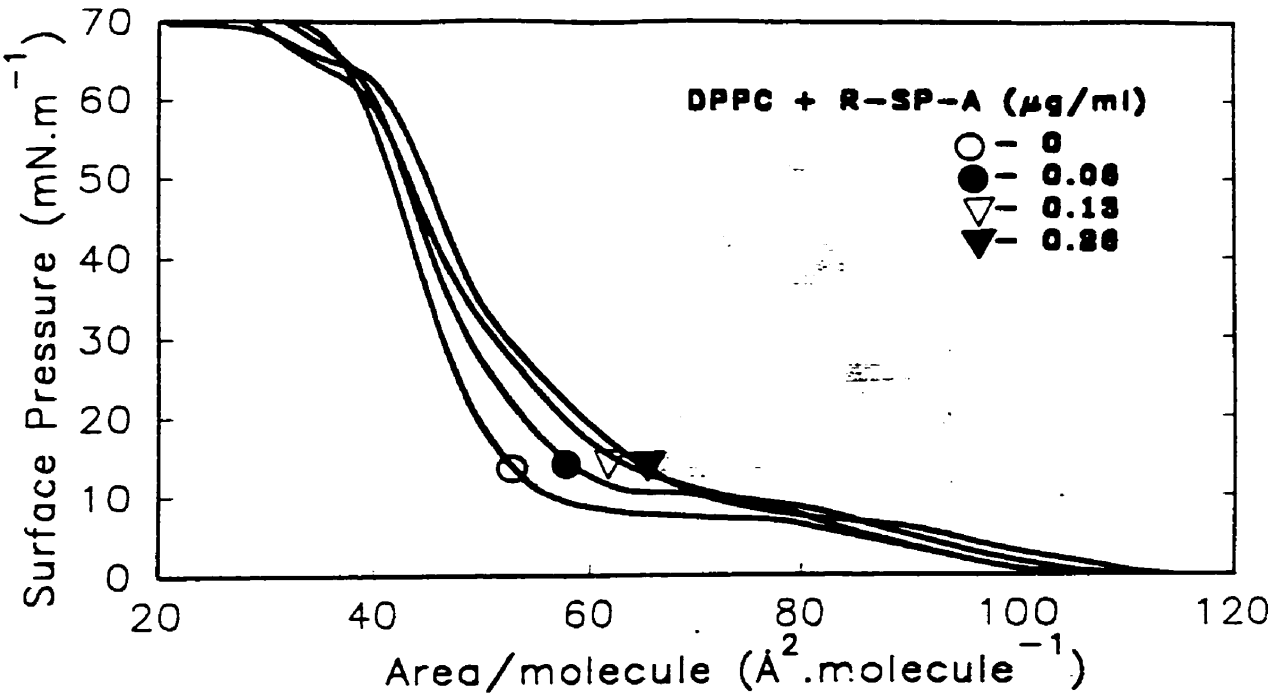
DPPC + R-SP-A (μg/ml)
○ – 0
● – 0.06
▽ – 0.13
▼ – 0.26
Surface Pressure (mN.m^{-1})
Area/molecule (Å^2.molecule^{-1})
0
10
20
30
40
50
60
70
20
40
60
80
100
120

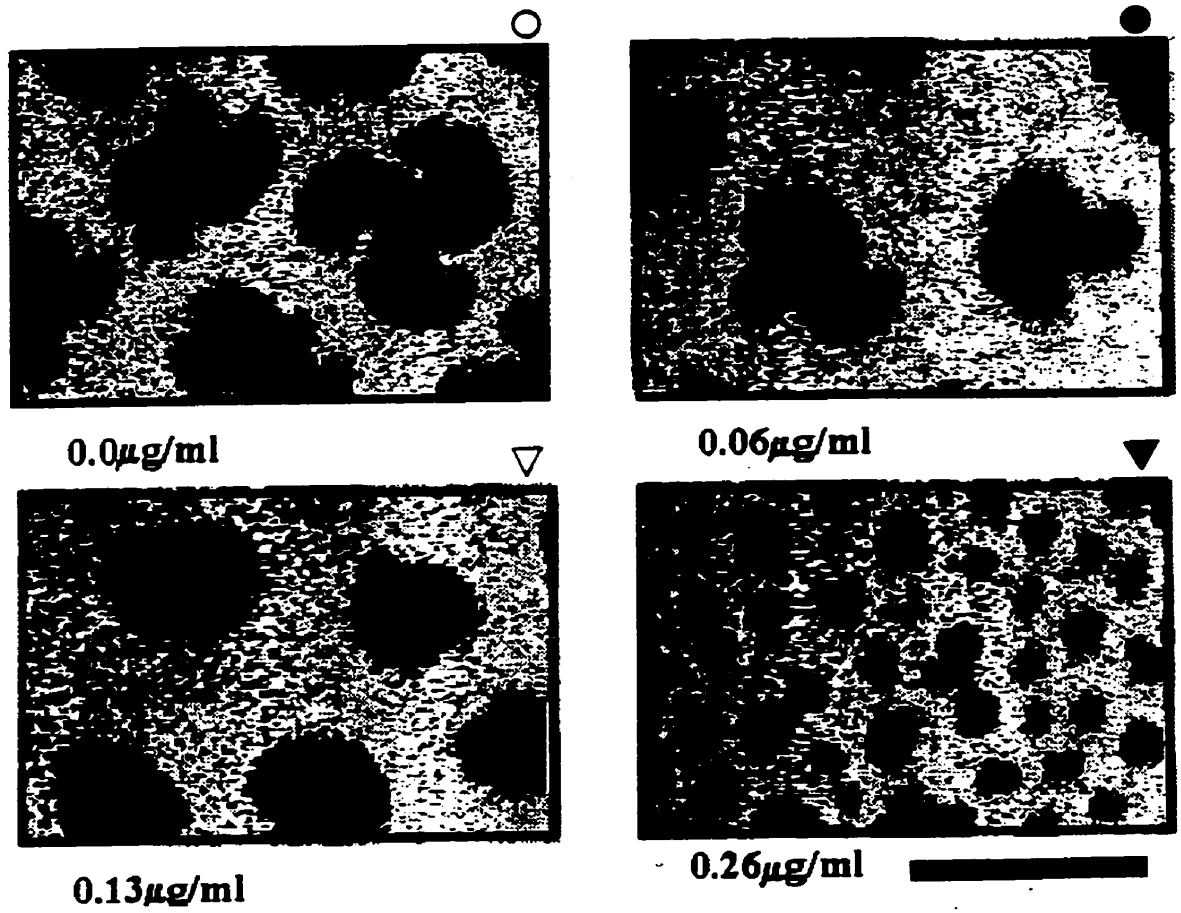
○
0.0μg/ml
●
0.06μg/ml
▽
0.13μg/ml
▼
0.26μg/ml

(top), and typical images observed in such monolayers from NBD-PC fluorescence at a $\pi \sim 12$ mN/m (bottom). Increasing amounts of R-SP-A caused a shift of the monolayer isotherms to the right from that of the lipid alone and this shift appeared to be pronounced between a π of 10-30 mN/m. The shifts in the isotherms indicate that the protein or some parts of it possibly penetrated the monolayer and affected the phase transition of DPPC.

Figure 10.6 shows the average area (A), number (B) and total amount (C) of the black or LC domains seen in films of DPPC containing 0 - 0.26 μg/ml of R-SP-A in the subphase as a function of surface pressure. The average area (A) and the total number (C) of LC domain profiles indicated that increasing amounts of R-SP-A decreased the size and the total amount of the black phase in the monolayers of DPPC at comparable π, although the number of domains (B) remained constant except for the highest amount of R-SP-A (0.26 μg/ml) used. This indicated that at equivalent surface pressures, R-SP-A decreased the amount of condensed phase of the DPPC films, and higher π were required to form equivalent amounts of condensed phase and suggested that R-SP-A perturbed the packing of DPPC films.

To observe if there was any electrostatic interaction between R-SP-A and the lipids, visual inspections of monolayers of DPPC containing some acidic lipid (DPPC:DPPG, 7:3, mol/mol) and in the presence of modified ionic environments of the protein (altering the pH and inclusion of calcium in the subphase) were performed. Typical images seen in monolayers of DPPC:DPPG (7:3, mol/mol) with 0.13 ug/ml of R-SP-A in the subphase at a pH of 7.4 and 4.5, and with 2 mM calcium (at pH 7.4) in

Figure 10.6 Average size (A), number (B) and total amount (C) of the black regions or LC phase seen in monolayers of DPPC containing 0 (○), 0.06 (●), 0.13 (▽) and 0.26 (▼) μg/ml (key in C) of R-SP-A plotted as a function of surface pressure. Ten randomly selected images were analyzed from such films at each individual π. The error bars represent $\pm$ one standard deviation.

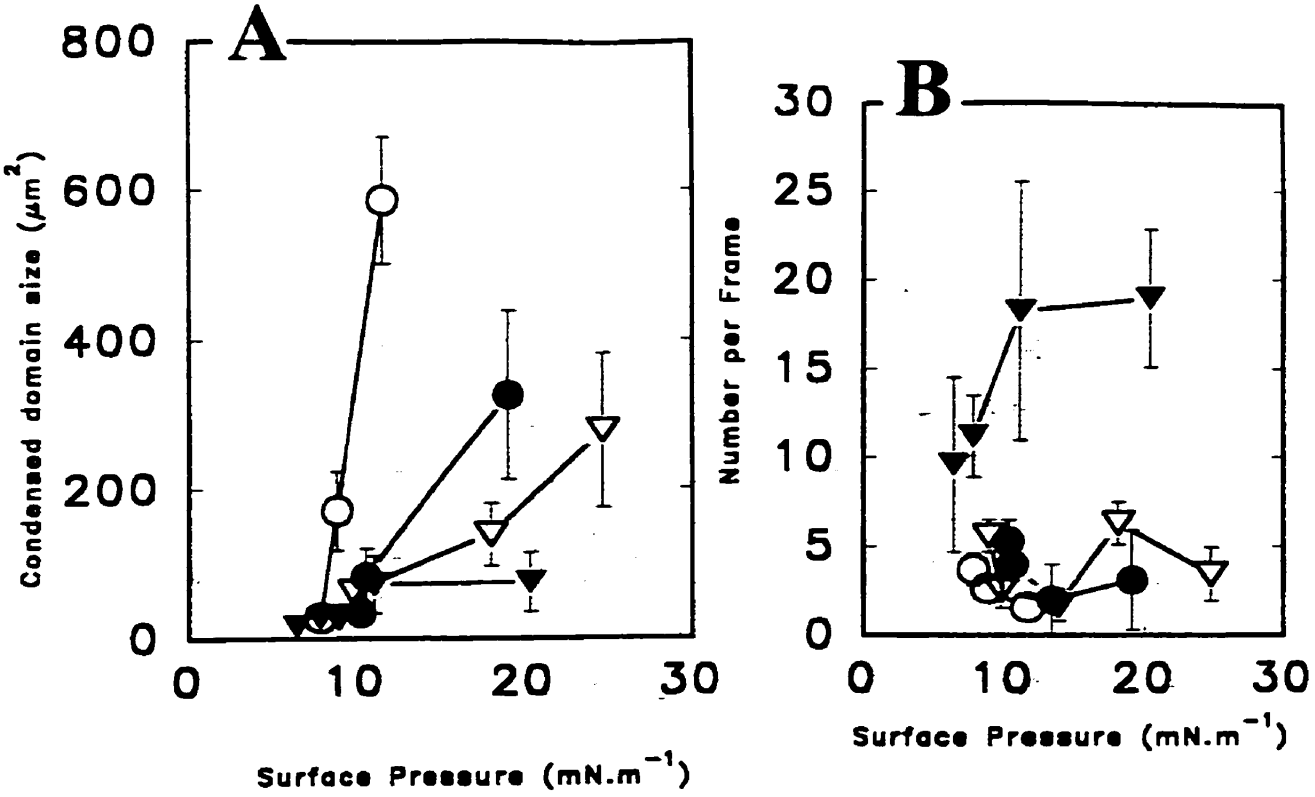
A
800
600
400
200
0
Condensed domain size (μm^2)
0
10
20
30
Surface Pressure ($mN.m^{-1}$)
B
30
25
20
15
10
5
0
Number per Frame
0
10
20
30
Surface Pressure ($mN.m^{-1}$)

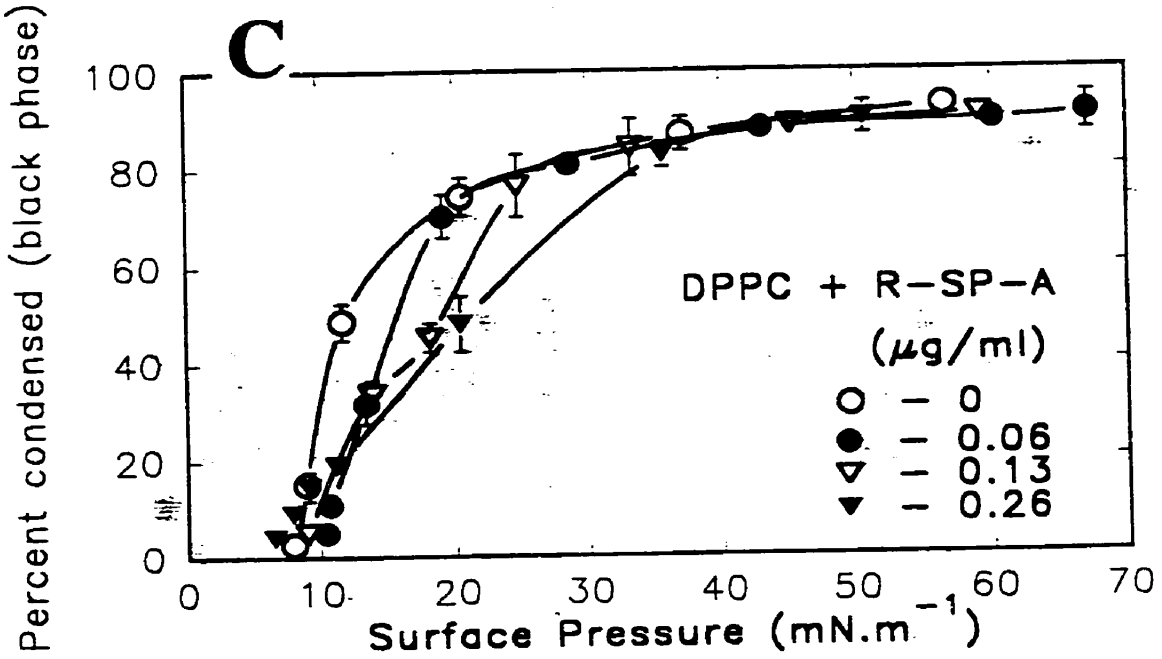
C
100
80
60
40
20
0
Percent condensed (black phase)
0
10
20
30
40
50
60
70
Surface Pressure ($mN.m^{-1}$)
DPPC + R-SP-A
($\mu g/ml$)
○ – 0
● – 0.06
▽ – 0.13
▼ – 0.26

Figure 10.7 Typical images seen in films of DPPC:DPPG (7:3, mol/mol) containing 0.13 μg/ml of R-SP-A. The green regions indicate fluorescence observed from NBD-PC (left) and the red from R-SP-A (right) at π indicated at the top of each image. Scale bar is 25 μm.

The conditions of subphase of the films are: panel A - DPPC:DPPG (7:3, mol/mol) pH 7.4; panel B - DPPC:DPPG (7:3, mol/mol) pH 4.5; panel C - DPPC:DPPG (7:3, mol/mol) + 5 mM calcium, pH-7.4.

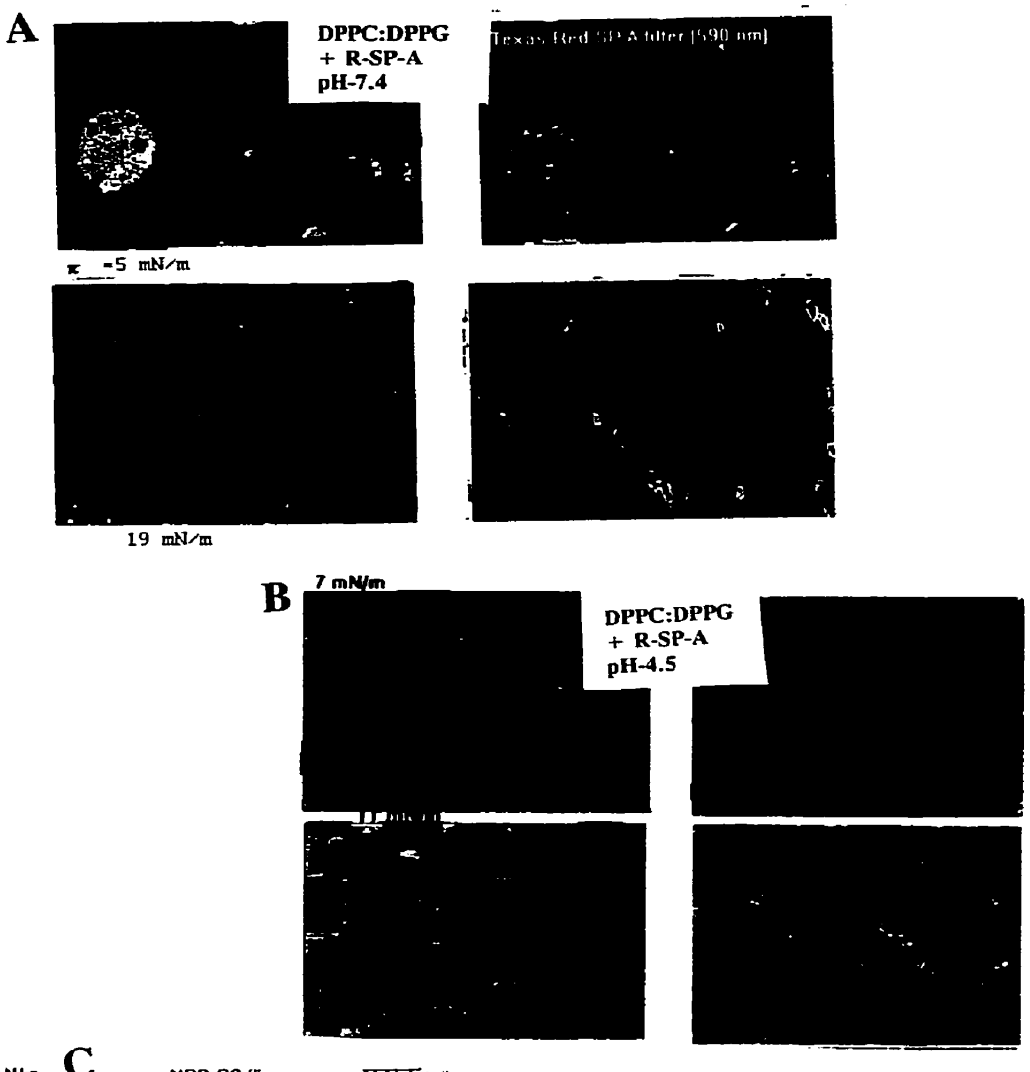
A
DPPC:DPPG
+ R-SP-A
pH-7.4
Texas Red SP-A filter (590 nm)
π -5 mN/m
19 mN/m
B
7 mN/m
DPPC:DPPG
+ R-SP-A
pH-4.5
C
5 mN/m
NBD-PC fl
R-SP-A fl
DPPC:DPPG
+ R-SP-A
pH-7.4
+ 5mM Ca2+
11 mN/m

the subphase are shown in Figure 10.7. These images suggested that by altering the ionic condition of the films (using acidic lipid DPPG) (panel A, Figure 10.7) or by changing the ionic conditions of R-SP-A environment (pH-4.5 or 2 mM calcium, panel B and C, Figure 10.7), the interaction of the protein with the lipids was altered. Using small amounts of acidic lipids changed the distribution of the protein aggregates around the gel phase boundaries, calcium caused aggregation of the protein into large circular domains. [Details of these interactions will be discussed elsewhere by M. L. F. Ruano in his PhD thesis and to be published as Ruano et al., 1997).

The images observed in DPPC films containing 10 wt % fluorescein labelled SP-B (F-SP-B) with 0.13 μg/ml of R-SP-A in the subphase, seen from the fluorescence of the proteins alone, are shown in Figure 10.8. The images in the left panel indicate that fluorescent labelled SP-B (F-SP-B, green) in the presence of SP-A had a different arrangement in DPPC films, than in its absence (Chapter 9, Figure 9.2). Fluorescent labelled SP-B in the absence of SP-A occupied the fluid or LE phase of DPPC films (Figure 9.2), whereas in the presence of R-SP-A (Figure 10.8) the protein aggregated in the LE-LC boundaries. This indicated that SP-B in the presence of SP-A mostly segregated out of the fluid phase, and formed aggregated structures or domains which attached to the LC domain (black) phase boundaries. These aggregates of F-SP-B also fluoresced when observed through the R-SP-A fluorescence (right panel, Figure 9.2) indicating that SP-A and SP-B closely associated with each other in the presence of the lipids in films.

Since the fluorescein label of SP-B has a broad emission spectrum between 480

Figure 10.8 Typical images observed in solvent spread films of DPPC + 10 wt % of F-SP-B, with 0.13 μg/ml of R-SP-A dissolved in the subphase, at the π given above each image. Scale bar is 25 μm.

The green in the left panels represents the fluorescence observed from fluorescein labelled SP-B (F-SP-B) and the red in the right panel the fluorescence from Texas-Red labelled SP-A (R-SP-A). The excitation and emission wavelengths (or colour) of each fluorophore is shown in the coloured bars in top of each column.

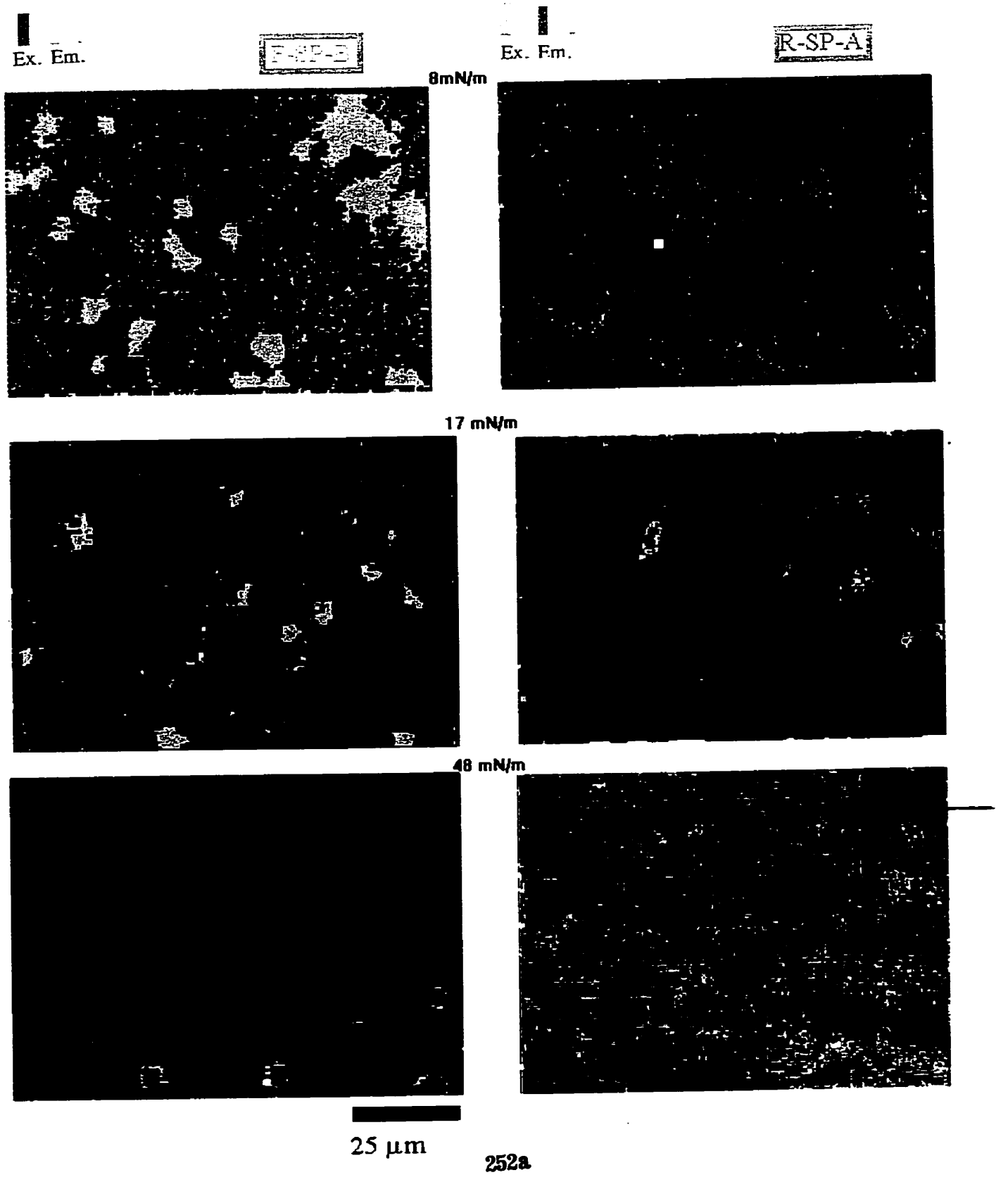

252a

Figure 10.9 Typical images observed in a DPPC film containing F-SP-B and R-SP-A (as in last figure), from excitation of fluorescein (F-SP-B) and emission of Texas-Red (R-SP-A) by fluorescence resonance energy transfer. The excitation and emission wavelength of each fluorophore is indicated by the coloured bars in the top. Scale bar is 25 μm.

The red patches in the images are fluorescence observed from the R-SP-A/F-SP-B aggregates as seen individually in the Figure 10.9 as green or red, from fluorescence of the individual proteins.

13 mN/m

Ex. Em.

17 mN/m

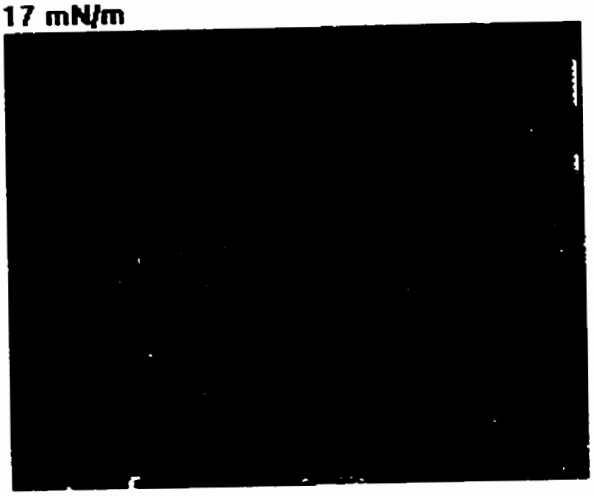

70 mN/m

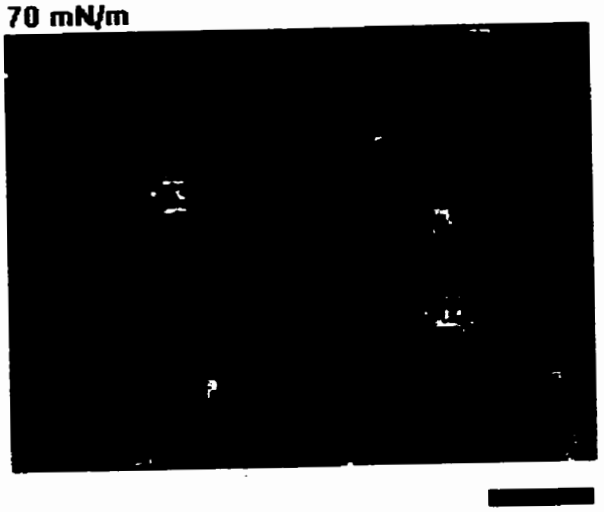

253a

and 600 nm, the tail end of which includes the maximum excitation wavelength of Texas-Red label of SP-A (-589 nm), the emission energy of F-SP-B (fluorescein) could be transferred to excite the R-SP-A by resonance energy transfer (Texas Red-excitation 589 and emission - 615), if such fluorophores or the proteins were in close proximity to each other. Figure 10.9 indicates images from a DPPC/F-SP-B/R-SP-A film with increasing π which were obtained by excitation of F-SP-B and fluorescence from R-SP-A (red). The images in Figure 10.9 indicated that SP-A and SP-B or their fluorescent labels were in close proximity to each other with some fluorescence energy transfer occurring between the two fluorophores.

10.41] SP-A associates with LE-LC phase boundaries of DPPC.

From the studies of Kuroki and Akino (1991) using radio-iodinated ^{125}I-SP-A binding to specific phospholipids on thin layer chromatography (TLC) plates, it was shown that the protein had strong affinity for DPPC, although the structural orientation and phase of the lipids on TLC plates are not easily defined. Their studies also indicated that the binding was strong for phosphatidylcholine (PC) having chain lengths greater than 14 carbons, such as DPPC (16:0) and DSPC (18:0), but not for unsaturated PC, possibly indicating that the lipids had to be in a gel-like state (rigid chains) for binding to occur (Kuroki and Akino, 1990). From turbidity measurements of DPPC/SP-A suspension, King and co-workers observed that the protein removed the usual calorimetrically detectable sharp phase transition of DPPC at 42°C (King and Macbeth, 1979). They later showed from measurements of temperature sensitivity of SP-A/lipid associations that SP-A had more affinity for the lipids in gel phase than in liquid crystalline phase (King et al., 1986). Their other studies have indicated that lipid-protein association was strongest when such suspensions contained DPPC plus small amounts of other lipids, suggesting that association may have been linked with phase boundaries (King et al., 1983). The association of fluorescently labelled SP-A (R-SP-A) with DPPC films as seen in this study seems to indicate similar lipid-protein association, since the protein was mainly found surrounding the condensed (or gel-like) and fluid phase boundaries (Figure 10.1 a and b). Whether such R-SP-A/DPPC association indicates

"binding" of the protein to the lipid, or exclusion of the protein by the gel-like phase, with the possibility that most of the protein being found aggregated at the phase boundaries, is inconclusive from this study. Albeit comparison between the DPPC/R-SP-A images with those of DPPC/Con A (Figure 10.1c) and SP-A/DPPC:DPPG (Figure 10.7) films tended to suggest that the SP-A/DPPC association is somewhat specific.

10.42] Specific or preferential association of SP-A with DPPC.

This study indicates that SP-A penetrated the DPPC films from the subphase, mainly aggregated around the edges of the condensed phase domains, although some protein was also present in the fluid or loosely packed phase at low surface pressure (Figure 10.1 (a), dull red fluorescence is seen in the fluid phase) and that the protein was probably squeezed-out of the lipid monolayers at high π. Studies on interaction of water soluble proteins with lipid films tend to indicate that the proteins penetrate the lipid monolayers at low surface pressure (π) and are squeezed out of such films at high π, without any specific lipid-protein interactions occurring. Figure 10.10 shows the conceptualised arrangement of SP-A in bilayers (A) and monolayers (B).

Taneva et al. (1984) had shown that serum albumin in lipid films has a different conformation than in the bulk phase, and is desorbed (squeezed out) from the lipid films in high compression states. Hepatitis A viral protein VP3 inserted into lipid films of DPPC, DSPC and DOPC, with maximal insertion occurring at π between 2-6 mN/m (the π at which LE-LC phase coexist in DPPC and DSPC films, but not in the DOPC films) (Bogdam et al., 1994). This may be due to the preference of the VP3 protein to

Figure 10.10 Possible arrangement of SP-A in bilayer (A) and a monolayer (B).

SP-A adsorbed onto the condensed-fluid (or LC-LE) phase boundaries in monolayers (B), although some protein was probably present in the expanded phase. [The figure was generously provided by Dr. Jesus Perez-Gil, of University of Madrid]

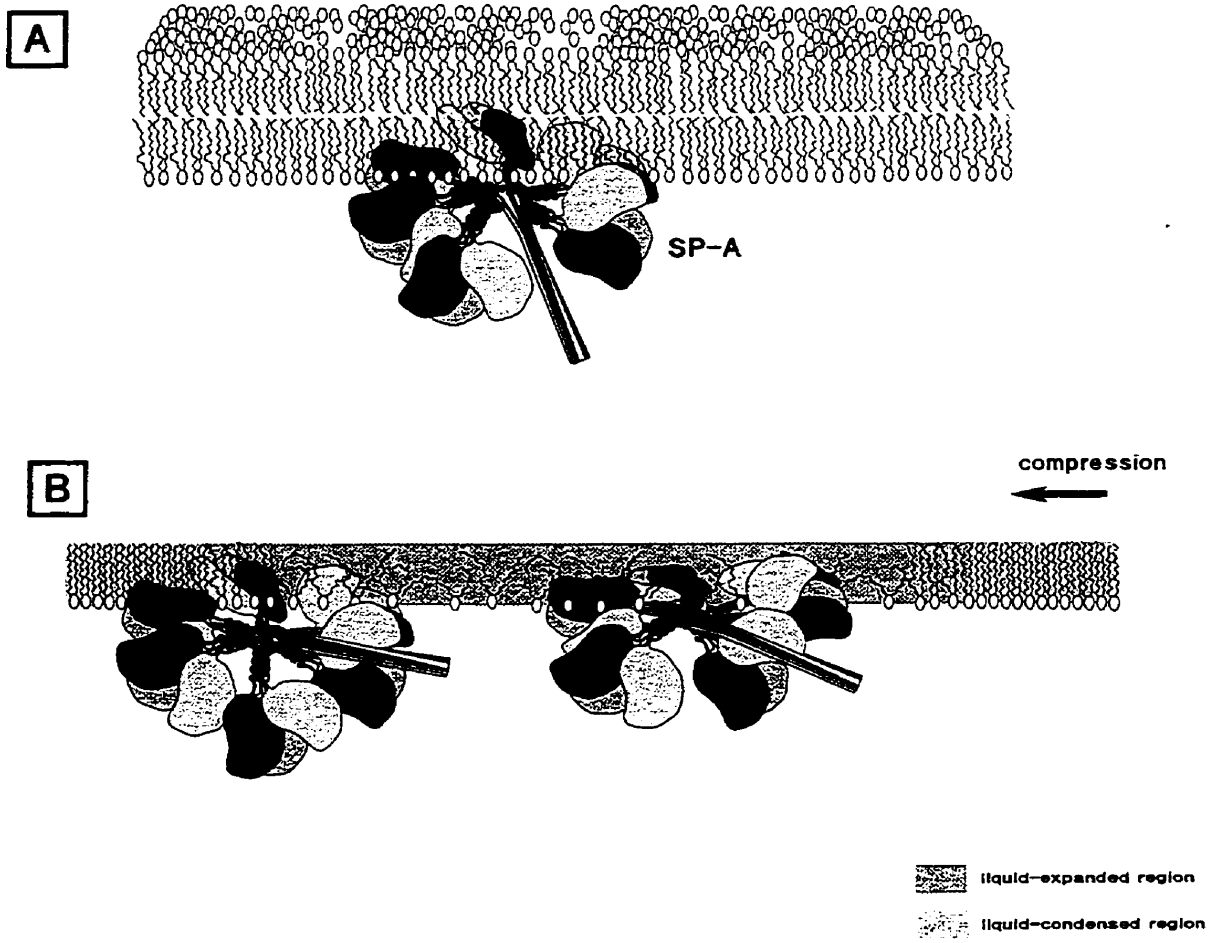
A
SP-A
B
compression
liquid-expanded region
liquid-condensed region

insert in the LE-LC phase boundaries of DPPC films, but not in the completely fluid DOPC films (Bogdam et al., 1994). By fluorescently labelling cytochrome b/c and bacterial antennae proteins others have shown that the proteins non-specifically and slowly adsorbed or penetrated into the fluid phase of phospholipid monolayers (Heckl et al., 1985; Möhwald, 1990; Peschke and Möhwald, 1987). Also recently it was demonstrated by fluorescence microscopy that, insertion of wheat lipid transfer protein into spread DPPG films increased the surface area of the lipid monolayers held at constant π, and insertion was accompanied by an increase in the size of condensed lipid domains (Subirade et al., 1995). Our studies of fluorescent labelled SP-B and SP-C suggested that the hydrophobic proteins were partitioned in the fluid or loosely packed phase of DPPC monolayers (Chapter 6, 8 and 9). These studies of interaction of various proteins with lipid films compared to the one with SP-A would suggest that the interaction and association of SP-A with DPPC in films may have both non-specific (such as adsorption to the fluid phase), and specific (aggregation at the boundaries of the LC phase) components. In the alveoli, SP-A has been found to direct DPPC for uptake by the type-II pneumocytes for subsequent recycling into the secreted material (Kuroki et al., 1996), and such SP-A/DPPC interactions such as those seen here may have some relevance *in vivo*.

The arrangement and distribution of SP-A aggregates surrounding the gel or LC phase of DPPC is somewhat more directed and less punctate than its more random distribution in DPPC:DPPG films (Figure 10.8), or in comparison to the more random appearance of Con A in DPPC films (Figure 10.1c). This indicates the possibility of

some specific interactions of SP-A with DPPC. The protein Con A is also a lectin type glycoprotein having no specific interaction with DPPC, and it tended to arrange in a more random fashion in DPPC films, similar to R-SP-A arrangements in DPPC:DPPG films (compare Figure 10.1c with Figure 10.7, Con A panel). Other proteins have also been seen near or surrounding LC phase boundaries. Specific hydrolysis of DPPC in films by phospholipase A_2 in the subphase has been shown to occur at the boundaries of LE-LC phase (Grainger et al., 1990), the LC phase is hydrolyzed and the enzyme attach to the edges of the condensed (or LC) domains. No binding or hydrolysis of the DPPC films were observed when the D-α-isomer of the lipid was used (Grainger et al., 1990). Specific recognition and formation of two-dimensional domains of biotin-labeled lipid by streptavidin protein have been demonstrated by measuring shifts in π-A isotherms and the binding of the protein to the condensed phase domains (Ahlers et al., 1989). Others however have suggested that the aggregation of fluorescently labelled Con A around the condensed domains of DMPE films is an example of non-specific, lipid-protein interactions (Haas and Möhwald, 1989; Möhwald, 1990; Netz et al., 1996). When small amounts of glycolipid which specifically binds to Con A were included in such films, no aggregation of Con A around the condensed domains was observed, rather the shape of such domains changed (Haas and Möhwald, 1989).

10.43] Significance of lipid binding of SP-A in pulmonary surfactant.

The binding of SP-A to DPPC may have relevance to pulmonary surfactant dynamics. The protein by binding to DPPC may allow for "surface sorting" or specific

adsorption of DPPC to the air-alveolar interface, thereby enriching the surface films with the DPPC (Schürch et al., 1992b). Also specific binding of DPPC, allows for it to be directed to the type-II cells for re-utilization as suggested by others (Kuroki et al., 1996). Since some small amount of SP-A is present in or near films of DPPC at high surface pressure, this may cause enhancement of lipid re-spreading upon film expansion as suggested by others (Taneva et al., 1995). Recent *in vitro* studies have shown that the adsorption of pulmonary surfactant to an air-water interface was inhibited by C-reactive protein (CRP) as this protein specifically binds to phosphatidylcholine (PC) headgroup (McEachren et al., 1995). If SP-A binds to DPPC, it may prevent the inhibitory effects of CRP (or other inhibitory proteins), by specifically protecting the PC molecules from CRP attachment by a competitive process, although this needs yet to be tested. Similarly, removal of inhibitory effects of plasma proteins by SP-A on pulmonary surfactant has been observed *in vivo*, and SP-A has been suggested to play a protective role in pulmonary surfactant activity (Yukitake et al., 1994).

10.44] Effect of SP-A on the phase transition of DPPC.

Earlier studies on SP-A/DPPC interactions by turbidity measurements of suspensions showed that upon SP-A binding to the lipid in presence of calcium, the usual phase transition of DPPC was abolished (King and Macbeth, 1979). Later King et al., (1986) observed from DSC melting curves of SP-A/DMPC, that SP-A shifted the main transition temperature only slightly. They concluded that the interaction of SP-A with the lipid could induce only small perturbation of the bilayer packing of the lipid. Others

have shown using FTIR of deuterated DPPC-d_{62}:DPPG (85:15, mol/mol) suspensions containing high amounts (1:1, lipid:protein, mol/mol) of SP-A that although the effect of the protein on the melting of DPPC was small, the protein ordered the chains of the lipids in the liquid crystalline (fluid) phase (Reilly et al., 1989). Enhanced intrinsic fluorescence observed from tryptophan of SP-A in presence of DPPC but not egg-PC tends to indicate that the protein conformation changed in the presence of gel state lipids (Casals et al., 1993).

Our study indicates that increasing amounts of SP-A slightly decreased the size and amount of condensed phase formed at equivalent surface pressures (Figure 10.6c). These results taken in consideration with the other models proposed in bilayers suggest that SP-A probably "removes" some lipids (by binding them ?) from undergoing their usual disorder-order (expanded - condensed) phase transitions in mono- or bi- layers. This conclusion is further substantiated by the way the SP-A interacted with DPPC:DPPG films. In this system the protein formed large aggregates, and with calcium even larger protein domains (Figure 10.7). Preliminary analysis of the data from this system (not presented here, see Ruano et al., 1997) indicated that there was absolutely no perturbation of the condensed phase packing by SP-A, although R-SP-A could be observed to penetrate such films (Figure 10.7, DPPC:DPPG/R-SP-A panel). This would indicate that SP-A did not affect the expanded to condensed phase transitions of DPPC:DPPG films, since it could not bind the phospholipids in either phase, and thus could not deter them from undergoing transitions from one phase to the other (fluid to condensed).

10.45] Interaction of SP-A with SP-B in DPPC films.

Previous studies on the effect of SP-A on lipid mixing between vesicles suggested that there was increased lipid exchange between vesicle populations containing SP-A, when small amount of SP-B was present in such vesicles (Poulain et al., 1992; 1996). As mentioned, SP-B and SP-A are required for *in vitro* reconstitution of tubular myelin in presence of surfactant lipids and calcium (Poulain et al., 1992; Williams, 1992). Recent studies have suggested that the process of membrane fusion induced by SP-B is enhanced 2-3 fold by the presence of SP-A (Poulain et al., 1996). Others have shown that SP-A-lipid mixtures showed lower adsorptivity compared to mixtures containing small amounts of SP-B in addition to SP-A (Efrati et al., 1987). These studies would tend to indicate that there are possibly additive or "synergistic" effects of SP-A and SP-B on each other (Efrati et al., 1987; Poulain et al., 1992; 1996; Ross et al., 1986). To produce such synergistic effects, the proteins would likely have to interact and be in close proximity in lipid systems, with each other. As seen in our film studies, SP-A and SP-B associated (or interacted) with each other in DPPC films. Individually the proteins associated with the DPPC film phases in one fashion, SP-A with the LC-LE phase boundaries (Figure 10.4a) and SP-B being distributed throughout the LE phase (Figure 9.2), whereas the results here (Figure 10.8) tend to indicate when SP-A and SP-B are present together, a marked attraction or association of the proteins with each other occur in lipid films. The association of the proteins as seen from the fluorescence resonant energy transfer experiments (Figure 10.9) tend to suggest that SP-A and SP-B can form

compact aggregates (green or red patches in Figures 10.8/10.9) in the presence of lipid, so that fluorescence energy transfer between the proteins fluorphores can easily occur. Such association between the proteins may be involved in the transformations seen in pulmonary surfactant during assembly of tubular myelin (Efrati et al., 1987; Poulain et al., 1992; 1996), or in enhancing adsorptivity of pulmonary surfactant lipids.

10.46] Electrostatic interactions of SP-A.

SP-A has been shown to self associate and aggregate under the influence of divalent cations such as calcium (Hawgood, 1992; Ruano et al., 1996). The structure, surface activity and assembly of tubular myelin are strongly dependent on presence of millimolar amounts of calcium ions (Efrati et al., 1987). Also it has been indicated that the *in vitro* reconstitution of tubular-myelin like structures in the absence of calcium was possible when the pH of the medium was lowered from 7 to 4.4, suggesting strong conformational and activity changes of SP-A under different ionic environments (Efrati et al., 1987; Hawgood, 1992). Our studies on lipid-SP-A films under different conditions of pH (Figure 10.4), acidic phospholipid PG and calcium (Figure 10.7) tend to suggest that the interaction and association of the protein with the lipids can be altered by ionic changes of the proteins environment. At a lower pH of 4.5 (Figure 10.4), more SP-A associated with the LE/LC phase boundaries, than occurred at higher pH. With calcium in the subphase and in DPPC:DPPG films the protein probably self aggregated into large domains (Figure 10.7), and such domains may not tend to interact with the phospholipids (The quantitative analysis of these ionic/SP-A systems are to be presented

in Ruano et al., (1997).

The alteration of activity and structure of SP-A under conditions of lower pH have been attributed to the neutralization of the COOH termini of the protein (Efrati et al., 1987), and as our studies suggest this charge neutralization had a profound effect on the association of SP-A with the lipids in films. The large SP-A domains seen in films of DPPC:DPPG films (Figure 10.7), tend to suggest that R-SP-A although adsorbed on to such films, were immiscible with its surrounding lipids. Taneva et al., (1995) have suggested from π-A measurements on DPPC:DPPG/SP-A films, that electrostatic repulsions between SP-A and the acidic DPPG in the film, accounts for the immiscibility of the protein with the lipids. When the charge of the COOH termini of SP-A was neutralized by lowering the pH (Figure 10.7/panel (C)or the films of DPPC:DPPG/SP-A at pH 4.5), the protein associated completely with the fluid phase of the phospholipids.

These film studies of SP-A with phospholipids indicate that there are ionic and probably specific interactions of the protein with the major lipid components of pulmonary surfactant. Also some of the lipid-protein associations presented here may indicate the general arrangement of glycoproteins in lipid matrices as models of biological membrane.

Chapter 11

PORCINE LIPID SURFACTANT EXTRACTS (LSE)

INTRODUCTION

Surface active material of lungs, or pulmonary surfactant (PS), lines the air-alveolar fluid interface, with a surface active monomolecular film and prevents lung collapse at low volumes. The current understanding of the complex lipid-protein material secreted by the type-II pneumocytes is that the material undergoes multiple transformations at the air-alveolar fluid interface. PS is secreted in multi-lamellar (bilayer) form called lamellar bodies (LB) which transform into unusual tube-like structures with bilayer walls called tubular myelin (TM) which are thought to be the precursor of the surface active film. *In vitro* PS shows two specific surface active properties, rapid adsorption to an air-water interface to form surface active films and the reduction of the surface tension of the interface to low values on compression of such films. These two properties are currently the basis of many studies of functional implications of pulmonary surfactant.

PS is normally obtained by lavaging or washing the alveoli and studying the extracted material by centrifugation. Lavaged material from the lungs shows various sub-fractions under centrifugation, varying in their biochemical composition, morphometry and surface activity (see Figure 1.3). Normally three distinct subfractions at 3000-10,000 g, 60,000 g and 100,000 g have been identified (Gross, 1995a; Gross and Naraine, 1989; Magoon et al., 1983; Putz et al., 1994). Analysis of the morphology of each of these subfractions reveal various structural forms such as ones rich in vesicular aggregates, tubular myelin and lamellar bodies (Benson et al., 1984; Williams, 1992; see

sections 1.2 and 1.3 for discussion on these structures). Biochemical analyses of the material indicates different proportions of surfactant lipids and proteins in such subfractions (Gross and Naraine, 1989; Hall et al., 1992; 1994; Knells et al., 1995). The characteristics and properties of the subfractions have helped us to model the structure-function relationship of surfactant components in the alveolar lining and has been termed as the "extracellular metabolism of pulmonary surfactant", to ultimately achieve and maintain surface active films in the alveoli (Gross, 1995a). The lining film undergoes enrichment with DPPC by either selective adsorption of "pools" of secreted materials from the subphase of the film, or by non-DPPC materials being "squeezed out" of the film during successive cycling of the surfactant at the air-alveolar fluid interface or a combination of both processes (Goerke and Clements, 1986; Keough, 1992; Schürch et al., 1992a; 1994; Schürch and Bachofen, 1995). The excluded materials are found as vesicular and other types of aggregates in the alveolar fluid (or the subphase for the films), and some of the excluded materials are probably destined for alveolar type - II cells for recycling (Gross, 1995a; Wright, 1990). Therefor the material extracted from the lungs known as "pulmonary surfactant" may contain various products or remnants of extracellular metabolism and possibly the materials which make up the alveolar film. Although films of surfactant materials have been recently demonstrated to exist in the alveoli (Schürch and Bachofen, 1995), it is not clear to date what the composition of such films are *in vivo* or *in vitro*, and if all or some of the components of PS are involved in maintenance of such films.

Numerous studies exist to date on analysis of films of the material extracted from

the lungs in Langmuir and adsorption balances, bubble surfactometers and captive bubbles, and some of the resultant surface chemistry of the material *in vitro* has been reviewed (Goerke and Clements, 1986; Possmayer, 1991; Keough, 1992). From the information gained from such studies it has been inferred that surfactant films in the alveoli are almost solid-like in density and highly enriched in DPPC (Bangham, 1987). However there are only a few reports in the literature to date on studies of the physical states of such films or their phase properties (Dluhy et al, 1989; King and Clements, 1972b; Träuble, et al., 1974) or extracted whole surfactant in bilayers (Ge et al., 1995; Gulik et al., 1994; Hook et al., 1984; Keough et al., 1985; Mautone et al., 1987; Träuble, 1974; Teubner et al., 1983).

Two decades ago King and Clements, (1972b; 1972c) detected that the compressibility of surfactant films in surface balances change abruptly in a small temperature range. Later some physical properties of surfactant in bilayers determined using fluorescence probe orientations and light scattering indicated, that the material underwent a broad thermotropic phase transition, and that pulmonary surfactant films may also undergo phase transitions at the air-alveolar fluid interface (Keough, 1992; Keough et al., 1985; Träuble, 1974). Later, other studies have indicated that the broad thermotropic transition of surfactant from most mammalian species occurred between 10 - 40°C, and was influenced by certain factors (Keough, 1992). The phase transition of surfactant was influenced by the hydration states (Teubner et al., 1983), unsaturated lipid content (Hook et al., 1984) and calcium (Mautone et al., 1987). These studies also indicated that the thermotropic phase transition of pulmonary surfactant is a diffusely co-

operative chain order-disorder type transition. Such order-disorder phase transition was also detected from surfactant films from infra-red spectroscopic measurements of C-H stretching modes of lipids chains (Dluhy et al., 1989). Recently it was shown that the ordering of the chains and the phase transition of surfactant in bilayers could be influenced by calcium and surfactant protein-A (Ge et al., 1995). Other than an unpublished report (noted in Keough, 1992), some of our previously unpublished observations, recently Hall and co-workers have demonstrated using fluorescence and Brewster angle microcopies, that an expanded to condensed, two-dimensional phase transition in solvent spread calf lipid surfactant extracts (CLSE) films occur with increasing packing of such films (Hall et al., 1995a; 1995b; Kocakova et al., 1996a; 1996b). These workers showed that condensed domains in CLSE films occur at intermediate packing of the films, and by semi-quantitative analysis of the domain structures justified that they are made of mainly DPPC (Discher et al., 1996).

We have studied the various components of pulmonary surfactant in films utilizing fluorescence microscopy (Chapters 3-10). Here we show the phase transitions in spread and adsorbed films of porcine lipid surfactant extracts (LSE) using epifluorescence microscopy of such films. We determined the effects of compression rates, dynamic cycling, calcium ions and surfactant protein - A, on the phase structures of LSE films. We also indicate some specific properties of the phase transition in LSE films which correlate well with our previous studies on simpler surfactant component films.

MATERIALS AND METHODS

Pulmonary surfactant was extracted by broncheo-alveolar lavaging porcine lungs and purified by Dr. Svetla G. Taneva and Mrs. June Stewart in our laboratory by methods discussed in detail elsewhere (Keough et al., 1988). The general procedures were the following. Freshly obtained porcine lungs were lavaged intratracheally with 0.15 M NaCl (4°C). The lavage was centrifuged to remove cell and debris for 10 minutes at 1000 x g, and the supernatant obtained at 20,000 x g for 1 hour to pellet the surfactant. The pelleted surfactant was used to extract the hydrophobic materials using chloroform:methanol:water combinations by the method of Bligh and Dyer (1956). LSE normally contains all the pulmonary surfactant components except the water soluble proteins (i.e. SP-A and SP-D). The extracted material probably contained all the lipids and the hydrophobic protein components of porcine pulmonary surfactant (SP-B and SP-C), and is referred to as the lipid surfactant extract (LSE). The phospholipid content of the LSE was determined using a phosphorous assay of Bartlett, (1959) as modified by Keough and Kariel (1987). Fluorescently labelled SP-A (Texas-Red-SP-A or R-SP-A) was obtained as above (Chapter 10).

The LSE in chloroform:methanol (3:1, vol/vol) was mixed with 1 mol percent of fluorescent phospholipid probe NBD-PC (obtained as above) in the same solvent, based on the phospholipid content of LSE. This was spread on a buffered saline subphase (150 mM NaCl, 5 mM Tris-HCl, pH-6.9, $\pm$ 5 mM calcium), in the epifluorescence microscopic surface balance to form solvent-spread LSE monolayers. Suspensions of the

material formed by vortexing dried LSE films in the same buffer were injected into the modified adsorption balance (discussed in chapter 7), to form the adsorbed LSE monolayers. The solvent spread LSE films were compressed and expanded at an initial rate of 20 (slow) or 707 (fast) $mm^2.sec^{-1}$ in 20 or 50 steps, and compressions were stopped for 1-5 minutes at each of the 20-50 steps for visual observation and recordings. The images were observed, video recorded and analyzed by methods discussed in Appendix A.

Suspension of LSE containing 1 mol% NBD-PC were prepared by drying the chloroform:methanol solutions of LSE (plus probe) in glass vials under a stream of N_2, and vortexing such dried LSE materials in buffer. Adsorption of LSE suspensions was monitored by the fluorescence emission from the monolayers formed at the air-buffer interface in the modified adsorption balance. In some experiments small amounts of fluorescently labelled R-SP-A (0.13 μg/ml final concentration) were dissolved in the subphase buffer and LSE films were solvent-spread on top of this subphase.

RESULTS

The surface pressure - area (π-A) isotherms obtained during dynamic cycling of spread films of lipid surfactant extract (LSE) (top), and the surface pressure - time (π-t) adsorption isotherms of an adsorbed LSE film (bottom) are shown in Figure 11.1. The π-A isotherms indicated that spread LSE film could be compressed to high surface pressure $\sim$ 70 mN/m or a low surface tension of $\sim$1 mN/m over a number of compression cycles. Upon expansion the π of such films dropped to 0 mN/m. The isotherm (top) also indicated that there was a plateau in the compression isotherms at around 45 mN/m. The plateaus persisted for a number of cycles, although their width decreased with increasing numbers of π-A cycles. The difference of area between the compression and expansion part of the cycles or hysteresis, changed with increasing number of cycles. The adsorption isotherm in Figure 11.1 (bottom) was obtained by injecting 70 μg/ml (final concentration) under a buffered subphase in the modified adsorption apparatus (discussed in chapter 7), and by monitoring the surface pressure over time. The adsorption isotherm (bottom in Figure 11.1) indicates that LSE adsorbed rapidly to an air-buffer interface and a equilibrium π of 45 mN/m was reached in a few minutes. These surface properties of LSE were in close agreement with the ones previously reported on pulmonary surfactant extracts from canine (King and Clements, 1972b) or porcine lungs (Keough, 1992).

Typical compression isotherm and images observed from a LSE plus 1 mol% NBD-PC film, performed on a buffered saline subphase (without calcium) are shown in

Figure 11.1 Surface pressure - area per phospholipid molecule (π-A) compression-expansion isotherms of lipid extracts of pulmonary surfactant (LSE) (top), and a surface pressure - time adsorption isotherms of a 0.07 mg/ml LSE suspension to an air-buffered saline interface (bottom).

The π-A isotherms were obtained by dynamically compressing and expanding solvent spread films at a relatively fast rate of 707 $mm^2.sec^{-1}$ on an air-buffer interface at a temperature of 22°C.

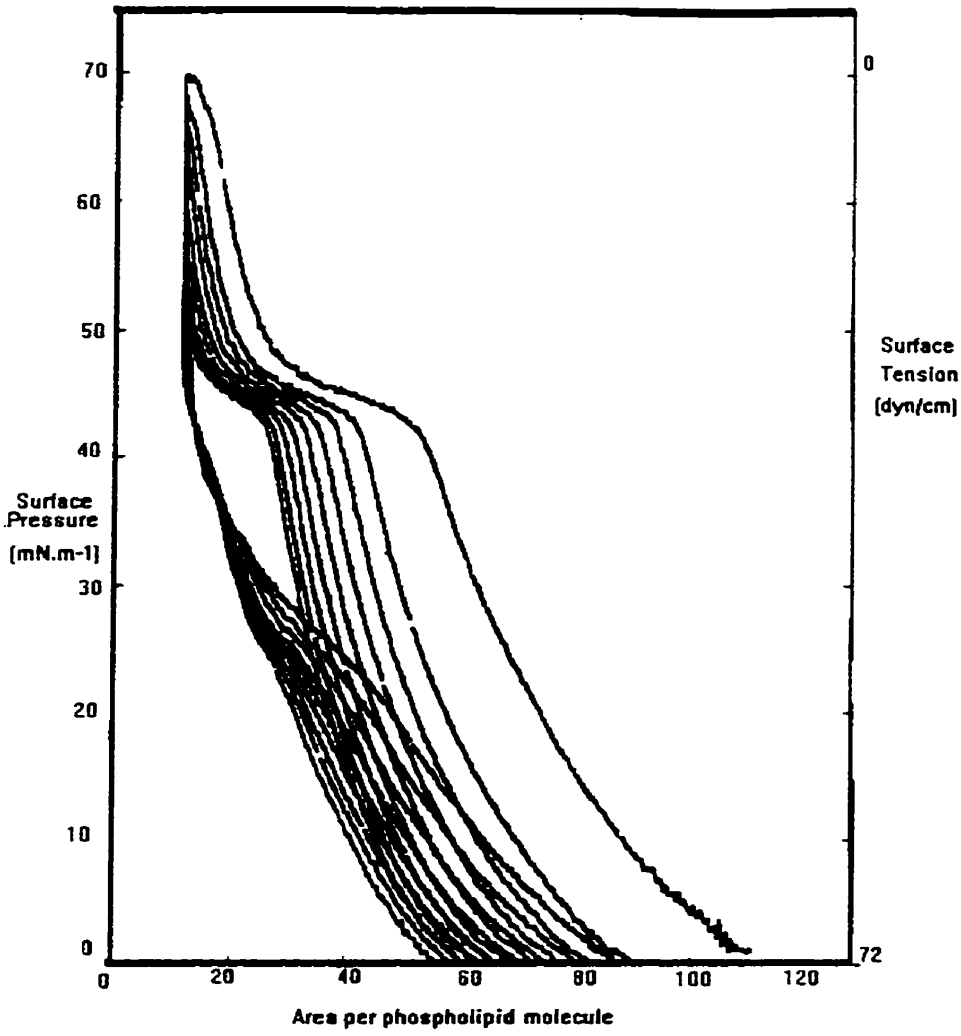
70
60
50
40
30
20
10
0
Surface Pressure (mN.m-1)
0
20
40
60
80
100
120
Area per phospholipid molecule
0
Surface Tension (dyn/cm)
72

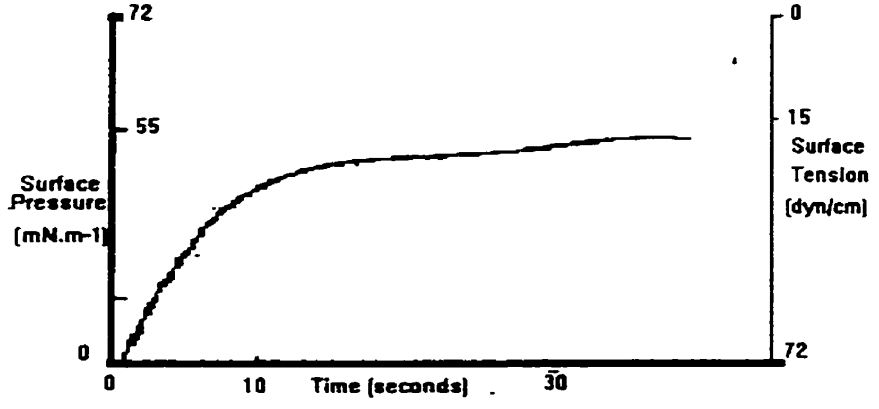
72
55
0
Surface Pressure (mN.m-1)
0
10
Time (seconds)
30
0
15
Surface Tension (dyn/cm)
72

Figure 11.2. The isotherm was obtained by compressing the LSE film at a relatively slow rate, in 50 steps, and a five minute waiting period was introduced between each step, giving a overall compression speed of 0.38 $Å^2$.molecule^{-1}.min^{-1} (based on initial area and phospholipid load). Such a relatively slow speed was chosen to observe any quasi-equilibrium features of condensed domains in such films (such as the typical kidney bean shaped domains of DPPC). The typical images observed after the 5 minute wait period after each step indicated that at low surface pressure of around 5 mN/m the monolayer was homogenously fluorescent (A). The condensed (black or LC phase) domains appeared at π above 13 mN/m grew in size (B and C) with increasing π, and then "decreased" in size at π above 40 mN/m (D). Above the plateau region at 45 mN/m, the condensed domains mostly disappeared and the monolayer fluorescence became heterogenous (E) and appeared to be a meshwork of thin black filamentous regions coexisting with regions of intense fluorescence. The filaments in the mesh-work seemed to be very thin and almost beyond the optical resolution of the camera-microscope combination. Such images as in (E) were also difficult to visually observe and video record, since the heterogeneous distribution of fluorescent probe, decreased the contrast between the black (filamentous) and fluorescent regions.

Some of the images seen at intermediate π in Figure 11.2 (B and C), showed some condensed domains (black regions) which appeared to be kidney bean shaped (see arrow mark in C), as was observed in DPPC films under equilibrium conditions (Flörsheimer and Möhwald, 1989; Nag et al., 1991; Weis and McConnell, 1990 and Figure 2.5). Some of the unusual (visual) features of LSE films, such as appearance and

Figure 11.2 Surface pressure - area per phospholipid isotherm of porcine LSE containing 1 mol % NBD-PC (top) and the typical images obtained from such films at surface pressures indicated by the letters in the isotherms (bottom). The film was spread from organic solvents onto an air-buffer interface (without calcium) at an temperature of 22 ± 2°C.

The films were compressed at a slow rate of 20 $mm^2.sec^{-1}$ in 50 steps, with a 5 minute wait period introduced at each step (the total time for compression of the film was 4.5 hours). The black regions in the images (A-D, bottom) represent the condensed or gel phase and the white the NBD-PC probe containing phase. The scale bar is 25 μm.

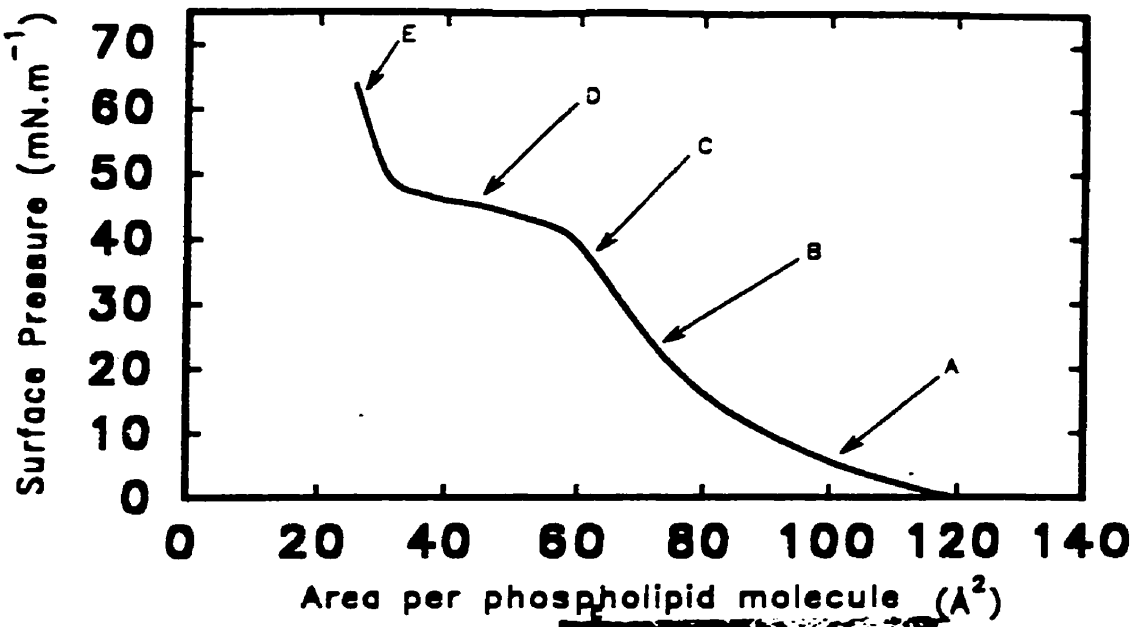
Surface Pressure (mN.m^{-1})
70
60
50
40
30
20
10
0
0
20
40
60
80
100
120
140
Area per phospholipid molecule (Å^2)
E
D
C
B
A

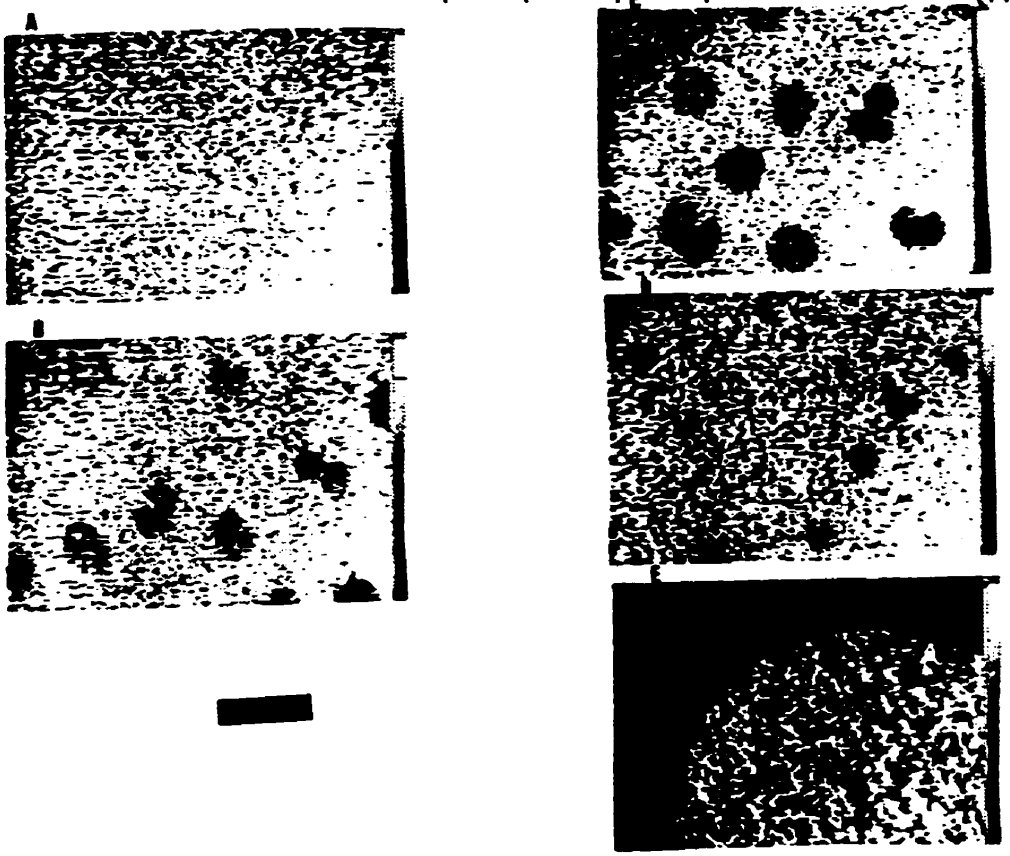
A
B
C

disappearance of condensed domains with increasing π, have also been reported also by others in films of calf lung surfactant extracts (CLSE) studied using fluorescence microscopy and without fluorescent probe by Brewster angle microscopy (Hall et al., 1995a; 1995b; Kocakova et al., 1996a; 1996b). Such features of decreasing size of condensed domains with increasing π were also observed in simple DPPC/DOPC films (Nag and Keough, 1993; chapter 3).

The frequency distributions of condensed domains for relatively fast and slow compression of LSE films are shown in Figure 11.3 (a), and the distribution at a similar surface pressure with images (inset) at that π in (b). The pattern in Figure 11.3 (a) indicated a difference in the frequency distribution of the condensed domains sizes for the rapidly and slowly compressed LSE films. In the film compressed at the faster rate the largest sizes of condensed domains were about 50 square μm^2 at 28 mN/m, whereas in the slowly compressed film at the same π, the maximum size was 100 μm^2. The figure also indicates that in case of the fast compression, greater numbers of smaller domains were formed compared to the slowly compressed films. An example of these properties is displayed in the inset images figure 11.3 (b) which were obtained at a similar π of 29 mN/m. Also, the distribution of the condensed domains in the case of the fast compression was less dispersed at all π compared to those of slowly compressed films. The patterns indicate that the frequency and size of condensed domains in LSE films are controlled by the rates of compression of the films, with kinetic factors probably controlling the nucleation, size and distribution of such domains. A similar pattern of the effect of compression rate on domain size and frequency has been

Figure 11.3 Frequency distribution of sizes of condensed (black) domains seen in LSE films compressed at relatively fast (left panel) and slow (right panel) rates (a); and the typical frequency distribution from these films at a π of 29 mN/m with inset images observed at that π (b), the top panel from fast and the bottom from slowly compressed films. The frequency distribution of size of condensed domains were obtained by analyzing 10 randomly selected images at π indicated on top of the plots.

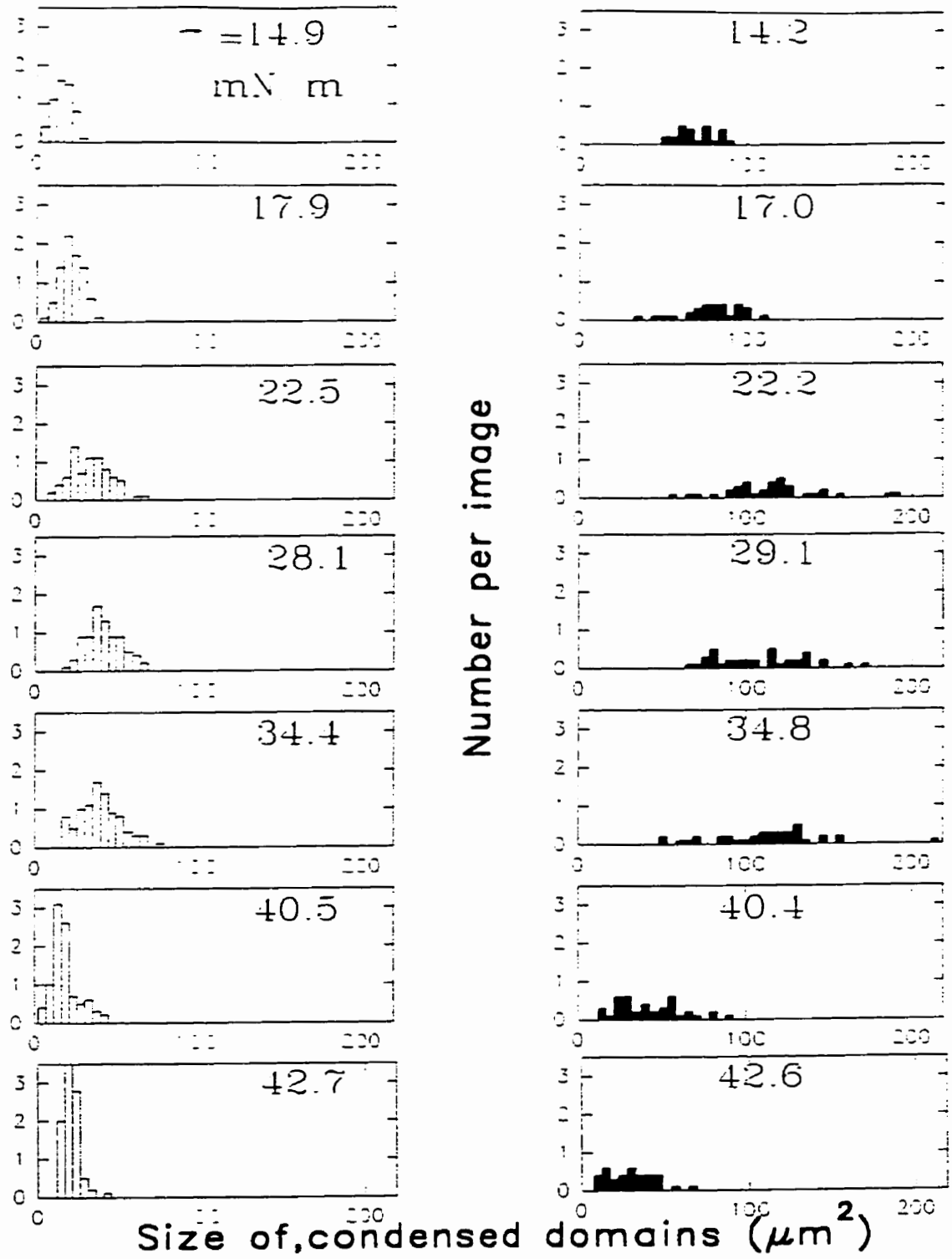
π =14.9
mN m
14.2
17.9
17.0
22.5
22.2
28.1
29.1
34.4
34.8
40.5
40.4
42.7
42.6
Number per image
Size of condensed domains (μm²)

277a

(a)

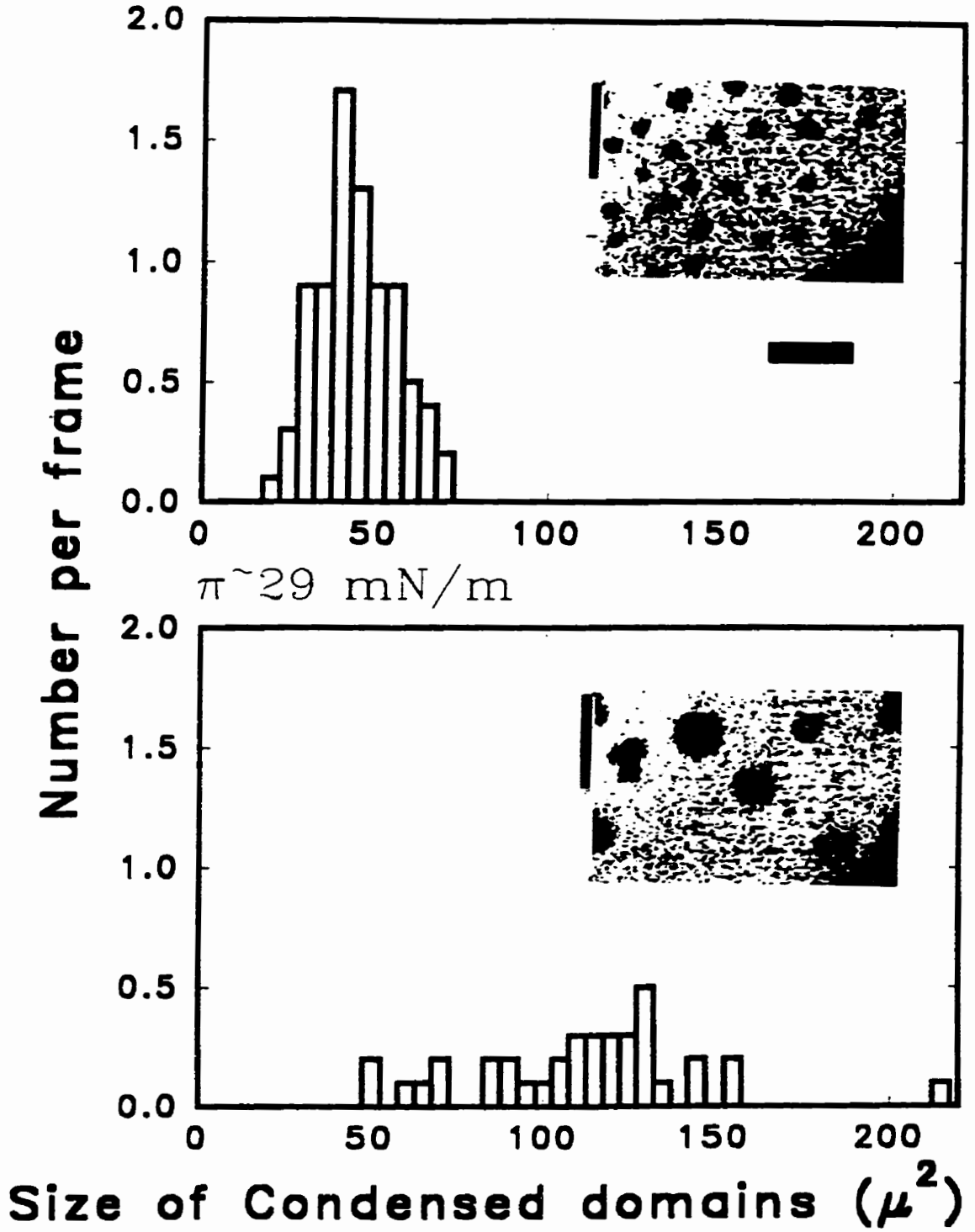
2.0
1.5
1.0
0.5
0.0
0
50
100
150
200
π~29 mN/m
Number per frame
Size of Condensed domains (μ²)

277b

(b)

previously observed by us in films of DPPC compressed at different rates (Nag et al., 1991). Some of the condensed domains in LSE films had typical kidney bean shapes as seen in films of DPPC, suggesting that such domains were made of or enriched with that lipid.

Figure 11.4. shows the average size (A), number (B) and total amount of black or condensed phase (C) plotted as a function of π, for LSE films compressed at slow and fast rates. The domain sizes are larger and their numbers lower in the films compressed at the slow rate compared to the fast, whereas the total amount of the condensed or black (C) phase is not significantly different in the two systems with different compression conditions. This may indicate that the condensed regions in LSE films are a particular phase formed due to the process of phase transition (say from fluid to gel-like states) since the process is independent of the conditions used to transit from one phase to the other. The other interesting feature of the LSE films phase transition is that the condensed phase decreased at π above 30 mN/m, a phenomenon previously observed in simple films of DPPC with DOPC (Chapter 3). We had previously explained this process in the DPPC/DOPC films as an effect of the probe on the lipids phase transition. In light of the recent studies on calf LSE films by Hall and co-workers (Hall et al., 1995a; 1995b; Discher et al., 1996), using Brewster angle microscopy (which does not require fluorescent probes), which reported that a similar decrease of condensed phase with increasing π above a critical value occurred, we speculate that there may be a second phase change occurring in LSE films at π above 30 mN/m. This phase transition may be of a type where the condensed phase (black regions) merges into a

Figure 11.4 Average area (A), number (B) and the total amounts (C) of condensed (black) domains in films of LSE plotted as a function of surface pressure for the relatively slowly (open symbols) and fast (closed symbols) compressed systems as in Figure 11.3. The data were obtained by analyzing 10 randomly selected frames at each π. The error bars indicate $\pm$ one standard deviation.

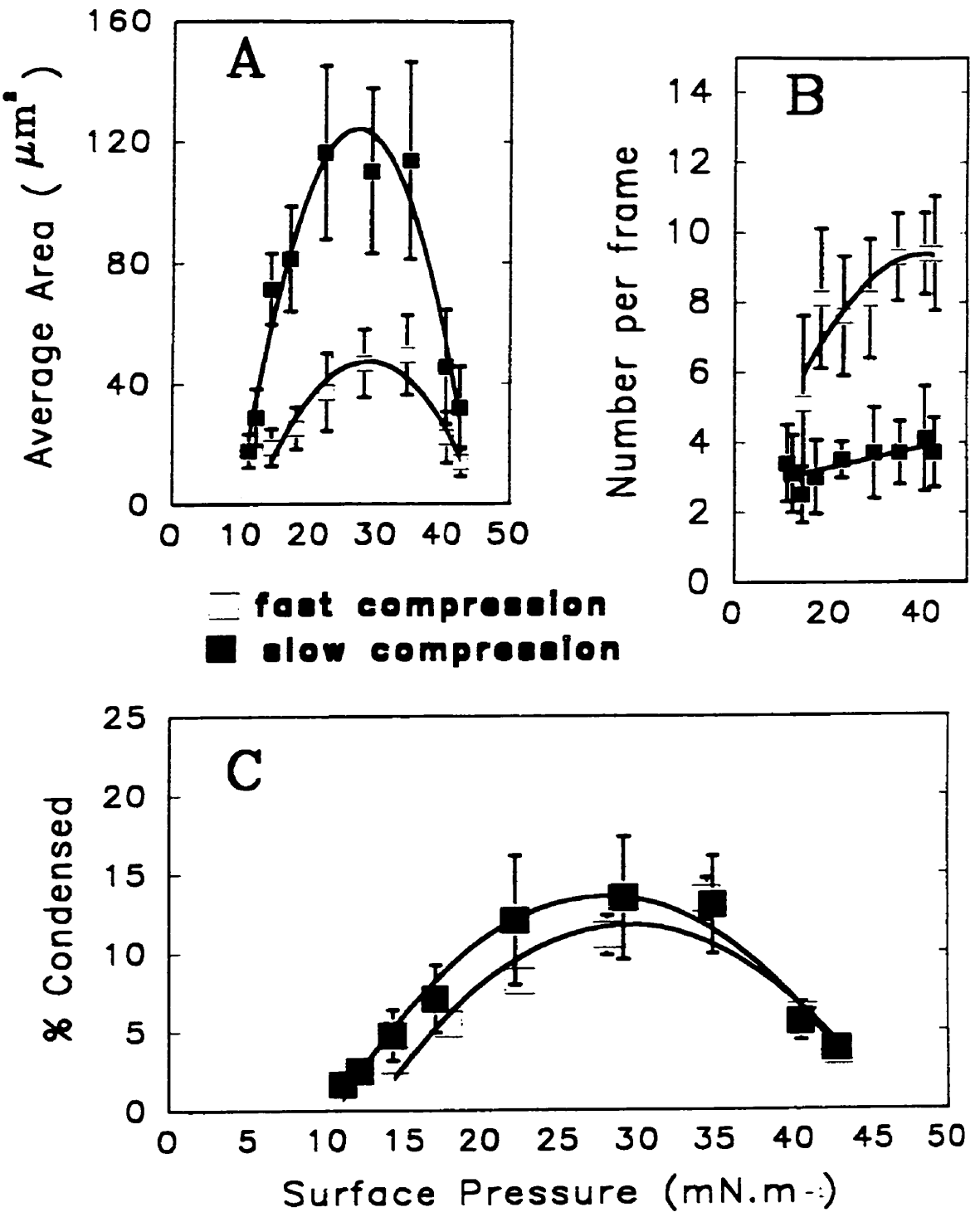
A
B
C
Average Area (μm²)
Number per frame
% Condensed
Surface Pressure (mN.m⁻¹)
fast compression
slow compression
0
40
80
120
160
0 10 20 30 40 50
2
4
6
8
10
12
14
0 20 40
5
15
20
25
0 5 10 15 20 25 30 35 40 45 50

more solid-like phase, and the solid-like phase increases with increase in π at the expense of the condensed phase. The images at π above 50 mN/m (Figure 11.2) would tend to indicate that the solid-like phase of LSE film was made of filamentous domain meshwork, and the probe was excluded from this phase into small regionalized aggregates distributed heterogeneously in the films.

The typical π-A isotherm of a LSE film dynamically compressed and expanded eleven times, spread at a initial π of 35 mN/m (top), and the typical images seen in the first and eleventh compression (bottom) are shown in Figure 11.5 (a). The data on number (A), size (B) and total amount (C) of condensed domains, plotted as a function of π from the first and the eleventh compression are shown in Figure 11.5 (b). The images in 11.5 (a) indicate that the distribution of the domains are different in the eleventh cycle compared to the first. The total amount, size and number of domains are also increased at equivalent π during the eleventh compression compared to the first. The amount of condensed phase in the eleventh compression is about 5 % higher than that seen in the first compression. This indicates that the amount of the material forming the black or condensed domains in LSE films is increased, or that the film in the eleventh cycle is enriched in the component which forms black domains in such films. It is possible that some of the components are irreversibly lost from the surface film, a process termed as "squeeze out", with the materials which are lost from the film being ones which do not form condensed domains. These results support our previous assumptions that fluidizing lipids (Chapter 3, 5) and protein components (Chapter 9) may be squeezed out of pulmonary surfactant films, eventually refining and enriching the

Figure 11.5 Typical π-A isotherms of a LSE film compressed and expanded 11 times (top) (at a rate of 20 $mm^2.sec^{-1}$ for the first and 11^{th} cycle and 707 $mm^2.sec^{-1}$ for the cycles in between) and the typical images observed in the first and the eleventh cycle at a similar π (bottom) (a); and the size (A); number (B) and total amount (C) of condensed phase estimated from a first (open symbol) and the 11^{th} compression (closed symbols) of LSE films (b). Scale barin (a) is 25 μm. The standard deviations are for 10 randomly selected images analyzed images at each π. [Similar dynamic compression-expansion cycling was performed for DPPC/DOPC films to monitor irreversible squeeze-out of materials from such films, and was discussed above in section 3.3 and 3.43]

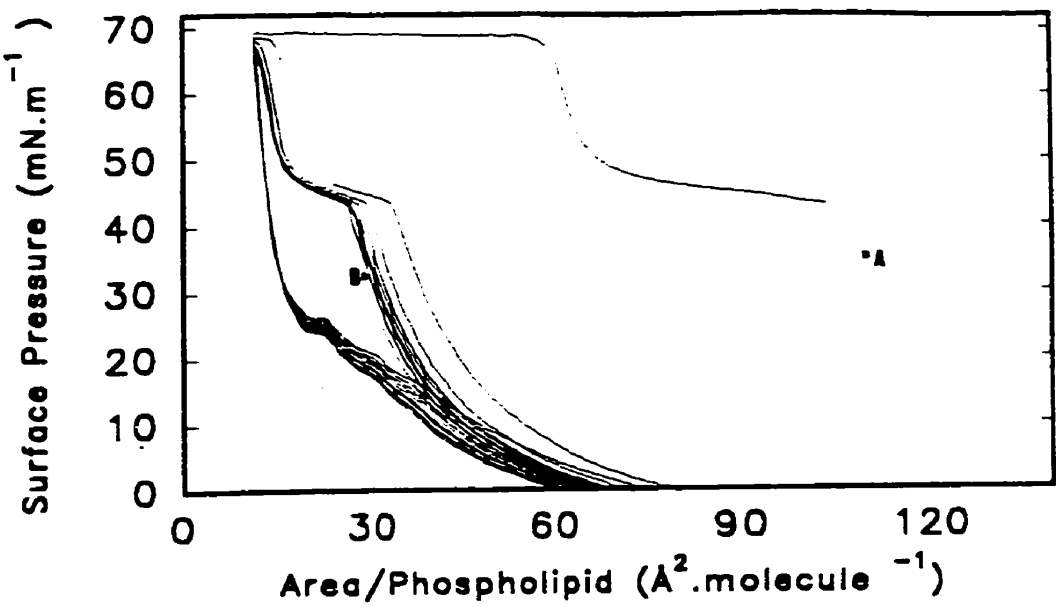
Surface Pressure (mN.m^{-1})
70
60
50
40
30
20
10
0
0
30
60
90
120
Area/Phospholipid (Å^2.molecule^{-1})
A
B

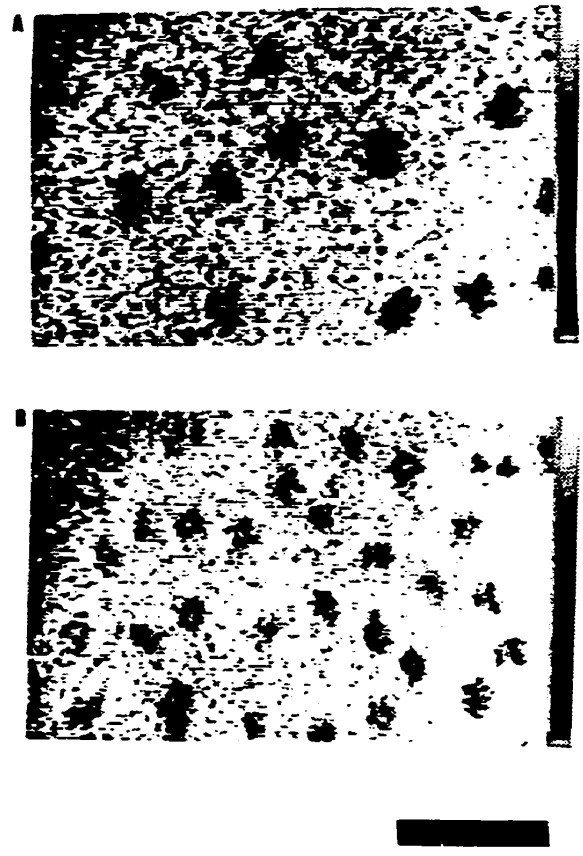
A
B

(a)

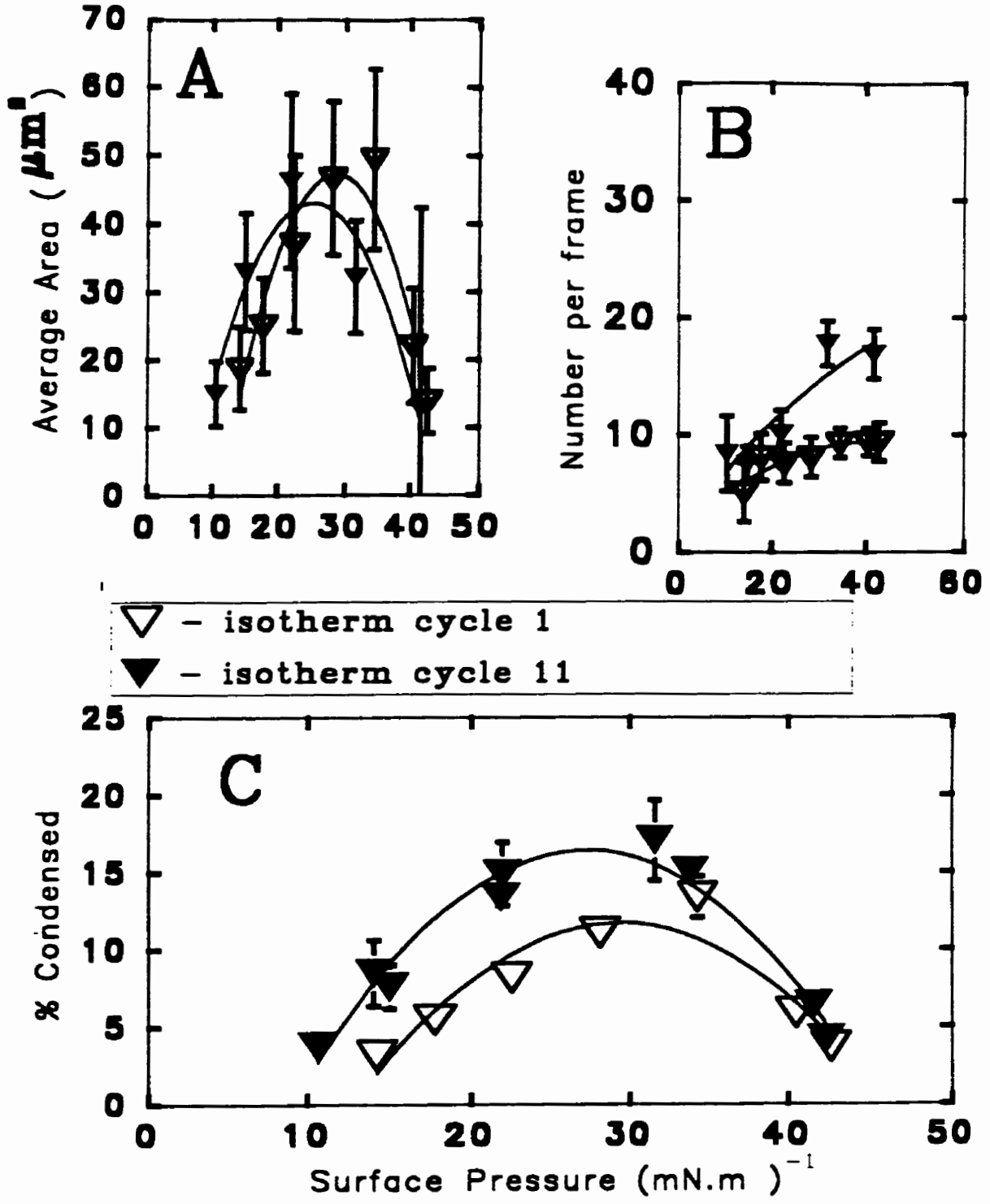
A
Average Area (μm^2)
70
60
50
40
30
20
10
0
0 10 20 30 40 50
B
Number per frame
40
30
20
10
0
0 20 40 60
▽ – isotherm cycle 1
▼ – isotherm cycle 11
C
% Condensed
25
20
15
10
5
0
0 10 20 30 40 50
Surface Pressure (mN.m)$^{-1}$

(b)

films with DPPC.

The slowly compressed π-A isotherms of a LSE film containing 1 mol % NBD-PC on a buffered subphase containing 5 mM calcium and the typical images observed in such films are shown in Figure 11.6(a). The number (A), size (B) and amount (C) of condensed domains in such a film plotted as a function of π, compared to the ones without calcium under similar conditions are shown in Figure 6 (b). Although the isotherm of the LSE film in Figure 11.6 (a) is not significantly different than the one without calcium (Figure 11.2, top), the images, especially those at π above 40 mN/m were quite different from those seen in the films without calcium (Figure 11.2, bottom). The visual features at π above 40 mN/m in the films in the presence of calcium, had bright circular regions or fluorescent (white) domains dispersed in a background of grey phases. These white regions or domains also had small black spots in the centre (image E in Figure 11.6 (a)). Such domains or fluorescent regions may be a separate phase induced by calcium in LSE films, and indicate that there may be an altered packing of the lipids and proteins under such induction. Although above π of 45 mN/m, the total amounts (Figure 11.6 (b), C) of the dark domains decreased, their numbers (B) and average size (B) were increased drastically at all π in the films containing calcium compared to the ones without. At a π of 40 - 45 mN/m, the amount of condensed phase in LSE films with calcium is about double the amount in the ones without calcium. Eventually at high π ($>$ 45 mN/m) the total amount of condensed phase decreased in the films with calcium. This fact indicated that calcium increased the condensed phase or condensation in LSE films, as was observed previously in simple films of DPPC/DPPG

Figure 11.6 Typical π-A isotherms of LSE films on a buffer subphase containing 5 mM calcium (top), compressed at a relatively slow rate as in Figure 11.2, and the typical images observed (bottom) in such films at π indicated by letters in the isotherms (a); and the size (A), number (B) and total amount (C) of the condensed (black) phase observed in such films (b). Scale bar for the images in (a) is 25 μm.

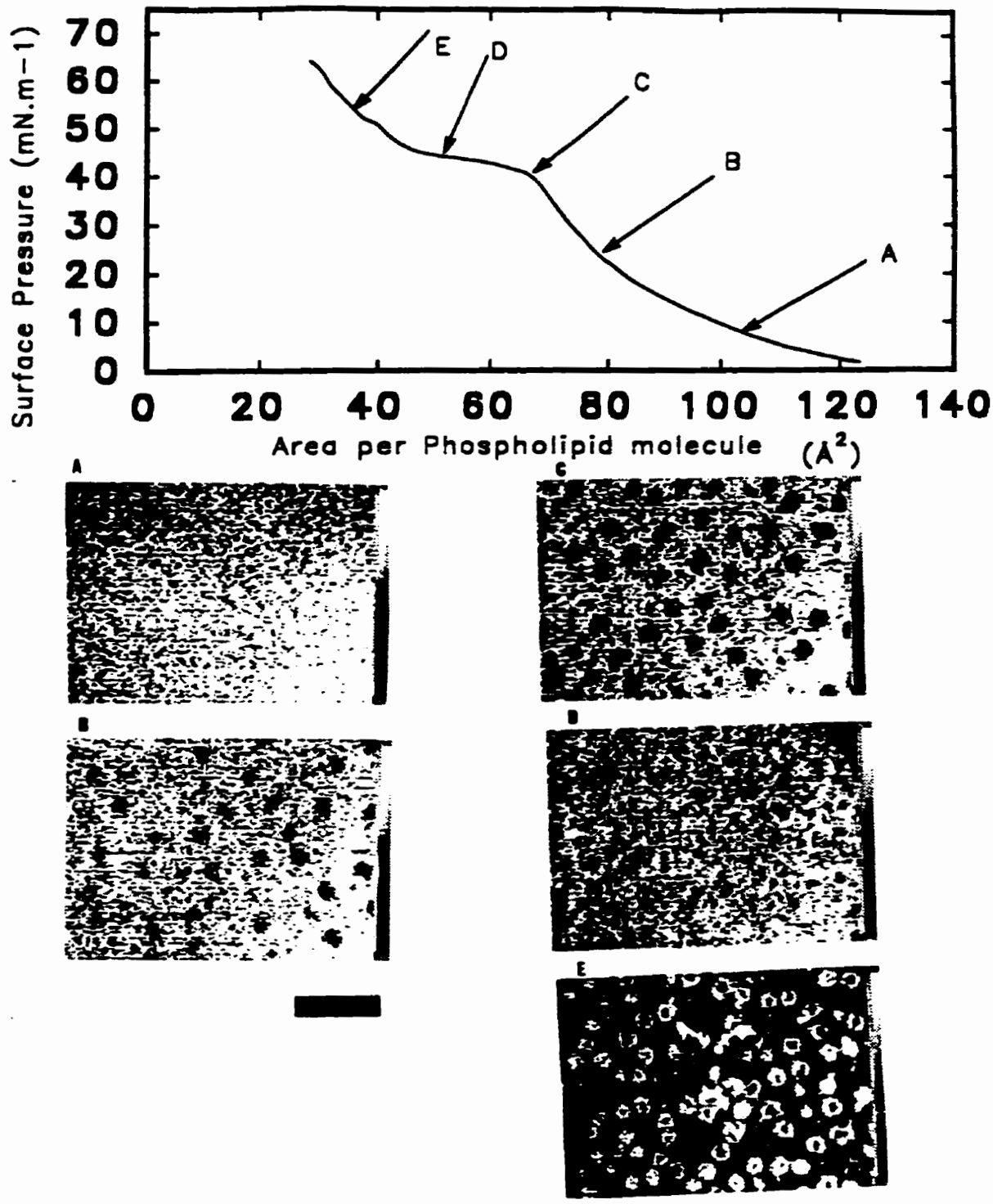
Surface Pressure (mN.m-1)
70
60
50
40
30
20
10
0
E
D
C
B
A
0
20
40
60
80
100
120
140
Area per Phospholipid molecule (Å²)
A
C
B
B
E

(a)

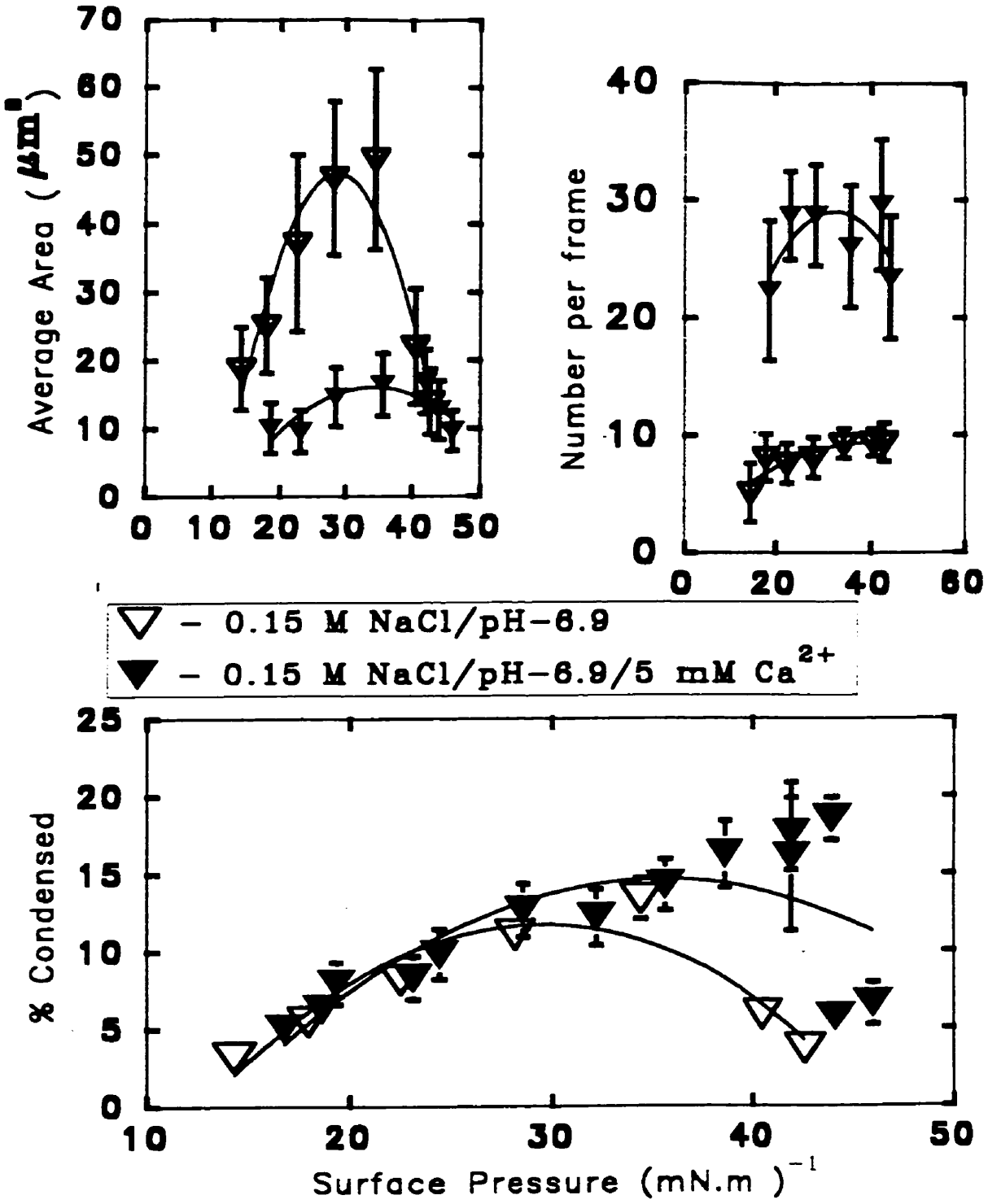
Average Area (μm^2)
Number per frame
▽ – 0.15 M NaCl/pH–6.9
▼ – 0.15 M NaCl/pH–6.9/5 mM Ca^{2+}
% Condensed
Surface Pressure (mN.m)$^{-1}$

(b)

(Chapter 4). The increased ordering in LSE films induced by calcium seemed also to somewhat increase the upper limit of π at which such condensed domains were observed. As discussed earlier (Chapter 4), calcium probably bound the acidic lipid headgroups of LSE lipids, and increased the condensation of such films or increased the amount of the dark phase domains.

Typical isotherms and images of adsorbed LSE films formed by injecting LSE suspensions containing 1 mol% of fluorescent probe, under air-buffer interface are shown in Figure 11.7. The isotherm in Figure 11.7 (top) is from the adsorbed film where higher amounts (0.06 μg/ml) of LSE suspension were injected and the one in the bottom from a film where a ten fold lower concentration of LSE suspension (0.006μg/ml) was injected. The material when injected under a buffered subphase at the higher concentration (top) increased the surface pressure of the air-buffer interface in a few seconds to 45 mN/m. The images observed at 45 mN/m from the adsorbed LSE films, showed a grey phase with regions of aggregated probe (Figure 11.7, A). When injected at the lower concentration of 0.006 mg/ml (bottom) the surface pressure increased slowly to 10 mN/m after 15 minutes, and the adsorbed films had the appearance of an almost homogenous fluid phase (B). In this system (bottom) the surface pressure reached about 15 mN/m after 30 minutes, and condensed domains appeared (C) in the field of view. Such domains increased in number and size (D and E) over a 2 hour period of further adsorption. These observations suggested that the process of an expanded to condensed phase transition seen in spread LSE films with compression (Figure 11.2) also occurred in adsorbed films formed from LSE suspensions as a function of increasing amount of

Figure 11.7. Typical π-t isotherms and images of LSE + 1 mol % of NBD-PC adsorbed films formed by injecting different amounts of LSE suspensions under the air-buffer interface (0.06 μg/ml; top, and 0.006 μg/ml; bottom). A smaller amount of LSE suspension was injected under the buffer (bottom), to obtain a slowly adsorbing film in which the fluid to condensed transition could be observed. The arrows indicate the surface pressures at which the images were obtained. The scale bar is 25 μm.

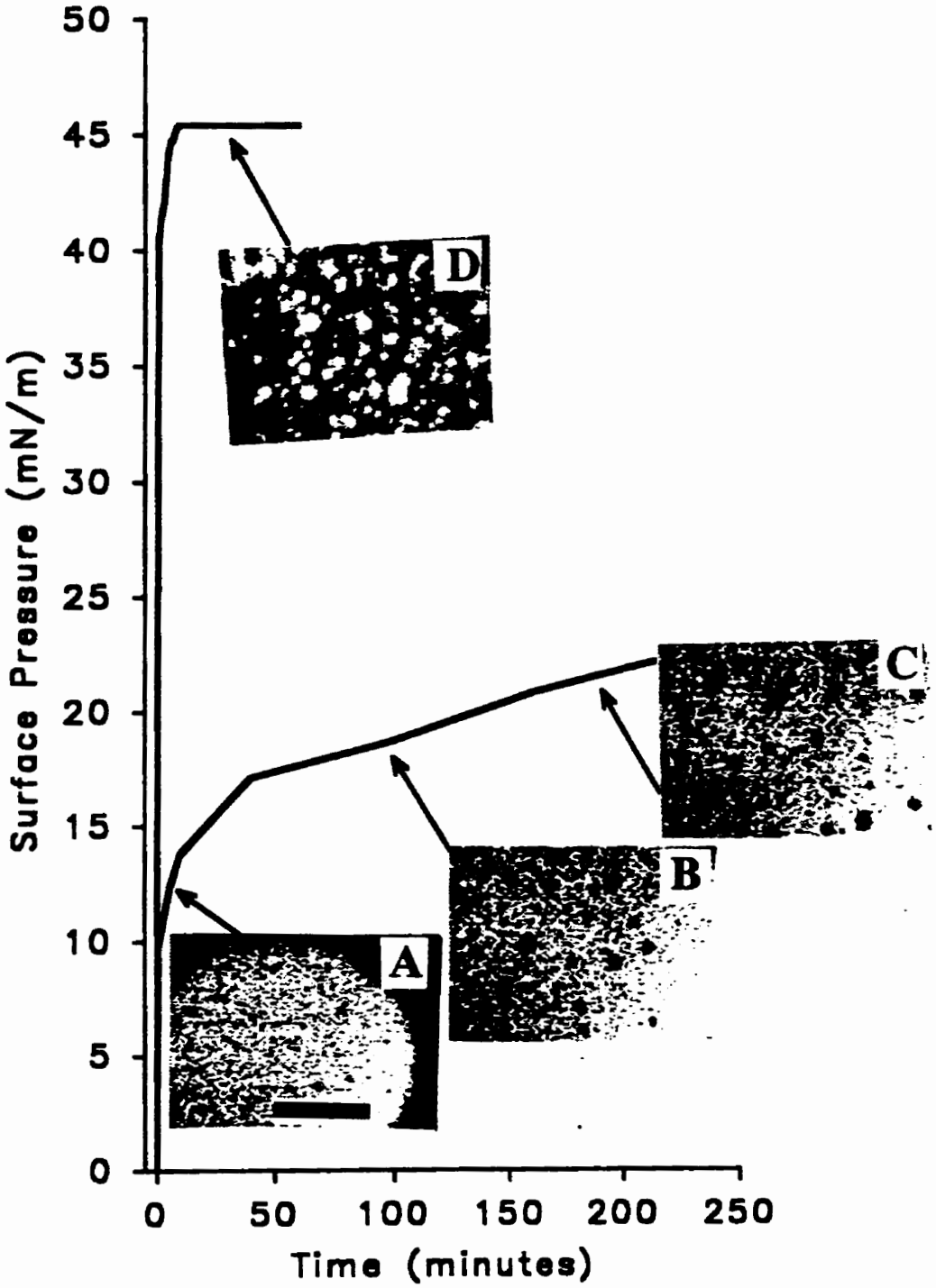
Surface Pressure (mN/m)
50
45
40
35
30
25
20
15
10
5
0
0
50
100
150
200
250
Time (minutes)
A
B
C
D

materials adsorbing into such films with time. The similarity of structures seen in the adsorbed and spread LSE films indicated that both types of films may be equivalent at similar packing densities or π, as seen previously for films of simple mixtures of components of pulmonary surfactant (Chapter 7).

Films of LSE were solvent spread and compressed on top of a buffered subphase containing fluorescent labelled R-SP-A, to observe any effect of the protein on such spread LSE films. The typical images observed in such spread LSE films at a π of 35 mN/m (with subphase containing 0.13 μg/ml of fluorescently labelled SP-A; methodology discussed in chapter 10) are shown in Figure 11.8. The images on the top panel are without and the bottom with 2 mM calcium. The images in the left were observed from the fluorescence of NBD-PC and the ones in the right from the fluorescence of R-SP-A. The images indicated that the distribution of condensed domains in the LSE films were modified in the presence of R-SP-A, and that the condensed domains were aggregated compared to the ones without the protein (Figure 11.2). The images in the right panel (B/B'), observed from the fluorescence of the protein (R-SP-A), indicated that SP-A also adsorbed into or was present very near the LSE films, and in case of the films containing calcium, that R-SP-A aggregated into large domains (Figure 11.8, bottom right image). Visual observations of such films ($\pm$ calcium) at high π, by switching the optical filters very quickly to observe the same field of view from lipid probe and R-SP-A fluorescence, indicated that the aggregated condensed domains of LSE had R-SP-A located in such aggregates. These results indicate that R-SP-A had interactions with LSE films and associated with the condensed domains (somewhat differently) as seen in some

Figure 11.8 Typical images observed in solvent spread LSE (+ 1 mol % NBD-PC) films containing 0.13 μg/ml R-SP-A on the buffered subphase without (top panel) and with 5 mM calcium (bottom panel), at a π of 35 mN/m. The images in the left (A, A′) were observed from the fluorescence of NBD-PC and the right from R-SP-A (B, B′). The scale bar is 25 μm.

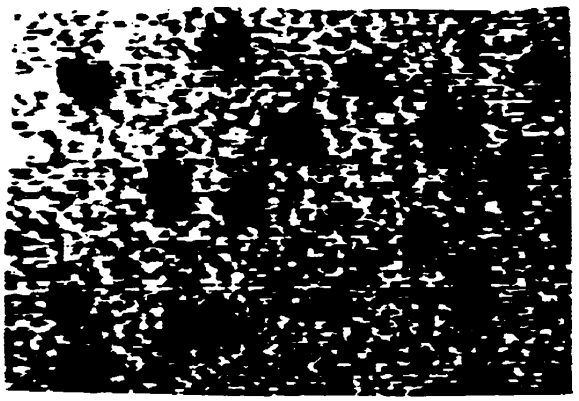

A

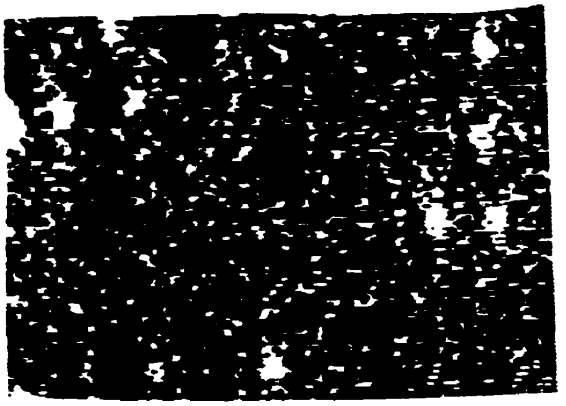

B

A′

B′

of the simpler systems of pulmonary surfactant components (Chapter 10).

11.41] Condensed domains in LSE are made of mainly DPPC.

From early studies on the thermotropic phase transitions of pulmonary surfactant or its lipid extracts (LSE), it was proposed that the principle component of the surfactant responsible for an ordered to fluid transition during heating was DPPC (Träuble et al., 1974). Others have detected by changing the temperature of canine surfactant films, that the "squeeze-out" plateau and surface compressibility changed abruptly over a temperature range of 30-35°C (King and Clements, 1972b). Electron paramagnetic resonance (EPR) studies of rabbit surfactant suspensions have indicated that the material is fluid at room temperature, and the fluidity was due to the presence of a significant amount of unsaturated lipids (Hook et al., 1984). Others have indicated by DSC measurements of rabbit surfactant suspensions that the material is partly fluid at 37°C and not very fluid at room temperature (Keough et al., 1985). Dluhy et al. (1989), using infrared spectroscopy of surfactant suspensions and films have indicated that a continuous decrease of the CH_2 stretching frequency of the C-C bonds of the acyl chains of surfactant lipids occurred with increased packing of such films, and that in highly compressed bovine surfactant films, most of such chains were in all *trans* configuration. The ordered or condensed domains observed in the porcine LSE films studied here support these observations, that a fluid to ordered transition occurs in pulmonary surfactant films with increasing packing or compression. The kidney shape of some of the condensed (dark) domains in the LSE films observed when the films were compressed

at quasi-equilibrium conditions (slowly), would tend to indicate that such domains are probably enriched in, or made of, DPPC. Recent calculations performed on the amounts of condensed phase in spread films of calf lung surfactant indicate there is a direct proportionality of the amount of DPPC present in surfactant with the highest amount of condensed phase found in such films (Hall et al., 1995a; Korcakova et al., 1996; Discher et al., 1996). The decrease in total amounts of condensed domains at higher pressures can also be due to disintegration of such domains in either sub-micron structures which are not detectable by optical microscopy. The images observed at π above 50 mN/m in LSE films also tend to indicate that fine filamentous structures exist which are barely visible through fluorescence microscopy. This may indicate that possibly the condensed domains may undergo some form of transition to more filamentous sub-micron range phases, not detectable by optical microscopy (Hwang et al., 1995).

There are also significant differences between the phase properties of LSE and DPPC films. At higher surface pressures in LSE films, the appearance of heterogenous irregular probe distribution (Figure 11.2) and the decrease of observable condensed phase (Figure 11.3, C) would indicate that the phase transitions in LSE films are not a simple liquid expanded (LE) to liquid condensed (LC) change as seen in films of pure DPPC. Also the appearance of condensed domains in LSE films at a higher $\pi \sim$ 11-15 mN/m (Figure 11.4) indicates that such films are more fluid than DPPC at equivalent π. Some of the features such as the appearance and disappearance of condensed domains in LSE films with increase in π, show that LSE films behave more like simple lipid mixtures (DPPC/DOPC) compared to films of pure DPPC. Also, since calcium increased the

amount of condensed phase in LSE films compared to those without the cation at equivalent π, this indicated that the LSE condensed domains or at least some of them contained acidic lipids, as also seen in films of DPPC/DPPG (Chapter 4). The increased fluidity of the LSE films at all packing densities compared to DPPC films, can be understood as the effect of unsaturated lipids, cholesterol, and the hydrophobic proteins SP-B/SP-C on DPPC film packing, since all these components are present in LSE and perturb the packing of the DPPC in such films (Chapters 3-9). Hall and co-workers have suggested that the condensed domains in films of lipids of calf lung surfactant (without SP-B and SP-C) are larger than the ones observed in the CLSE films at similar π, and also suggested that the amount of cholesterol or neutral lipids of surfactant may be the main deciding factor controlling the size and amounts of condensed domains (and thus the fluidity) of lung surfactant films (Hall et al., 1995a).

The functional significance of condensed domains in pulmonary surfactant *in vitro* is not clear, but an interesting proposition has been put forward by Bangham, (1987) (see also Keough, 1992). This proposition is based on the observations that the surfactant film in the lung alveoli are almost made of condensed or "solid lipids" or DPPC. Such films can have regions or "solid islands" existing in a "sea" of fluid lipids (Bangham, 1987). The solid lipid regions act as small "splints" in the alveolar wall, and prevent them from collapsing with decreasing alveolar wall area or volume (Bangham, 1987; Keough, 1992). Such splinting would occur if each of the alveoli is assumed as a "geodesic dome" or a dodecahedron (Kimmel and Budiansky, 1991) or the inside surface made of many small flat surfaces, where each side of the alveolar wall would provide a

surface on which such splints reside (Keough, 1992; Bangham, 1987). Whether the condensed domains in LSE films can fulfil the properties of such splints *in situ* in the alveoli may be too speculative from this *in vitro* study, but the existence of condensed domains of micrometer size in pulmonary surfactant films, may open up new possibilities in modelling pulmonary surfactant at the air-alveolar fluid interface.

11.42] Fluidity of LSE films and squeeze out.

The pressure - area dynamic cycling of LSE films (Figure 11.5) and the decrease of condensed phase with higher π (Figure 11.4), would indicate that the effects of fluidizing lipids and probably proteins on such films are quite profound. Since we have reported earlier that in films of simple DPPC/DOPC mixtures (Chapter 3) that the condensed phase decreased in such films at high π, it seems that the LSE films are also influenced by its fluid components. Upon dynamic compression and expansion some of the fluid components were probably squeezed out or irreversibly lost from the films, enriching the LSE films with DPPC (as also seen in films of DPPC/DOPC, Chapter 3). As shown in Figure 11.5, there was a small (5%) but probably significant increase in the amounts of condensed phase in the eleventh cycle compared to the first, and the appearance of the black domains occurred at a lower π (10 mN/m) in the eleventh cycle compared to the first. These factors tend to indicate that the film was enriched by DPPC possibly by about 5%. Since the number of condensed domains were also increased in such films in the eleventh cycle (Figure 11.5, B), the enrichment of DPPC probably occurred in the eleventh cycle with increasing DPPC rich areas or nucleations compared

to the first cycle. The difference of the amounts of condensed phase seen between the first and eleventh cycle was not very prominent, since LSE films probably contained other components which were not irreversibly lost during compression, but were rapidly re-adsorbed back into the films upon expansion. These components could be the hydrophobic surfactant proteins SP-B and SP-C, which were found to remain in films on high compressions and after number of cycles in the simpler surfactant component film studies (Chapter 8 and 9). Also the dynamically cycled films of LSE studied here were solvent spread (and did not allow for selective insertion from a subphase pool) and did not contain SP-A, and thus may not reflect the exact properties of lung surfactant films in the alveoli, and some of the processes such as selective enrichment as may occur *in situ*.

In the lungs the surface tension of the air-alveolar fluid interface is near 0 mN/m (Schürch et al., 1976), and probably the only component of surfactant which can reach such low values upon compression was indicated to be DPPC (Goerke and Clements, 1986; Keough, 1992; Possmayer, 1991). Later detailed theoretical and experimental studies *in vitro* on surface activity of pulmonary surfactant have indicated that the material near an air-water interface showed a rich variety of complex phenomena, such as molecular adsorption-desorption, squeeze-out, spreading-re-spreading, a combination of one or all these processes is involved in achieving lung stability in situ (Otis et al., 1994; Scarpelli and Mautone, 1994; Yu and Possmayer, 1993). In excised rabbit lungs, measurements indicated that the alveolar geometry, pressure-volume (P-V) and surface tension-volume (γ-V) characteristics showed

hysteresis loops (Bachofen et al., 1987; Pattle, 1977; Schürch et al., 1985) indicating that probably some of the surface pressure - area characteristics of surfactant films contribute to these phenomena. Upon dynamic cycling of rat surfactant adsorbed films in captive bubbles, it was shown that after a few cycles of compression-expansion of the material, the π-A hysteresis became negligible, and the surface tension, collapse rates and compressibility were decreased (Schürch et al., 1992a). These and other studies of dynamic cycling of pulmonary surfactant have suggested that the surface films are enriched by DPPC, and the enrichment probably occurred by loss of low surface activity components (Gross, 1995a; Gross and Naraine, 1989) or selective adsorption of higher surface active component such as DPPC (Schürch, 1992; 1994). Similarly in this study the LSE films were somewhat enriched by a more surface active component, possibly DPPC. Others have indicated that some of the subfractions (squeezed-out material from alveolar films ?) detected in extracting pulmonary surfactant (Magoon et al., 1983; Putz et al., 1994), showed lower surface activity (Gross, 1995a), which would tend to indicate that a process of surface refining may also occur *in situ*. Schürch et al. (1992; 1994), have suggested that surfactant adsorbed films have a reservoir or pool of lipids under the surface film which enriches the surface with DPPC, and SP-A and calcium enhances the adsorption of DPPC to the surface (Schürch and Bachofen, 1995). Since the LSE films studied here in the dynamic cycling experiment were spread from solvent, and the subphase possibly could not have contained any reservoir, the enrichment of such films was probably nominal but conservatively 5 %, after eleven cycles, consistent with the "squeeze out" of some components occurring. The condensed domains of LSE need to

be studied in adsorbed films, and in combinations with SP-A, so that a closer examination of the dynamics and phase state of the pulmonary surfactant in situ can be comprehended.

11.43] Ionic interactions of LSE with calcium.

It was known for some time that ionic conditions determine morphology and functional properties of pulmonary surfactant. A number of previous studies have indicated that the physical and surface properties of pulmonary surfactant can be altered by altering pH and ionic changes in the environment of bilayers and films. Removal of calcium ions changed the structures of tubular myelin, which were restored by their addition (Benson et al., 1984). *In vitro* studies have shown that increasing the pH of the subphase of surfactant films above 7, decreased the ability of calf lung surfactant to reach low surface tension upon compression (Amirkhanian and Merrit, 1995; Amirkhanian and Taeusch, 1993; Haddad et al., 1994). Calcium and acidic pH increased the ability of surfactant to adsorb at an air-fluid interface (Efrati et al., 1987). Recent surface balance studies have indicated that the surface activity of pulmonary surfactant was also lowered by cationic polyamino acids (Brummer et al., 1995). Proteins which may bind to one or more phospholipid headgroups of surfactant such as C-reactive protein to DPPC, inhibited surfactant adsorption to the air-water interface (McEachren and Keough, 1995). These studies tend to indicate that some hydrophobic components of pulmonary surfactant have specific electrostatic interactions with ions, although proteins such as SP-A which have strong interactions with calcium are likely also affected. Our study of LSE films

directly indicates the sensitivity of such electrostatic interactions, as seen by the higher amounts of condensed phase in LSE films induced by millimolar amount of calcium in the subphase compared to the ones without calcium present (Figure 11.6b). Since our LSE films studied with calcium (Figure 11.6b) did not contain any SP-A the ionic interactions were probably between acidic phospholipid in the films and calcium in the subphase.

Teubner et al., (1983) reported, from measuring thermal transitions by DSC of pulmonary surfactant (PS) suspensions of sheep, under different states of hydration, that fully hydrated PS showed a 20°C change of the peak transition temperature (T_c) compared to dehydrated samples. They suggested that hydration of some of the specific components of PS was responsible for thermotropic properties of pulmonary surfactant (Teubner et al., 1993). Others have observed by FTIR of surfactant suspensions from rabbit, that 5 to 10 mM calcium increased the onset T_c of the thermotropic transition of the material, and the ion bound to the phosphate head group of the lipids, detected by measuring the phosphate stretching frequencies directly from such suspensions (Mautone et al., 1987). Recent studies using FTIR of calf lipid surfactant extracts (CLSE) have also indicated that millimolar amounts of calcium interacted with acidic phospholipid of surfactant, and increased the molecular order of such extracts (Ge et al., 1995). We have observed previously in films containing acidic lipid (DPPG) that calcium was able to increase the amount of condensed phase compared to neutral lipid films (Chapter 4). The amounts of condensed phase (Figure 11.6 (b), C) observed in films of LSE under the influence of calcium were observed to persist to a somewhat higher π before

disappearing, compared to the films without the cation. The number of condensed domains observed in such films containing calcium were also increased as much as two fold at similar π (Figure 11.6b, B) compared to the LSE films without calcium. These results suggests that calcium by increasing the number and amounts of condensed domains, induced an ordering or condensed LSE films.

In the LSE-calcium films, the fluorescent aggregates (Figure 11.6, E) observed at higher π were absent in films without the cation (Figure 11.2a, E), and tends to suggest that the divalent cation also caused possible re-arrangements of materials in LSE films at high π. The re-arrangements at the high π could be an indication of phase segregation of acidic lipid aggregated by binding of calcium. The presence of probe in the aggregates or domains would tend to indicate that their internal constituents were mostly fluid (the probe NBD-PC prefers the fluid phase). Since pulmonary surfactant also contains fluid acidic lipids, it is tempting to speculate that calcium regionalized the fluid acidic lipids into domains, and such regions could be easily squeezed out of the films upon further compression, as suggested previously by others (Boonman et al., 1987; Egberts et al., 1989; Fleming and Keough, 1988; Keough, 1992).

11.44] Adsorption of LSE.

Previous studies on adsorption of simple mixtures of surfactant components have indicated that unsaturated lipids, and SP-B and SP-C, enhance the adsorption of DPPC (see Chapter 7, and references there in). Since qualitative examination of the visual feature of adsorbed LSE films do not indicate any drastic difference with their solvent-

spread counterparts, although LSE-suspensions adsorption was more rapid compared to DPPC (Chapter 7), the hydrophobic proteins and unsaturated lipids indeed increased the rate of adsorption of DPPC in LSE. The typical visual features of adsorption of LSE suspensions (Figure 11.7) to an air-saline interface suggested that adsorbed and spread films of surfactant are similar, at equivalent π. Also, the adsorbed LSE films underwent fluid to condensed phase transitions, as seen from the appearance and growth of condensed domains with increasing packing of the materials at the interface. Previously we indicated that some spread and adsorbed films of surfactant components were similar at equivalent packing densities (Chapter 7), the studies on LSE suspensions also further support the proposal that spread and adsorbed LSE films are equivalent. Although such adsorbed LSE films were not studied in detail, this study indicates that some of the components of LSE such as DPPC (which form condensed domains) do reach the air-water interface in the LSE adsorbed films, and that such films are not further enriched with this component compared to their solvent spread counterparts. This would suggest that the processes discussed above such as selective adsorption or enrichment of adsorbed pulmonary surfactant films with DPPC, may require more complex processes rather than simple adsorption. Dynamic cycling of such adsorbed LSE films and ones containing SP-A may indicate if such processes do occur, and should be performed in future. Instrumental limitations restrict us from doing such studies at present, since the adsorption balance is not modified enough to allow for compression-expansion of adsorbed films (see chapter 7, for details).

11.45] Association of SP-A with LSE films.

As discussed previously (Chapter 10), pulmonary surfactant protein SP-A may specifically interact and associate with surfactant lipids in films. The preliminary observations made in this study (Figure 11.8) indicate that SP-A interacts and induces condensed domain aggregation in LSE films. SP-A penetrated or adsorbed onto LSE films at low π, and the protein by itself formed large aggregates or domains in the LSE films in the presence of calcium. The condensed domains (black regions) in Figure 11.8, show that SP-A aggregated the condensed domains into large clusters. This may be due to the binding of SP-A to the condensed lipid domains, since observation of the fluorescent label of SP-A from the film indicated that the protein was localized with the condensed domain clusters. As in the previous study of interaction of SP-A with DPPC/DPPG films (Chapter 10), the association of the protein with condensed lipids or gel-like phases is also observed in films of LSE.

This arrangement of condensed domains in LSE films induced by SP-A (aggregation of domains) seems to be somewhat different from those lipid-protein arrangements previously seen in simpler systems such as in DPPC/SP-A films, where the protein associated with the liquid condensed (LC) domain boundaries only but did not aggregate the condensed domains (Chapter 10). This difference of arrangement of SP-A in LSE films compared to the ones seen in DPPC system, may be due to the fact that LSE films contained other components such as hydrophobic proteins and other lipids, which possibly allowed SP-A to interact with lipids differently with such films compared to the ones seen in simpler systems of surfactant components. It was previously observed

by a number of workers that SP-A caused extensive aggregation of vesicles of pulmonary surfactant lipid extracts. This process was indicated to occur by binding of SP-A to individual lipid vesicles, and such vesicles showing tendency to aggregate and fuse around the protein (see Casals et al., 1993; Ruano et al., 1996 and the references therein). This LSE film study with SP-A tend to reflect similar aggregation induced by SP-A, except in this case it occurred with condensed domains of LSE. This may implicate SP-A in aggregating vesicles by binding to specific phase structures of the bilayer of vesicles and thereby aggregating them.

The study indicates that pulmonary surfactant lipid extract films undergo liquid-expanded to liquid-condensed and perhaps higher order phase transitions upon compression. The condensed domains of such films display some similar properties to those of simpler pulmonary surfactant components. Spread and adsorbed films of lipid surfactant extract (LSE) are similar and calcium and SP-A interact with such films.

SUMMARY AND CONCLUSIONS

Pulmonary surfactant lines the air-alveolar fluid interface with a putative monomolecular film which is responsible for lowering surface tension of that interface and maintaining alveolar stability. Monolayer films are also good models for biological membranes. It is somewhat unclear to date, how the lipids and proteins of surfactant associate, interact and organize in films at an air-water interface, nor if some or all of the components responsible are present in the alveolar films. The purpose of this thesis was to answer some of these questions, utilizing a novel technique of epifluorescence microscopy of films of surfactant components, and especially to observe the interactions of surfactant lipids and protein with its major component DPPC. The epifluorescence microscopic surface balance technique allowed us to quantitatively study the microscopic organization of surfactant lipids and proteins at an air-water interface. Such organization also pertain to models of lipid-protein association in biological membranes.

These studies indicated that unsaturated lipid can alter the organization of rigid or condensed domains of DPPC films, increase the fluidity of such films, and probably be squeezed out of such films allowing the films to be enriched in DPPC. Increased fluidity of surfactant can allow it to rapidly adsorb at the air water interface. Enrichment of surfactant films with DPPC, may allow such films to achieve low surface tension at the air-alveolar fluid interface. Phosphatidylglycerol can mix with DPPC in films in condensed and fluid phase. Calcium can condense such films. Condensed films can reach low surface tension upon maximal compression, and such films may exclude or

segregate other surfactant components allowing for further enrichment with DPPC to achieve low surface tension. Cholesterol altered the packing of DPPC condensed domains, increased the fluidity of DPPC-cholesterol films, and it remained in such films at high packing density. By increasing fluidity, cholesterol may allow surfactant films to rapidly re-spread from its highly packed states achieved at high surface pressure or low surface tension.

Hydrophobic surfactant proteins SP-B and SP-C perturbed the packing of DPPC films, some amounts remained in such films at low surface tension and increased the adsorption of this component to the air-water interface. The proteins were found to affect the DPPC phase structures differently, indicating their individual structure-function relationships may be an important factor in surfactant dynamics and lipid-protein associations. The hydrophobic proteins may allow for surfactant films to be rapidly formed (by adsorption) at the air-alveolar interface, and rapidly re-spread from highly compressed states. The water soluble glycoprotein SP-A associated with (or bound to) the condensed fluid phase boundaries of surfactant phospholipid films, and interacted with the hydrophobic protein SP-B as well as the phospholipid. Such interactions were modulated by films ionic environment. SP-A, by binding to condensed or gel-phase phospholipids in surfactant, may allow for the material to be re-directed towards type-II pneumocytes for re-utilization. By interacting with SP-B and calcium in DPPC environments, SP-A may allow for formation of the unusual tubular myelinic structures, which are presumed surfactant film precursors.

Hydrophobic surfactant extracts formed similar films at an air-water interface

either from solvent spreading or by adsorption. Such films exhibited fluid to condensed phase transitions upon compression, and such transitions were affected by dynamic cycling, calcium and SP-A. The condensed domains of surfactant films exhibited characteristics of DPPC, and such films displayed properties which could be co-related to the ones exhibited by simpler surfactant lipid-protein component films.

These studies thus indicate most of the components of pulmonary surfactant components associate and interact at the air-water interface in films, and the micro-organization of such films are similar whether they are adsorbed or solvent-spread. Not only are spread and adsorbed surfactant films similar, fluorescent probes can be easily incorporated in adsorbed films. This opens up future possibilities of studying organization of films of adsorbed natural surfactant and its subfractions, especially the elusive surface active film (if such layers can be isolated intact from the lungs), using fluorescence microscopy. Also biophysical processes involved in such film formation, maintenance, inhibition and re-utilization may be studied in surface balances, allowing for development of artificial surfactants which show all or most of their properties. If such films can be transferred into solid-substrates, using recently developed techniques such as atomic force, scanning tunnelling, near field scanning and plasma desorption microcopies, in combination with neutron diffraction, synchrotron radiation methods, would yield further information of the molecular and atomic organization of surfactant in the lungs.

REFERENCES

Adachi., H., H. Hyashi, H. Sato, K. Dempo & T. Akino (**1989**) Characterization of phospholipids accumulated in pulmonary surfactant compartments of rats intratrachially exposed to silica. *Biochem. J.*, 262 : 781 - 786.

Adamson, A. W. (**1990**) *Physical Chemistry of Surfaces.* 5th edition. John Wiley & Sons, Inc., New York., chapters III - V., pp. 53 - 159.

Ahlers, M., R. Blankenburg, D. W. Grainger, P. Meller, H. Ringsdorf & C. Salesse (**1989**) Specific recognition and formation of two-dimensional streptavidin domains in monolayers: Application to molecular devices. *Thin Solid Films*, 180 : 93 - 99.

Ahlers, M., R. Blankenburg, H. Haas, D. Möbius, H. Möhwald, W. Müller, H. Ringsdorf & H.-U. Siegmund (**1991**) Protein interactions with ordered lipid films : specific and unspecific binding. *Adv. Mater.*, 3 : 39 -46.

Akino. T. (**1992**) Lipid components of the surfactant system. In *Pulmonary Surfactant : from molecular biology to clinical practice.* Eds. B. Robertson, L. M. G. VanGolde and J. J. Batenburg. Elsevier Science Publishers B.V., Amsterdam, Chapter 2, pp. 19 - 31.

Albrecht, O., H. Gruler & E. Sackmann (**1978**) Polymorphism of phospholipid monolayers. *J. Physiq. (France)*, 39 : 301 - 313.

Albrecht, O., H. Gruler & E. Sackmann (**1981**) Pressure-composition phase diagrams of cholesterol/lecithin, cholesterol/phosphatidic acid and lecithin/phosphatidic acid mixed monolayers : a Langmuir film balance study. *J. Coll. Interf. Sci.*, 79 : 319 - 338.

Amirkhanian, J. D. & T. A. Merrit (**1995**) The influence of pH on surface properties of lung surfactant. *Lung*, 173 : 243 - 254.

Amirkhanian, J. D. & H. W. Taeusch (**1993**) Reversible and irreversible inactivation of preformed pulmonary surfactant surface films by changes in subphase constituents. *Biochim. Biophys. Acta*, 1165 : 321 - 326.

Amrein, M., M. Schenk, A. VonNahmen, M. Sieber & R. Reichelt (**1995**) A novel force-sensing arrangement for combined scanning force/scanning tunnelling microscopy applied to biological objects. *J. Micros.*, 179 : 261 - 265.

Andelman, D., & P. G. DeGennes (**1988**) Chiral discrimination in a Langmuir monolayer. *C. R. Acad. Sci.* 307 : 233.

Andelman, D., F. Brochard & J.-F. Joanny (**1987**) Phase transitions in Langmuir

monolayers of polar molecules. *J. Chem. Phys.*, 86 : 3673 - 3683.

Ansfield, M. J. & B. T. Benson (**1980**) Identification of the immunosuppressive components of canine pulmonary surface active material. *J. Immunol.*, 125 : 1093 - 1098.

Avery, M. E. & J. Mead (**1959**) Surface properties in relation to atelectasis and hyaline membrane disease. *Am. J. Dis. Child.*, 97 : 517 - 523.

Baatz, J. E., B. Elledge & J. A. Whitsett (**1990**) Surfactant protein SP-B induces ordering at the surface of model membrane bilayers. *Biochemistry*, 29 : 6714 - 6720.

Baatz, J. E., V. Sarin, D. R. Absolom, C. Baxter & J. A. Whitsett (**1991**) Effects of surfactant-associated protein SP-B synthetic analogous on the surface activity of model membrane bilayers. *Chem. Phys. Lip.*, 60 : 163 - 178.

Bachofen, H., S. Schürch, M. Urbenelli & E. R. Weibel (**1987**) Relations among alveolar surface tension, surface area, volume and recoil pressure. *J. Appl. Physiol.*, 62 : 1878 -1887.

Bangham, A. D. (**1987**) Lung surfactant: How it does and does not work. *Lung*, 165 : 17 - 25.

Bangham, A. D., C. J. Morley & M. C. Phillips (**1979**) The physical properties of an effective lung surfactant. *Biochim. Biophys. Acta.*, 573 : 552 - 556.

Bartlett, G. R. (**1959**) Phosphorous assay in column chromatography. *J. Biol. Chem.*, 234 : 466 - 468.

Bashford, C. L., C. C. Morgan & G. K. Radda (**1976**) Measurement and interpretation of fluorescence polarization in phospholipid dispersions. *Biochim. Biophys. Acta*, 46 : 157 - 172.

Bastacky, J., C. Y. C. Lee, J. Goerke, H. Kaushafen, D. Yager, L. Kenaga, T. P. Speed, Y. Chen & J. A. Clements (**1995**) Alveolar lining layer is thin and continuous. Low temperature scanning electron microscopy of rat lung. *J. Appl. Physiol.*, 79 : 1615 - 1628.

Beers, M. F. (**1996**) Inhibition of cellular processing of surfactant protein C by drugs affecting intracellular pH gradients. *J. Biol. Chem.*, 271 : 14361 - 14370.

Beers, M. F. & A. B. Fisher (**1992**) Surfactant protein C: A review of its unique properties and metabolism. *Am. J. Physiol.*, 263: 151 - 160.

Benson B. J., M. C. Williams, K. Sueshi, J. Goerke & T. Sargeant (**1984**) Role of

calcium ions in the structure and function of pulmonary surfactant. *Biochim. Biophys. Acta*, 793 : 18 - 27.

Birdi, K. S. (**1989**) *Lipid and Biopolymers Monolayers at Liquid Interfaces*. Plenum Press., New York.

Blume A. A. (**1979**) A comparative study of the phase transitions of phospholipid bilayer and monolayers. *Biochim. Biophys. Acta*, 557 : 32 - 44.

Bogdam K., M. A. Alsina, I. Haro, I. Martin & F. Reig (**1994**) Interaction of the HAV-VP3 (61-78) peptide with mono and bilayers. *Langmuir*, 10 : 4618 - 4623.

Boonman A., F. H. J. Machiels, A. F. M. Snik & J. Egberts (**1987**) Squeeze-out from mixed monolayers of dipalmitoylphosphatidylcholine and egg phosphatidylglycerol. *J. Coll. Interf. Sci.*, 120 : 456 - 468.

Boyle, F & J. Seelig (**1983**) Hydration of Escherichia coli lipids : Deuterium T_1 relaxation time studies of phosphatidylglycerol, phosphatidylethanolamine and phosphatidylcholine. *Biochim. Biophys. Acta*, 735 : 131 - 136.

Bredlow, A, H. T. Galla & L. D. Bergelson (**1992**) Influence of fluorescent lipid probes on the packing of their environment. A monolayer study. *Chem. Phys. Lip.*, 62 : 293 -

301.

Bretscher, M. S. (**1985**) The molecules of the cell membrane. *Sci. Amer.*, 253 : 100 - 108.

Bringezu, F., G. Brezesinski, P. Nuhn & H. Möhwald (**1996**) Chiral discrimination in a monolayer of a triple-chain phosphatidylcholine. *Biophys. J.*, 70 : 1789 - 1795.

Brumm, T., C. Naumann, E. Sackmann, R. A. Rennie, R. K. Thomas, D. Kanellas, J. Penfold & T. Bayerl (**1994**) Conformational changes of the lecithin headgroups in monolayers at the air -water interface. A neutron reflection study. *Eur. Biophys. J*, 23 : 289 - 295.

Brummer, P. M., S. Aziz & M. N. Gillespie (**1995**) Inhibition of pulmonary surfactant biophysical activity by cationic polyamino acids. *Pharmaceut. Res.*, 12 : 1658 - 1663.

Bruni, R., H. W. D. Taeusch & A. J. Waring (**1991**) Surfactant protein SP-B:lipid interactions of the synthetic peptides representing the amino terminal amphipathic domain. *Proc. Natl. Acad. Sci. USA*, 88 : 7481 - 7455.

Bruno, M. A., R. J. Bohinski, J. E. Carter, K. A. Foss & J. A. Whitsett (**1995**) Structural and functional analysis of the mouse surfactant protein B gene. *Am. J.*

Physiol., 268 : 381 - 389.

Cadenhead, D. A. (**1985**) Monomolecular films as biomembrane models. In *Structure and Properties of Cell Membranes.* Vol. III, Ed. Georghe Benga. CRC Press, Boca Raton, Florida., chapter 2., pp 21 - 62.

Casals, C., E. Miguel & J. Perez-Gil (**1993**) Tryptophan fluorescence study on the interaction of pulmonary surfactant protein with phospholipid vesicles. *Biochem. J.*, 296 : 585 - 593.

Chao, F-F., L. M. Amende, E. J. Blanchette-Mackie, S. I. Skarlatos, W. Gamble, J. H. Resau, P. Mergner & H. S. Kruth (**1988**) Unesterified cholesterol-rich lipid particles in atherosclerotic lesions of human and rabbit aortas. *Am. J. Pathol.*, 131 : 73 - 83.

Cherry, R. J., U. Muller, C. Holnstein & M. P. Heyn (**1980**) Lateral segregation of proteins induced by cholesterol in bacteriorhodopsin-phospholipid vesicles. *Biochim. Biophys. Acta*, 596 : 145 - 151.

Chi, L. F., A. Anders, H. Fuchs, R. R. Johnston & H. Ringsdorf (**1993**) Domain structures in Langmuir-Blodgett films investigated by atomic force microscopy. *Science*, 259 : 213 - 216.

Clark, J. C., S. E. Wert, C. J. Bachurski, M. T. Stahlman, B. R. Stripp, T. E. Weaver & J. A. Whitsett (**1995**) Targeted disruption of the surfactant protein B gene disrupts surfactant homeostasis, causing respiratory failure in newborn mice. *Proc. Natl. Acad. Sci. USA*, 92 : 7794 - 7798.

Clements J. A. (**1956**) Dependence of pressure volume characteristics of lungs on intrinsic surface active material. *Am. J. Physiol.*, 187 : 592A.

Clements J. A. (**1977**) Functions of the alveolar lining. *Am. Rev. Respir. Dis.*, 115 : 67 - 71.

Clements, J.A. (**1957**) Surface Tension of lung extracts. *Proc. Soc. Exp. Biol. Med.*, 95 : 170 -172.

Clercx, A., G. Vandenbussche, T. Curstedt, J. Johansson, H. Jörnvall & M. J. Ruysschaert (**1995**) Structural and functional importance of the C-terminal part of the pulmonary surfactant polypeptide SP-C. *Eur. J. Biochem.*, 229 : 465 - 472.

Cochrane, C. G., & S. D. Revak (**1991**) Pulmonary surfactant protein B (SP-B): structure function relationships. *Science*, 254 : 566 - 568.

Collins, J. J. & M. C. Phillips (**1982**) The stability and structure of cholesterol-rich co-

dispersions of cholesterol and phosphatidylcholine. *J. Lipid Res.*, 23 : 291 - 298.

Comroe, J. H. (**1977**) Premature Science and Immature Lungs. In *Retrospectroscope: Insights Into Medical Discovery*. Von Gehr Press, Menlo Park, CA., pp 140 - 182.

Creuwels, L. A. J. M., E. H. Boer, R. A. Demel, L. M. G. VanGolde & H. P. Haagsman (**1995**a) Neutralization of the positive charges of surfactant protein C. Effects on structure and function. *J. Biol. Chem.*, 270 : 16225 - 16229.

Creuwels, L. A. J. M., R. A. Demel, L. M. J. VanGolde & H. P. Haagsman (**1995**b) Characterization of a dimeric canine form of surfactant protein C (SP-C) *Biochim. Biophys. Acta* 1254 : 326 - 332.

Creuwels, L. A. J. M., R. A. Demel, L. M. G. Van Golde, B. J. Benson & H. P. Haagsman. (**1993**) Effect of acylation on structure and function of surfactant protein C at the air-liquid interface. *J. Biol. Chem.*, 268 : 26752 - 26758.

Cruz, A., C. Casals & J. Perez-Gil (**1995**) Conformational flexibility of pulmonary surfactant proteins SP-B and SP-C, studied in aqueous organic solvents. *Biochim. Biophys. Acta*, 1255 : 68 - 76.

Cŝerhati, T. & M. Sžogyi (**1994**) Interaction of phospholipids with proteins and peptides.

New advances IV. *Int. J. Biochem.*, 26 : 1 - 18.

Curstedt, T., J. Johansson, J. Barros-Söderling, B. Robertson, G. Nilsson, M. Westberg & H. Jörnvall (**1988**) Low-molecular-mass surfactant protein type 1. The primary structure of a hydrophobic 8-kDa polypeptide with eight half-cysteine residues. *Eur. J. Biochem.*, 172 : 521 -525.

Curstedt, T., J. Johansson, P. Persson, A. Eklund, B. Robertson & H. Jörnvall (**1990**) Hydrophobic surfactant-associated polypeptides. SP-C is a lipopeptide with two palmitoylated cysteine residues, whereas SP-B lacks covalently linked fatty acyl groups. *Proc. Natl. Acad. Sci. USA*, 87 : 2985 - 2989.

Curstedt, T., H. Jörnvall, B. Robertson, T. Bergman & P. Berggren (**1987**). Two hydrophobic low-molecular mass protein fractions of pulmonary surfactant : characterization and biophysical activity. *Eur. J. Biochem.*, 168 : 255 - 262.

Daillant, J., J. J. Benattar & L. Bosio (**1990**) X-ray reflectivity study of monolayers of amphiphilics at the air-water interface. *J. Phys. (Cond. Matt.)*, 2 : 405 - 410.

Daniels, C. B., H. A. Bann, J. H. T. Power & T. E. Nicholas (**1990**) Body temperature alters lipid composition of pulmonary surfactant in the lizard. *Expt. Lung. Res.*, 16 : 435 - 449.

Daniels C. B., S. Orgeig & A. W. Smits (**1995**) The evolution of vertebrate pulmonary surfactant. *Physiol. Zool.* 68 : 539 - 566.

Davis, P. J., K. P. Coolbear & K. M. W. Keough (**1980**) Differential scanning calorimetric studies of the thermotropic phase behaviour of membranes composed of Dipalmitoyl lecithin and mixed acid unsaturated lecithins. *Can. J. Biochem.*, 58 : 851 - 858.

DeFontanges A., F. Bonte, C. Taupin & R. Ober (**1984**) Pressure-Area curves of single and mixed monolayers of phospholipids and possible relevance to properties of lung surfactant. *J. Coll. Interf. Sci.*, 101 : 301 - 308.

DeGennes, P. G. (1992) Soft Matter (Nobel Lecture). *Angewandate Chemie Int. Ed. Engl.*, 31 : 842 - 845.

DeJongh, H. H. J., E. Goormaghtigh & J. A. Killian (**1994**) Analysis of circular dichroism spectra of oriented protein-lipid complexes: Toward a general application. *Biochemistry*, 33 : 14521 - 14528.

Denicourt, N., P. Tancréde & J. Teissié (**1994**) The main transition of dipalmitoylphosphatidy- lcholine monolayers. A liquid expanded to solid condensed high order transition. *Biophys. Chem.* 49 : 153 - 162.

Dietrich, C., W. H. Goldmann, E. Sackmann & G. Isenberg (**1993**) Interaction of NBD-Talin with lipid monolayers. A film balance study. *FEBS Lett.* 324: 37 - 40.

Discher, B. M., K. M. Maloney, W. R. Scheif, D. W. Grainger, V. Vogel & S. B. Hall (**1996**) Lateral phase seperation in interfacial films of pulmonary surfactant. *Biophys. J.* 71: 2583 - 2590.

Dluhy, R. A., K. E. Reilly, R. D. Hunt, M. L. Mitchell, A. J. Mautone & R. Mendelsohn (**1989**) Infrared spectroscopic investigation of pulmonary surfactant. Surface film transition at the air - water interface and bulk phase thermotropism. *Biophys. J.* 56 : 1173 - 1181.

Efrati, H., S. Hawgood, M. C. Williams, K. Hong & B. J. Benson (**1987**) Divalent cation and hydrogen ion effects on the structure and surface activity of pulmonary surfactant. *Biochemistry*, 26 : 7986 - 7993.

Egberts, J., A. Beintema-Dubbledam & A. DeBaers (**1987**) Phosphatidylinositol and not phosphatidylgycerol is the important minor phospholipid in rhesus - monkey surfactant. *Biochem. Biophys. Acta*, 919 : 90 - 92.

Egberts J., H. Sloot & A. Mazure (**1989**) Minimal surface tension, squeeze-out and transition temperatures of binary mixtures of dipalmitoylphosphatidylcholine and

unsaturated phospholipids. *Biochim. Biophys. Acta*, 1002 : 109 - 113.

Eklund K. K., J. Vurinen, J. Mikkola, J. A. Virtanen & P. K. J. Kinnunen (**1988**) Ca^{++}-Induced lateral phase separation in phosphatidic acid/phosphatidylcholine monolayers as revealed by fluorescence microscopy. *Biochemistry*, 27 : 3433 - 3437.

ElMashak E. M., F. Lakhdar-Ghazal & J. F. Tocanne (**1982**) Effect of pH, mono- and di-valent cations on the mixing of phosphatidylglycerol with phosphatidylcholine. *Biochim. Biophys. Acta* 688 : 465 - 474.

Estep, T. N., D. B. Mountcastle, R. L. Biltonen & T. E. Thompson (1978) Studies on the anomalous thermotropic behaviour of aqueous dispersions of dipalmitoylphosphatidylcholine-cholesterol mixtures. *Biochemistry*, 17 : 1984 - 1989.

Evert, L. L., D. Leckband & J. Israelachvili (**1994**). Structure and dynamics of ion-induced domains in free and supported monolayers and bilayers. *Langmuir*, 10 : 303 - 315.

Fan, B., R. Bruni, W. Taeusch & A. Waring (**1991**) Antibodies against synthetic amphipathic helical sequence of surfactant protein SP-B detect a conformational change in the native protein.
FEBS Lett. 282: 220 - 224.

Findley E.J. & P. G. Barton (**1978**) Phase behaviour of synthetic phosphatidylglycerols and binary mixtures with phosphatidylcholines in the presence and absence of calcium. *Biochemistry*, 17 : 2400 - 2405.

Fischer A. & E. Sackmann (**1984**) Electron microscopy and diffraction studies of phospholipid monolayers transferred from water to solid substrates. *J. Physiq. (France)*, 45 : 517 - 527.

Fischer, B., S. P. Heyn, M. Egger & H. E. Gaub (**1993**) Antigen binding to a pattern of lipid-anchored antibody-binding sites measured by surface-plasmon microscopy. *Langmuir* 9 : 136 - 140.

Flach, C. R., J. W. Brauner, and R. Mendelsohn (**1993**) Calcium ion interactions with insoluble phospholipid monolayer films at the a/w interface. External reflection-absorption IR studies. *Biophys. J.* 65 : 1994 - 2001.

Fleming, B. D. & K. M. W. Keough (**1988**) Surface respreading after collapse of monolayers containing major lipids of pulmonary surfactant. *Chem. Phys. Lip.* 49 : 81 - 86.

Fleming B. D., C. M. Raynor & K. M. W. Keough (**1983**). Some characteristics of monolayers of 1-palmitoyl,2-oleyl phosphatidylglycerol (POPG) with and without DPPC

during dynamic compression and expansion. *Biochim. Biophys. Acta*, 737 : 243 - 250.

Flörsheimer, M. & H. Möhwald (**1989**) Development of equilibrium domain shapes in phospholipid monolayers. *Chem. Phys. Lip.* 49 : 231 - 241.

Flörsheimer , M. & H. Möhwald (**1991**) Superimposed ordering transitions in phospholipid monolayers. *Coll. & Surf.* 55 : 173 - 189.

Gaines, G.L. (**1966**) *Insoluble Monolayers at liquid-gas interface. Wiley Interscience*, NY.

Gaines, G.L. (**1995**) Langmuir-Blodgett films. in *Characterization of Organic Thin Films. Surfaces, Interfaces, Thin Films. Material Characterization Series*, Ed. A. Ullman and L.E. Fitzpatrick. Butterworth, Heinman and Manning, MA.

Galla, H.-J., W. Hartmann, U. Thielen & E. Sackmann (**1979**). On two dimensional passive random walks in lipid bilayer and fluid pathways in biomembranes. *J. Membr. Biol.* 48 : 215 -236.

Gaub, H.E., V. T. Moy & H. M. McConnell (**1986**). Reversible formation of plastic two dimensional lipid crystals. *J. Phys. Chem.*, 90 : 1721 - 1725.

Ge, Z.C.W., C. W. Brown, J. G. Turcotte, F. Wang & R. H. Notter (**1995**). FTIR studies of calcium - dependant molecular order in lung surfactant and surfactant extract dispersions. *J. Coll. Interf. Sci.*, 173 : 471 - 477.

Gennis R. B. (**1989**) *Biomembranes: Molecular Structures and Function,* Springer Verlag, N.Y.

Georgallas, A & D. A. Pink (**1982**) Phase transitions in monolayers of saturated lipids. Exact results and Monte Carlo simulations. *J. Coll. Interf. Sci.*, 89 : 107 -116.

Gershfeld, N. L. (**1976**) Physical chemistry of lipid films at fluid interfaces. *Annu. Rev. Phys. Chem.* 27 : 349 - 368.

Gershfeld, N. L. (**1989**) The critical unilamellar lipid state: a perspective for membrane bilayer assembly. *Biochim. Biophys. Acta,* 988: 335-350.ad.

Ghosh, D., & J. Tinoco (**1972**) Monolayer interactions of individual lecithins with natural sterol. *Biochim. Biophys. Acta,* 266 : 41 - 49.

Gil, J. (**1985**) Histological preservation and ultrastructure of alveolar surfactant. *Annu. Rev. Physiol.* 47 : 753 - 763.

Glasser, S. W., T. R. Korfhagen, T. E. Weaver, T. PilotMatias, J. L. Fox and J. A. Whitsett (**1987**). cDNA and deduced amino acid sequence of human pulmonary surfactant-associated proteolipid SPL(Phe). *Proc. Natl. Acad. Sci. USA.*, 84 : 4007 - 4011.

Gluck, L. (**1995**). Surfactant development and lung maturity prediction. *Appl. Cardiopulm. Pathophysiol.*, 5(sup1): 53 - 58.

Goerke, J. (**1974**) Lung surfactant. *Biochim. Biophys. Acta*, 344 : 241 - 264.

Goerke, J. (**1992**) Surfactant and lung mechanics. in *Pulmonary Surfactant: From Molecular Biology to Clinical Practice*. Ed. B. Robertson, L. M. G. Van Golde & J.J. Battenburg, Elseiver, Amsterdam. Ch. 8.

Goerke, J. & J. A. Clements (**1986**) Alveolar surface tension and lung surfactant. in *Handbook of Physiology - The Respiratory System III, Mechanics of Breathing*. Ed. P. T. Macklem and J.Mead, American Physiological Society, Washington, 247 - 261.

Gorter E. & F. Grendel (**1925**) On bimolecular layers of lipid on the chromatocytes of the blood. *J. Exp. Med.*, 41 : 439 - 443.

Grainger D. W., A. Reichert, H. Ringsdorf & C. Salesse (**1989**) An enzyme caught in

action:direct imaging of hydrolytic function and domain formation of phospholipase A_2 in phosphatidylcholine monolayer. *FEBS Lett.*, 252 : 73 - 82.

Grainger, D. W., A. Reichert, H. Ringsdorf & C. Salesse (**1990**) Hydrolytic action of phospholipase A_2 in monolayers in the phase transition regions: direct observations of enzyme domain formation using fluorescence microscopy. *Biochim. Biophys. Acta,* 1023 : 365 - 379.

Gregory T.J., W. J. Longmore, M. A. Morley, J. A. Whitsett, C. R. Reed, A. A. Fowler, R. J. Maunder, C. Crim & T. M. Hyers (**1991**). Surfactant chemical composition and biophysical activity in acute respiratory distress syndrome. *J. Clin. Invest.*, 88 : 1976 - 1981.

Griffith, O. H., P. J. Dehlinger & S. P. Van (**1974**) Shape of the hydrophobic barrier of the phospholipid bilayer: Evidence of water penetration in biological membranes. *J. Membr. Biol.*, 15 : 159 - 192.

Gross N. J. (**1995**a) Extracelluar metabolism of pulmonary surfactant. The role of a new serine protease. *Annu. Rev. Physiol.* 57 : 135 - 150.

Gross, N. J. (**1995**b) Pulmonary surfactant : Unanswered questions. *Thorax*, 50 : 325 - 327.

Gross, N. J. & K. R. Naraine (**1989**) Surfactant subtypes of mice:metabolic relationships and correlation in vitro. *J. Appl. Physiol*, 67 : 414 - 421.

Gross, N. J. & R. M. Schultz (**1992**) Requirements for extracellular metabolism of pulmonary surfactant. tentative identification of serine protease. *Am. J. Physiol.*, 262 : 446 - 453.

Grotberg, J. B., D. Halpren & O. E. Jenson (**1995**) Interaction of exogenous surfactant and endogenous surfactant: spreading-rate effects. *J. Appl. Physiol.*, 78 : 750 - 756.

Groves J. T. & H. M. McConnell (**1996**) Chiral discrimination in two dimensions. *Biophys. J.* 70: 1573 - 1574.

Gulik, A., P. Tchoreloff & J. Proust (**1994**) A conformation transition of lung surfactant lipids probably involved in respiration. *Biophys. J.* 67 : 1107 - 1112.

Günther, A., R. Schmidt, F. Nix, C. Seibert, S. Zeigler, G. Guth, H. Morr & W. Seeger (**1995**) Alteration of biochemical and biophysical surfactant properties in interstitial lung disease. *Appl. Cardiopulm. Pathophysiol.*, 5(su. 3)46: A39.

Gustafsson, M, G. Vandenbussche, T. Curstedt, J. M. Ruysschaert & J. Johansson (**1996**) The 21-residue surfactant peptide ($LysLeu_4$)$Lys(KL_4)$ is a transmembrane α-helix

with mixed non-polar / polar surface. *FEBS Lett.*, 384 : 185 - 188.

Haagsman, H. P. (**1994**) Structure-function relationships in lung surfactant: Protein-lipid interactions. *Prog. Respir. Res.*, 27 : 15 - 24.

Haas, M. A. & W. J. Longmore (**1980**) Regulation of lung surfactant cholesterol metabolism by serum lipoproteins. *Lipids*, 15 : 401 - 406.

Haas, H. & H. Möhwald (**1989**) Specific and unspecific binding of concanavalin A at monolayer surfaces. *Thin Solid Films*, 108 : 101 - 110.

Haddad. L. Y., B. A. Holm, L. Hlavaty & S. Matalon (**1994**) Dependence of surfactant function on extracellular pH : mechanisms of modification. *Am. J. Physiol.* 76 : 657 - 772.

Hadley, N. F. (**1985**) *The adaptive role of lipids in biological systems.* Wiley Intersci. NY.

Hall, S. B, K. Maloney, B. Korcakova, D. W. Grainger, W. Schief & V. Vogel (**1995**a) Ordered domains in films of pulmonary surfactant. *Am. J. Respir. Crit. Care Med.*, 151 : A312.

Hall, S. B, K. Maloney, B. Korcakova, D. W. Grainger, W. Schief & V. Vogel (**1995b**) Ordered domains in films of pulmonary surfactant. *Biophys. J.*, 68 : A214.

Hall, S. B., A. R. Venkitaraman, J. A. Whitsett & R. Notter (**1992**) Importance of hydrophobic apoproteins and constituents of clinical exogenous surfactant. *Am. Rev. Respir. Dis.*, 145 : 24 -30.

Hall, S. B., Z. Wang & R. H. Notter (**1994**) Separation of subfractions of the hydrophobic components of lung surfactant. *J. Lip. Res.*, 35 : 1386 - 1394.

Hallman, M. (**1992**) Antenatal diagnosis of lung maturity in pulmonary surfactant. in *Pulmonary Surfactant: From Molecular Biology to Clinical Practice.* Ed. B. Robertson, L. M. G. Van Golde & J. J. Battenburg, Elseiver, Amsterdam. Ch. 18.

Hallman, M. (**1995**) Sixteen years of surfactant research. *Appl. Cardiopulm. Pathophysiol.* 5(su. 1): 59 - 63.

Hallman, M. & L. Gluck (**1976**). Phosphatidylglycerol in lung surfactant. III. Possible modifier of surfactant function. *J. Lip. Res.* 17 : 257 - 262.

Hallman, M. & J. K. Terano (**1981**). Measurement of the lecithin/sphingomyelin ratio and phosphatidylglycerol in amniotic fluid. An accurate method for the assessment of

fetal maturity. Brit. *J. Obstet. Gynaec.* 88 : 806 - 813.

Hallman, H, B. H. Feldman, E. Kirkpatrick, & L. Gluck (**1977**) Absence of phosphatidylglycerol (PG) in respiratory distress syndrome in newborns. *Pediat. Res.*, 11 : 714 - 720.

Hallman, M., M. Kulovich, E. Kirkpatrick, R. A. Sugarman & L. Gluck (**1976**) Phosphatidylinositol and phosphatidylglycerol in amniotic fluid : indices of lung maturity. *Am. J. Obstet. Gynecol.*, 125 : 613 - 617.

Hallman, M., R. Spragg, J. H. Harrel, K. M. Moser & L. Gluck (**1982**). Evidence of lung surfactant abnormality in respiratory failure. Study of bronchioalveolar lavage phospholipid surface activity, phospholipase activity and plasma myoinositol. *J. Clin. Investig.*, 70 : 673 - 683.

Hauser, H., I. Pascher, R. H. Pearson & S. Sundell (**1981**) Preferred conformation and molecular packing of phosphatidylethanolamine and phosphatidylcholine. *Biochim. Biophys. Acta*, 650 : 21 - 51.

Haverstick D. M. & M. Glaser (**1989**) Influence of proteins on the reorganization of phospholipid bilayers into large domains. *Biophys. J.*, 55 : 677 - 682.

Haverstick, D. M., & M. Glaser (**1987**) Visualization of a Ca^{2+} - induced phospholipid domains. *Proc. Natl. Acad. Sci. USA.*, 84 : 4475 - 4479.

Haverstick, D. M. & M. Glaser (**1988**) Visualization of domain formation in the inner and outer leaflets of a phospholipid bilayer. *J. Cel. Biol.* 106 : 1885 - 1892.

Hawco, M. W., K. P. Coolbear, P. J. Davis & K. M. W. Keough. (**1981**a) Exclusion of fluid lipid during compression of monolayers of mixtures of dipalmitoylphosphatidylcholine with some other phosphatidylcholines. *Biochim. Biophys. Acta.* 646 : 185 - 187.

Hawco, M. W., P. J. Davis & K. M. W. Keough. (**1981**b) Lipid fluidity in lung surfactant: monolayers of saturated and unsaturated lecithins. *J. Appl. Physiol.*, 51 : 509 - 515.

Hawgood, S. (**1991**) Surfactant : composition, structure and metabolism. in *The Lung : Scientific Foundations,* Eds. R. G. Crystal, J. B. West, P. J. Barnes, N. S. Cher & E.R. Weibel., Raven Press, NY. Ch. 3.1.10.

Hawgood S. (**1992**) The hydrophillic surfactant protein SP-A: Molecular biology, structure and function. in *Pulmonary Surfactant: from Molecular Biology to Clinical Practice.* Eds. B. Robertson, L. M. G. Van Golde & J. J. Battenburg. Elsevier Science

Publisher. Ch. 3.

Hawgood S. & J. A. Clements (**1990**) Pulmonary surfactant and its apoproteins *J. Clin. Investig.*, 86 : 1 - 6.

Hawgood, S. & K. Shiffer. (**1991**) Structure and properties of surfactant associated proteins. *Ann. Rev. Physiol.*, 53 : 375 - 394.

Hawgood, S., B. J. Benson, J. Schilling, D. Damm, J. A. Clements & R. T. White. (**1987**) Nucleotide and amino acid sequences of pulmonary surfactant protein SP 18 and evidence for cooperation between SP 18 and SP 28-36 in surfactant lipid adsorption. *Proc. Natl. Acad. Sci. USA.*, 84 : 66 - 70.

Hayashi, H., K. Adachi, H. Kataoka, T. Sato & T. Akino (**1990**) Molecular species profiles of acidic phospholipids in lung fractions of adult and perinatal rabbits. *Biochim. Biophys. Acta.*, 1042 : 126 - 131.

Heckl, W. M., D. A. Cadenhead & H. Möhwald. (**1988**) Cholesterol concentration dependence of quasi-crystalline domains in mixed monolayers of the cholesterol-dimyristoylphosphatidic acid system. *Langmuir*, 4 : 1352 - 1358.

Heckl, W. M., M. Lösche, D. A. Cadenhead & H. Möhwald. (**1986**) Electrostatically

induced growth of spiral lipid domains in the presence of cholesterol. *Eur. Biophys. J.* 14 : 11 - 17.

Heckl, W. M., M. Lösche, H. Scheer & H. Möhwald (**1985**) Protein/lipid interactions in phospholipid monolayers containing the bacterial antennae protein B800-850. *Biochim. Biophys. Acta*, 810 : 73 - 83.

Heckl, W.M., B. N. Zaba & H. Möhwald. (**1987**) Interactions of cytochrome b_5 and c with phospholipid monolayers. *Biochim. Biophys. Acta.*, 903 : 166 - 176.

Hénon S., & J. Meunier (**1991**) Microscope at the Brewster angle: Direct observation of the first-order phase transitions in monolayers. *Rev. Sci. Instrum.*, 62 : 936 - 939.

Heyn, S. P., M. Egger & H. E. Gaub.(**1990**) Lipid and lipid-protein monolayers spread from a vesicle suspension: a microfluorescence film balance study. *J. Phys. Chem.*, 94 : 5073 -5078.

Hickel, W, D. Kamp & W. Knoll (**1989**) Surface-plasmon microscopy. *Nature*, 339 : 186 - 186.

Hifeda, Y. F. & G. W. Rayfield (**1992**) Evidence for first-order phase transition in lipid and fatty acid monolayers. *Langmuir*, 8 : 197 - 200.

Hildebran, J. N., J. Goerke & J. A. Clements. (**1979**) Pulmonary surface film stability and composition. *J. Appl. Physiol.*, 47 : 604 - 610.

Hillenkamp, F., M. Karas, R. C. Beavis, and B. T. Chait. (**1991**) Matrix-assisted laser desorption/ionization mass spectrometry of biopolymers. *Anal. Chem.* 63 : 1193 - 1203.

Hirschfeld, C. L. & M. Seul. (**1990**) Critical mixing in monomolecular films: pressure-composition phase diagram of a two-dimensional binary mixture. *J. Phys. (France).* 51 : 1537 -1552.

Honig, D. & D. Möbius. (**1991**) Direct visualization of monolayers at the air water interface by Brewster angle microscopy. *J. Phys. Chem.*, 95 : 4590 - 4592.

Hook, G. E. R, J. W. Spalding, M. J. Ortner, E. G. Tombropoulos & C. F. Chignell (**1984**) Investigation of phospholipid of the pulmonary extracellular lung lining by electron paramagnetic resonance. The effects of phosphatidylglycerol and unsaturated phosphatidylcholines on the fluidity of dipalmitoylphosphatidylcholine. *Biochem. J.*, 223 : 533 - 542.

Hörber, J. K. H., C. A. Lang, T. W. Hänsch, W. M. Heckl & H. Möhwald (**1988**) Scanning tunnelling microscopy of lipid films and embedded biomolecules. *Chem. Phys. Lett.* 145 : 151 - 158.

Horowitz, A. D. (**1995**) Exclusion of SP-C, but not SP-B, by gel phase palmitoyl lipids. *Chem. Phys. Lip.*, 76 : 27 - 39.

Horowitz, A. D., J. E. Baatz & J. Whitsett. (**1993**) Lipid effects on aggregation of pulmonary surfactant protein SP-C studied by fluorescence energy transfer. *Biochemistry.*, 32 : 9513 -9523.

Horowitz, A. D., B. Elledge, J. A. Whitsett & J. A. Baatz. (**1992**) Effects of lung surfactant proteolipid SP-C on the organization of model membrane lipids a fluorescence study. *Biochim. Biophys. Acta.*, 1107 : 44 - 54.

Houslay M. D. & K. K. Stanley (**1983**) *Dynamics of biological membranes. Influence on synthesis, structure and function.* John Wiley and Sons Ltd., Ch. 2.

Hui, S.W. (**1981**) Geometry of phase - separated domains in phospholipid bilayer by diffraction-contrast electron microscopy. *Biophys. J.* 34 : 383 - 395.

Hui, S. W. & H. Yu (**1993**) Electron diffraction studies of molecular ordering and orientation in phospholipid monolayer domains. *Biophys. J.* 64 : 150 - 156.

Hunt, R. A., M. L. Mitchell & R. A. Dluhy (**1989**) The interfacial structure of phospholipid monolayer films: an infrared reflectance study. *J. Mol. Str.*, 214 : 93 - 109.

Hwang, J., L. K. Tamm, C. Böhm, T. S. Ramalingam, E. Betzig & M. Edidin (**1995**) Nanoscale complexity of phospholipid monolayers investigated ny near-field scanning optical microscopy. *Science*, 270 : 610 - 614.

Ibadah, J. A., S. Lund-Katz & M. C. Phillips. (1989) Molecular packing of high-density and low-density lipoprotein surface lipids and apolipoprotein A-1 binding. *Biochemistry,* 28 : 1126 -1133.

Jähnig, F. (**1984**) Lipid exchange between membranes. *Biophys J.* 46 : 687 - 694.

Johansson, J., T. Curstedt & H. Jörnvall (**1991**). Surfactant protein B: disulphide bridges, structural properties and Kringle similarities. *Biochemistry*, 30 : 6917 - 6921.

Johansson, J., H. Jörnvall & T. Curstedt (**1992**) Human surfactant polypeptide SP-B: disulphide bridges, C-terminal end, and peptide analysis of the airway form. *FEBS Lett.*, 301 : 165 -167.

Johansson, J., T. Curstedt & B. Robertson. (**1994**a). The proteins of the surfactant system. *Eur. Respir. J.*, 7 : 372 - 391.

Johansson, J., T. Szyperski, T. Curstedt & K. Wuthrich. (**1994**b). The NMR structure of the pulmonary surfactant-associated polypeptide SP-C in an apolar solvent contains

valyl rich α - helix. *Biochemistry*, 33 : 6015 - 6023.

Johansson, J., T. Szyperski & K. Wüthrich (**1995**) Pulmonary surfactant-associated polypeptide SP-C in lipid micelles: CD studies of intact SP-C and NMR secondary structure determination of dipalmitoyl-SP-C(1-17) *FEBS Lett.*, 362 : 261 - 265.

Jones, M. N. & R. J. Davies (**1987**) Human erythrocyte intrinsic membrane proteins and glycoproteins in monolayer and bilayer systems. in *Proteins at Interfaces : Physicochemical and Biochemical Studies*. Eds. J. L. Brash & T. A. Horbett, American Chemical Society, Washington DC. 134 - 152.

Kahn, M. C., G. J. Anderson, & S. B. Hall (**1995**a) Phosphatidylcholine molecular species of calf lung surfactant. *Am. J. Repir. Crit. Care Med.*, 151 : A315.

Kahn, M. C., G. J. Anderson, W. R. Anyan & S. B. Hall (**1995**b) Phosphatidylcholine molecular species of calf lung surfactant. *Am. J. Physiol.*, 269 : 567 - 573.

Katyal S.L. & A. Singh (**1981**) Analysis of pulmonary surfactant apoproteins by electrophoresis. *Biochim. Biophys. Acta*, 670 : 323 - 331.

Keller, A., H. R. Eisetter, T. Voss & K. P. Schafer (**1991**) The pulmonary surfactant protein C (SP-C) precursor is a type II transmembrane protein. *Biochem. J.* 277 : 493 -

499.

Keough, K. M. W. (**1985**) Lipid fluidity and respiratory distress syndrome. in *Membrane Fluidity in Biology. Disease Processes,* Vol. 3, Eds. R. C. Aloia & J. M. Boggs, Acad Press, Inc., NY. Ch. 2.

Keough K. M. W. (**1984**) Physical chemical properties of some mixtures of lipids and their potential for use in exogenous surfactant. *Prog. Respir. Res.* 18 : 257 - 262.

Keough K. M. W. (**1992**) Physical chemistry of pulmonary surfactant in the terminal air spaces. in *Pulmonary Surfactant: From Molecular Biology to Clinical Practice.* Eds. B. Robertson, L. M. G. Van Golde & J.J. Battenburg, Elseiver, Amsterdam. Ch. 7.

Keough, K. M. W. & N. Kariel (**1987**) Differential scanning calorimetric studies of aqueous dispersions of phosphatidylcholines containing two polyenoic chains. *Biochim. Biophys. Acta.* 902 : 11 - 18.

Keough, K. M. W., C. S. Parsons, P. T. Dheng & M. A. Tweedale. (**1988**) Interactions between plasma proteins and pulmonary surfactant : surface balance studies. *Can. J. Physiol. Pharmacol.*, 66 : 1166 - 1173.

Keough, K. M. W., G. Simatos, J. Perez-Gil, K. Nag, L. A. Alwood & M. R. Morrow.

(**1992**) Pulmonary surfactant protein SP-C and phosphatidylcholines in bilayers and monolayers. *Thin Solid Films*, 210/211 : 720 - 722.

Keough, K. M. W., E. Farrel, M. Cox, G. Harrel & H. W. Taeusch (**1985**) Physical, chemical and physiological characteristics of isolates of pulmonary surfactant from adult rabbits. *Can. J. Physiol. Pharamacol.*, 63 : 1043 - 1051.

King, R. J. (**1984**) Isolation and chemical composition of pulmonary surfactant. in *Pulmonary Surfactant*. Eds. B. Robertson, L. M. G. Van Golde & J. J. Battenburg. Elsevier, Amsterdam, 1 - 15.

King R. J. & J. A. Clements (**1972**a) Surface active materials from dog lungs. I. Method of Isolation. *Am. J. Physiol.*, 223 : 707 - 714.

King R. J. & J. A. Clements (**1972**b) Surface active materials from dog lungs. II. Composition and physiological correlations. *Am. J. Physiol.*, 223 : 715 - 726.

King R. J. & J. A. Clements (**1972**c) Surface active materials from dog lungs. III. Thermal analysis. *Am. J. Physiol.* ,223 : 727 - 733.

King, R. J., M. C. Carmichael & P. M. Horowitz (**1983**) Reassembly of lipid-protein complexes of pulmonary surfactant. Proposed mechanism of interaction. *J. Biol. Chem.*,

258 : 10672 -10680.

King R. J. & M. C. Macbeth (**1979**) Physiochemical properties of dipalmitoyl phosphatidylcholine after interaction with an apolipoprotein of pulmonary surfactant. *Biochim. Biophys. Acta*, 577: 86 - 101.

King, R. J., M. C. Phillips, P. M. Horowitz & S. C. Dang (**1986**) Interaction between the 35 kDa apolipoprotein of pulmonary surfactant and saturated phosphocholines. Effect of temperature. *Biochim. Biophys. Acta*, 879 : 1 - 13.

King R. J., D. Simon & P. M. Horowitz (**1989**) Aspects of secondary and quartenary structure of surfactant protein A from canine lungs. *Biochim. Biophys. Acta*, 1001 : 294 - 301.

Kinnunen, P. K. J., A. Kõiv, J. Y. A. Lehtonen, M. Rytöma & P. Mustonen (**1994**) Lipid dynamics and peripheral interactions of proteins with membranes. *Chem. Phys. Lip.*, 73 : 181 - 207.

Kjaer, K., J. Als-Nielsen, C. A. Helm, P. Tippmann-Kayer & H. Möhwald (**1988**) An X-ray scattering study of lipid monolayers at the air-water interface and on solid supports. *Thin Solid Films*, 159 : 17 - 28.

Kleeman, W. & H. M. McConnell. (**1976**) Interaction of proteins and cholesterol with lipids in bilayer membrane. *Biochim. Biophys. Acta.*, 419 : 206 - 222.

Klopfer, K. J. & T. K. Vanderlick (**1996**) Isotherms of dipalmitoylphosphatidylcholine (DPPC) monolayers: Features revealed and features obscured. *J. Coll. Interf. Sci.*, 182 : 220 - 229.

Knells, G., M. K. Ahmed, R. M. Dass, M. R. Oulton, H. H. Mantsch & J.E. Scott. (**1995**) Fourier transform infrared spectroscopic analysis of lung surfactant: Subfraction associated phospholipid and protein profiles. *Chem. Phys. Lip.*, 77 : 193 - 201.

Knobler C. M. (1990) Seeing phenomena in flatland: Studies of monolayers by fluorescence microscopy. *Science*. 249 : 870 - 874.

Knobler, C. M. & R. C. Desai (**1992**) Phase transitions in monolayers. *Ann. Rev. Phys. Chem.*, 43 : 207 - 236.

Korcakova, B, K. M. Maloney, W. R. Scheif, D. W. Grainger, V. Vogel & S. B. Hall (**1996**) Line tension of condensed domains in interfacial films of pulmonary surfactant. *Biophys. J.* 70 : A350.

Kooyman, R. P. H. & U. J. Krull (**1991**) Surface plasmon microscopy of two crystalline

domains in a lipid monolayer. *Langmuir*, 7 : 1507 - 1509.

Krebs, K. E., J. A. Ibadah & M. C. Phillips. (**1988**) A comparison of the surface activities of human apolipoproteins A-I and A-II at the air-water interface. *Biochim. Biophys. Acta,* 959 : 229 - 237.

Krebs, K. E. & M. C. Phillips. (**1983**) The helical hydrophobic moments and surface activities of serum apolipoproteins. *Biochim. Biophys. Acta.*, 754 : 227 - 230.

Krill, S. L., S. L. Gupta & T. Smith (**1994**) Pulmonary lung surfactant synthetic peptide concentration-dependent modulation of DPPC and POPG acyl chain order in a DPPC:POPG:palmitic acid lipid mixture. *Chem. Phys. Lip.* 71 : 47 - 59.

Krill, S. L. & S. L. Gupta (**1994**) Effect of bovine lung surfactant protein isolate (SP-B/C) on egg phosphatidylglycerol acyl chain order in a lipid mixture with dipalmitoylphosphatidylcholine and palmitic acid. *J. Pharm. Sci.* 83 : 539 - 541.

Kuhn, H. (**1989**) Present status and future prospects of Langmuir - Blodgett film research. *Thin Solid Films*, 178 : 1 - 16.

Kuroki Y. & T. Akino (**1991**) Pulmonary surfactant protein - A (SP-A) specifically binds dipalmitoylphosphatidylcholine. *J. Biol. Chem.* , 266 : 3068 - 3073.

Kuroki, Y., M. Shiratori, Y. Ogasawra, A. Hattori, W. Tsunezawa, T. Honma & T. Akino (**1996**) Interaction of phospholipid liposomes with plasma membrane isolated from type -II cells: effect of pulmonary surfactant protein A. *Biochim. Biophys. Acta*, 1281 : 53 - 59.

Lachmann, B. (**1995**) Preface. *Appl. Cardiopulm. Pathophysiol.* 5(su.1):1.

Ladbrooke, B. D., R. M. Williams & D. Chapman. (**1968**) Studies on lecithin-cholesterol-water interactions by differential scanning calorimetry and x-ray diffraction. *Biochim. Biophys. Acta*, 150 : 333 - 340.

Langmuir I. (**1936**) Two-dimensional gases, liquids and solids. *Science*, 84 : 379 - 383.

Lau M. J. & K. M. W. Keough (**1981**) Lipid composition of lung lavage fluid from map turtles (Malaclarys geographica) maintained at different environmental temperatures. *Can. J. Biochem.*, 59 : 208 - 219.

Lawrie, G. A., P. B. Schneider, B. J. Batters, G. T. Barnes & H. K. Cammenga (**1996**) Spreading properties of dimyristoyl phosphatidylcholine at the air/water interface. *Chem. Phys. Lip.*, 79 : 1 - 8. .

Leckband, D. E., C. A. Helm & J. Israelachvili (**1993**) Role of calcium in the adhesion

and fusion of bilayers. *Biochemistry*,. 32 : 1127 - 1140.

Lee, A. G. (**1977**) Lipid phase transitions and phase diagrams: I. Lipid phase transitions. *Biophys. Biochim. Acta*, 472 : 237 - 281.

Lee, A. G., N. J. M. Birdsall, J. C. Metcalfe, P. A. Toon & G. B. Warren (**1974**) Clusters in lipid bilayers and the interpretation of thermal effects in biological membranes. *Biochemistry* 13 : 3699 - 3705.

Lee, K. Y. C. & H. M. McConnell. (**1993**) Quantized symmetry of liquid monolayer domains. *J. Phys. Chem.* 97 : 9532 - 9539.

Lee, K. Y. C., J. F. Klingler & H. M. McConnell. (**1994**) Electric field-induced concentration gradients in lipid monolayers. *Science*, 263 : 655 - 658.

Lentz B. R., Y. Barenholz & T. E. Thompson. (**1976**) Fluorescence depolarization studies of phase transitions and fluidity in phospholipid bilayer. 2. Two-component phosphatidylcholine liposomes. *Biochemistry*, 15 : 4529 - 4536.

Lentz, B. R., D. R. Alford, M. Hoechli & F. A. Dombrose (**1982**) Phase behaviour of mixed phosphatidylglycerol / phosphatidylcholine multi-lamellar and uni-lamellar vesicles. *Biochemistry*, 21 : 4212 - 4219.

Leonard, J. & S. J. Singer (**1966**) Protein conformation in cell membrane, preparations as studied by optical rotatory dispersions and circular dichroism. *Proc. Natl. Acad. Sci. USA.*, 56 : 1828 - 1835.

Leufgen, K. M., H. Rulle, A. Benninghaven, M. Sieber & H. J. Galla (**1996**) Imaging time-of-flight secondary ion mass spectrometry allows visualization and analysis of co-existing phases in Langmuir-Blodgett films. *Langmuir*, 12 : 1708 - 1711.

Lewis, J. F. & R. A. W. Veldhuizen (**1995**) Factors influencing efficiency of exogenous surfactant in acute lung injury. *Biol. Neonate*, 67(su.) : 48 - 60.

Longo, M. L., A. M. Bisagno, J. A. N. Zasadzinski, R. Bruni & A. J. Waring (**1993**) A function of lung surfactant protein SP-B, *Science*, 261 : 453 - 456.

Longo, M. L., A. Waring & J. A. N. Zasadzinski (**1992**) Lipid bilayer surface association of lung surfactant protein SP-B, amphipathic segments detected by flow immunofluorescence. *Biophys. J.*, 63 : 760 - 773.

Lösche M. & H. Möhwald (**1984**a) Fluorescence microscope to observe dynamical processes in monomolecular layers at the air /water interface. *Rev. Sci. Intrum.*, 55 : 1968 - 1972.

Lösche, H. & H. Möhwald (**1984b**) Fluorescence microscopy of monomolecular films at the air/water interface. *Coll. & Surf.*, 10 : 217 - 224.

Lösche, M., H. P. Duwe & H. Möhwald (**1988**). Quantitative analysis of surface textures in phospholipid monolayer phase transition. *J. Coll. Interf. Sci.*, 126 : 432 - 444.

Lösche, M. & H. Möhwald (**1989**). Electrostatic interaction in phospholipid membranes. II. Influence of divalent ions on monolayer structure. *J. Coll. Interf. Sci.*, 131 : 56 - 67.

Luna, E. G. & H. M. McConnell (**1978**) Multiple phase equilibria in binary mixtures of phospholipid. *Biochim. Biophys. Acta*, 509 : 462 - 473.

Lund-Katz, S., H. M. Laboda, L. R. McLean & M. C. Phillips. (**1988**) Influence of molecular packing and phospholipid type on rates of cholesterol exchange. *Biochemistry*, 27 : 3416 - 3423.

Macklin, C. C. (**1954**) The pulmonary alveolar mucoid film and the pneumocytes. *Lancet*, 1 : 1099 - 1104.

Magoon, M. W., J. R. Wright, A. Bourtussio, M. C. Williams, J. Goerke, B. J. Benson, R. L. Hamilton & J. A. Clements (**1983**). Subfractionation of lung surfactant.

Implication for metabolism and surface activity. *Biochim. Biophys. Acta*, 750 : 18 - 31.

Maloney, K. M. & D. W. Grainger (**1993**) Phase separated anionic domains in ternary mixed lipid monolayers at the air- water interface. *Chem. Phys. Lip.*, 65 : 31 - 42.

Marsh, D. (**1995**) Lipid protein interactions and heterogenous lipid distribution in membranes. *Mol. Member. Biol.* 12 : 59 -64. ibm.

Mattjus, P. & J. P. Slotte. (**1994**) Availability for enzyme-catalyzed oxidation of cholesterol in mixed monolayers containing both phosphatidylcholine and sphingomyelin. *Chem. Phys. Lip.*, 71 : 73 - 81.

Mattjus, P., G. Hedström & J. P. Slotte. (**1994**) Monolayer interaction of cholesterol with phosphatidylcholines: effects of phospholipid acyl chain length. *Chem. Phys. Lipids.* 75 : 195 -203.

Mautone, A. J., K. E. Reilly & R. Mendelsohn (**1987**) Fourier transform infrared and differential scanning calorimetric studies of surface - active material from rabbit lung. *Biochim. Biophys. Acta*, 896 : 1 - 10.

McConnell, H. M. (**1991**) Structures and transitions in lipid monolayers at the air-water interface. *Ann. Rev. Phys. Chem.*, 42 : 171 - 195.

McConnell. H. M. (**1993**) Surface dipole densities in lipid monolayers. *J. Phys. Chem.* 97 : 6686 - 6691.

McConnell, H. M., P. A. Rice & D. J. Benvegnu (1990) Brownian motion of lipid domains in electrostatic traps in monolayers. *J. Phys. Chem.*, 94 : 8965 - 8968.

McEachren, T. & K. M. W. Keough (**1995**) Phosphocholine reverses inhibition of pulmonary surfactant adsorption caused by C-reactive protein. *Am. J. Physiol.*, 269 : 492 - 497.

McLean, L. R., & J. E. Lewis. (**1995**) Biomimectic pulmonary surfactant. *Life Sciences*, 56 : 363 - 378.

Mead, J., J. L. Whittenberger & E. P. Radford. Jr. (**1957**). Surface tension as a factor in pulmonary volume - pressure hysteresis. *J. Appl. Physiol.*, 10 : 191 - 196.

Meller, P. (**1988**) Computer-assisted video microscopy for the investigation of monolayers on liquid and solid substrates. *Rev. Sci. Instrum.* 59 : 2225 - 2231.

Mendelsohn, R., J. W. Brauner & A. Geircke (**1995**) External infrared reflection adsorption spectrometry of monolayer films at the air-water interface. *Ann. Rev. Phys. Chem.*, 46 : 305 -334.

Merkel, R. & E. Sackmann (**1994**) Non stationary dynamics of excimer formation in two-dimensional fluids. *J. Phys. Chem.* 98 : 4428 - 4442.

Mikrut, J. M., P. Dutta, J. B. Ketterson & R. C. MacDonald (**1993**) Atomic-force and fluorescence microscopy of Langmuir-Blodgett monolayers of L-α-dimyristoylphosphatidic acid. *Phys. Rev. B*, 48 : 14479 - 14487.

Mischel, M. J., J. Seelig, L. F. Braganza & G. Buldt. (**1987**) A neutron diffraction study of the headgroup conformation of phosphatidylglycerol from Escherechia coli membranes. *Chem. Phys. Lip.*, 43 : 237 - 246.

Möhwald, H. (**1990**) Phospholipid & phospholipid-protein monolayers at the air/water interface. *Ann. Rev. Phys. Chem.* 41 : 441 - 476.

Möhwald, H., A. Dietrich, C. Böhm, G. Brezesinski & M. Thoma (**1995**) Domain formation in monolayers. *Mol. Membr. Biol.*, 12 : 29 - 38.

Möhwald H., H. Haas & S. Kirsten. (**1988**) Pattern formation of molecules adsorbing on lipid monolayers. in *Random Fluctuation and Pattern Growth: Experiments and Models*. Eds. H. E. Stanley & N. Ostrowsky, NATO/ASI Series E., Cargese, France. 110 - 116.

Montero, M. T., J. Hernandez-Borrel, K. Nag & K. M. W. Keough. (**1994**). Fluoroquinolone distribution in a phospholipid environment studied by spectrofluorimetry. *Anal. Chim. Acta* 2900 : 58 - 64.

Morley, C. J., A. D. Bangham, P. Johnson, G. D. Thorburn & G. Jenkins (**1978**). Physical and physiological properties of dry lung surfactant. *Nature*. 271 : 162 - 163.

Morrow, M. R., J. Perez-Gil, G. Simatos, C. Boland, J. Stewart, D. Absolom, V. Sarin & K. M. W. Keough. (**1993**a) Pulmonary surfactant-associated protein SP-B has little effect on the acyl chains in dipalmitoylphosphatidylcholine dispersions. Biochemistry, 32 : 4397 - 4402.

Morrow, M. R., S. Taneva, G. A. Simatos, L. A. Alwood & K. M. W. Keough. (**1993**b) ^{2}H NMR studies of the effect of pulmonary surfactant SP-C on the 1,2-dipalmitoyl-sn-glycero-3-phosphocholine headgroup: A model for transbilayer peptides in surfactant and biological membrane. *Biochemistry*, 32 : 11338 - 11344.

Mouritsen, O. G. , J. H. Ipsen & M. Zuckerman (**1989**) Lateral density fluctuation in the chain - melting phase transition of lipid monolayers. *J. Coll. Interf. Sci.*, 129 : 32 - 40.

Müller-Landau, F. & D. A. Cadenhead. (**1979**) Molecular packing in steroid-lecithin

monolayers, part II: mixed films of cholesterol with dipalmitoylphosphatidylcholine and tetradecanoic acid. *Chem. Phys. Lip.*, 25 : 315 - 328.

Müller-Landau, F., D. A. Cadenhead & B. M. J. Kellner (**1980**) The nature of the liquid expanded/liquid condensed phase change in insoluble monolayers at the air - water interface. *J. Coll. Interf. Sci.*, 73 : 264 - 266.

Munakata, H., R. B. Nimberg, G. L. Snider, A. G. Robins, H. VanHalbeek, J. F. G. Vligenthart & K. Schmid (**1982**) The structure of the new carbohydrate units of 36 kDa glycoprotein derived from lung lavage of a patient with alveolar proteinosis by high resolution ^{1}H-NMR spectroscopy. *Biochim. Biophys. Res. Commun.*, 108 : 1401 - 1405.

Nag, K. (**1991**) An epifluorescence microscopic surface balance to observe monolayers at the air-water interface. *MSc Thesis*, Memorial University of Newfoundland.

Nag, K. & K. M. W. Keough. (**1993**) Epifluorescence microscopic studies on monolayers containing mixtures of dioleyl and dipalmitoylphosphatidylcholine. *Biophys. J.*, 65 : 1019 - 1026.

Nag, K., N. H. Rich, C. Boland & K. M. W. Keough (**1990**) Design and construction of an epifluorescence microscopic surface balance for the study of lipid monolayer phase transitions. *Rev. Sci. Instrum.*, 61 : 3425 - 3430.

Nag, K., N. H. Rich, C. Boland & K. M. W. Keough (**1991**) Epifluorescence microscopic observation of monolayers of dipalmitoylphosphatidylcholine: dependence of domain size on compression rates. *Biochim. Biophys. Acta,* 1068 : 157 - 160.

Nag, K., N. H. Rich & K. M. W. Keough (**1994**). Interaction between dipalmitoylphosphatidylglycerol and phosphatidylcholines and calcium. *Thin Solid Films,* 244 : 841 - 844.

Nagle, J. F. (**1980**) Theory of the main lipid bilayer phase transition. *Ann. Rev. Phys. Chem.*, 31 : 157 - 195.

Netz, R. R., D. Andelman & H. Orland (**1996**) Protein adsorption on lipid monolayers at their coexistence region. *J. Physiq. (France)*, 6 : 1023 - 1047.

Nielson D.W. (**1986**) Electrolyte composition of pulmonary alveolar subphase in anaesthetized rabbits. *J. Appl. Physiol.* 60 : 972 - 979.

Nielson, D. W. & M. B. Lewis. (**1988**) Calcium increases in pulmonary alveolar fluid in lambs at birth. *Pediat. Res.*, 24 : 322 - 325.

Notter, R. H., H. Holcomb & R. D. Mavis (**1980a**). Dynamic surface properties of phosphatidylglycerol - dipalmitoyl phosphatidylcholine mixed films. Chem. Phys. Lip.

27 : 305 -319.

Notter, R. H., S. A. Tabak & R.D. Mavis. (**1980**b) Surface properties of binary mixtures of some pulmonary surfactant components. *J. Lip. Res.*, 21 : 10 - 22.

Notter, R. H., D. Shapiro, B. Ohning & J. A. Whitsett. (**1987**) Biophysical activity of synthetic phospholipids combined with purified lung surfactant 6000 dalton apoprotein. *Chem. Phys. Lip.*, 44 : 1 - 17.

Obalden M. (**1992**) History of surfactant research. in *Pulmonary Surfactant: from molecular biology to clinical practice.* Eds. B. Robertson, L. M. G. Van Golde & J. J. Batenburg. Elsevier Science Publishers B.V., Amsterdam. Ch. 1.

Ohmer-Schröck, D., C. Schlatterer, H. Plattner & J. Schlepper-schäfer (**1995**) Lung surfactant protein A (SP-A) activates a phosphoinositide/calcium signalling pathway in alveolar macrophages. *J. Cel. Sci.*, 108 : 3695 - 3702.

Oosterlaken-Dijksterhuis, M. A., H. P. Haagsman, L. M. G VanGolde & R. A. Demel (**1991**a) Characterization of lipid insertion into monomolecular layers mediated by surfactant protein SP-B and SP-C. *Biochemistry*, 30 : 10965 - 10971.

Oosterlaken-Dijksterhuis, M. A., H. P. Haagsman, L. M. G. VanGolde & R.A. Demel

(**1991**b) Interaction of lipid vesicles with monomolecular layers containing lung surfactant proteins SP-B or SP-C. *Biochemistry*, 30 : 8276 - 8281.

Otis, D.R.(Jr), E. P. Ingenito, R. D. Kamm & M. Johnson (**1994**). Dynamic surface tension of surfactant TA : Experiments and theory. *J. Appl. Physiol.*, 77 : 2681 - 2688.

Oyarzun, M.J., J. A. Clements & A. Baritussio (**1980**) Ventilation enhances pulmonary alveolar clearance of radioactive dipalmitoylphosphatidylcholine in liposomes. *Am. Rev. Respir. Dis.*, 121 : 709 - 721.

Pallas, N.R. & B. A. Pethica (**1985**) Liquid - expanded to liquid condensed transitions in lipid monolayers at the air/water interface. *Langmuir*, 1 : 509 - 513.

Panaiotov, I., Tz. Ivanova, J. Proust, F. Boury, B. Denizot, K. Keough & S. Taneva (**1996**) Effect of hydrophobic protein SP-C on structure and dilational properties of the model monolayers of pulmonary surfactant. *Coll. & Surf.*, 6: 243 - 260.

Pastrana, B., A. J. Mautone, & R. Mendelsohn. (**1991**) Fourier transform infrared studies of secondary structure and oreintation of pulmonary surfactant SP-C and its effects on the dynamic surface properties of phospholipids. *Biochemistry*, 30 : 10058 - 10064.

Pastrana-Rios, B, C. R. Flach, J. W. Brauner, A. T. Mautone & R. Mendelsohn (**1993**) A direct test of the " Squeeze-Out" hypothesis of lung surfactant function. External reflection FT-IR at the air-water interface. *Biochemistry.*, 33 : 5121 - 5127.

Pastrana-Rios, B., S. Taneva, K. M. W. Keough, A. J. Mautone & R. Mendelsohn (**1995**) External reflection absorption infrared spectroscopy study of lung surfactant proteins SP-B and SP-C in phospholipid monolayers at the air water interface. *Biophys. J.*, 69 : 2531 - 2540.

Pathy, L. (**1991**) Homology of the precursor of pulmonary surfactant associated protein SP-B with prosaposin and sulphated glycoprotein-1. *J. Biol. Chem.*, 266 : 6035 - 6037.

Pattle, R. E. (**1955**) Properties, function and origin of the alveolar lining layer. *Nature*, 175 : 1125 - 1126.

Pattle, R. E. (**1977**) The relation between surface tension and area in the alveolar lining film. *J. Physiol. (London)*, 269 : 591 - 604.

Pattus, I., C. Rothlen, M. Streit & P. Zahler. (**1981**) Further studies on the spreading of biomembranes at the air/water interface: structure, composition, enzymatic activities of human erythrocyte and sarcoplasmic reticulum membrane films. *Biochim. Biophys. Acta*, 647 : 29 -39.

Perez-Gil, J., C. Casals & D. Marsh (**1995**) Interactions of hydrophobic lung surfactant proteins SP-B and SP-C with dipalmitoylphosphatidylcholine and dipalmitoylphosphatidylglycerol bilayers studied by electron spin resonance. *Biochemistry*, 34 : 3964 - 3971.

Perez-Gil, J., A. Cruz & C. Casals (**1993**) Solubility of hydrophobic surfactant proteins in organic solvent/water mixtures. Structural studies on SP-B and SP-C in aqueous organic solvents and lipids. *Biochim. Biophys. Acta*, 1168 : 261 - 270.

Perez-Gil J., J. L. Lopez-Lacomba, A. Cruz, A. Beldarrain & C. Casals. (**1994**) Deacylated pulmonary surfactant protein SP-C has different effects on the thermotropic behaviour of bilayers of dipalmitoylphosphatidylglycerol(DPPG) than the native acylated protein. *Biochem. Soc. Trans.*, 22 : 372S.

Perez-Gil, J., K. Nag, S. Taneva & K. M. W. Keough. (**1992**a) Pulmonary surfactant protein SP-C causes packing rearrangements of dipalmitoylphosphatidylcholine in spread monolayers. *Biophys.J.*, 63 : 197 - 204.

Perez-Gil, J., J. Tucker, G. Simatos & K. M. W. Keough. (**1992**b). Interfacial adsorption of simple lipid mixtures combined with hydrophobic surfactant protein from pig lung. *Biochem. Cel. Biol.*, 70 : 332 - 338.

Peschke, J. & H. Möhwald. (**1987**) Cytochrome C interaction with phospholipid monolayers and vesicles. *Coll. & Surf.*, 27 : 305 - 323.

Peters, R. & K. Beck. (**1983**) Translational diffusion in phospholipid monolayers measured by fluorescence microphotolysis. *Proc. Natl. Acad. Sci. USA.*, 80 : 7184 - 7187.

Phillips, M. C. & D. Chapman. (**1968**) Monolayer characteristics of saturated 1,2-diacyl phosphatidylcholines (lecithins) and phosphatidylethanolamines at the air-water interface. *Biochim. Biophys. Acta*, 163 : 301 - 313.

Phillips M. C., B. D. Ladbrooke & D. Chapman. (**1970**) Molecular interaction in mixed lecithin systems. *Biochim. Biophys. Acta* 196 : 35 - 44.

Pink, D. A. (**1984**) Theoretical studies of phospholipid bilayers and monolayers. Perturbing probes, monolayer phase transitions and computer simulation of lipid-protein bilayers. *Can. J. Bioch. Cel. Biol.*, 62 : 760 - 777.

Pison U., J. R. Wright & S. Hawgood (**1992**) Specific binding of surfactant apoprotein SP-A to rat alveolar macrophages. *Am. J. Physiol.* 262 : 412 - 417.

Possmayer, F. (**1988**) A proposed nomenclature for pulmonary surfactant-associated

proteins. *Am. Rev. Respir. Res.*, 138 : 990 - 998.

Possmayer, F. (**1991**) Biophysical activities of pulmonary surfactant. In *Fetal and Neonatai Physiology*. Eds. R. A. Polin & W. W. Fox., W. B. Saunders Co., Philadelphia. Ch. 90. 949 - 962.

Post, A., A. V. Nahmen, M. Schmitt, M. Ruths, H. Riegler, M. Seiber & H.-J. Galla. (**1995**) Pulmonary surfactant protein C containing lipid films at the air-water interface as a model for the surface of lung alveoli. *Mol. Membr. Biol.*, 12 : 93 - 99.

Poulain, F. R., L. Allen, M. C. Williams, R. L. Hamilton & S. Hawgood (**1992**) Effects of surfactant apolipoproteins on liposome structure: implication for tubular myelin formation. *Am. J. Physiol.*, 262 : 730-739.

Poulain, F.R., S. Nir & S. Hawgood (**1996**) Kinetics of phospholipid membrane fusion induced by surfactant apoproteins A and B. *Biochim. Biophys. Acta*, 1278 : 169 - 175.

Putz, G., J. Goerke & J. A. Clements. (**1994**) Surface activity of rabbit pulmonary surfactant subfraction at different concentration in a captive bubble. *J. Appl. Physiol.*, 77 : 597 - 605.

Quanbar, R. & F. Possmayer (**1995**) On the surface activity of surfactant-associated

protein C (SP-C): effects of palmitoylation and pH. *Biochim. Biophys. Acta*, 1255 : 251 - 259.

Rana F. R., A. T. Mautone & R. A. Dluhy (**1993**) Surface chemistry of binary mixtures of phospholipids in monolayers. Infrared studies of surface composition at varying surface pressures in a pulmonary surfactant model system. *Biochemistry*, 32 : 1169 - 3177.

Reichert, A., H. Ringsdorf & A. Wagenecht (**1992**) Spontaneous domain formation of phospholipase A_2 at interfaces: fluorescence microscopy of the interaction of phospholipase A_2 with mixed monolayers of lecithin, lysolecithin and fatty acid. *Biochim. Biophys. Acta*, 1106 : 178 - 188.

Reilly, K. E., A. J. Mautone & R. Mendelsohn (**1989**) Fourier-Transform Infrared Spectroscopy studies of lipid/protein interactions in pulmonary surfactant. *Biochemistry*, 28 : 7368 - 7373.

Rice, P. A. & H. M. McConnell. (**1989**) Critical shape transitions of monolayer lipid domains. *Proc. Natl. Acad. Sci. USA.*, 86 : 6445 - 6448.

Rice, W. R., V. K. Sarin, T. L. Fox, J. Baatz, S. Wert & J. A. Whitsett (**1989**). Surfactant peptides stimulate uptake of phosphatidylcholine by isolated cells. *Biochim.*

Biophys. Acta., 1006 : 237 - 245.

Robertson, R. N. (**1983**) *The Lively Membranes*. Cambridge University Press., NY.

Rodgers, W. & M. Glaser (**1991**) Characterization of lipid domains in erythrocyte membranes. *Proc. Natl. Acad. Sci. USA.*, 88 : 1364 - 1368.

Ross, G. F., R. H. Notter, J. Merit & J. A. Whitsett (**1986**) Phospholipid binding and biophysical activity of pulmonary surfactant associated protein (SAP-35) and its non-collagenous COOH-terminal domains. *J. Biol. Chem.*, 261 : 14283 - 14291.

Ruano, M. L. F., E. Miguel, J. Perez-Gil & C. Casals (**1996**) Comparison of lipid aggregation and self aggregation activities of surfactant-associated protein A. *Biochem. J.*, 313 : 683 - 689.

Ruano, M. L. F., K. Nag, C. Casals, J. Perez-Gil & K. M. W. Keough (**1997**) Differential partitioning of pulmonary surfactant protein SP-A in liquid-condensed and liquid-expanded regions of spread monolayers of dipalmitoylphosphatidylcholine and DPPC/dipalmitoylphosphatidylglycerol. *Biophys. J.* submitted.

Rüstow, B., R. Haupt, P. A. Stevens & D. Kunze (**1993**) Type-II pneumocytes secrete vitamin E together with surfactant lipids. *Am. J. Physiol.*, 265 : 133 - 139.

Rüstow B, I. Kalleck, F. Guthmann, R. Haupt, D. Kunze & P.A. Stevens (**1994**). Synthesis and secretion of plasmalogens of type-II pneumocytes. *Biochem. J.*, 302 : 665 - 668.

Ryba N. J. P. & D. Marsh. (**1992**) Protein rotational diffusion and lipid/protein interaction in recombinant of bactereorhodopsin with saturated diacyl phosphatidylcholines of different chain lengths studied by conventional and saturation transfer electron spin resonance. *Biochemistry*, 31 : 7511 - 7518.

Sacré M. M. & J. F. Tocanne (**1977**). Importance of glycerol and fatty acid residues on the ionic properties of phosphatidylglycerols at the air-water interface. *Chem. Phys. Lip.*, 18 : 334 -354.

Salesse, C., D. Duchrame & R. M. Leblanc. (**1987**) Direct evidence for the formation of a monolayer from a bilayer. *Biophys. J.*, 52 : 351 - 352.

Sankaram, M. B., D. Marsh & T. E. Thompson (**1992**) Determination of fluid and gel domain sites in two - component, two - phase lipid bilayer. An electron spin resonance spin label study. *Biophys. J.*, 63 : 340 - 349.

Sarin, V. K., S. Gupta, T. K. Leung, V. E. Taylor, B. L. Ohning, J. A. Whitsett & J . L. Fox (**1990**). Biophysical and biological activity of a synthetic 8.7 kDa hydrophobic

pulmonary surfactant protein SP-B. Proc. *Natl. Acad. Sci. USA.*, 87, 2633-2637.

Scarpelli, E. M. & A. T. Mautone (**1994**). Surface biophysics of the surface monolayer theory is incompatible with regional lung function. *Biophys. J.*, 67 : 1080 - 1089.

Scherer, P. G & J. Seelig (**1987**) Structures and dynamics of the phosphatidylcholine and the phosphatidylethanolamine headgroup in L-M fibroblast studied by deuterium nuclear magnetic resonance. *EMBO J.*, 6 : 2915 - 2922.

Schindler, H. (**1979**) Exchange and interactions between lipid layers at the surface of a liposome solution. *Biochim. Biophys. Acta*, 555 : 316 - 336.

Schindler, H. (**1989**) Planar lipid-protein membranes: strategies of formation and detecting dependence of ion transport function on membrane conditions. *Meth. Enzymol.*, 171 : 225 - 253.

Schroeder, F., J. K. Woodford, J. Kavecansky, W. G. Wood & C. Joiner. (**1995**) Cholesterol domains in biological membranes. *Mol. Memb. Biol.*, 12 : 113 - 119.

Schürch S. & H. Bachofen (**1995**) Biophysical aspects in the design of a therapeutic surfactant in *Surfactant Therapy for Lung Diseases*. Eds. B. Robertson & H. W. Tauesch., Mercel Dekker, Inc., NY, 3 - 32.

Schürch, S., H. Bachofen, J. Goerke & F. Green (**1992**a). Surface properties of rat pulmonary surfactant studied with the captive bubble method: adsorption, hysteresis, and stability. *Biochim. Biophys. Acta*, 1103 : 127 - 136.

Schürch, S. H. Bachofen, J. Goerke & F. Possmayer (**1989**). A captive bubble method reproduces the in situ behaviour of lung surfactant monolayers. *J. Appl.Physiol.* 67 : 2389 -2396.

Schürch, S., H. Bachofen & E. R. Weibel (**1985**). Alveolar surface tensions in excised rabbit lungs: Effect of temperature. *Respir. Physiol.* 62 : 31 - 45.

Schürch, S., J. Goerke & J. A. Clements. (**1976**) Direct determination of surface tension in the lungs. *Proc. Natl. Acad. Sci. USA.*, 73 : 4698 - 4702.

Schürch, S., J. Goerke & J. A. Clements. (**1978**) Direct determination of volume- and time- dependence of alveolar surface tension in excised lung. *Proc. Natl. Acad. Sci. USA.*, 75 : 3417 - 3421.

Schürch, S., F. Possmayer, S. Cheng & A. M. Cocksutt (**1992**b) Pulmonary SP-A enhances adsorption and appears to induce surface sorting of lipid extract surfactant. *Am. J. Physiol.*, 163 : 210 - 218.

Schürch, S., D. Schürch, T. Curstedt & B. Robertson (**1994**) Surface activity of lipid extract surfactant in relation to film area compression and collapse. *J. Appl. Physiol.*, 77 : 974 - 986.

Schürholz, T., & H. Schindler. (**1991**) Lipid-protein surface films generated from membrane vesicles: self assembly, composition, and film structure. *Eur. Biophys. J.*, 20 : 71 - 78.

Seager, W, A. Elssrer, A. Gunther, A. Knamer & H. O. Kalinowshi (**1993**) Lung surfactant phospholipid associate with polymerizing fibrin: loss of surface activity. *Am. J. Respir. Cel. Mol. Biol.*, 9 : 213 - 220.

Seelig J. & A. Seelig (**1980**) Lipid conformation in model and biological membranes. *Quart. Rev. Biophys.*, 13 : 19 - 61.

Seul, M. (**1990**) Domain wall fluctuations and instabilities in monomolecular films. *Physica A.* 168 : 198 - 209.

Seul, M. & D. Andelman (**1995**) Domain shapes and patterns : The phenomenology of modulated phases. *Science*, 267 : 476 - 483.

Seul, M. & M. J. Sammon (**1990**) Competing interactions and domain-shape instabilities

in a monomolecular film at an air-water interface. *Phys. Rev. Lett.*, 64 : 1903 - 1906.

Seul, M., M. J. Sammon & L. R. Monar (**1991**) Imaging of fluctuating domain shapes : Methods of image analysis and their implementation in a personal computing environment. *Rev. Sci. Instrum.* 62 : 784 - 792.

Shiffer, K., S. Hawgood, N. Düzgünes & J. Goerke (**1988**) Interactions of the low molecular weight group of surfactant-associated proteins (SP 5-18) with pulmonary surfactant lipids. *Biochemistry*, 27 : 2689 - 2695.

Shiffer, K., S. Hawgood, H. P. Haagsman, B. Benson, J. A. Clements & J. Goerke (**1993**) Lung surfactant proteins, SP-B and SP-C, alter the thermodynamic properties of phospholipid membranes: A differential calorimetry study. *Biochemistry*, 32 : 590 - 597.

Shimomura, M.R., R. Fuji, T. Shimamura, M. Oguchi, E. Shinohara, Y. Nagata, M. Matsubara & K. Koshishi (**1992**) Effect of thermal treatment on crystal growth of the surface monolayer. *Thin Solid Films*, 210/211 : 98 - 100.

Signor, G., S. Mammi, E. Peggion, H. Ringsdorf & A. Wagenknecht. (**1994**). Interaction of bombolitin III with phospholipid monolayers and liposomes and effect on the activity of phospholipase A_2. *Biochemistry,* 33 : 6659 - 6670.

Simatos, G., K. B. Forward, M. R. Morrow & K. M. W. Keough. (**1990**) Interaction between predeuterated dimyristoylphosphatidylcholine and low molecular weight pulmonary surfactant protein SP-C. *Biochemistry*, 29 : 5807 - 5814.

Singer S. J. & G. L. Nicholson (**1972**) The fluid mosaic model of the structure of cell membrane. *Science*, 175 : 720 - 731.

Slotte, J. P. (**1995**) Lateral domain formation in mixed monolayers containing cholesterol and dipalmitoylphosphatidylcholine or N-palmitoylsphingomyelin. *Biochim. Biophys. Acta*, 1235 : 419 - 427.

Slotte, J. P., & P. Mattjus. (**1995**) Visualization of lateral phases in cholesterol and phosphatidylcholine monolayers at the air/water interface- a comparative study with two different reporter molecules. *Biochim. Biophys. Acta*, 1254 : 22 - 29.

Smaby, J. M., H. L. Brockman & R. E. Brown. (**1994**) Cholesterol's interfacial interactions with sphingomyelins and phosphatidylcholines: hydrocarbon chain structure determines the magnitude of condensation. *Biochemistry*, 33 : 9135 - 9142.

Smith, B.T. (**1995**) Surfactant research: conclusions and perspectives for the future. *Appl. Cardiopulm. Pathophysiol.*, 5(su.1): 3 - 5.

Smith, G.B., H. W. Taeusch, D. S. Phelps & K. M. W. Keough (**1988**) Mixtures of low molecular weight surfactant proteins and dipalmitoylphosphatidylcholine duplicate the effects of pulmonary surfactant in Vitro and in Vivo. *Pediatr. Res.*, 23 : 484 - 489.

Smutzer G., & P. L. Yeagle. (**1985**) A fluorescence anisotropy study on the phase behaviour of dimyristoylphosphatidylcholine / cholesterol mixtures. *Biochim. Biophys. Acta*. 814 : 274 -280.

Snik, A. F. M., A. J. Kruger & P. Joos. (**1978**) Dynamical behaviour of monolayers of dipalmitoyl lecithin and cholesterol. *J. Coll. Interf. Sci.*, 66 : 435 - 439.

Stern, L., R. D. Angeles, E.W. Outerbridge & P. H. Beaudry (**1970**) Negative pressure artificial respiration: use in treatment of respiratory failure of the newborn. *Can. Med. Assoc. J.*, 102 : 595 - 601.

Stine K.J. (**1994**) Investigations of monolayers by fluorescence microscopy. *Micr. Res. Tech.*, 27 : 439 - 450.

Subirade, M., C. Salesse, D. Marion & M. Pézelot (**1995**) Interaction of a nonspecific lipid transfer protein with phospholipid monolayers imaged by fluorescence microscopy and studied by infrared spectroscopy. *Biophys. J.*, 69 : 974 - 988.

Subramaniam, S. & H. M. McConnell. (**1987**) Critical mixing in monolayer mixtures of phospholipid and cholesterol. *J. Phys. Chem.*, 91 : 1715 - 1718.

Suzuki, Y., T. Curstedt, G. Grossman, T. Kobayashi, R. Nilsson, K. Nohara & B. Robertson (**1986**) Experimental studies on the role of the low-molecular weight (< 15,000-dalton) apoproteins of pulmonary surfactant. *Eur. J. Respir. Dis.*, 69 : 336 - 345.

Suzuki, Y., Y. Fujita & K. Kogishi (**1989**) Reconstitution of tubular myelin from synthetic lipids and proteins associated with pig pulmonary surfactant. *Am. Rev. Respir. Disease.*, 140 : 75 -81.

Swalen, J. D., D. L. Allara, J. D. Andrade, E. A. Chandross, S. Garoff, J. Israelachvilli, T.J. McCarthy, R. Murray, R. F. Pease, J. F. Robolt, K. J. Wynne & H. Yu (**1987**) Molecular monolayers and films. *Langmuir*, 3 : 932 - 950.

Takahashi, A. & T. Fujiwara. (**1986**) Proteolipid in bovine lung surfactant: its role in surfactant function. *Biochim. Biophys. Res. Commun.*, 135 : 527 - 532.

Takahasi, A., A. J. Waring, J. Amirkhanian, B. Fan, & H. W. Taeusch (**1990**) Structure function relationships of bovine pulmonary surfactant proteins SP-B and SP-C. *Biochim. Biophys. Acta*, 1044 : 43 - 49.

Tanaka, Y., T. Takei, T. Aiiba, K. Masuda, A. Kiushi & T. Fujiwara, (**1986**) Development of synthetic lung surfactants. *J. Lip. Res.*, 27 : 475 - 485.

Taneva, S., & K. M. W. Keough. (**1995**). Calcium ions and interactions of pulmonary surfactant proteins SP-B and SP-C with spread monolayers at the air-water interface. *Biochim. Biophys. Acta,* 1236 : 185 - 195.

Taneva, S., & K. M. W. Keough. (**1994**). Dynamic surface properties of pulmonary surfactant proteins SP-B and SP-C and their mixtures with dipalmitoylphosphatidylcholine. *Biochemistry*, 33 : 14660 - 14670.

Taneva, S. & K. M. W. Keough (**1994**a) Pulmonary surfactant proteins SP-B and SP-C in spread monolayers at the air-water interface: I. Monolayers of pulmonary surfactant protein SP-B and phospholipids. *Biophys. J.*, 66: 1158-1168.

Taneva, S. & K. M. W. Keough. (**1994**b). Pulmonary surfactant proteins SP-B and SP-C in spread monolayers at the air-water interface: II. Monolayers of pulmonary surfactant protein SP-C and phospholipids. *Biophys. J.*, 66 : 1149 - 1157.

Taneva, S. & K. M. W. Keough. (**1994**c) Pulmonary surfactant proteins SP-B and SP-C in spread monolayers at the air-water interface: III. Proteins SP-B plus SP-C with phospholipids in spread monolayers. *Biophys. J.*, 66 : 1158 - 1168.

Taneva, S., T. McEachren, J. Stewart & K. M. W. Keough (**1995**) Pulmonary surfactant protein SP-A with phospholipids in spread monolayers at the air-water interface. *Biochemistry*, 34 : 10279 - 10289.

Taneva, S, I. Panaiotov & L. Ter-Minassian-Saraga (**1984**) Effect of surface pressure on mixed dipalmitoyl lecithin - serum albumin monolayer composition. *Coll. & Surf.*, 10: 101 - 111.

Tchoreloff P., A. Gulik, B. Denizot, J. E. Proust & F. Puisieux. (**1991**) A structural study of interfacial phospholipid and lung surfactant layers by transmission electron microscopy after Blodgett sampling: influence of surface pressure and temperature. *Chem. Phys. Lip.*, 59 : 151 -165.

Teubuer, J. K., R. A. Gibson & E. J. McMurchie (**1983**) The influence of water on the phase transition of sheep lung surfactant, a possible mechanism for surfactant phase transition in vivo. *Biochim. Biophys. Acta*, 750 : 521 - 525.

Thewalt, J. L. & M. Bloom. (**1992**) Phosphatidylcholine: cholesterol phase diagrams. *Biophys. J.*, 63 : 1176 - 1181.

Thompson, N. L., H. M. McConnell & T. P. Burghardt (**1984**) Order in supported phospholipid monolayers detected by the dichroism of fluorescence excited with polarized

evanescent illumination. *Biophys. J.*, 46 : 739 - 747.

Thompson, T. E, M. B. Sankaram & R. L. Biltonen (**1992**) Biological membrane domains functional significance. *Comments in Mol. Cell. Biophs.* 8 : 1 - 15.

Tocanne, J.-F., L. Cézanne, A. Lopez, B. Piknova, V. Schram, J.-F. Tournier and M. Welby (1994) Lipid domains and lipid/protein interactions in biological membranes. Chem. Phys. Lip. 73 : 139 - 158. Ibm.

Tocanne, J. F. & J. Teissié (**1990**). Ionization of phospholipid and phospholipid-supported interfacial lateral diffusion of protons in membrane model system. *Biochim. Biophys Acta*, 1031 : 111 - 142.

Träuble, H., & E. Sackman (**1972**) Studies of the crystalline - liquid crystalline phase transition of lipid model membranes. III. Structure of a steroid - lecithin system below and above the lipid phase transition. *J. Am. Chem. Soc.*, 94 : 4499 - 4510.

Träuble, H., H. Eibl & H. Sawada (**1974**). Respiration a critical phenomenon ? Liquid phase transition in the lung alveolar surfactant. *Naturwissenchaften*, 61 : 344 - 354.

Tredgold, R. H. (**1994**) *Order in Thin Organic Films*. Cambridge University Press, Cambridge (England).

Ueda, T., M. Ikegami & A. H.Jobe (**1995**) Clearance of surfactant protein A from rabbit lungs. *Am. J. Respir. Cell Mol. Biol.*, 12 : 89 - 94.

Ullman A. (**1991**) *An Introduction to Ultra Thin Organic Films, from Langmuir - Blodgett to Self Assembly*. Academic Press, Inc., San Diego, CA., Ch. 1.1 - 1.4.

Vandenbussche, G., A. Clercyx, M. Clercyx, T. Curstedt, J. Johansson, H. Jörnvall & J.-M. Ruysschaert (**1992**a) Secondary structure and orientation of the surfactant protein SP-B in a lipid environment: A Fourier transform infrared spectroscopy study. *Biochemistry*, 31 : 9169 - 9176.

Vandenbussche, G., A. Clercx, T. Curstedt, J. Johansson & H. Jornvall. (**1992**b). Structure and orientation of the surfactant-associated protein C in a lipid bilayer. *Eur. J. Biochem.*, 203 : 201 - 209.

Vanderlick, T. K. & H. Möhwald (**1990**) Mode selection and shape transitions of phospholipid monolayer domains. *J. Phys. Chem.*, 94 : 886 - 890.

VanGolde, L. M. G. (**1995**) Potential role of surfactant proteins A and D in innate lung defence against pathogens. *Biol. Neonate*, 67:2 - 17.

VanGolde, L. M. G., J. J. Battenburg & B. Robertson (**1994**) The pulmonary surfactant

system. *News in Physiol. Sci.*, 9 : 13 - 20.

Vaz, W. L. C., E. C. C. Melo & T. E. Thompson (**1989**) Translational diffusion and fluid domain connectivity in a two-component, two phase phospholipid bilayer. *Biophys. J.*, 56 : 869 -876.

Veldhuizen, R. A. W., K. Inchley, S. A. Hearn, J. F. Lewis & F. Possmayer. (**1993**) Degradation of surfactant associated protein B (SP-B) during in vitro conversion of small surfactant aggregates. *Biochem. J.*, 295 : 141 - 147.

Venkitaraman, A. R., S. B. Hall, J. A. Whitsett & R. H. Notter (**1990**) Enhancement of biophysical activity of lung surfactant extracts and phospholipid-apoprotein mixtures by surfactant protein A. *Chem. Phys. Lip.* ,56 : 185 - 184.

Verkileij, A. J., B. DeKruyff, P. H. J. Th. Ververgaert, J. F. Tocanne & L. L. M. VanDeenen (**1974**) The influence of pH, Ca^{2+} and protein on the thermotropic behaviour of negetively charged phospholipid, phosphatidylglycerol. *Biochim. Biophys. Acta*, 339 : 432 - 437.

Vincent, J. S., S. D. Revak, D. Cochrane & I. W. Levin (**1993**) Interactions of model human pulmonary surfactant with a mixed phospholipid bilayer assembly: Raman spectroscopic studies. *Biochemistry*, 32 : 8228 - 8238.

Vincent, J. S., S. D. Revak, D. Cochrane & I. W. Levin (**1991**) Raman spectroscopic studies of model human pulmonary surfactant systems: phospholipid interactions with peptide paradigms for the surfactant protein SP-B. *Biochemistry*, 30 : 8394 - 8401.

Vist, M. R. & J. H. Davis (**1990**). Phase equilibria of cholesterol / dipalmitoylphosphatidylcholine mixtures: ^{2}H nuclear magnetic resonance and differential scanning calorimetry. *Biochemistry*, 29 : 451 - 464.

Von Tscharner V. & H. M. McConnell (**1981**) An alternative view of phospholipid phase behaviour at the air - water interface. *Biophys. J.*, 36 : 409 - 419.

Voorhout, W. F., T. Veenendaal, H. P. Haagsman, A. J. Verkleij, L. M. G. VanGolde & H. J. Geuze (**1991**) Surfactant protein A is localized at the corners of the pulmonary tubular myelin lattice. J. Histochem. Cytochem. 39 : 1331 - 1336.

Wang, M., C. Sun, W. J. P. VanEnckevort, J. VanEsch, G. Wildburg, R. W. Peng, N.B. Ming, P. Bennema, H. Ringsdorf & R. J. M. Nolte (**1996**) Pattern formations in lipid monolayers under illumination. *Phys. Rev. (E)*, 53 : 2580 - 2587.

Waring, A., M. Longo, J. Zasadzinski, R. Bruni & W. Taeusch (**1994**) Studies on the conformation, orientation and molecular topography of synthetic SP-B N-terminus in surfactant lipid films. *Prog. Respir. Res.*, 27 : 29 - 32.

Waring, A., W. Taeusch, R. Bruni, J. Amirkhanian, B. Fan, R. Stevens & J. Young (**1989**) Synthetic amphipathic sequences of surfactant protein-B mimic several physicochemical and in vivo properties of native pulmonary surfactant proteins. *Peptide Res.*, 2 : 308 - 313.

Watkins, J. C. (**1968**). The surface properties of pure phospholipid to those of lung extracts. *Biochim. Biophys. Acta,* 152 : 293 - 306.

Weaver T. E. & J. A. Whitsett (**1991**). Function and regulation of expression of pulmonary surfactant-associated proteins. *Biochem. J.*, 273 : 249 - 264.

Weibel E. R. & J. Gill (**1968**). Electron microscopic demonstration of an extracelluar duplex lining layer of alveoli. *Respir. Physiol.*, 4 : 42 - 47.

Weidemann, G. & D. Volhardt (**1996**) Long-range tilt orientational order in phospholipid monolayers: A comparative study. *Biophys. J.* ,70 : 2758 - 2766.

Weis, R. M. (**1991**) Fluorescence microscopy of phospholipid monolayer phase transitions. *Chem.Phys. Lip.*, 57 : 227 - 239.

Weis, R. M., & H. M. McConnell (**1985**) Cholesterol stabilizes the crystal-liquid interface in phospholipid monolayers. *J. Phys. Chem.* 89 : 4453 - 4459.

Weis, R. M. & H. M. McConnell. (1984) Two-dimensional chiral crystals of phospholipid. *Nature*, 310 : 47 - 49.

Welti, R. & M. Glaser (**1994**) Lipid domains in model and biological membrane. *Chem. Phys. Lip.*, 73 : 121 - 137.

White R. T., D. Damm, J. Miller, K. Spratt, H. J. Schilling, S. Hawgood, B. Benson & B. Cordell (**1985**) Isolation and characterization of the human pulmonary surfactant apoprotein gene. *Nature*, 317 : 361 - 363.

Whitsett, J.A., L. M. Nogee, T. E. Weaver & A. D. Horowitz (**1995**) Human surfactant protein B: Structure, function, regulation and genetic diseases. *Physiol. Rev.*, 75 : 749 - 757.

Wildeboer-Venema, F. (**1978**) A model for the study of physical behaviour of the lung-surfactant film in vitro. *Respir. Physiol.* 32 : 225 - 237.

Wilson, T. A. & H. Bachofen. (**1982**) A model for mechanical structure of the alveolar duct. *J. Appl. Physiol.*, 52 : 1064 - 1070.

Williams M. C. (1992) Morphologic aspects of the surfactant system. in *Pulmonary Surfactant: From Molecular Biology to Clinical Practice*. Eds. B. Robertson, L. M. G.

Van Golde & J.J. Battenburg, Elseiver, Amsterdam. Ch. 6.

Williams, M. C., S. Hawgood & R. L. Hamilton. (**1991**) Changes in lipid structure produced by surfactant proteins SP-A, SP-B and SP-C. *Am. J. Respir. Cell Mol. Biol.*, 5 : 41 - 50.

Wojciak J.F., R. H. Notter & A. Oberdöster (**1985**) Size stability of phosphatidylcholine - phosphatidylglycerol aerosols and a dynamic film compression state from their interfacial impaction. *J. Coll. Interf. Sci.*, 106 : 547 - 557.

Woodle, M. C. & D. Papahadjopoulos. (**1989**) Liposome preparation and size characterization. *Meth. Enzymol.*, 171 : 193 - 217.

Worcester, D. L. & N. P. Franks (**1976**). Structural analysis of hydrated egg lecithin and cholesterol bilayer. II. Neutron Diffraction. *J. Mol. Biol.* ,100 : 359 - 378.

Wright J. R. (**1990**) Clearance and recycling of pulmonary surfactant. *Am. J. Physiol.*, 259 : 1 - 12.

Wright J. R., B. J. Benson, M. C. Williams, J. Goerke & J. A. Clements. (**1984**) Protein composition of rabbit alveolar surfactant subfractions. *Biochim. Biophys. Acta*, 791 : 320 - 3327.

Yeagle, P.L. (**1985**) Cholesterol and the cell membrane. *Biochim. Biophys. Acta.* 822 : 267 -287.

Yeagle, P. L. (**1993**) The biophysics and cell biology of cholesterol: an hypothesis for the essential role of cholesterol in mammalian cells. in *Cholesterol in Membrane Models.* Ed. L. Finegold, CRC Press, Boca Raton, Florida. 1-12. ch.

Yu H. and S. W. Hui. (**1991**). Epifluorescence microscopy and spectroscopy studies of phosphatidylcholine monolayers. *Biophys. J.*, 59 : 629A.

Yu, S.-H. & F. Possmayer (**1993**) Adsorption, compression and stability of surface films from natural, lipid extract and reconstituted pulmonary surfactants. *Biochim. Biophys. Acta*, 1167 : 264 - 271.

Yu, S.-H. & F. Possmayer. (**1988**) Comparative studies on the biophysical activities of the low molecular weight hydrophobic proteins purified from bovine pulmonary surfactant. *Biochim. Biophys. Acta.*, 961 : 337 - 350.

Yu, S.-H., & F. Possmayer (**1990**) Role of bovine pulmonary surfactant associated proteins in the surface-active property of phospholipid mixtures. *Biochim. Biophys. Acta*, 1046 : 233 - 241.

Yu, S. -H, P. G. R. Harding & F. Possmayer (**1983**). Bovine pulmonary surfactant : Chemical composition and physical properties. *Lipids*, 18 : 522 - 529.

Yu, S.-H., & F. Possmayer (**1990**) Role of bovine pulmonary surfactant associated proteins in the surface-active property of phospholipid mixtures. *Biochim. Biophys. Acta*, 1046 : 233- 241.

Yukitake, K., C. L. Brown, M. A. Schlueter, J. A. Clements & S. Hawgood (**1995**) Surfactant apoprotein A modifies the inhibitory effect of plasma proteins on surfactant activity in vivo. *Pediat. Res.*, 37 : 21 - 25.

APPENDIX A

Image processing and analysis were performed using JAVA 1.4® (Jandel Video Analysis Software, Jandel Scientific, San Rafael, CA) software, in a IBM 486 personal computer. The programme (JAVA 1.4) requires a TARGA M8® (Truevision, AT & T, San Francisco, CA) video frame grabber board and a minimum memory of 612 kilo bytes or more. A video cassette recorder (VCR), feeds the frame grabber (installed in the PC) with analogue black and white images, which are frame grabbed by TARGA M8 and saved in memory of JAVA 1.4 digitally. Each image requires at least 198 kbyte of memory. These stored digital images can be later displayed on a TV monitor connected to the TARGA board, for processing and analysis. The total area of the images have been calibrated in the programme to be 7700 μm^2 (or 100 μm (breadth) x 77 μm (length). Randomly selected frames of monolayers (which look the most clear to the eye on the TV monitor) are frame grabbed, saved, processed and analyzed by the following steps:

Frame Grabbing:

The JAVA 1.4 is executable by typing in "newjava" at the DOS C:\ prompt. Once entered the programme displays the screen with menus as shown on the right Figure (A). By moving the mouse cursor to function *F3 Inten*, the intensity menu is entered. In this menu the *F2 Freeze* function frame grabs any image being played in the VCR. The frame grabbed image is saved by entering the *F6 Disk* command, and by typing in a name for the image (maximum 8 characters), and such images are stored as

*.TIFF files (198 kbytes) in the hard disk of the computer.

Image Processing:

The typical saved images (*.TIFF) are processed by loading them from the disk menu by successive commands of *F2 Image*, *F7 From Disk* and *F2 Load* (Figure B shows a typical loaded/digitized image). Then in the morphometric menu (Figure A), by using *^F3 Intern* and *IP* the image processing menu can be entered. In this menu an area of interest *F8 AOI* (rectangular box in the Figure (B) is selected for image processing, by moving the mouse cursor to the four ends of a rectangle or a

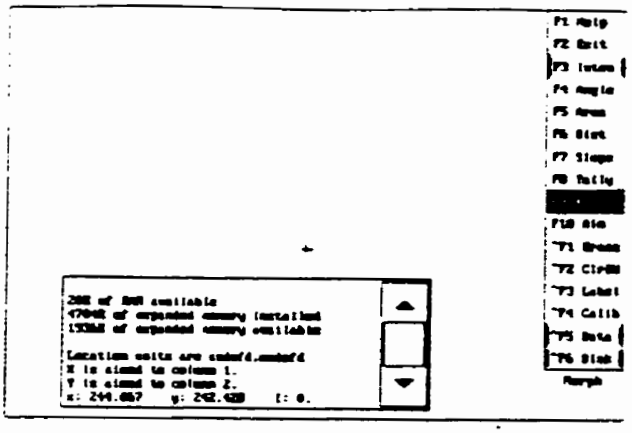

Figure 1 Morph Menu is Appears When Running

A

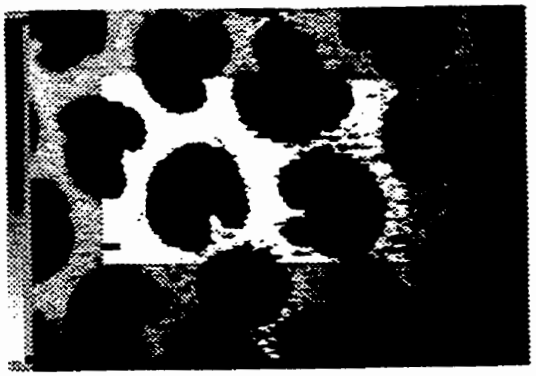

B

selected area of interest. The contrast of the AOI is increased by using *F3 Cont.En* cursor in the Log Intensity Histogram (Greyish histogram in Figure C) twice, and a typical processed area of interest (high contrast, rectangular box) as shown in Figure (B) is obtained.

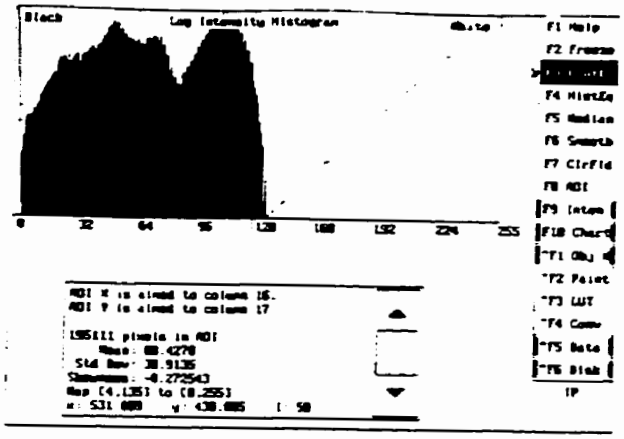

C

Image Analysis:

The image analysis is performed by using the Object Number menu (D). This menu can be accessed by using *^F1 Obj N* in the image processing menu. In the object number menu a threshold for the images is set by executing the *F7 Thres* command, to subtract the white background of the images and leave the images

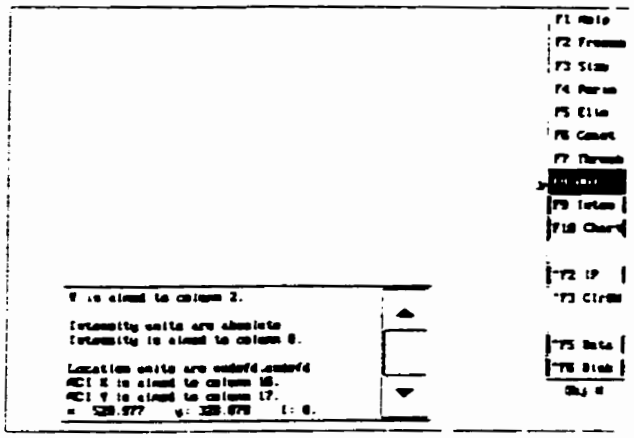

D

with only black pixels (condensed domains) to be measured. To measure and count such objects the *F6 Count* command is used twice, first to count and measure the objects and then to transfer the measurements to a data work sheet file. The counting is performed by the programme by measuring the number and x/y axis location of each black pixel in the image, and the movement of small black lines on the two end of the boxed image in Figure (B) which indicates the progress of such measurements. Then by entering *^F5 Data*, the data work sheet is accessed.

In the data work sheet the data is saved as area, number and pixel amounts in various columns. The data work sheet can be saved by using *F3 AscData* and *F8 ToDisk* commands and are saved as *.PRN or DOS accessible print files. Such data is analyzed by the statistical sub-programmes (transforms) found in this menu.

The total amount of condensed (or black) phase is calculated from the amounts of black area per frame, normally for 10 frames, at each surface pressure. These are converted to percentage condensed by using % condensed = (average black area per frame (μm^2)/total frame area or area of interest (μm^2) x 100). Other analysis of the data such as the individual area of the condensed (black) domains, their number and frequency distributions can also be performed using the various statistical sub-programmes (transforms) in the data work sheet menus of JAVA 1.4.

[The Figures A, C and D are reprinted from the JAVA 1.4 manual with the permission from publisher, ©Jandel Scientific, San Rafael, California).

APPENDIX B

PUBLICATIONS: REFEREED

1] Worthman, L. A., **K. Nag**, P. J. Davis and K. M. W. Keough (1996) Cholesterol in condensed and fluid phosphocholine monolayers studied by epifluorescence microscopy. *submitted.*

2] **Nag, K.**, S. Taneva, J. Perez-Gil, A. Cruz and K. M. W. Keough (1996) Association of fluorescently labelled pulmonary surfactant proteins SP-B and SP-C with DPPC in spread monolayers during dynamic cycling: An epifluorescence microscopic study. *Biophys. J. in press.*

3] **Nag, K** and K. M. W. Keough, M. T. Montero, J. Trias, M. Pons and J. Hernandez-Borrel (1996) Segregation of a quinoline antibiotic in dipalmitoylphosphatidylcholine bilayers and monolayers. *J. Liposome Res. 6: 713-736.*

4] **Nag, K.**, J. Perez-Gil, A. Cruz, N. H. Rich and K. M. W. Keough (1996) Spontaneous interfacial monolayers formation during adsorption of lipid-protein vesicles. *Biophys. J. 71:1356-1363.*

5] **Nag, K.**, J. Perez-Gil, A. Cruz and K. M. W. Keough (1996) Epifluorescence microscopic studies on interaction of fluorescently labelled pulmonary surfactant protein - C (SP-C) with phospholipids and calcium in spread monolayers. *Biophys. J. 71:246-256.*

6] **Nag K.**, N. H. Rich and K. M. W.Keough (1994) Interaction between dipalmitoylphosphatidylglycerol and phosphatidylcholine and calcium. *Thin Solid Films 244:841-844.*

7] Montero, M. T., J. Hernandez-Borrel, **K. Nag** and K.M.W. Keough (1994) Fluoroquinone distribution in a phospholipid environment studied by fluorometry. *Analytica Chimica Acta 290:58-64.*

8] Khan, R.A., D. Barker, R. Hooper, E. M. Lee, K. Ryan and **K. Nag** (1994) Histopathology in Pleuronectus americanus living adjacent to pulp and paper mills. *Archives of Environmental Contamination and Toxicology. 26:95-102.*

9] **Nag K.** and K. M. W. Keough (1993) Epifluorescence microscopic studies of monolayers containing mixtures of dioleoyl and dipalmitoyl phosphatidylcholines. *Biophys. J 65:1019-1026.*

10] Khan R. A. and **K. Nag** (1993) Estimation of Hemosiderosis in seabirds and fish exposed to petroleum. *Bulletin of Environmental Contamination and Toxicology. 50:125-131.*

11] Perez-Gil J., **K. Nag**, S. Taneva and K. M. W. Keough (1992) Pulmonary surfactant protein SP-C causes packing rearrangements of dipalmitoylphosphatidylcholine in spread monolayers. *Biophys. J 63:197-204.*

12] Keough K. M. W., G. Simatos, J. Perez-Gil, **K. Nag**, L. Allwood and M. Morrow (1992) Surfactant protein SP-C and phosphatidylcholines in bilayers and monolayers. *Thin Solid Films 210/211:720-722.*

13] Keough K. M. W., J. Perez-Gil, G. Simatos, J. Tucker, **K. Nag**, C. Boland, J. Stewart, L. Taylor, S. Taneva, L. Alwood and M. Morrow. (1991) Hydrophobic pulmonary surfactant proteins in model lipid systems. *in Progress in Membrane Biotechnology. ed. Gomezfernandez J.C., D.Chapman and L.B.Packer. Birkhauser Verlag, Basel. pp 241-252.*

14] **Nag K.**, C. Boland, N. H. Rich and K. M. W. Keough (1991) Epifluorescence microscopic observation of monolayer of dipalmitoylphosphatidylcholine : Dependence of domain size on compression rates. *Biochim. Biophys. Acta 1068:157-160.*

15] **Nag K.**, C. Boland, N. H. Rich and K. M. W. Keough (1990) Design and construction of an epifluorescence microscopic surface balance for the study of lipid phase transition. *Rev. Sci. Instr. 61:3425-3430.*

16] Goswami T. and **K. Nag.** (1989) The ultradian rhythm of nasal airway resistance: A computer analyzed study. *Otolaryngol. 18:44-47.*

17] **Nag K.** and H. Chattopadhyay. (1987) A computer analyzed study of the ultradian rhythm of nasal airway resistance in college students. *Ind. J. Physiol. 41:19-23.*

PROCEEDINGS AND ABSTRACTS:

1] **Nag, K.**, N. Chattopadhyay and H. Chattopadhyay (1989) Effect of moderate exercise and axial pressure on the nasal cycle activity of male and female college students. *INDIAN SCIENCE CONGRESS, MADURAI. A52.*

2] **Nag, K.**, N.H. Rich and K.M.W. Keough (1990) Epifluorescence microscopic observation of dynamic changes during lateral phase transition of DPPC monolayers at the air water interface. *CANADIAN FEDERATION OF BIOLOGICAL SOCIETIES. HALIFAX. A361.*

3] **Nag, K.**, N.H. Rich and K.M.W. Keough (1990) Observation of lateral phase transition in monolayers of dipalmitoyl phosphatidylcholines. *CONGRESS OF*

CANADIAN ASSOCIATION OF PHYSICIST. ST.JOHN'S. APP4.

4] **Nag, K.**, N.H. Rich and K.M.W. Keough (1990) An epifluorescence microscopic surface balance for characterization of phospholipid monolayer architecture during pressure induced phase transition. *X^th INTERNATIONAL BIOPHYSICS CONGRESS. VANCOUVER. A.P.3.1.1.*

5] **Nag, K.** and K.M. Keough. (1990) Dynamics of phospholipid domain formation in monolayers as studied by epifluorescence microscopy. *XX^th FEDERATION OF EUROPEAN BIOCHEMICAL SOCIETY MEETING. BUDAPEST, HUNGARY. A.P-TH 227.*

6] **Nag, K.** and K.M.W. Keough. (1991). Epifluorescence microscopic observation of monolayers of a DOPC:DPPC mixture at the air-water interface. *CANADIAN FEDERATION OF BIOLOGICAL SOCIETIES. KINGSTON. AP-143.*

7] Perez-Gil, J., **K. Nag** and K.M.W. Keough. (1991) Pulmonary surfactant protein SP-C and packing arrangements in monolayers of dipalmitoylphosphatidylcholine. *XXV^th BIOPHYSICAL SOCIETY ANNUAL MEETING. CALIFORNIA. USA. (Biophys. J.59:623a)*

8] Keough, K.M.W., J. Perez-Gil, G. Simatos and **K. Nag** (1991) The effects of pulmonary surfactant protein SP-C on packing of saturated phosphatidylcoline monolayers and bilayers. *INTERNATIONAL CONFERENCE OF AMERICAN THORACIC SOCIETY. CALIFORNIA. USA. (Respir. Dis. 143:A307).*

9] Keough, K.M.W., J. Perez-Gil, G. Simatos, J. Stewart, L. Taylor, **K. Nag,** C. Boland, M. Morrow, K. Sarin, C. Baxter and D. R. Absolom (1991) Pulmonary surfactant hydrophobic proteins in phosphatidylcholine(PC) arrays. *VII^th INTERNATIONAL CONFERENCE OF SURFACE AND COLLOID SCIENCE. COMPEIGNE, FRANCE. A C1/CL-20.*

10] Keough, K.M.W., G. Simatos, J. Perez-Gil, **K. Nag** and M. Morrow (1991) Pulmonary surfactant protein SP-C in bilayers and monolayers. *V^th INTERNATIONAL CONFERENCE ON LANGMUIR-BLODGETT FILMS. PARIS, FRANCE. AIP-1.*

11] Keough, K.M.W., G. Simatos, J. Perez-gil, **K. Nag**, L.A. Alwood, L. Taylor and M. Morrow (1991) Influence of hydrophobic surfactant proteins on lipids in bilayers and monolayers. *LV^th ANNUAL MEETING OF THE ROYAL COLLEGE OF PHYSICIANS AND SURGEONS OF CANADA. QUEBEC. (Clin. Invest. Med. A99)*

12] Keough, K.M.W., J. Perez-Gil, G. Simatos, J. Tucker, **K. Nag,** C. Boland, J. Stewart, L. Taylor, S. Taneva, L. Alwood and M. Morrow. (1991) Hydrophobic pulmonary surfactant proteins in model lipid systems. *IV^th INTERNATIONAL*

WORKSHOP ON MEMBRANE BIOTECHNOLOGY AND BIOMATERIALS. LA MANGA, SPAIN. A24.

13] Perez-Gil, J., **K.Nag** and K.M.W.Keough (1991) Utilizacion de microscopia dee epifluoreceencia en el estudio de interacciones lipido-proteina. *III CONGRESS OF THE SPANISH BIOPHYSICS SOCITY. A515.*

14] Taneva, S., **K. Nag** and K.M.W. Keough (1992) Pulmonary surfactant protein SP-B and lipids in spread monolayers at the air-water interface. *AMERICAN ASSOCIATION OF MOLECULAR BIOLOGY/BIOPHYSICAL SOCIETY MEETING. HOUSTON. Texas. (Biophys.J A498)*

15] **Nag, K.** and K.M.W. Keough (1992) Epifluorescence studies of monolayers containing mixtures of dioleoyl and dipalmitoyl phosphatidylcholine. *AMERICAN ASSOCIATION OF MOLECULAR BIOLOGY/BIOPHYSICAL SOCIETY MEETING. HOUSTON, Texas (Biophys. J A2144)*

16] Keough, K.M.W. and **K. Nag** (1992) Epifluorescence of monolayers of dipalmitoylphosphatidylglycerol (DPPG) at the air water interface. *CANADIAN FEDERATION OF BIOLOGICAL SOCIETIES. VICTORIA. British Columbia. A 379.*

17] Keough, K.M.W., M. Morrow, S. Taneva, **K.Nag**, J.Perez-gil and G.Simatos (1992) Interaction of pulmonary surfactant protein SP-B with dipalmitoylphosphatidylcholine. *NATO-FEBS INTERNATIONAL SUMMER SCHOOL ON NEW DEVELOPEMENTS IN LIPID-PROTEIN INTERACTIONS AND RECEPTOR FUNCTION. Aug.92. GREECE.*

18] Hernandez-Borrel, J., I. Carreira, **K. Nag** and K.M.W. Keough (1992) Segregation of one quinolone from dipalmitoyl phosphatidylcholine monolayers and bilayers. *IInd LIPOSOME RESEARCH DAYS. LEIDEN. THE NETHERLANDS. P39.*

19] Keough, K.M.W. and **K. Nag** (1993) Epifluorescence studies of monolayers containing dipalmitoylphosphatidylglycerol (DPPG) and dipalmitoylphosphatidylcholine (DPPC). *INTERNATIONAL MEETING OF THE AMERICAN THORACIC SOCIETY. SAN FRANCISCO. USA.*

20] Keough, K.M.W. and **K. Nag** (1993) Effect of Calcium with dipalmitoylphosphatidylglycerol (DPPG) and dipalmitoylphosphatidylcholine (DPPC). *36 th CANADIAN FEDERATION OF BIOLOGICAL SOCIETY. WINDSOR. A 154.*

21] **Nag, K.**, N.H. Rich and K.M.W. Keough (1993) Interaction between dipalmitoylphosphatidylglycerol (DPPG) and dipalmitoylphosphatidylcholine (DPPC) and calcium. *VIth INTERNATIONAL CONFERENCE OF LANGMUIR-BLODGETT FILMS. TROIS-RIVIERA. CANADA. p480.*

22] Montero, M.T., J. Hernandez Borrel, **K. Nag** and K.M.W. Keough (1993) Fluoroquinone distribution in a phospholipid environment studied by fluorometry. *Vth INTERNATIONAL SYMPOSIUM ON QUANTITATIVE LUMINESCENCE SPECTROMETRY IN BIOMEDICAL SCIENCES. GHENT.*

23] Keough, K.M.W., **K.Nag**, S.Taneva and J.Perez-gil (1993) Pulmonary surfactant (PS) protein in monolayers of PS lipids. *39th CANADIAN SPECTROSCOPY CONFERENCE A096 LAVAL, QUEBEC.*

24] Keough, K.M.W., J.Perez-Gil and **K.Nag** (1994) Adsorption and monolayer formation of some pulmonary surfactant components visualized by epifluorescence microscopy. *INTERNATIONAL CONFERENCE OF THE AMERICAN THORACIC SOCIETY. BOSTON (Am. J. respir. Crit. Care Med. 149 (4) A95)*

25] **Nag, K.**, J. Perez-Gil and K..M.W.Keough (1994) Epifluorescence microscopy of spread monolayers of some pulmonary surfactant components. *CONGRESS OF THE INTERNATIONAL UNION OF BIOCHEMISTRY AND MOLECULAR BIOLOGY. NEW DELHI. INDIA. P-11-11.*

26] Perez-Gil, J. **K.Nag** and K.M.W.Keough (1994) Lipid-protein interactions in surfactant associated protein C (SP-C)/DPPC monolayers studied by epifluorescence microscopy. *NATO ADVANCED STUDY INSTITUTE: NATO-ASI MEETING ON TRAFFICKING OF INTRACELLULAR MEMBRANE:FROM MOLECULAR SORTING TO MEMBRANE FUSION. ESPINHO, PORTUGAL.*

27] **Nag, K.**, N.H.Rich and K.M.W.Keough (1994) Epifluorescence microscopy of shape transitions in lipid monolayers at the air-water interface. *THE GEOMETRY OF FORMS IN EQUILIBRIUM AND NON EQUILIBRIUM SYSTEMS. ST.JOHN'S. CANADA.*

28] **Nag, K.**, J.Perez-Gil and K.M.W.Keough (1995) Epifluorescence microscopy of vesicle adsorbed monolayers of some pulmonary surfactant components. *39thANNUAL MEETING OF THE BIOPHYSICAL SOCIETY. SAN FRANCISCO. CALIFORNIA (Biophys. J. 68 (2) A304).*

29] Davis, P.J., L.A.Worthman, **K.Nag** and K.M.W.Keough (1995) Monolayer interaction of cholesterol with dipalmitoylphosphatidylcholine (DPPC) studied by epifluorescence microscopy. *86th AMERICAN OIL CHEMISTS SOCIETY ANNUAL MEETING. SAN ANTONIO. TEXAS. (INFORM 6 (1) 511 A191)*

30] Keough, K. M. W., S.Taneva, J.Perez-Gil and **K.Nag** (1995) Pulmonary surfactant proteins SP-B and SP-C remain associated with phospholipid in monolayers compressed to high surface pressure at the air-saline interface. *AMERICAN THORACIC SOCIETY MEETING. (Am. J. Respir. Crit. Care Med. 151 (4) 306)*

31] Ruano, M. L. F.,**K. Nag**, J.Perez-Gil, K.M.W.Keough and C.Casals (1995) Interaction of surfactant protein A (SP-A) with bilayers and monolayers of dipalmitoylphosphatidylcholine (DPPC) at acidic and neutral pH.*PORTUGESE-SPANISH BIOPHYSICS CONGRESS, LISBON. PORTUGAL.*

32] Perez-Gil, J., **K. Nag**, M. L. F. Ruano, A. Cruz, C. Casals and K. M. W. Keough (1995) Preferential distribution of fluorescently labelled pulmonary surfactant proteins in condensed and fluid regions of DPPC monolayers studied by epifluorescence microscopy. *V CONGRESO DE LA SOCIEDAD DE BIOFISICA DE ESPANA, LISBON, PORTUGAL.*

34] **Nag, K.**, M.L.F. Ruano, J. Perez-Gil, C. Casals and K. M. W. Keough. (1996) Adsorption of pulmonary surfactant protein - A (SP-A) on to dipalmitoylphosphatidylcholine monolayers studied by epifluorescence microscopy. *40th BIOPHYSICAL SOCIETY ANNUAL MEETING. BALTIMORE (Biophys J. 70 (2), A349).*

34] Keough, K. M. W., M.L.F. Ruano, J. Perez-Gil, C. Casals and **K. Nag** (1996) Distribution of pulmonary surfactant protein-A (SP-A) in dipalmitoylphosphatidylcholine (DPPC) and phosphatidylglycerol (DPPG) in spread monolayers. *AMERICAN THORACIC SOCIETY INTERNATIONAL CONFERENCE. NEW ORLEANS (Am. Rev. Respir. Crit. Care. Med. 153 (4) A106)..*

35] Worthman, L. D., **K. Nag**, P.J. Davis and K.M.W. Keough (1996) High amounts of cholesterol induce similar surface textures in monounsaturated and saturated phospholipid monolayers. *39th CANADIAN FEDERATION OF BIOLOGICAL SOCIETIES MEETING, London, Ontario, A087.*

36] **Nag, K.**, J.Perez-Gil, M.L.F. Ruano, C. Casals and K.M.W.Keough (1996) Association of fluorescently labelled pulmonary surfactant protein A (SP-A) and -B (SP-B) with dipalmitoylphosphatidylcholine (DPPC) monolayer films. *39th CANADIAN FEDERATION OF BIOLOGICAL SOCIETIES MEETING, London, Ontario, A088.*

☺ **END** ☻